Characterization of the D-Amino Acid Oxidase Interactome

Michael Popiolek

A thesis submitted to the University College London for the degree of Doctor of Philosophy in Pharmacology

April 2010

I, Michael Popiolek, confirm that the work presented in this thesis is my own. Where the information has been derived from other sources, I confirm that this has been indicated in the thesis.

Abstract

Schizophrenia is a psychiatric disorder affecting about 1% of the world's population and manifests itself as positive symptoms (eg. hallucinations), negative symptoms (eg. social withdrawal) in conjunction with cognitive impairments (eg. working memory). Evidence suggests that schizophrenia is, in part, a heritable disease. Candidate susceptibility genes implicate the glutamatergic neurotransmitter system, reinforcing clinical observations of N-methyl-D-aspartate receptor (NMDAR) hypofunction in schizophrenia. One of those genes, D-amino acid oxidase (DAO), is genetically associated with schizophrenia and its function includes degradation of D-serine, the NMDAR co-agonist. DAO is a candidate gene of high interest due to schizophrenic patients' manifestation of reduced D-serine levels, increased DAO expression and increased DAO activity.

Despite mounting evidence for DAO involvement in schizophrenia, its regulation is poorly understood. Characterization of DAO may lead to a more thorough understanding of its function and biology and ultimately to the identification of novel targets for this disorder. To this end, DAO-specific antibodies were utilized to identify DAO-interacting proteins through co-immunoprecipitation from rat cerebellum, where DAO expression is especially high. Subsequent mass spectroscopy analysis of associating proteins yielded twenty-four putative DAO interactors. The most abundant and interesting interactors include known presynaptic active zone members such as bassoon (BSN) and piccolo (PCLO). The DAO interaction with BSN was confirmed through co-immunoprecipitation and both proteins were shown to localize in the presynaptic junction. These data suggest that BSN is a novel DAO interactor and defines a previously unappreciated localization of DAO perhaps as a result of a physiologically important interaction with BSN. Furthermore, BSN was found to partially inhibit DAO enzymatic activity in transiently transfected human embryonic kidney (Hek293) cells. Collectively these novel findings suggest that synaptic D-serine concentration may be under tight regulation by BSN via proximally localized DAO. DAO may thus play a role in modulating the functions of the presynaptic active zone via its interaction with BSN.

Acknowledgements

I am very grateful to several people including Margaret Lie, Stan Nawoschik and Dr. Kevin Pong who thought me key biochemistry and tissue culture techniques even prior to enrollment in the doctorate program. Through their assistance I was able to hit the ground running in respect to DAO research detailed in this thesis. I am very thankful to Dr. John Ross for assistance with identification of DAO interacting proteins through mass spectroscopy. His expertise in designing suitable mass spectroscopy experimental controls was critical in our identification of the DAO interactome. I am thankful to Brian Strassle for teaching me everything in respect to imaging starting from animal perfusion all the way to tissue preparation, staining and imaging. Brian's' expertise made my imaging experience very pleasurable indeed.

I am very deeply grateful to my Wyeth advisers: Dr. Mark Pausch and Dr. Nick Brandon for selecting me as a doctorate degree candidate. Their support, encouragement and advice throughout my studies allowed me to grow scientifically and think independently. I am especially thankful to Dr. Brandon for initiating the doctorate program and to Dr. Pausch for mentoring me during the program and many years prior to it. Dr. Steve Moss has been instrumental to my progress and I thank him for his advice and mentorship. I would also like to thank the Brandon lab for their support.

Contents

Chapter 7: Discussion

Chapter 8: Materials and Methods

List of Tables

List of Figures

List of Abbreviations

7-TM	7-Transmembrane
AD	Activating domain
Ade	Adenine
AMPA	Aalpha-3-hydroxy-5-methyl-4-isoxazolepropionate
ASC-1	Alanine-serine-cysteine transporter-1
Asp	D-aspartate
ATP	Adenosine-5'-triphosphate
BA9	Brodmann area 9
BACS	Brief Assessment of Cognition in Schizophrenia
BD	Binding domain
BHK	Baby hamster kidney
BLAST	Basic local alignment search tool
BPRS	Brief psychiatric rating scale
BSA	Bovine serum albumin
BSN	Bassoon
BVMT	Brief Visuospatial Memory Test
CAZ	Cytomatrix assembled at active zone
CCTCC	Cortico-cerebellar-thalamo-cortical circuit
CGI	Clinical global impression
CGN	Cerebellar granule neurons
CHL	Chinese hamster lung
CHO	Chinese hamster ovary
CMT	Charcot-Marie-Tooth
CNV	Copy number variants
Co-IP	Protein complex immunoprecipitation
CONSIST	Cognitive and negative symptoms of schizophrenia trial
COS7 cells	CV-1 in Origin, and carrying the SV40 genetic material
CPT-IP	Continuous Performance Test - Identical Pairs
CSF	Cerebrospinal fluid
C-terminal	Carboxy-terminal
D2	Dopamine 2 receptor
DAO	D-amino acid oxidase
DAOA	DAO activator; G72/G30
DDO	D-aspartic acid oxidase
DLPFC	Dorso-lateral prefrontal cortex
DMP	Dimethyl pimelimidate dihydrochloride
DNA	Deoxyribonucleic acid
DSM	Diagnostic and Statistical Manual of Mental Disorders
DTT	Dithiothreitol
EAAT	Excitatory Amino Acid Transporter
EC50	Half maximal effective concentration
ELISA	Enzyme-linked immunosorbent assay
EM	Electron micrography
EPS	Extrapyramidal side effects
EPSCs	Excitatory postsynaptic currents

FAD	Flavin adenine dinucleotide
fMRI	Functional magnetic resonance imaging
GABA	γ-Aminobutyric acid
GAD	Glutamic acid decarboxylase
GAS	Global assessment scale
GAT	GABA transporter
GCP II	Glutamate carboxypeptidase II
GFP	Green fluorescent protein
GH4C1	Clonal rat pituitary tumor
GlyT1	Glycine tranporter-1 receptor
GMS	Glycine modulatory site
GRIK4	Glutamate receptor, ionotropic, kainate 4
GRIP	Glutamate-receptor-interacting protein
GRM3	Metabotropic glutamate receptor 3
GTP	Guanosine-5'-triphosphate
Ham-D	Hamilton rating scale for depression
Hek293	Human embryonic kidney cells
HeLa	Human carcinoma cell line derived from Henrietta Lacks
HET	Heterozygous
His	Histidine
HRP	Horseradish peroxidase
HVLT	Hopkins Verbal Learning Test
IC50	Half maximal inhibitory concentration
IgG	Immunoglobulin G
KLH	Keyhole Limpet Hemocyanin
KO	knock-out
Leu	Leucine
MAP2	Microtubule associated protein 2
MATRICS	Measurement and Treatment Research to Improve Cognition in Schizophrenia
MCCB	MATRICS Consensus Cognitive Battery
mGluR	Metabotropic glutamate G-protein-coupled receptor
MK-801	Dizocilpine
MRI	Magnetic resonance imaging
mRNA	Messenger ribonucleic acid
MSCEIT	Mayer-Salovey-Caruso Emotional Intelligence Test
NAA	N-acetyl aspartyl
NAAG	N-acetyl aspartyl glutamate
NAB	Neuropsychological Assessment Battery
NADH	Nicotinamide adenine dinucleotide
NCBI	National Center for Biotechnology Information
NIH 3T3	Mouse embryonic fibroblast cells
NIMH	National Institute of Mental Health
NMDAR	N-methyl-D-aspartate receptor
PAM	Positive allosteric modulator
PANSS	Positive and negative syndrome scale
PBS	Phosphate buffered saline
PCLO	Piccolo

PCP	Phencyclidine
PCR	Polymerase chain reaction
PET	Positron emission tomography
PIP2	Phosphatidylinositol (4,5)-bisphosphate
RAB	RAS oncogene family
RFU	Relative fluorescence unit
RIPA	Radioimmunoprecipitation assay buffer
SANS	Scale for the assessment of negative symptoms
SDS-PAGE	Sodium dodecyl sulfate polyacrylamide gel electrophoresis
Ser	D-serine
SNPs	Single-nucleotide polymorphisms
SNARE	Soluble N-ethylmaleimide-sensitive factor attachment protein receptors
SPECT	Single photon emission computed tomography
SRR	Serine racemase
TNIK	TRAF2 and NCK interacting kinase
Trp	Tryptophan
UAS	Upstream activating sequence
VAMP	Vesicle-associated membrane protein
VTA	Ventral tagmental area
WBP2	WW domain binding protein 2
WCST	Wisconsin card sorting task
WMS	Wechsler Memory Scale
WT	Wildtype
Y2H	Yeast-two-hybrid

1.1 Schizophrenia symptoms, diagnosis, and costs

Schizophrenia is a chronic, severe, disabling brain disorder that generally has an onset in the early adulthood and may persist throughout life (Lewis and Lieberman, 2000). It affects around 1% of the population worldwide (Harrison and Owen, 2003) and is highly heritable (80%) with a concordance rate of approximately 50% in monozygotic twins, 12% to 17% for dyzygotic twins and first-degree relatives (Gotesman, 1991; Sullivan et al., 2003). The lack of complete concordance rate in identical twins suggests that environmental and epigenetic factors influence the phenotype with strong evidence for perinatal insults (Tsuang, 2000).

Schizophrenia manifests itself through positive symptoms including delusions, hallucinations, and though disorder; negative symptoms such as flattening of emotional responses, apathy and social withdrawal (Andreasen, 1995; Crow, 1985); and cognitive symptoms with impairments in attention, memory and executive functions (Elvevag and Goldberg, 2000). The disease is heterogeneous and the diagnosis is based on symptoms and their progression (Andreasen, 1995) classified by the Diagnostic and Statistical Manual (DMS-IV; American Association of Psychiatry, 1994; Table 1.1).

Schizophrenia is burdensome on the patient as well as the society as the disease has economical implications through productivity loss of the patient and the immediate family, cost of law-enforcement, homeless shelters, hospital stay and treatment. It is estimated that schizophrenia is the seventh most costly medical illness in the world (Freedman, 2003). In the United States alone the economic burden associated with schizophrenia in 2002 was estimated at $62.7 billion with about 9% of that sum made up by cost of drugs (Wu et al., 2005). The data highlights the need for a pharmacological intervention in treatment of this debilitating disease.

Table 1.1: DSM-IV Diagnostic criteria for schizophrenia

A. Characteristic symptoms. Two (or more) of the following, each present for a significant portion of time during a 1 month period (or less if successfully treated).
   a. Delusions
   b. Hallucinations
   c. Disorganized speech (e.g. frequent derailment of incoherence)
   d. Grossly disorganized or catatonic behavior
   e. Negative symptoms, i.e. affective flattening, alogia or avolition
B. Social/occupational dysfunction. For a significant portion of the time since the onset of the disturbance, one or more major areas of functioning such as work, interpersonal relations, or self-care are markedly below the level achieved prior to the onset (or when the onset is in childhood or adolescence, failure to achieve the expected level of interpersonal, academic or occupational achievement).
C. Duration. Continuous signs of the disturbance persists for at least 6 months. This 6-month period must include at least 1 month of symptoms (or less if successfully treated) that meet criterion A (i.e. active-phase symptoms) and may include periods of prodromal or residual symptoms. During these prodromal or residual periods, the signs of the disturbance may be manifested by only negative symptoms or two or more symptoms listed in Criterion A present in an attenuated from (e.g. odd beliefs, unusual perceptual experiences).
D. Schizoaffective and Mood Disorder exclusion. Schizoaffective Disorder and Mood Disorder with Psychotic Features have been ruled out because either
   a. No Major Depressive, Manic, or Mixed episodes have occurred concurrently with the active-phase symptoms; or
   b. If mood episodes have occurred during active-phase symptoms, their total duration has been brief relative to the active and residual periods.
E. Substance/general medical condition exclusion. The disturbance is not due to the direct physiological effects of a substance (e.g. a drug of abuse, a medication) or a general medical condition.
F. Relationship to a Pervasive Developmental Disorder. If there is a history of Autistic Disorder or another Pervasive Developmental Disorder, the additional diagnosis of Schizophrenia is made only if prominent delusions or hallucinations are present for at least a month (or less if successfully treated).

Diagnostic criteria for Schizophrenia subtypes
1. Paranoid Subtype. A type of schizophrenia in which the following criteria are met:
   a. Preoccupation with one or more delusions or auditory hallucinations
   b. None of the following is prominent: disorganized speech, disorganized or catatonic behavior, or flat or inappropriate affect
2. Disorganized subtype. A type of Schizophrenia in which the following criteria are met:
   a. All of the following are present; i)Disorganized speech; ii)Disorganized behavior; iii) flat or inappropriate affect
   b. The criteria are not met for catatonic type
3. Catatonic Subtype. A type of schizophrenia in which the clinical picture is dominated by at least two of the following:
   a. Motoric inability as evidenced by catalepsy (including waxy flexibility or stupor)
   b. Excessive motor activity (that is apparently purposeless and not influenced by external stimuli)
   c. Extreme negativism (an apparently motiveless resistance to all instructions or maintenance of a rigid posture against attempts to be moved) or mutism
   d. Peculiarities of voluntary movement as evidenced by posturing (voluntary assumption of inappropriate or bizarre postures), stereotyped movements prominent mannerisms, or prominent grimacing
   e. Echolalia or echopraxia
4. Undifferentiated subtype. A type of Schizophrenia in which the symptoms that meet Criterion A are present but the criteria are not met for the Paranoid, Disorganized, or Catatonic Type.

Adapted from American Association of Psychiatry, 1994

1.2 Major pathways associated with schizophrenia

Dopamine research has been recognized to be central to schizophrenia studies for many years and resulted in development of several drugs that treat the disease (outlined in dopamine hypothesis of schizophrenia section 1.2.1 and in treatment of schizophrenia section 1.4). Abnormalities in glutamate neurotransmission have been highlighted more recently but have already been implicated in schizophrenia especially in symptoms where the dopaminergic treatment has limitations. The glutamate neurotransmission deficits are complementary to the dopaminergic hypothesis and also impinge upon other important neurotransmitters such as GABA described below.

1.2.1 Dopamine hypothesis of schizophrenia

For nearly half a century, schizophrenia was though to be a disease of dopaminergic neurotransmission dysregulation (Carlsson, 1988). The dopamine hypothesis was based upon two fundamental observations. First, blocking dopamine re-uptake and increasing dopamine release through psycho stimulants such as amphetamine and cocaine can cause psychosis in healthy volunteers that resemble the positive symptoms of schizophrenia while exacerbating those symptoms in schizophrenic patients (Bunney et al., 1973; Einhorn et al., 1988; Lieberman et al., 1987; Satel and Edell, 1991; Shi et al., 2000). Secondly, the typical antipsychotic medications such as haloperidol and chlorpromazine block dopamine D2 receptors. Their affinity at the D2 receptors, in turn, highly correlates with their clinical potency in psychosis relief (Creese et al., 1976; Kapur et al., 2000; Peroutka and Synder, 1980; Seeman et al., 1976). Thus the dopamine hypothesis of schizophrenia was based on the dopamine hyperactivity resulting in symptoms of schizophrenia (Matthysse, 1973).

There are four main dopaminergic pathways in the brain that impinge on abnormalities found in schizophrenic patients. They include the mesocortical, mesolimbic, tuberoinfundibular and nigrostriatal tracts. The origin and respective target regions for each is highlighted in Figure 1.1. The mesolimbic pathway is important for memory and for motivating behavior. Through blockage of this pathway antipsychotics reduce intense emotions associated with schizophrenia.

Overactive mesocortical pathway is though to result in hallucinations and disorderly thinking thus toning down this pathway through antipsychotics may have a desirable effect in schizophrenic patients. The nigrostriatal pathway is involved in motor control and excessive dopaminergic inhibition may result in extra pyramidal side effects. The tuberoinfundibular pathway plays a role in hormonal secretion such as prolactin.

With additional data the focus of blocking dopamine receptors and limiting excess dopaminergic transmission shifted to a more compartmentalized approach (Davis et al., 1991; Matthysse, 1973; Snyder, 1976). Specifically it was observed that the destruction of dopamine afferents within the prefrontal cortex resulted in a chronic subcortical dopamine hyperactivity which manifested as increased dopamine turnover and up-regulation of postsynaptic receptors (Pycock et al., 1980). These findings are strikingly similar to those of schizophrenia postmortem findings (Weinberger and Kleinman, 1986). Positron emission tomography (PET) suggested a regional brain dysfunction because of observed reduced cerebral blood flow in frontal cortex of schizophrenic patients (Meyer-Lindenberg et al., 2002). The single most widely replicated brain dopaminergic changes are from PET studies of acutely psychotic patients showing elevated presynaptic striatal dopamine (Howes and Kapur, 2009). Consequently, the dopaminergic hyperactivity theory was then refined to suggest a hyperfunction of mesolimbic projections and a hypofunction of mesocortical projections as symptomatic of schizophrenia (Davis et al., 1991; Weinberger, 1987).

The limitation of the dopamine hypothesis is that neither negative symptoms nor cognitive impairments are adequately treated with dopamine D2 receptor antipsychotics (Laruelle et al., 1999; Meltzer, 1997). Further undermining the importance of this hypothesis in schizophrenia were inconsistent findings in post mortem studies which were not able to demonstrate consistent up regulation or excessive activation of the D2 receptors (Farde et al., 1990; Howes et al., 2009). Thus the disease as a whole is unlikely to be explained solely by the dopaminergic alterations (Carlsson et al., 2001).

Figure 1.1: The four dopaminergic pathways.

Mesocortical tract: projects from VTA to cortical regions, especially the prefrontal cortex

Mesolimbic tract: projects from VTA to limbic regions including hippocampus, nucleus accumbens and amygdala

Nigrostriatal tract: projects from the substantia nigra to the caudate and putamen

Tuberinfundibular tract: projects from the hypothalamus to the pituitary stalk

Taken from thebrain.mcgill.ca

1.2.2   Glutamate and schizophrenia

Glutamate is the major excitatory neurotransmitter in the brain and is utilized by 40 percent of all synapses (Tsai and Coyle, 2002). The postsynaptic effects of glutamate are mediated by three families of glutamate-gated ion channels: the AMPA, kainate and NMDA receptors. The AMPA receptors are primarily involved in generation of the excitatory postsynaptic currents (EPSCs) which are responsible for initiating action potentials. While the NMDARs also contribute to the EPSCs and dendritic spikes they are known to have a critical role in synaptic plasticity. Kainate receptors are found in pre- and postsynaptic neurons (Huettner, 2003) where they can affect neurotransmitter release (Schmitz et al., 2001). The fourth family of glutamate receptors is the 7-TM G-protein coupled metabotropic glutamate receptors (mGluRs), which are known to modulate glutamatergic neurotransmission both pre and postsynaptically (Coyle, 2006; Halassa et al., 2007).

1.2.2.1 N-methyl-D-aspartate receptor and schizophrenia

Since NMDARs are central to my thesis they are described in more detail. NMDARs are voltage dependent ionotropic glutamate receptors responsible for synaptic plasticity and memory function (Li and Tsien, 2009). NMDARs assemble as multi-subunit tetramers including at least one NR1 subunit and one or more NR2 or NR3 subunits. Seven subtypes (NR1a–g) of the NR1 subunit are generated by alternative splicing from a single gene while the NR2 and NR3 subunits exist as multiple subtypes (NR2A-D and NR3A-B) each encoded by a distinct gene (Dingledine et al., 1999). The NR2 subunits contribute to functional diversity by conferring on NMDARs distinct biophysical and pharmacological properties (Cull-Candy and Leszkiewicz, 2004; Paoletti and Neyton, 2007). NMDAR subunits are organized into three functionally distinct domains, an extracellular N-terminal glutamate-binding domain, the transmembrane domain composed of three membrane-spanning helices containing the ion-channel pore forming loop, glycine/D-serine modulatory and kynurenic acid inhibitory sites and the cytoplasmic C-terminal tail that determines subcellular trafficking of the receptor and coupling to various intracellular signaling pathways (Figure 1.2). Occupancy of the modulatory site by glycine or D-serine affects channel open time and desensitization rate in the presence of glutamate but does not induce channel opening in the absence of glutamate, making these endogenous ligands obligatory co-agonists. Glutamate in concert with glycine/D-serine binding to the co-agonist modulatory site (GMS) leads to the induction of Ca^{2+} currents through the ionic pore of the NMDAR. The Ca^{2+} influx, in turn mediates learning and memory, long-term changes in the synaptic plasticity and neural development (Oliet and Mothet, 2006).

The NR1 subunit is expressed in neurons at all developmental stages throughout the mammalian brain while NR2 subunits display distinct regional and developmental expression patterns. The NR2B and NR2D subunits predominate in the embryonic brain while NR2A and NR2C are absent. In the adult brain, NR2A is ubiquitously expressed, NR2B is restricted to forebrain areas and NR2C is highly enriched in the cerebellum (Akazawa et al., 1994; Monyer et al., 1994;

Watanabe et al., 1992). While the NMDARs also contribute to the EPSCs and dendritic spikes they are known to have a critical role in synaptic plasticity.

Figure 1.2: Diagram of NMDAR and its modulatory sites.
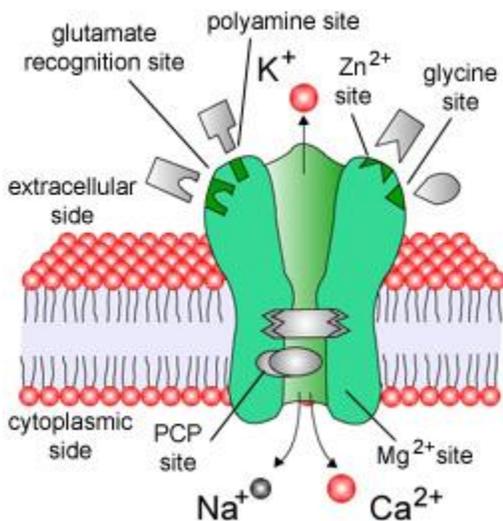
Taken from Institute of Organic Chemistry and Biochemistry AS CR.

Considerable evidence has accumulated in support of glutamate hypofunction as a contributor to schizophrenia etiology. Data from NMDAR antagonist studies, pharmacologic intervention studies, postmortem studies and genetic studies converged on and reinforced the NMDAR hypofunction hypothesis (Coyle, 2006). In the 1950's and 60's dissociative anesthetics such as ketamine and phencyclidine (PCP) were observed to result in a psychotic syndrome in healthy individuals (Luby et al., 1959) and were found to exacerbate those symptoms in schizophrenic patients (Itil et al., 1967; Lahti et al., 1995). Although Javitt and Zukin (Javitt and Zukin, 1991) proposed that PCP induced NMDAR blockade resulted in schizophrenia-like symptoms the NMDAR involvement in schizophrenia was not widely embraced until Krystal *et al*. (Krystal et al., 1994) demonstrated that administration of chronic low doses of ketamine led to negative and minor positive symptoms and subtle cognitive impairments in healthy volunteers. Subsequently, declarative memory

(Newcomer et al., 1999), and thought disorders similar to those found in schizophrenia (Adler et al., 1999), were shown to be affected by administration of low doses of ketamine in healthy volunteers. Together the NMDAR antagonist studies in humans suggested the glutamate receptor hypofunction with schizophrenic symptoms.

To build on the glutamate receptor hypofunction hypothesis, pharmacological agents were used to reverse the deficit and ascertain their behavioral outcome in patients. However, since direct activation of the NMDAR may lead to excitotoxicity and neuronal degradation (Lynch and Guttmann, 2001; Misztal et al., 1996; Wolf et al., 1990), NMDAR functional enhancement through application of co-agonists has been used. D-cycloserine is a partial agonist at the NMDAR with 60% of the efficacy of glycine (Sheinin et al., 2001). In clinical trials D-cycloserine administered at 50 mg/day in conjunction with typical antipsychotics to schizophrenic patients characterized with prominent negative symptoms resulted in reduction in negative symptoms and improvement in cognitive impairments but no relief of the positive symptoms (Goff et al., 1995; Heresco-Levy et al., 2002). Increasing synaptic glycine concentration through inhibition of GlyT1 by administration of sarcosine was tested in patients with chronic schizophrenia as an adjunct to resperidone or typical antipshychtics. Significant reductions in negative symptoms, increase in cognitive performance, and improvement in positive symptoms were observed versus placebo-controlled patients (Tsai et al., 2004). Similarly administration of glycine (30-60 g/day) in conjunction with typical antipsychotics to chronic schizophrenic patients showed significant improvements in negative symptoms and cognitive impairments (Leiderman et al., 1996). Milacemide is an acetylated prodrug of glycine, which converts into glycine upon deacetylation (O'Brien et al., 1991). When administered to drug-free patients milacemide did not improve psychotic symptoms (Rosse et al., 1991; Tamminga et al., 1992) however, co-administration with conventional antipsychotics may have a different outcome as seen with other NMDAR co-agonists. While d-cycloserine and glycine administration had encouraging early outcomes recent CONSIST clinical trial showed data that neither of the two compounds had any affect on negative symptoms or cognitive

impairment in schizophrenic patients (Buchanan et al., 2007). The CONSIST study had a differential response between inpatients versus outpatients and used a fixed dose of glycine at 60 g/day which may not be optimal for some patients (Buchanan et al., 2007). While these recent results carry negative outcome for the glycine modulatory site (GMS) (see figure 1.2) modulation through administration of d-cycloserine and glycine other NMDAR co-agonists such as D-serine and D-alanine were reported to have encouraging findings (described in D-serine section 1.7). The clinical application of GMS and their respective outcomes are summarized in table 1.2.

Initial studies analyzing the CSF of schizophrenic patients reported decreased concentration of glutamate but this finding has not been consistently reproduced (Goff and Coyle, 2001; Kim et al., 1980). Schizophrenic postmortem glutamate concentrations were found to be reduced in prefrontal cortex and hippocampus, brain regions implicated in schizophrenia, versus controls while NAAG, NMDAR antagonist and mGluR3 agonist, were increased in hippocampus of patients. Furthermore, glutamate carboxypeptidase II (GCP II), which metabolizes NAAG to glutamate and NAA was reduced in frontal cortex, temporal cortex, and the hippocampus in patients (Tsai et al., 1995). Through magnetic resonance spectroscopic studies the NAA levels were confirmed to be lower in schizophrenics (Bertolino et al., 2000). Kynurenic acid, an NMDAR antagonist, was also increased in postmortem samples of schizophrenic hippocampus (Schwarcz et al., 2001). Expression of NMDAR 2D subunit was increased in prefrontal cortex but the NR-1 subunit was decreased in the hippocampus of schizophrenic patients. Despite this altered expression ligand-binding studies did not indicate NMDAR alterations (Akbarian et al., 1996; Gao et al., 2000). Some of the postmortem studies, while not always reproducible, support NMDAR involvement albeit indirectly through alterations in levels of glutamate receptor antagonists in schizophrenic patients.

Schizophrenia appears to follow a complex inheritance pattern with multiple genes contributing small effects in the emergence of the phenotype (Kirov et al., 2005; Purcell et al., 2009). Several possible risk genes based on linkage and association studies (highlighted in Table 1.4) have been implicated in

this disease. Several of the candidate genes are known to modulate the NMDAR. For example, some dysbindin variants are concentrated on the presynaptic glutamatergic terminals where they modulate vesicular release of glutamate (Numakawa et al., 2004). Furthermore, dysbindin expression in the prefrontal cortex and hippocampus of schizophrenics is reduced (Talbot et al., 2004; Weickert et al., 2004). mGluR3 activity may be elevated in schizophrenia and the activation of mGluR3 is known to down regulate the release of glutamate providing supporting evidence for the glutamate hypofunction (Coyle, 2006). Neuregulin directly reduces NMDAR currents in cortical primary neurons (Gu et al., 2005) and animals with a null mutation in neuregulin display lower expression of NR1 subunit (Falls, 2003). Both G72 and DAO have been implicated in NMDAR activation through metabolism of its mandatory co-agonist D-serine (Chumakov et al., 2002). The association data is supportive of NMDAR importance in schizophrenia. The risk genes, in general, are not directly associated with proteins within the serotonergic, muscarinic, histaminergic or dopaminergic systems.

Several other observations, related to the NMDAR, suggest that glutamate alterations may play a critical role in brain development. NMDAR are critically involved during development when they guide axons to their targets and continue to maintain synapses and influence synaptic plasticity (Coyle and Tsai, 2004a; Harrison et al., 2003) and NMDAR may be relevant in synaptic pruning (Feinberg, 1990). This evidence is complementary to the neurodevelopmental hypothesis described in genetics and aetiology of schizophrenia section 1.5.

Data suggest that the dopaminergic abnormalities observed in the schizophrenic patients may be accounted for by glutamatergic hypofunction. Dissociative anesthetics such as PCP and MK-801 were shown in preclinical trials to increase dopamine release in frontal cortex and ventral striatum to the same magnitude as amphetamine (Breier et al., 1998; Verma and Moghaddam, 1996; Vollenweider et al., 2000). Likewise, antagonists at the glycine site of the NMDAR increased midbrain dopamine neuronal firing (Linderholm et al., 2007; Schwieler et al., 2006). Inhibition of glutamate transmission in the ventral tegmental area was shown to result in increased dopaminergic release in the

mesolimbic pathway and reduced dopaminergic release in the mesocortical pathway (Takahata and Moghaddam, 2000). Subanesthetic doses of ketamine produce an increased striatal release of dopamine in normal humans with amphetamine challenge similar to that of schizophrenic patients (Kegeles et al., 2000).

Likewise, glutamatergic hypofunction is complementary with the GABAergic deficits found in schizophrenia. The GABA transporter 1 (GAT1) and glutamic acid decarboxylase (GAD67) have been shown to be expressed at a lower level in chronically treated rats with MK-801 reflecting observations made in schizophrenic patients (Guidotti et al., 2000; Paulson et al., 2003; Volk et al., 2000).

1.3 Brain regions implicated in schizophrenia

In addition to important pathways associated with this disorder, several brain regions have been identified as disease relevant through functional imaging, neuropathological findings and clinical observations. Some of those regions include dorso-lateral prefrontal cortex (DLPFC) and hippocampus which have been implicated in cognitive, negative and positive symptoms of schizophrenia (Boyer et al., 2007; Harrison, 1999). More recently, evidence suggests that the cerebellum may be an important brain region involved in cognition and displaying abnormalities in schizophrenia (Andreasen and Pierson, 2008). Hence, the three brain regions are discussed below.

1.3.1 DLPFC

Any disease related changes within the DLPFC may be especially relevant for schizophrenia cognitive dysfunction as the DLPFC is known to participate in attention, executive function and working memory. While schizophrenic patients show performance deficits in nearly all functional neuropsychological studies, working memory is generally most severely affected (Saykin et al., 1991; Saykin et al., 1994). DLPFC gray matter volume is reduced in schizophrenic patients and positively correlated with cognitive dysfunction and severity of negative symptoms (Cannon et al., 2002).

Table 1.2: Antipsychotic effects of glycine site potentiators adopted from Shim (Shim et al., 2008)

Clinical Trials	Sample size	Dur of trial (weeks)	AD	Clinical observations	Observ.
Glycine					
(Waziri, 1988)	11	~35	DR	clin observ	I psychotic/ Psychosocial
(Costa et al., 1990)	6	5	C	BRPS	I
(Potkin et al., 1992)	18	6	C	CGI, SANS, BPRS	I BPRS
(Javitt et al., 1994)	14	8	C	PANSS	I negative
(Leiderman et al., 1996)	5	8	C/A	PANSS/SANS	I negative
(Heresco-Levy et al., 1996a; Heresco-Levy et al., 1996b)	11	6	C/A	PANSS/BPRS	I negative
(Heresco-Levy et al., 1999)	22	6	C/A	PANSS/BPRS	I negative
Milacemide					
(Rosse et al., 1990)	5	5	DR	SANS/BPRS/CGI	E negative
(Rosse et al., 1991)	4	4	DR	SANS/BPRS/CGI	NI
(Tamminga et al., 1992)	6	6	DR	BPRS	NI
D-serine					
(Tsai et al., 1998)	28	6	C	PANSS, SANS, CGI, WCST, Ham-D	I cognitive
D-Alanine					
(Tsai et al., 2006)	32	6	C	PANSS, SANS, CGI	I neg/cog/ psychopathology
D-cycloserine					
(Simeon et al., 1970)	10	2-14	DR	clin observ	E
(Cascella et al., 1994)	7	6	C	CGI, SANS, BPRS	E pos/neg/ gen psychopatholo
(Goff et al., 1995)	9	2	C	SANS, BPRS	E negative
(Rosse et al., 1996)	13	4	molindone	SANS, BPRS, CGI	NI
(van Berckel et al., 1996)	7	3	C	PANSS, CGI	I negative
(van Berckel et al., 1999)	25	8	C	PANSS, CGI	E pos/general Psychopathology
(Goff et al., 1999)	39	8	C	PANSS, SANS, GAS *cognitive, Ham-D	I negative
(Heresco-Levy et al., 2002)	16	6	C/A	PANSS, SANS, Ham-D	I negative
(Duncan et al., 2004)	22	4	C	PANSS, SANS, BPRS *cognitive	NI
(Goff et al., 2005)	26	26	C	PANSS, SANS, BPRS	NI
Sarcosine					
(Tsai et al., 2004)	38	6	C/risperid	PANSS, SANS, Ham-D	I positive/negative/ general psychopathol
(Lane et al., 2006)	65	6	risperidone	PANSS, SANS	I positive/ negative/general psychopathol

Rating scale: PANSS (positive and negative syndrome scale), SANS (scale for the assessment of negative symptoms), BPRS (brief psychiatric rating scale), CGI (clinical Rating scale: PANSS (positive and negative syndrome scale), SANS (scale for the assessment of negative symptoms), BPRS (brief psychiatric rating scale), CGI (clinical global impression), GAS (global assessment scale), Ham-D (Hamilton rating scale for depression), WCST (Wisconsin card sorting task, *cognitive (Abrams and Tayler rating scale, Sternbery memory/continuous performance)
Symptoms outcomes: I (improved), E (exacerbated), NI (not improved)
AD = antipsychotic drugs; DR = drug free; C = conventional; A = atypical

Within layer III of schizophrenic patients DLPFC pyramidal cells are smaller (Pierri et al., 2001; Rajkowska et al., 1998), have decreased spine density (Glantz and Lewis, 2000), less dendritic arborization and complexity (Kalus et al., 2000), decreased synaptic connectivity (Mirnics et al., 2001), and increased neuronal density (Selemon et al., 1998). Likewise, similar findings were reported in layer V in respect to pyramidal cell soma size (Cotter et al., 2002) and dendritic spine density (Black et al., 2004). Neuronal mis-connectivity may play a relevant role in schizophrenic DLPFC as evidenced by decreased levels of synaptic proteins such as SNAP-25 and synaptophysin (Karson et al., 1999; Thompson et al., 1998), complexin I (Sawada et al., 2002), synaptobrevin (Halim et al., 2003) and synapsin III (Porton and Wetsel, 2007). Interestingly, both NMDA and AMPA receptors are enriched in the above mentioned DLPFC pyramidal cell layers (Beneyto and Meador-Woodruff, 2004; Conti et al., 1999; Huntley et al., 1997) suggesting glutamatergic modulation may be relevant in this brain region and altered in patients.

1.3.2 Hippocampus

The hippocampus plays an important role in memory consolidation, transfer of memory from short-term to long-term memory and navigation (Heckers and Konradi, 2002). Single photon emission computed tomography (SPECT), PET and magnetic resonance imaging (MRI) functional studies suggest hypofunction of the hippocampus in schizophrenic patients which manifests in memory impairments (Weiss and Heckers, 2001). Other studies suggested

augmented hippocampal activity in medication-free schizophrenic patients (Lahti et al., 2006; Medoff et al., 2001; Nordahl et al., 1996; Weiss et al., 2006). Furthermore, anatomical hippocampal abnormalities in schizophrenia patients including decrease in area and volume were demonstrated (Harrison, 1999; Nelson et al., 1998; Weiss et al., 2005; Wright et al., 2000). The volumetric decrease in schizophrenia was explained by neuronal loss (Falkai and Bogerts, 1986), reduced neuronal size (Arnold et al., 1995), and pyramidal cell disarray (Conrad et al., 1991). The reduced neuronal size is hypothesized to be a result of a less extensive or abnormal synaptic connections (Harrison and Eastwood, 2001). Also, decreased expression of synaptic proteins such as synaptophysin (Davidsson et al., 1999; Vawter et al., 1999), synapsins (Browning et al., 1993), SNAP-25 (Young et al., 1998), complexins I and II (Sawada et al., 2005), and rab3a (Davidsson et al., 1999) provide more evidence of decreases in synapses. Abnormalities in the hippocampal architecture of schizophrenic patients have been observed (Arnold et al., 1997).

1.3.3 Cerebellum

The cerebellum has been primarily thought of as a coordinator of motor function. However, recent neurodevelopmental and neuroimaging studies imply a much greater role of the cerebellum in cortical function as well as potential involvement in schizophrenia (Andreasen et al., 1996; Andreasen and Pierson, 2008; Ichimiya et al., 2001; Weinberger et al., 1980). The cerebellum and the prefrontal cortex are the only two brain regions greatly enlarged in the humans as compared to other higher primates (Middleton and Strick, 1994) suggesting an involvement and coordination of the two regions in higher level thinking associated with humans. This hypothesis is supported by a positive correlation of intelligence and cerebellar volume in healthy individuals (Andreasen et al., 1993; Paradiso et al., 1997).

The cerebellum is proposed to be the "cognitive coordinator" through the cortico-cerebellar-thalamo-cortical circuit (Figure 1.3). Cerebellar atrophy has been shown to result in thought disorders and emotional disturbances (Schmahmann, 2004). Functional MRI showed involvement of the cerebellum in

cognition and linked schizophrenic deficits in cognition to this brain region (Honey et al., 2005). Working interactively with the cortex, cerebellum may help coordinate both motor and cognitive performance (Andreasen et al., 1996). Cerebellar involvement in coordination in part stems from the inhibitory Purkinje cells and the excitatory granule cells. Working together, the Purkinje and granule cells help to modulate and coordinate the activity of the cerebral cortex by providing input to deep nuclei such as the dentate nucleus. The deep nuclei, in turn, provide the sole output from the cerebellum to the cerebral cortex (Manto, 2009). Thus Purkinje cells have the important role of deciding what information is or is not returned to the cerebral cortex through inhibition of the output nuclei. Furthermore the Purkinje cells are implicated in schizophrenia because they display an eight percent reduction in size in schizophrenic patients (Katsetos et al., 1997; Tran et al., 1998). The observed Purkinje cell size reduction may be at least in part due to drug use as there was a significant correlation with antipsychotic drug dose (Tran et al., 1998).

Figure 1.3: The CCTCC pathway and alterations found within the pathway among schizophrenic patients primarily affected with positive and/or negative symptoms as compared to normal controls.
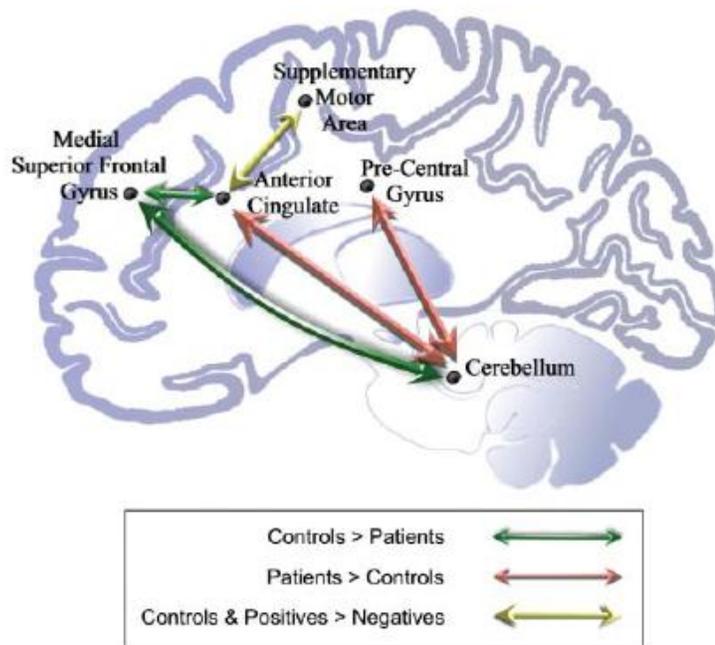
Taken from Honey (Honey et al., 2005)

1.4 Treatment of Schizophrenia

Schizophrenia drug discovery research, in large part, focused on addressing deficits in the dopaminergic and glutamatergic pathways. About sixty years ago, chloropromazine was one of the first generation typical antipsychotic and discovered by an accident as it was initially developed for surgical anesthesia but later found to be particularly effective in episodes of psychosis (Turner, 2007). Chloropromazine belongs to a group of drugs that share a common mechanism of action centered on blockade of dopamine D2 receptors (Snyder, 2006). Typical antipsychotics' affinity for the dopamine D2 receptor strongly correlates with their clinical potency (Kapur et al., 2000; Seeman et al., 1976). While the first generation antipsychotics are effective in reducing the positive symptoms they are associated with a propensity to cause extrapyramidal side effects (EPS), including tremor, rigidity, dystonia, bradykinesia and dyskinesia (Kurz et al., 1995; Peacock et al., 1996).

Second generation antipsychotics, including clozapine and olanzapine, also known as atypical antipsychotics have a more diverse pharmacological profile targeting for example several of the 5-HT receptors and their D2 affinity does not correlate as well with clinical efficacy (Kim et al., 2009). The atypical antipsychotics came about due to the need for reduction in EPS associated with the typical antipsychotics (Farah, 2005). As such the second generation antipsychotics have reduced risk for EPS but are associated with a greater risk for obesity, hyperlipidemia, and type II diabetes (Miyamoto et al., 2005). Despite the claims of better atypical efficacy, in a head-to-head comparison between perphenazine, a typical antipsychotic, and the newer atypical antipsychotics no major differences in efficacy or tolerability were found in schizophrenic patients (Geddes et al., 2000; Leucht et al., 2009; Lieberman et al., 2005). A notable exception to this finding was clozapine which has been shown to be effective in treatment resistant schizophrenics and particularly useful in targeting the negative symptoms (Davis et al., 2003; Kane et al., 1988; McEvoy et al., 2006). The observed effectiveness of clozapine may stem from its modulation of the glutamatergic system (Coyle and Tsai, 2004b), however its applicability is limited by agranulocytosis, or a decrease in number of white blood cells, a potentially

dangerous side effect (Alvir et al., 1993). In another comparative study, haloperidol, a typical antipsychotic was compared to several atypical drugs. Patients on haloperidol had significantly greater rate of discontinued treatment than atypicals but symptom reductions were the same in all groups suggesting that there may not be an advantage to atypical administration (Kahn et al., 2008). Similar findings were reported by Jones (Jones et al., 2006) where second generation antipsychotics excluding clozapine did not have the expected benefit over first generation antipsychotics.

Many patients fail to respond to current medications, are noncompliant due to adverse side effects, and even when the positive symptoms are treated the patients are for the most part still incapable of living a normal productive life (Browne et al., 1996; Conley and Buchanan, 1997; Fenton et al., 1997). It became apparent that schizophrenia may have to be treated on the basis of individual symptoms of cognitive impairment, negative symptoms and positive symptoms instead of treatment of the disorder as a whole (Lewis and Gonzalez-Burgos, 2006). Based on this fractional approach alternative targets to the D2 receptor became heavily researched including the glutamatergic system due to its likelihood of ameliorating negative and cognitive symptomology which have not been successfully addressed with either the typical or the atypical antipsychotics (as discussed in glutamate and schizophrenia section 1.2.2).

To facilitate and guide the development of cognitive enhancing antipsychotic agent in schizophrenia the National Institute of Mental Health (NIMH) Initiative, Measurement and Treatment Research to Improve Cognition in Schizophrenia (MATRICS) was designed. The MATRICS Consensus Cognitive Battery (MCCB) was one objective for the consortium which allows for an evaluation of key cognitive domains relevant to schizophrenia (Table 1.3).

Table 1.3: MATRICS Consensus Cognitive Battery

Speed of Processing
Category Fluency
Brief Assessment of Cognition in Schizophrenia (BACS) - Symbol-Coding
Trail Making A
Attention/Vigilance
Continuous Performance Test – Identical Pairs (CPT-IP)
Working Memory
Verbal:
Letter-Number Span
Nonverbal:
Wechsler Memory Scale (WMS) - III Spatial Span
Verbal Learning
Hopkins Verbal Learning Test (HVLT) – Revised
Visual Learning
Brief Visuospatial Memory Test (BVMT) – Revised
Reasoning and Problem Solving
Neuropsychological Assessment Battery (NAB) – Mazes
Social Cognition
Mayer-Salovey-Caruso Emotional Intelligence Test (MSCEIT) – Managing Emotions

Taken from http://www.matrics.ucla.edu

1.4.1 Advantages of allosteric modulation of ionotropic glutamate receptor

The advantage of a positive allosteric modulator (PAM) over an agonist is that it is unlikely to saturate the receptor with an allosteric modulator thus it is difficult to overdose and the receptor signal can be boosted under endogenous stimulation with a PAM instead of being continuously activated with an agonist (Yang and Svensson, 2008). Full agonists have been shown to de-sensitize receptors while enhancement of the endogenous signal is unlikely to play that role (Kinney et al., 2005). This is especially relevant with the NMDAR where direct and persistent stimulation was shown to result in excitotoxicity, seizures, memory loss, and brain damage (Lynch and Guttmann, 2001; Misztal et al., 1996; Wolf et

al., 1990). Finally PAMs are more likely to display better receptor subtype selectivity (Christopoulos and Kenakin, 2002).

NMDAR can be activated through PAMs on the NR1 subunit GMS. It has been shown that both glycine and D-serine are obligatory co-agonists of the NMDAR at the GMS (Curras and Pallotta, 1996; Dingledine et al., 1990). The NMDAR channel opens only when glycine/D-serine binds to the GMS on the NR1 subunit and simultaneously glutamate binds to the glutamate binding site on the NR2 subunit (Cull-Candy and Leszkiewicz, 2004; Curras and Pallotta, 1996). The combination of NR1 and NR2 subunits determines the affinity of glycine and D-serine. Both of the obligatory co-agonists have a ten-fold higher affinity for the NR2B, NR2C or NR2D over NR2A (Buller et al., 1994; Laurie and Seeburg, 1994; Matsui et al., 1995; Priestley et al., 1995). This selectivity over NMDAR subunits suggests that instead of targeting ubiquitously expressed NR2A, D-serine and glycine selectively target NMDAR subunits enriched during embryonic brain, and adult forebrain and cerebellum.

1.5 Genetics and Aetiology of Schizophrenia

In large part (~80%), schizophrenia is believed to be a heritable disease. Twin studies show that environment and epigenetic factors also influence the phenotype (Sullivan et al., 2003). Attempts to identify the genetics underlying schizophrenia have proven to be difficult. Given the apparent genetic complexity involved in schizophrenia the most promising approach to identify the most relevant genes may be genome-wide and hypothesis-free taking into account all brain regions and all genes. Such studies are likely to focus on regions most likely to host genes contributing to the manifestation of schizophrenia. In fact, hot spots were identified through meta-analyses of over 30 studies in chromosome regions 2p, 6p, 8p, 20p, 1q, 5q, 11q, 13q, 14p and 22q which may contain one or more risk genes (Badner and Gershon, 2002; Lewis et al., 2003). Since the above mentioned regions may each be encompassing multiple genes, association studies were undertaken to identify the most interesting candidates. Association is analysis of transmission of single-nucleotide polymorphisms (SNPs) within a gene in a family or a control sample but in itself SNP may not be causative.

Several putative susceptibility genes were identified through association studies (Table 1.4) and are supportive of the glutamate hypothesis. Contrary to these findings recent genome-wide assessment of SNPs and copy number variants (CNVs) concluded that very few schizophrenia patients share common genomic causative variants but instead very rare deleterious variants may be more important in schizophrenia predisposition (Need et al., 2009). CNVs tend to be unique to families and are unlikely to account for more then a few percent of schizophrenia (2008; O'Donovan et al., 2008).

Non-genetic factors including maternal starvation (Susser et al., 1996), maternal infections (Brown et al., 2000; Buka et al., 2001a; Buka et al., 2001b; Mednick et al., 1988), Rhesus blood-type incompatibility (Hollister et al., 1996), perinatal anoxic birth injuries (Rosso et al., 2000; Zornberg et al., 2000), obstetric complications (Geddes, 1999; Verdoux et al., 1997), season of birth (Torrey et al., 1996), and cannabis use in adolescence (Hall and Degenhardt, 2000; Veen et al., 2004) have all been shown to increase the risk of developing schizophrenia.

Individuals who went on to develop schizophrenia displayed subtle abnormalities in cognition, social interaction, motor function, and physical morphology prior to the onset of the disease suggesting that it is neurodevelopmental in nature (Niemi et al., 2003). The hypothesis takes into account both the genetic and the environmental factors into the most likely pathogenic model of schizophrenia. In this model, genetically predisposed individuals under the disadvantageous influence of environment beginning as early as *in utero* developed psychopathology which manifested most often between 15 and 24 years of age (Messias et al., 2007). Both negative and cognitive symptoms are less common and less severe in the early stages of schizophrenia but are more likely to become prominently manifested as the disorder advances suggesting a neurodevelopmental aspect (McGlashan and Fenton, 1993; Wyatt, 1991). The neurodevelopmental theory is further supported by brain imaging studies which showed a progressive enlargement of ventricles and reductions of cortical gray matter in schizophrenic patients (Davis et al., 1998; Gur et al., 1998; Shenton et al., 2001). The mechanism underlying the

observed phenotypic changes may be attributed to key schizophrenia genetic susceptibility factors such as NRG1 and DISC1 (Jaaro-Peled et al., 2009).

1.6 Astrocytic involvement in NMDAR activity

Astrocytes are proximally positioned to the synapse where they can participate in neurotransmission (Figure 1.4) by modulating neurons (Schousboe, 2003). Astrocytes express many key enzymes and transporters associated with maintaining glutamate, glycine and D-serine synaptic levels for optimal stimulation of the glutamate receptors. Astrocytes provide glutamine for glutamate synthesis at the synaptic terminal, express EAAT1 and 2, the two glutamate transporters which protect against excitotoxicity by inactivating synaptic glutamate (Schluter et al., 2002). The glycine transporter1 (GlyT1) responsible for synaptic glycine regulation (Zafra et al., 1995), serine racemase (SRR), which synthesizes D-serine and DAO, which breaks down D-serine have all been localized to astrocytes (Harrison and Weinberger, 2005; Kirkpatrick et al., 2001; Schell, 2004; Wolosker et al., 1999a). Presynaptic mGluR3, responsible for down regulating glutamate release is activated by NAAG (Wroblewska et al., 1997). NAAG, in turn is degraded by glutamate carboxypeptidase II (GCP II) which is concentrated in astrocytes (Berger et al., 1999). Astrocytes are the source of kynurenic acid, an endogenous competitive antagonist of the NMDAR at the glycine site (Jentsch and Roth, 1999). This evidence suggests that astrocytes sense the level of synaptic activity and augment synaptic activity by release of neuromodulators (Haydon, 2001; Volterra and Meldolesi, 2005).

Table 1.4: Candidate schizophrenia susceptibility genes

Gene	Locus	Association with Schizophrenia	Linkage to gene locus
COMT	22q11	++	++++
DTNBP1	6p22	+++++	++++
NRG1	8p12-21	+++++	++++
RGS4	1q21-22	+++	+++
GRM3	7q21-22	+++	+
DISC1	1q42	++++	++
DAOA(G72/G30)	13q32-34	+++	++
DAO	12q24	++	+
PPP3CC	8p21	+	++++
CHRNA7	15q13-14	+	++
PRODH2	22q11	+	++++
AKT1	14q22-32	+	+
GAD1	2q31.1	++	
ERBB4	2q34	++	
FEZ1	11q24.2	++	
MUTED	6p24.3	++++	++++
MRDS1(OFCC1)	6p24.3	++	++++
NPAS3	9q34	++	
GRIK4	11q23	++	+

Adapted from Straub (Straub and Weinberger, 2006). Many of the identified genes are relevant to glutamate hypothesis. COMT, Catechol-*O*-methyl transferase; DTNBP1, dysbindin; NRG1, neuregulin; RGS4, regulator of G-protein signaling; GRM3, metabotropic glutamate receptor 3; DISC1, disrupted in schizophrenia 1; DAOA (G72/G30), D-amino acid oxidase activator; PPP3CC, calcineurin gamma catalytic subunit; CHRNA7, alpha7 nicotinic acetylcholine receptor; PRODH2, proline dehydrogenase; AKT1, V-akt murine thymoma viral oncogene homolog 1; GAD1, glutamate decarboxylase 1; ERBB4, V-erb-a erythroblastic leukemia viral oncogene homolog 4; FEZ1, elongation protein zeta-1; MRDS1, orofacial cleft 1; NPAS3, neuronal PAS domain protein 3; GRIK4, glutamate receptor, ionotropic, kainate 4.

In addition to expressing key enzymes, in an eloquent study, astrocytes were shown to modulate neuronal activation via altering level of neuronal ensheathing. NMDAR transmission in the supra-optic nucleus is dependent on astrocytic coverage of the synapse (Panatier et al., 2006). During lactation, astrocytic ensheathing of neurons is reduced in the supra-optic nucleus resulting

in reduced NMDAR activation as compared to the virgin rats. This reduced NMDAR activation was shown to be due to reduced D-serine release from the astrocytes (Panatier et al., 2006). This data solidified an astrocytic role in postsynaptic control of excitatory neurotransmission by releasing D-serine.

Figure 1.4 Electron micrograph (EM) showing the close association of astrocytes (blue) with the presynaptic axonal bouton (green) and postsynaptic dendrytic spine head (yellow) at the synapse in hippocampus of a mature rat. Taken from Witcher (Witcher et al., 2007).
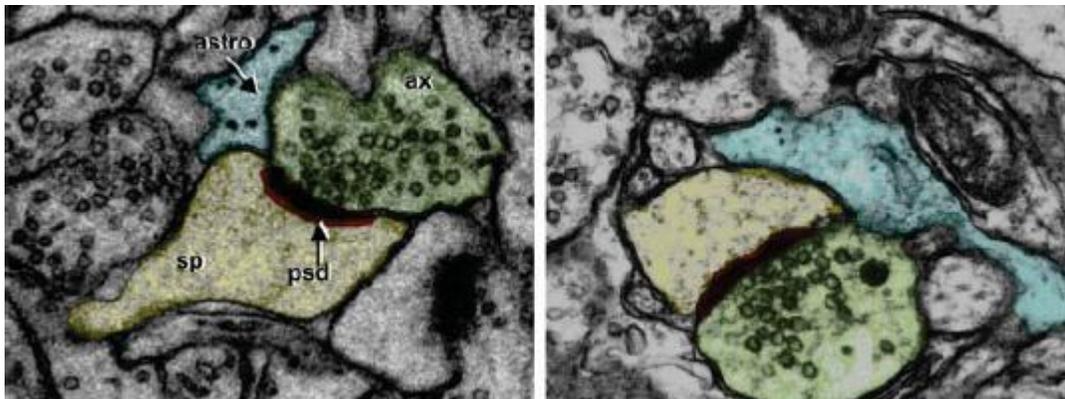
1.7 D-Serine: the NMDAR obligatory co-agonist

D-serine was thought of as an amino acid solely of bacterial origin so its presence in substantial quantities of about 300 nmol g^{-1} in the mammalian (Hashimoto et al., 1992; Hashimoto et al., 1993b; Hashimoto et al., 1993c; Hashimoto et al., 1995a; Hashimoto et al., 1995b) and about 100 nmol g^{-1} in human brain (Chouinard et al., 1993; Hashimoto et al., 1993a; Kumashiro et al., 1995; Nagata et al., 1995) was initially surprising. D-serine was also thought not to play a functional role in higher organisms (Corrigan, 1969) yet displacement of [^{3}H]glycine by D-serine on the rat brain NMDARs (McDonald et al., 1990) sparked interest in the physiological role of D-serine in the human brain. Recombinant NMDARs were found to be stimulated by D-serine application (Hess et al., 1996; McBain et al., 1989; Priestley et al., 1995) suggesting that D-serine may act as an NMDAR activator *in vivo*. Furthermore, application of

exogenous DAO reduced NMDAR function *in vivo* and *in vitro* (Gustafson et al., 2007; Mothet et al., 2000; Stevens et al., 2003; Yang et al., 2005).

D-serine is found at much higher concentrations in the brain than it is in the periphery (Wolosker et al., 2008), for example, in the brain for every two L-serine molecules there exists one D-serine molecule (Hashimoto et al., 1992; Hashimoto et al., 1993c). Brain microdialysis experiments revealed extracellular concentration of D-serine to be twice that of glycine in the striatum and comparable in the cerebral cortex (Hashimoto et al., 1995b). D-serine is enriched in rat forebrain areas abundant in NMDARs (Hashimoto et al., 1993a; Schell et al., 1997; Schell et al., 1995). Despite the high D-serine concentration the NMDAR were found not to be saturated *in vivo* (Wood et al., 1989) because exogenously applied D-serine to rat cortical (Li and Han, 2007) and hippocampal slices (Martina et al., 2003) potentiated NMDARs.

D-serine was found to display up to threefold higher affinity for the NMDAR than glycine (Furukawa and Gouaux, 2003; Matsui et al., 1995). Through crystal structure examination it was noted that D-serine displaces a water molecule from the NR1 binding site and makes three additional hydrogen bonds than glycine explaining the higher D-serine affinity for NMDAR (Furukawa and Gouaux, 2003). Furthermore, the L-serine isomer interacts unfavorably in the binding pocket due to the hydroxyl group specifically selecting for the D-serine isomer (Furukawa and Gouaux, 2003). These bidning affinities and structural observations are consistent with experiments showing that D-serine is 100x more effective than L-serine in stimulating NMDAR (McBain et al., 1989; Wood et al., 1990).

The model for NMDAR activation is through a cascade initiated by neuronal glutamate release which stimulates AMPA/Kainate receptors on glial cells to release D-serine from glia (Kim et al., 2005; O'Brien and Bowser, 2006). D-serine, in turn, acts as the co-agonist on the strychnine-insensitive GMS on the NR1 subunit to enhance NMDAR functional flux of Ca^{2+} current through the ionic pore. The Ca^{2+} influx mediates learning and memory, long-term changes in synaptic plasticity and neural development (Oliet and Mothet, 2006).

In vivo data from rodents is supportive of D-serine modulatory effects on the NMDAR. In rats the cognitive impairment induced by PCP could be reversed by treatment with D-serine (Andersen and Pouzet, 2004) while fMRI experiments in rats showed that administration of D-serine leads to an increase in hippocampal activity (Panizzutti et al., 2005). D-serine from glial cells seems to play a role in synaptic plasticity because synapses with reduced astrocytic coverage showed less NMDA-dependent activity and this activity could be restored by D-serine addition (Panatier et al., 2006) as discussed earlier.

1.7.1 Schizophrenia and D-serine

Multiple publications suggest deficits in D-serine levels in schizophrenia. Serum levels of D-serine in schizophrenic patients were significantly lower than those of healthy controls (Hashimoto et al., 2003). Schizophrenic CSF samples displayed reduced D/total (D+L) serine, but not D-serine levels per-se as compared with control subjects (Hashimoto et al., 2005b). Complementary to this observation was a significant 25% decrease in CSF D-serine levels in schizophrenia patients versus healthy control subjects (Bendikov et al., 2007). However, some studies did not correlate initial observations of altered D-serine plasma and CSF levels (Fuchs et al., 2008; Hons et al., 2008). While CSF and serum D-serine concentrations were found to be inconsistent, brain tissue D-serine concentration has been found to be unaltered (Bendikov et al., 2007; Hashimoto et al., 2003). However, there was a significant positive correlation between serum D-serine levels and total scores, positive symptom scores, and negative symptom scores on the BPRS among medicated patients (Hashimoto et al., 2003)**.**

Since schizophrenic patients may have decreased brain D-serine levels, their antipsychotic medications were supplemented with D-serine treatment resulting in psychotic symptom reductions. Chronic schizophrenia patients, poorly responsive to neuroleptics other then clozapine, with prominent negative symptoms were treated with administration of adjunct 30 mg/kg/day of D-serine. After six weeks of treatment the patients displayed significant reductions in negative symptoms, cognitive symptoms and positive symptoms. The serum D-

serine levels of patients were elevated 50-fold while serum glycine, glutamate, and aspartate levels were unchanged. The broad improvement of the symptoms significantly correlated with the treatment and with the serum D-serine levels (Tsai et al., 1998) (see Table 1.2). These clinical trials strongly suggest potential of NMDAR enhancement through D-serine administration as suitable adjunct treatment of schizophrenic symptoms. A meta analysis of eighteen clinical trials with 343-randomized patients confirmed that D-serine is effective in reducing negative symptoms and trends toward effectiveness in cognitive symptoms (Tuominen et al., 2005).

The clinical data with D-serine supplementation generated interest in proteins responsible for D-serine synthesis, transport and degradation. As such serine racemase, alanine-serine-cysteine transporter-1 and DAO will be described individually in the next section where their impact on D-serine will be assessed.

1.7.2 D-serine synthesis: Serine racemase (SRR)

Serine racemase (SRR) is a 37 kDa protein that exhibits a high degree of interspecies similarity (92% identity between rat and human and 96% identity between rat and mouse) (Konno, 2003). While multiple mRNAs have been proposed to encode SRR, only a single isoform appears to be expressed in the brain (Wolosker et al., 1999b; Xia et al., 2004; Yamada et al., 2005). SRR can inter-convert L-serine to D-serine with a six fold higher preference for conversion of L- to D-form (Wolosker et al., 1999b). Furthermore, SRR is highly selective toward L-serine as it fails to racemize other amino acids (Wolosker et al., 1999b). Regional localization of SRR coincides with that of D-serine suggesting a physiological role for D-serine synthesis (Wolosker et al., 1999a). An *in vivo* role of serine racemase and its involvement in D-serine synthesis came from SRR knockout animals where the D-serine levels declined by 80-90% (Wolosker et al., 2008). As expected, the SRR homozygous knockout mice displayed decreased NMDAR transmission, impaired long term potentiation of synaptic activity in the hippocampus, attenuated synaptic plasticity and spatial memory deficit (Basu et al., 2009; Wolosker et al., 2008). Recently an association between SRR and schizophrenia was found reinforcing the association of this enzyme in this

devastating disease (Labrie et al., 2009a). SRR expression data from schizophrenic patients is mixed. For example, SRR protein levels in schizophrenic patients were found to be marginally lower in the frontal cortex (BA9) and in the hippocampus (Bendikov et al., 2007). However, in a separate study, SRR immunoreactivity was increased in schizophrenia in the DLPFC but not in cerebellum, while SRR mRNA was unchanged in both regions (Verrall et al., 2007). More comprehensive SRR expression analysis is required to determine if SRR expression is linked to modified D-serine levels.

Several cofactors and modulators of SRR have been identified. The purified SRR enzyme requires cofactor pyridoxal 5'-phosphate (Wolosker et al., 1999b) and ATP that is not hydrolyzed during SRR activation (De Miranda et al., 2002). Interestingly, phosphatidylinositol (4,5)-bisphosphate (PIP2) competes with ATP for SRR binding resulting in physiological inhibition of the catalytic activity (Mustafa et al., 2009). The PIP2 inhibition has served as a bridge linking glutamate release with an increase in D-serine synthesis. The mechanism of this coordinated action was shown to be mediated through metabotropic glutamate transmission via mGluR5 which upon activation stimulates phospholipase C, degrades PIP2 and disinhibits serine racemase (Mustafa et al., 2009). NMDAR-mediated calcium entry into postsynaptic neurons may contribute to SRR inhibition through activation of calcium/calmodulin-dependent neuronal nitric oxide synthase and generation of nitric oxide (Baumgart and Rodriguez-Crespo, 2008). The nitric oxide, in turn, nitrosylates SRR in the ATP-binding region and inhibits SRR catalytic activity. Coincidentally, nitric oxide activates DAO activity further suppressing D-serine concentration (Shoji et al., 2006a; Shoji et al., 2006b). Thus ATP binding or lack there of plays a significant role in SRR activity modulation. Serine racemase is also positively modulated by divalent cations like Mg^{2+}, Mn^{2+} and Ca^{2+} (Cook et al., 2002; Neidle and Dunlop, 2002) while, glycine and L-aspartic acid metabolites such as asparagine and α,β-threo-3-hydroxyaspartic acid were found to competitively inhibit SRR (Dunlop and Neidle, 2005; Strisovsky et al., 2005). A yeast two-hybrid screen identified glutamate-receptor-interacting protein (GRIP), a scaffolding protein for AMPA receptors as SRR interactor. GRIP has been recognized as SRR activator leading

44

to a five-fold greater D-serine synthesis (Kim et al., 2005). Furthermore, activation of AMPA receptors increases SRR activity probably through dissociation of GRIP from activated AMPAR enabling AMPA neurotransmission to enhance D-serine synthesis and release (Kim et al., 2005).

SRR has also been shown to have an additional function. SRR was found to generate pyruvate and ammonia via α,β-elimination of water from L-serine. In fact the SRR elimination activity is stronger than racemization activity resulting in a synthesis of three pyruvate molecules per each D-serine molecule racemized (Strisovsky et al., 2003). The dual functionality of the SRR is likely to be influenced by the cellular needs. For example, the complex of ATP and Mg^{2+} was found to favor the elimination activity over the racemization activity (Foltyn et al., 2005). The resulting pyruvate can be used for lactate synthesis which is known to provide neuroprotection against oxidative stress and used for neuronal energy needs (Foltyn et al., 2005). D-serine was also shown to undergo α,β-elimination suggesting an alternative pathway for D-serine catabolism from that of DAO enzymatic breakdown (Foltyn et al., 2005).

SRR has a critical function in regulation of D-serine concentration. The modulation of SRR activity through the various protein interactions is a testament to the critical role SRR has in balancing D-serine levels. Association and behavioral studies further support SRR involvement in NMDAR hypofunction disease suggesting that SRR may have a relevant role in schizophrenia.

1.7.3 D-serine uptake: alanine-serine-cysteine transporter-1 (Asc-1)

The activity of the multi transmembrane-spanning amino acid uptake transporter of small neutral amino acids (Ala, Ser, Cys), Asc-1, has been shown to be a major mechanism for D-serine clearance from the extracellular space in forebrain and cerebellum. Asc-1 has been cloned from mouse (Fukasawa et al., 2000) and human (Nakauchi et al., 2000) and localized to presynaptic terminals, dendrites, and soma of neurons and glia where it could have the most impact on D-serine clearance from the synaptic cleft. It operates via an exchange mechanism where upon uptake of one amino acid there is an efflux of another (Fukasawa et al., 2000; Helboe et al., 2003; Matsuo et al., 2004; Nakauchi et al.,

2000). Convincing data for a key role for Asc-1 in D-serine regulation comes from experiments in Asc-1 knockout mice which show that [³H]D-serine uptake in forebrain synaptosomes is significantly reduced (Rutter et al., 2007). Furthermore, the Asc-1 knockout animals had elevated circulating D-amino acids, including D-serine, in the brain (Rutter et al., 2007). In fact, the elevated level of brain circulating D-serine may have lead to the seizure-propensity of these animals through over activation of the NMDAR (Xie et al., 2005). Administration of MK-801 to the KO animals significantly reduced the seizures suggesting that they were due to excessive NMDAR stimulation (Xie et al., 2005).

Interestingly, Asc-1 immunoreactivity was found to be decreased in schizophrenic DLPFC and cerebellum independent of drug treatment (Burnet et al., 2008b) suggesting that the NMDAR hypofunction is not due to excessive reuptake. Furthermore it may be a compensatory effect in response to reduced D-serine concentration found in schizophrenics.   However, decreased Asc-1 expression may not be necessary or sufficient for altered transporter activity (Aragon and Lopez-Corcuera, 2003; Zahniser and Doolen, 2001).   Although protein expression has been shown to be reduced, the same brain regions did not display a complementary decrease in Asc-1 mRNA suggesting that translational or post-translational modifications are responsible for the reduced protein expression (Burnet et al., 2008b).

1.7.4 D-serine degradation: D-amino acid oxidase (DAO)

Human DAO is 347 amino acids long protein (Momoi et al., 1988) encoded by a single gene found on chromosome 12 (Konno, 2001). It is composed of 11 exons and spans 20 kb (Fukui and Miyake, 1992). DAO is a flavoenzyme oxidase whose main function is degradation of certain D-amino acids selectively targeting those with small, neutral side chains such as D-serine and D-alanine (Leighton et al., 1968) with affinity (Km) of 1 to 10 mM (Kawazoe et al., 2007; Molla et al., 2006). The amino acids are degraded into imino acid and consequently into α-keto acids through hydration (Figure 1.5) (Pollegioni et al., 2007). During the amino acid oxidation the flavin adenine dinucleotide (FAD) is reduced which upon reoxidation generates hydrogen peroxide. FAD

may play a relevant role in modulating DAO's activity as it was observed that FAD-unbound DAO may be catalytically inactive (Caldinelli et al., 2009). In humans, FAD is weakly bound to DAO suggesting a mechanism for DAO regulation (Caldinelli et al., 2009).

DAO has been detected in kidney, liver, brain and at low concentration in leukocytes (Cline and Lehrer, 1969; Robinson et al., 1978), small intestine, epididymis (Gossrau, 1991), and preputial and adrenal glands (Goldenberg et al., 1975). Within the central nervous system of rats, DAO has been shown to be more abundant in the cerebellum and brainstem then in the forebrain (Horiike et al., 1994). While rat DAO was initially exclusively localized to astrocytes but not other glial cells or neurons (Arnold et al., 1979; Horiike et al., 1987) it was later found in humans and rats to be expressed in both neuronal and glial cells (Moreno et al., 1999; Verrall et al., 2007). However, human DAO regional expression differences were noted including predominant neuronal expression in DLPFC, and hippocampus, predominant glial in cerebellum and both neuronal and glial in substantia nigra pars compacta (Verrall et al., 2007). Furthermore, DAO expression is likely to be neurodevelopmentally regulated as kidney DAO activity is low at birth but reaches a maximum in 2-4 week old rats (Johkura et al., 1998; Stefanini et al., 1994). Likewise, a similar pattern of DAO expression was observed in the rat cerebellum where at birth no detectable DAO activity was found but by 3-4 weeks of age mice were expressing DAO at maximum levels (Wang and Zhu, 2003).

On a cellular level, DAO was first reported to be localized within peroxisomes (De Duve and Baudhuin, 1966). While in the periphery DAO has been confirmed to be confined to the peroxisomes in rat liver through enzymatic histochemical, immunohistochemical and electron microscopy imaging (Angermuller and Fahimi, 1988; Stefanini et al., 1985; Usuda et al., 1986) the brain expression may not be limited to this organelle. This observation is supported by a pericellular immunostaining of DAO brain samples from DLPFC, cerebellum, and hippocampus (Verrall et al., 2007) and lack of DAO expression overlap with peroxisomal markers (Sacchi et al., 2008). A pericellular distribution, potentially outside of the peroxisome, suggests that DAO may be

able to directly influence how much D-serine is being released perhaps into the synapse. The proposed mode for the altered DAO expression outside of the peroxisome is proteolysis of the peroxisomal targeting area from the c-terminal end of DAO (Campaner et al., 1998; Pollegioni et al., 1995) which in case of porcine (Tarelli et al., 1990) and yeast DAO (Yurimoto et al., 2000) have been shown to yield active DAO enzymes. An expression profile outside of the peroxisome may have very important consequences for the proposed interaction study as it exposes DAO to an alternative set of putative interacting proteins. An extra-peroxisomal localization also suggests an altered function or regulatory role for DAO which may be derived from the interactor study.

In schizophrenic patients where decreased levels of D-serine were reported DAO may exacerbate the NMDAR hypofunction (Bendikov et al., 2007; Hashimoto et al., 2003). In fact, DAO mRNA was increased in patients with schizophrenia as compared to control individuals while DAO immunoreactivity in the cerebellum showed a trend to being increased in schizophrenic patients (Verrall et al., 2007). In the DLPFC, where DAO is expressed to a lesser extent than in the cerebellum, DAO mRNA was unchanged in schizophrenia (Verrall et al., 2007). Furthermore DAO activity was increased as much as two-fold in the cerebellum in schizophrenia and DAO activity increased with duration of illness (Burnet et al., 2008a; Burnet et al., 2008b; Madeira et al., 2008). Hippocampa CA4 DAO mRNA levels were found to be increased in schizophrenic patients (Habl et al., 2009). Consistently with the increased mRNA expression, hippocampal DAO protein levels in schizophrenics significantly correlated with duration of illness but not with age, suggesting the possibility that increased breakdown of hippocampal D-serine is associated with the progressive nature of the severity of schizophrenia (Bendikov et al., 2007). DAO levels were unaltered in antipsychotic treated animals suggesting that the duration of illness correlation study is independent of drug use (Verrall et al., 2007).

Figure 1.5 Schematic diagram of d-amino acid catalyzed by DAO.
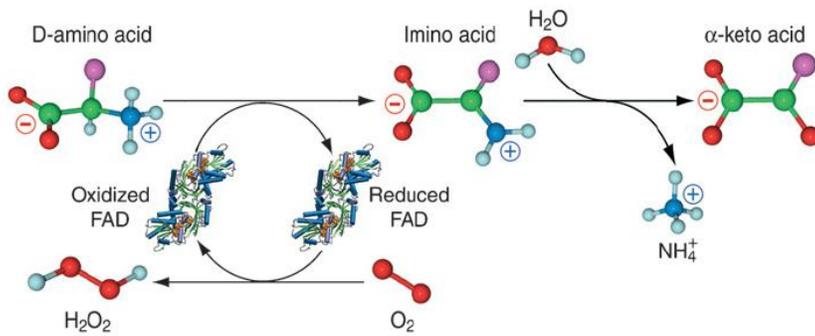
Taken from Pollegioni (Pollegioni et al., 2007)

In addition, a mutant mouse line has been important for looking at DAO function *in vivo*. This naturally occurring strain of mice with an inactive DAO enzyme (Konno and Yasumura, 1983) due to a glycine 181 to arganine mutation (Sasaki et al., 1992) has been identified but the expression of the inactive enzyme was found not to be altered in the mutated strain versus wildtype (Konno et al., 1991). These mice were examined for D-amino acid levels and compared to the wildtype mice. D-serine concentrations were largely unchanged in most brain regions tested including cerebrum and hippocampus, while, it was increased about ten-fold in the cerebellum and medulla oblongata. More interestingly, D-alanine, a good DAO substrate (D'Aniello et al., 1993), levels in the mutant mice were elevated on average four-fold in all seven brain regions tested. Increased D-alanine concentration was also found to be elevated fifteen fold in the mutant mice serum suggesting that catalytically inactive DAO throughout the body contributed to the increased D-alanine concentration by allowing for accumulation of D-alanine (Hamase et al., 2005). The increased D-alanine levels in DAO mutant mice may be relevant to the disease state in schizophrenia as D-alanine was found to act as an NMDAR co-agonist (Sakata et al., 1999; Tanii et al., 1994). The concentration of D-aspartate, known to be oxidized by D-aspartic acid oxidase (DDO) and not DAO, was not altered in the mutant mice (Hamase et al., 2005) suggesting that there are no compensatory changes in the mutant mice.

Mice lacking the DAO catalytic activity displayed diminution of stereotypy and ataxia elicited by MK-801 compared with wild-type mice

(Hashimoto et al., 2005a). Independently another group confirmed the observed increased occupancy of the NMDAR GMS as shown by attenuated effects of L-701,324, a NMDAR glycine site antagonist in the DAO mutant mice (Almond et al., 2006). DAO KO mice display enhanced spatial learning and long-term potentiation (LTP) in the hippocampus (Maekawa et al., 2005) suggesting that the increased D-serine/D-alanine levels at the NMDAR GMS could have contributed to enhanced behavioral responses relevant to schizophrenia. This suggestion was confirmed by pharmacologically blocking NMDAR in wildtype mice and reversing schizophrenia-like behaviors including hyperlocomotion, stereotypy, and ataxia through D-serine/D-alanine administration (Tanii et al., 1994). Double mutant mice, with the DAO mutation and NR1 aspartate 481 to asparagine mutation, which is characterized by a reduction in NMDAR glycine affinity, were found to outperform single mutant NR1 mice in tasks related to negative and cognitive symptoms of schizophrenia (Labrie et al., 2009b). Taken together, these animal data suggest that DAO may play a role in NMDAR regulation and pharmacological inhibition of DAO may be therapeutically relevant for schizophrenia.

Due to the evidence of DAO involvement in schizophrenia pharmacological inhibitors including AS057278 (5-methylpyrazole-3-carboxylic acid), CBIO (6-chlorobenzo[d]isoxazol-3-ol) and Merck Compound 8 (4H-thieno[3,2-b] pyrrole-5-carboxylic acid) were developed and tested in animal behavioral models (Hashimoto et al., 2009; Marino et al., 2008; Smith et al., 2009). All three compounds were found to increase peripheral and CNS D-serine levels with the exception of CBIO which only raised peripheral D-serine level (Williams, 2009). AS057278 was found to acutely and chronically normalize PPI in PCP induced mice and chronic but not acute PCP induced hypercolomotion (Marino et al., 2008). CBIO was found to potentiate D-serine attenuation of MK-801 induced PPI deficits (Hashimoto et al., 2009). When treated acutely with Merck Compound 8 rats displayed no effect in amphetamine-induced psychomotor activity, nucleus accumbens dopamine release, or a MK-801 induced deficit in novel object recognition (Smith et al., 2009). Pharmacological inhibition of DAO provides a mixed support for the therapeutic mechanism

inhibition of DAO in vivo at least when acutely treated but together with the DAO point mutant mice data, suggest that chronic DAO inhibition may be a suitable treatment alternative.

1.7.4.1 G72 and DAO protein-protein interaction suggests DAO involvement in schizophrenia

Considerable evidence exists for association of a molecule known as D-amino acid oxidase activator (DAOA), or G72, and schizophrenia. Association of G72 to schizophrenia was first demonstrated by Chumakov through high-density mapping of SNPs to a chromosome 13q region which is linked to schizophrenia (Chumakov et al., 2002). Markers in the 3' region of G72 such as M23 (rs3918342) and M24 (rs141292) were found to be particularly strongly linked to schizophrenia (Chumakov et al., 2002). Subsequent association studies have in most cases confirmed the association in a wide range of populations including, for example, Palestinian Arabs, Chinese, Scottish, and German subjects (Korostishevsky et al., 2006; Liu et al., 2006; Ma et al., 2006; Mulle et al., 2005; Schumacher et al., 2004; Wang et al., 2004; Zou et al., 2005). Furthermore, meta-analysis of association studies concluded that genetic variation in G72 and in particular in M23/M24 region supports schizophrenia association (Detera-Wadleigh and McMahon, 2006; Li and He, 2007; Shi et al., 2008). Likewise DAO has been shown to be associated with schizophrenia (Corvin et al., 2007; Liu et al., 2004; Schumacher et al., 2004; Wood et al., 2007) albeit weakly as a recent meta-analysis of 18 association studies found a significant DAO association in three of them (Shi et al., 2008).

Interest in DAO as a schizophrenic candidate gene grew as a direct consequence of identification of DAO as an interacting partner for G72 (Chumakov et al., 2002). Initially, through yeast-two-hybrid screen DAO was shown to interact with G72 and purified G72 increased the catalytic activity of DAO *in vitro* (Chumakov et al., 2002). This modulation, in turn, was hypothesized to be responsible, in part, for a lower D-serine concentration and consequently NMDAR hypoactivity. In contrast to the initial observations, it was reported that G72 does not bind with DAO (Kvajo et al., 2008). However, others

have since suggested that G72 inhibits DAO activity *in vitro* and *in vivo* when both G72 and DAO are overexpressed in U87 cells (Pollegioni et al., 2007; Sacchi et al., 2008). An interaction between the two proteins *in vivo* is likely as DAO was shown to co-immunoprecipitate with G72 from human cortex and both proteins were shown via immunohistochemistry to co-localize in cortical astrocytes slices from human brain (Sacchi et al., 2008). The proposed inhibitory activity of G72 on DAO may be relevant to NMDAR hypofunction if in the schizophrenic brain G72 is down regulated (Sacchi et al., 2008). While G72 expression in the dorsolateral prefrontal cortex of schizophrenia patients was shown to be increased in one study (Korostishevsky et al., 2004), G72 mRNA and protein from schizophrenic and control human brains were not quantifiable in another (Benzel et al., 2008). Taken together, the reported observations made it difficult to propose a satisfying explanation for the involvement of the two proteins in schizophrenic brain. Conflicting data in terms of the interaction, functional implication for such an interaction and the level of G72 expression *in vivo* has been used to question the validity and proposed implications of this interaction.

As G72 is only found in anthropoid primates (Chumakov et al., 2002), G72 overexpressing transgenic mice were generated in order to test behavioral changes associated with G72 expression (Otte et al., 2009). Interestingly, the mice were found to have impaired sensorimotor gating which was normalized with haloperidol treatment. Sensorimotor gating enables the organism to filter external information and was found to be impaired in schizophrenia (Braff et al., 2001). They were also more sensitive to PCP treatment suggesting NMDAR hypofunction in the transgenic mice or altered receptor expression. It remains to be seen whether DAO activity is altered in the transgenic animals and if the behavioral abnormalities are result of altered D-serine concentration.

1.8 Objectives and aims of this thesis

NMDAR hypofunction has been implicated through NMDAR antagonist studies, GMS pharmacological intervention studies, postmortem studies, DAO transgenic animal characterization and genetic studies as a significant contributor

to schizophrenia pathology. One way to restore NMDAR hypofunction is to increase the concentration of NMDAR co-agonists such as D-serine. In fact, this obligatory co-agonist has been shown to be reduced in schizophrenic patients' CSF and serum which may be a function of increased DAO activity. Supporting this hypothesis are findings of increased DAO activity in schizophrenic patients which is possible due to an increased DAO expression or potentially changes in activating pattern.

While DAO linkage and association studies had mixed results they were mostly suggestive of no linkage between DAO and schizophrenia. Yet G72, the putative DAO interactor, through positive linkage with schizophrenia implicates DAO in the disease. A case for DAO is somewhat like that for NMDAR which in itself did not genetically associate with schizophrenia yet many of the genes that do are modulators of the NMDAR. Through characterization of DAO interacting proteins we aim to increase our understanding of DAO function, biology and to identify novel schizophrenia targets. We hope to ascertain DAO's intracellular localization and the mechanism responsible for its presence outside of the peroxisome. Furthermore, we will explore the potential DAO interacting proteins for a modulatory role on DAO enzymatic activity resulting in the schizophrenic phenotype.

As part of our studies we set out to expand upon and identify additional potential DAO interacting proteins. To do this, two independent approaches were undertaken; a yeast-two-hybrid screen against a human fetal brain library using DAO as the bait protein and an immunoprecipitation mass spectroscopy approach from rat cerebellum. While the yeast-two-hybrid screen identified fifteen putative interactors, the samples generated from rat cerebellar co-immunoprecipitation against DAO antibody resulted in identification of twenty-four proteins likely to be interacting with DAO directly or through association of a complex of proteins one or more of which were interacting with DAO. In this thesis I will outline and describe novel DAO interacting proteins with an emphasis on DAO's interaction with BSN, a presynaptic active zone member, and suggest a novel DAO localization as a result of this interaction which is likely to be relevant in

monitoring synaptic D-serine concentrations and in understanding more fully the role of DAO in disease.

2. Generation of a DAO stable cell line and purification of DAO protein from bacterial cells

This chapter will focus on establishing tools necessary for validation of putative DAO interacting proteins and measuring functional effects they may have on DAO activity. An AmplexRed functional assay was established to ascertain the implications of interacting proteins on DAO's activity. Both hDAO and rDAO stable lines were established as well as purified hDAO enzyme to allow for *in vitro* experiments with putative interacting proteins.

2.1 AmplexRed functional assay for analysis of DAO activity

To ascertain the activity of DAO either in a stable cell line or as a purified enzyme and to enable the examination of the impact of DAO interacting proteins on the enzymatic activity of DAO, an in vitro assay was required. DAO catalyzes the degradation of D-amino acid substrates such as D-serine or D-alanine by oxidative deamination, yielding reaction products including pyruvate, ammonia (NH_3) and hydrogen peroxide (H_2O_2) (Pollegioni et al., 2007) (Figure 2.1). For each substrate molecule that DAO degrades, one molecule of hydrogen peroxide is released. In order to measure the production of substrates, a coupled reaction in which the hydrogen peroxide was utilized by horseradish peroxidase (HRP) in a one-to-one stoichiometric ratio converts Amplex Red (10-acetyl-3,7-dihydroxyphenoxazine), a non-fluorescent substrate, into resorufin, a red-fluorescent (544 nm excitation, 590 nm emission) product (Zhou et al., 1997). Thus, this assay is dependent on the activity of two enzymes, DAO and HRP, and the fluorescent signal is directly proportional to the rate at which DAO deaminates D-serine/D-alanine as illustrated in Figure 2.1. Should an interactor alter DAO configuration or modify substrate access to the catalytic site, the rate of reaction may be altered and measured using the Amplex Red assay.

Figure 2.1: Amplex Red assay measures the production of resorufin, a fluorescent molecule. DAO catalyzes the oxidative deamination of D-amino acids including D-alanine into pyruvate, ammonia and hydrogen peroxide. In the presence of horseradish peroxidase (HRP) the Amplex Red substrate (10-acetyl-3,7-dihydroxyphenoxazine) reacts with hydrogen peroxide with a one to one stoichiometry to produce resorufin, a fluorescent product. The rate of resorufin production is proportional to the D-alanine deamination reaction rate.
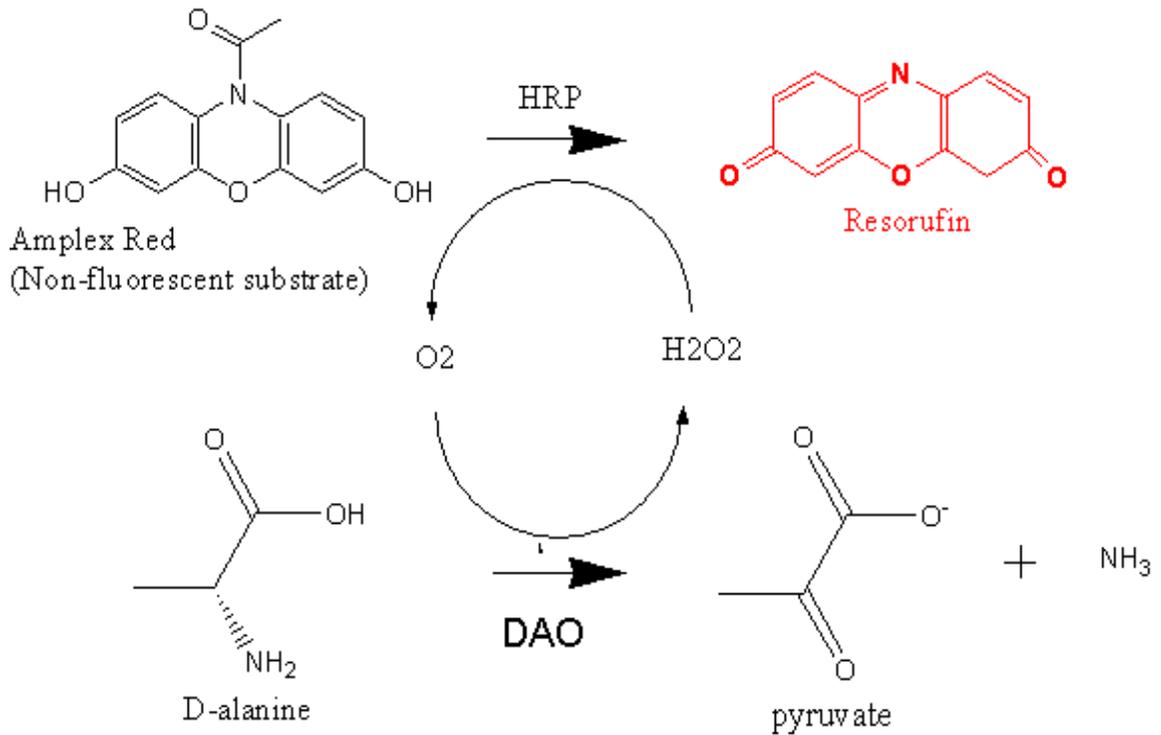
2.2 Selection of host cell type line for the DAO stable lines

In order to enable the assessment of DAO activity in a cellular context, ten host cell lines were considered for the generation of human and rat DAO stable cell lines. All of the lines were first examined in the Amplex Red assay with D-serine, D-aspartate and with no substrate and compared to signal generated without any cells (Figure 2.2) in order to choose a host cell line with the best signal to noise ratio and to identify lines that may already be expressing native DAO or D-aspartate oxidase (DDO), which shares a high homology with DAO sequence. In this respect, no substrate was used as negative control while D-aspartate as the substrate for DDO. Human embryonic kidney (Hek293) cells were selected as the line of choice as they produce the best balance of useful properties as they are readily adaptable to generation of stable cell line and had a low basal response in buffer as well as with treatment of D-serine and D-aspartate. While clonal rat pituitary tumor (GH4C1) cells and Chinese hamster lung (CHL) cells both had relatively low RFUs resembling that of the no cell control, GH4C1 are known to be slow growers and difficult to generate stable cell lines while CHL cells grow best as free floating cells which do not lend themselves well to high-throughput plate based assay formats in common use. The lines with the highest background noise were human cervical cancer cells taken from Henrietta Lacks (HeLa) and Chinese hamster ovary (CHO K1) cells. Baby hamster kidney (BHK-21) cells may naturally express some DAO as the signal from D-serine is twice that of D-aspartate or buffer. DAO is known to be highly expressed in the kidney (Koibuchi et al., 1995) so this finding may suggest functional DAO presence within this line. Confirmation of this activity could be made with a DAO specific inhibitor but we are interested in human and rat lines. Mouse embryonic fibroblast (NIH 3T3) cells may naturally express DDO since the responses of this line were elevated with the treatment of D-aspartate but not with buffer or D-serine.

Figure 2.2: Ten different host lines were examined for spontaneous activity with D-serine (blue), D-aspartate (maroon) and buffer (yellow) in the AmplexRed assay to identify the best candidate for the DAO stable cell line. The highest spontaneous activity using the Amplex Red assay was observed in CHO K1 cells while the lowest in CHL cells. Hek293 line was selected due to comparable RFUs to that of buffer alone, low maintenance and high probability of stable cell line generation.
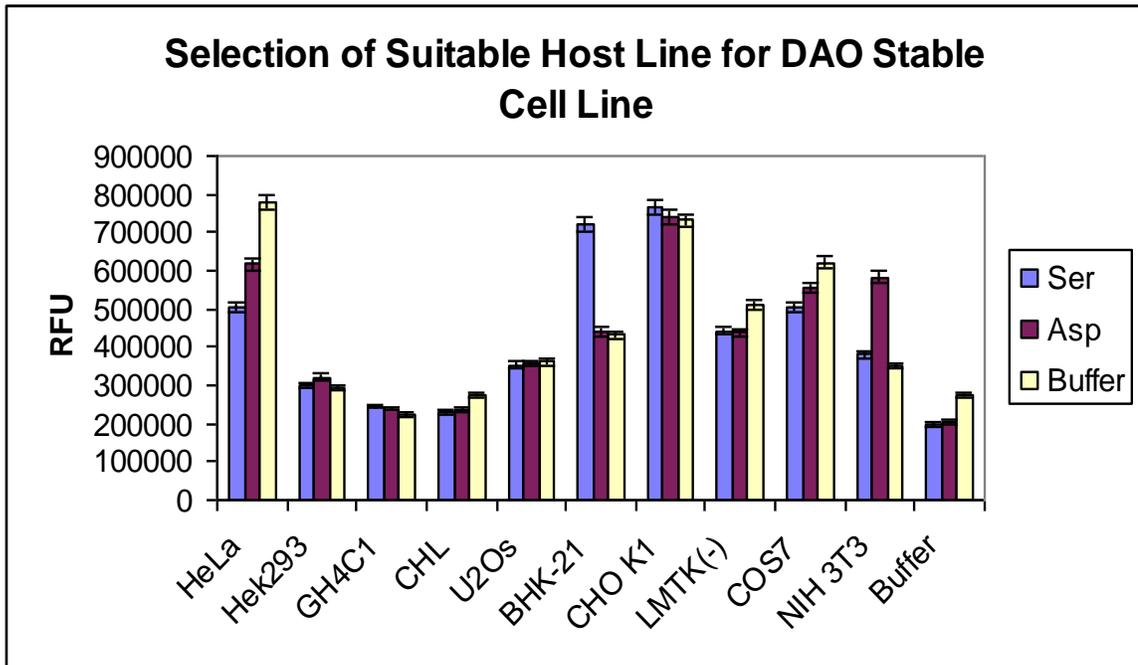
2.3 Identification of DAO stable cell lines

For the purpose of generating stable lines, both hDAO and rDAO inserts were independently cloned into pcDNA3.1 vectors which contain a hygromycin resistance selection marker. The DAO constructs were transfected into Hek293 cells through electroporation. Stable integration of the constructs in the cells was accomplished by subsequent selection for clones in hygromycin containing media over a three week span. Since transcription of DAO and hygromycin resistance were under two independent mammalian promoters and generation of stable line involves incorporation of the construct into the cell's genome some of the colonies may express hygromycin resistance without expressing DAO enzyme. However, sufficient numbers of clones were examined to guarantee that some may express both genes by virtue of a close proximity of the genes on the pcDNA3.1 constructs.

Nine hygromycin resistant colonies were examined for functional hDAO activity utilizing the Amplex Red assay with D-alanine as substrate. One of the nine colonies, designated hDAO #1, displayed a particularly high level of functional DAO activity as compared to Hek293 and buffer only controls (Figure 2.3 A). The remaining eight colonies displayed very modest functional increases over their respective controls and were deemed as not suitable for further analysis. Likewise, sixteen rDAO colonies were examined for functional DAO activity. The highest expressing lines were identified as rDAO #12 and #24 (Figure 2.3 B) with stable cell lines expressing intermediate and moderate levels of DAO activity identified as well. The functional activity of hDAO #1 is comparable to that of rDAO#12 and #24 as measured by the Amplex Red assay. The highest expressing lines were selected because they provide the best signal to noise ratio.

In order to confirm that the increased response in the selected hDAO and rDAO stable lines was due to DAO activity, WAY-396964, a tool DAO inhibitor originally made by the company Sepracor, was used to block the response (Fang et al., 2005). Because this compound specifically inhibits DAO enzymatic activity by competing with DAO's substrate a diminution of the Amplex Red assay in a dose dependent fashion by the inhibitor implies that the activity is that of DAO (Fang et al., 2005). The inhibitor was shown to have an IC50 of 163 nM

against hDAO #1 (Figure 2.4 A) and 108 nM against rDAO #12 (Figure 2.4 B) suggesting that both of those stable lines are expressing a functional DAO enzyme and that the inhibitor has about equal affinity for both DAO enzymatic species.

2.4 Purification of DAO from BL21 bacteria strain

Escherichia coli (*E. coli*) cells have been used routinely to successfully synthesize mammalian proteins (Liu et al., 2009). In order to generate DAO protein, BL21 DE3 cells were transformed with an inducible pTYB2 vector containing DAO construct encoding human DAO-intein fusion. Use of this vector allows for the bacterial over expression of target gene as a fusion construct with a 55 kDa self-cleavable intein affinity tag. As depicted in Figure 2.5, an intein has a high affinity for a chitin column which can be used to purify the fusion construct from the bacterial lysate. After selective retention of the fusion construct through the intein-chitin affinity and subsequent wash steps purified DAO enzyme was cleaved from intein through treatment with DTT whereby purified DAO was released leaving the intein on the chitin column.

In order to assess the efficacy of the purification procedure, samples from each step in the purification of hDAO were resolved by SDS-PAGE and stained using Coomassie blue (Figure 2.6). Within that figure a progression from total bacterial proteins representing the input, to those proteins retained on the chitin column, removed by the washing and finally resulting in collection of purified hDAO enzyme are shown. The concentration of purified hDAO was highest in the initial fractions and it gradually decreased until all of the cleaved DAO was eluted from the column. In fact, post elution beads show that most of the DAO was eluted off with the DTT cleavage. As a positive control and for the purposes of purity comparison a commercially available Sigma porcine DAO was used. The purity of the final DAO as determined by Coomassie stain is very good and compares very well with a commercially available porcine DAO enzyme. Whereas the commercial enzyme has visible contaminating bands at 51 kDa, 28 kDa and 20 kDa the human DAO generated through the intein pull-down does not have any visible contaminating bands.

Figure 2.3: The hDAO (A) and rDAO (B) stable lines were established in Hek293 cell line and selected based on functional activity through the Amplex Red assay. Several DAO colonies were identified and tested for functional expression of DAO enzyme. Human DAO stable line #1 was particularly active as compared to the Hek293 and buffer alone controls. Rat DAO stable line #12 and #24 represented the high expressing DAO lines. The other lines tested had intermediate to moderate enhancement of Amplex Red activity. Sigma porcine DAO was used as a positive control.

A
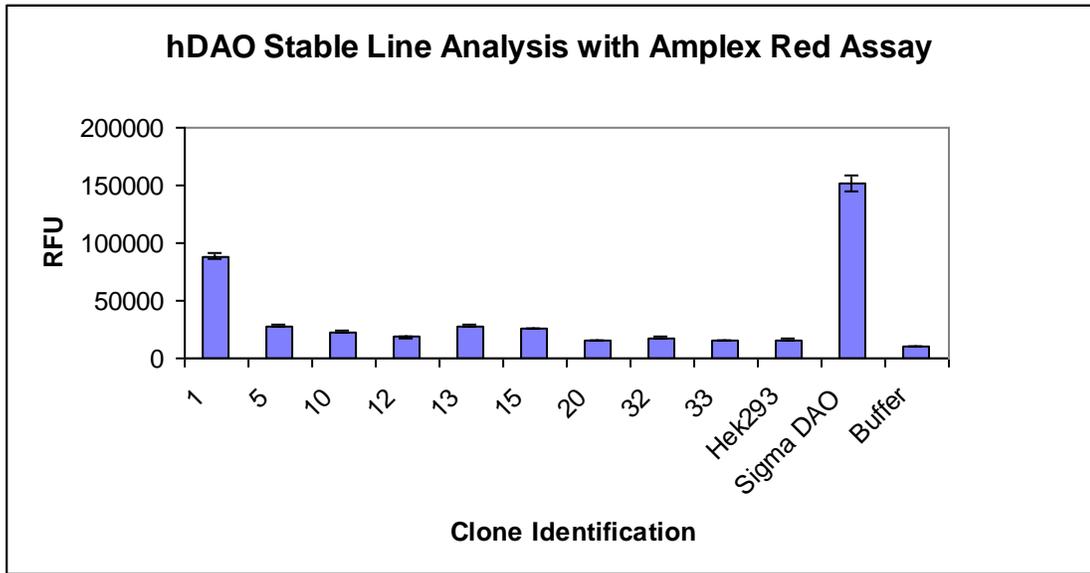
B
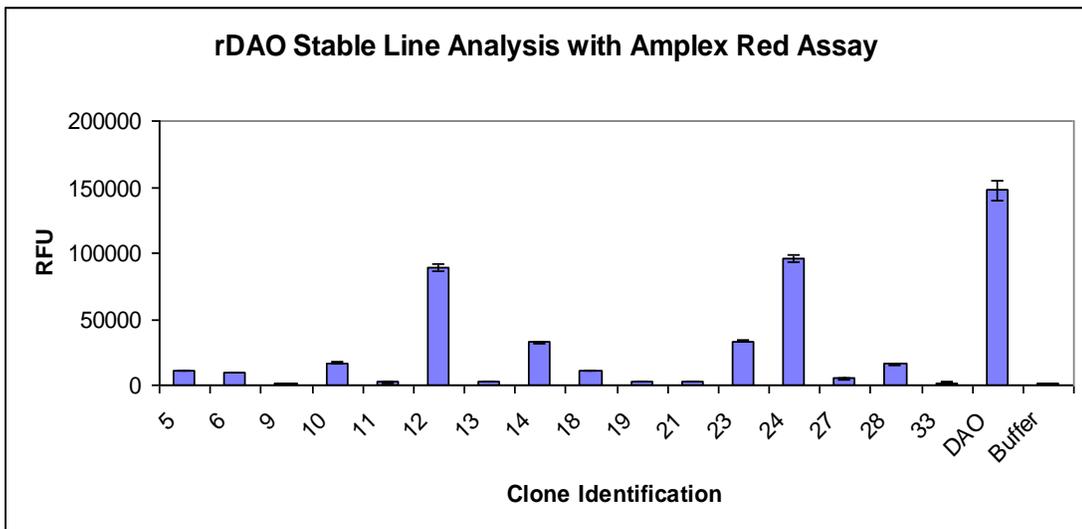
Figure 2.4: WAY-396964, a DAO inhibitor, completely abolishes hDAO #1 (A) and rDAO #12 (B) activity as determined by the Amplex Red assay. The respective IC50s generated against hDAO #1 and rDAO #12 are 163 nM and 108 nM.
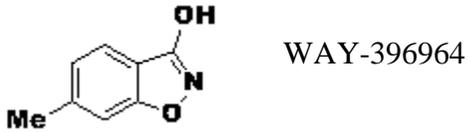
WAY-396964

	EC50
WAY-396964	1.631e-007

	EC50
WAY-396964	1.084e-007
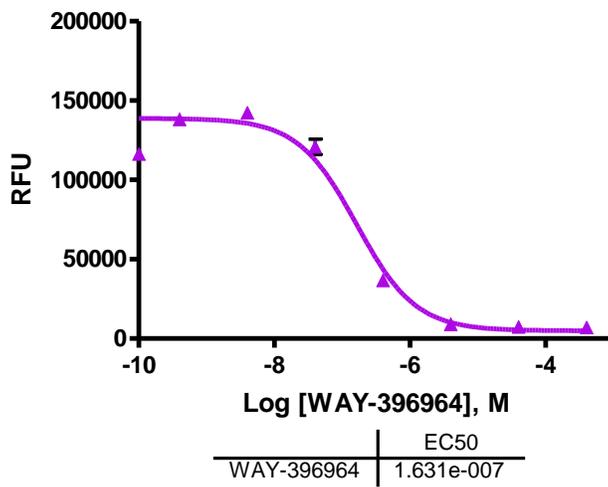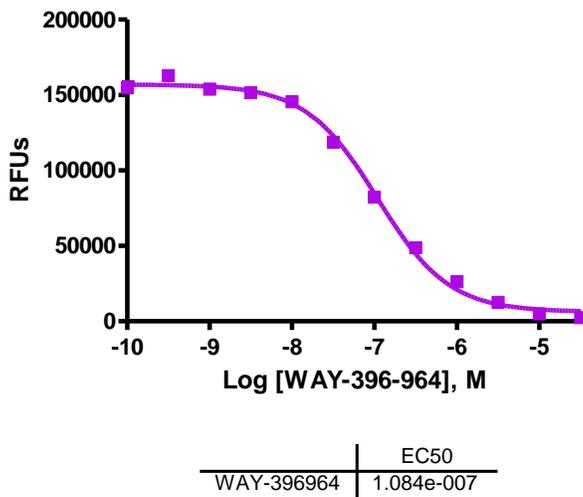
The protein concentration of eluates representing fractions #1 through #3 and illustrated by lanes 7 through 9 on the Coomassie gel in Figure 2.6 were measured with Bradford protein assay (compared to a standard curve prepared using BSA according to manufacturers instructions, Biorad) to determine the yield of purified hDAO from 750ml of bacteria media or 7.5g of wet mass. The yield from each fraction is listed in Table 2.1. The total hDAO yield was 2.69 mg with estimated purity of 100% as determined by absence of contaminating band on SDS-PAGE gel stained with Coomassie blue (Figure 2.6).

Table 2.1: hDAO purified enzyme yield from the intein column purification. Most of the soluble protein (~90%) was found in the first two eluates with a steep drop in yield between the second and third eluate.

	Collection volume (ml)	Concentration (mg)	Yield (mg/ml)
Fraction #1	**211**	**6.80**	**1.43**
Fraction #2	**156**	**6.67**	**1.04**
Fraction #3	**138**	**1.59**	**0.22**
Total			**2.69**

The purified DAO fractions were tested in the Amplex Red assay to determine if the purified DAO enzyme is functionally active and if the activity would correspond to the DAO concentrations found on the Coomassie gel. Figure 2.7 outlines the favorable outcome of this study showing a robust DAO activity especially in the first two fractions where most of the hDAO was found. The third fraction has some DAO activity while none is found in the fourth and last fraction. All of the DAO activity is inhibited by 10 μM WAY-396964, a DAO inhibitor, proving that the activity seen in the Amplex Red assay is due to DAO.

As part of our purification procedure we calculated how well DAO protein was purified in the final eluates as compared to the initial bacterial lysate and at what yield. With 7 ng of purified hDAO incubated for 30 minutes in the AmplexRed assay an output of about 300,000 RFUs was generated. This RFU corresponded with about 15 μM resorufin (see resorufin standard curve Figure 2.8). Consequently, the hDAO was generating about 15 μM of resorufin in 30 min or 0.5 μM/min. Since the volume in both the hDAO and resorufin was 40 μl then the hDAO was driving the production of 20 mol resorufin/min. Finally, if all of the 2.69 mg of purified hDAO were to be used instead of the 7 ng then about 7.68 million mol of resorufin/min could be generated with a specific activity of about 2.8 million mol of resorufin/min/mg. Same calculations were performed for the other samples in Table 2.2.

2.5 Conclusions

Through application of the Amplex Red assay a DAO assay suitable for use with purified enzyme and stable cell lines was generated. This assay was used to select HEK293 cells as host cell line with the least amount of background activity for the generation of hDAO and rDAO stable lines. DAO stable cell lines with significant and specific D-alanine Amplex Red signal were identified from among all of the colonies that grew in selective media and confirm their functional DAO expression by generating IC50's with a known DAO inhibitor, WAY-396964, in line with published data. Using these reagents functional hDAO enzyme was purified to homogenity. These tools will be used for analysis of the effects of DAO interactors on DAO enzymatic activity.

Figure 2.5: Schematic diagram for the hDAO intein tag purification. DAO fusion protein was expressed in BL21 *E. coli* cells and a chitin column was used to purify functional DAO enzyme. Taken from New England BioLabs Impact kit manual.
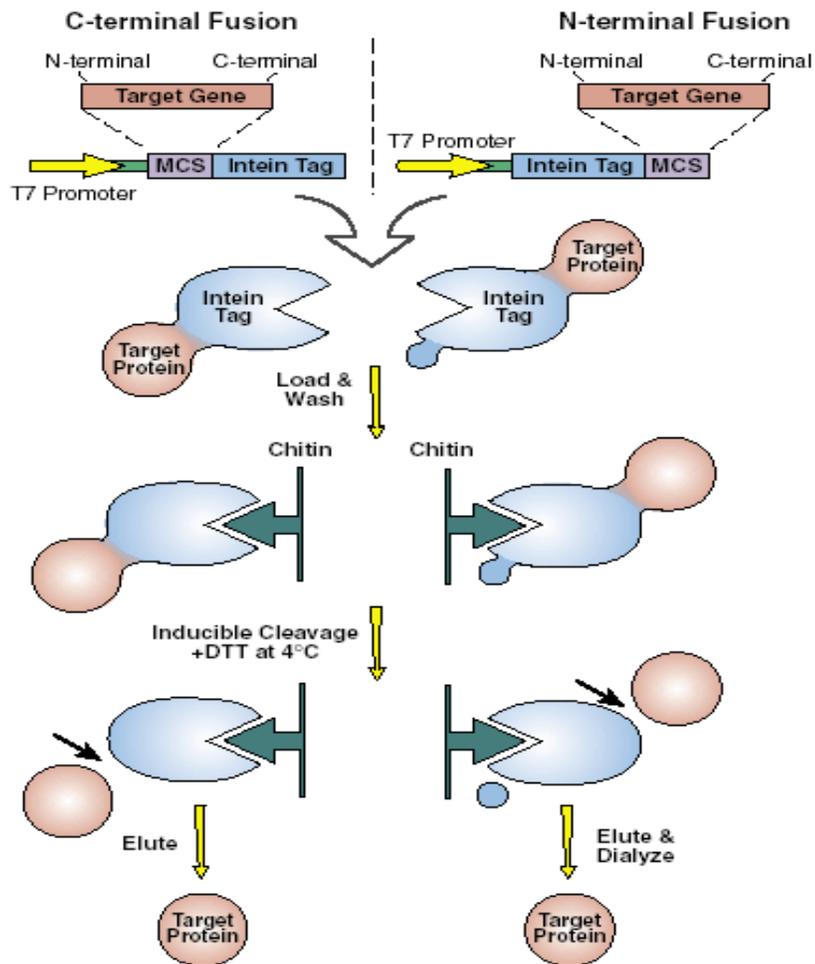
Figure 1: A schematic illustration of the IMPACT-CN System.

Figure 2.6: Coomassie stain of hDAO chitin column purification and the intermediate steps. Human DAO-intein fusion construct was expressed in bacteria and the bacterial lysate was applied to the chitin column. After washes with Buffer A and B (lanes 5 and 6) the columns containing chitin-hDAO were treated with DTT to cleave off hDAO. Fractions #1 through #3 (lanes 7-9) contain eluates of the purified hDAO which was used in subsequent enzymatic studies. As a control commercially available Sigma porcine DAO was used (lane 12).
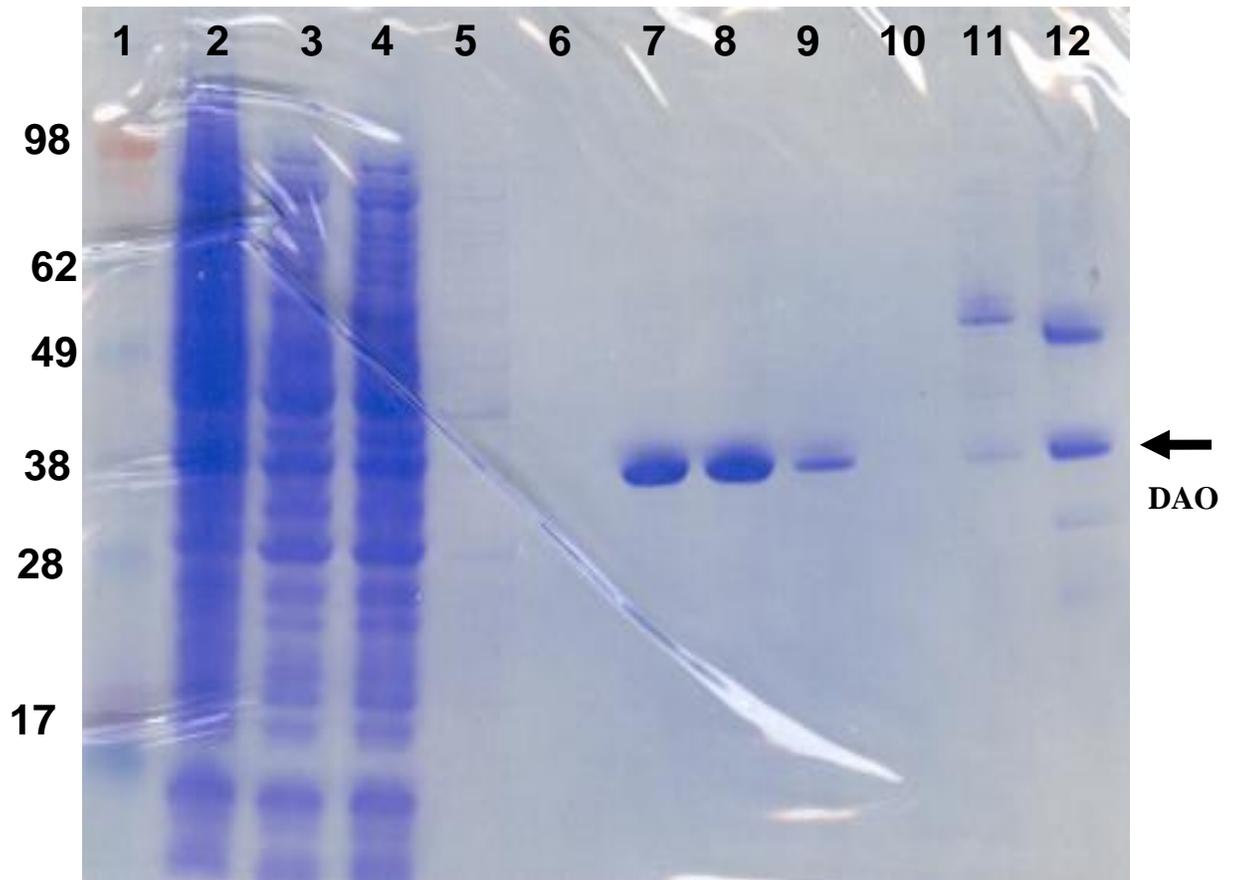
Legend:
Ln1: Protein ladder
Ln2: Cell lysate
Ln3: Lysate after sonication / centrifugation
Ln4: Lysate after chitin bead
Ln5: Elution from Buffer A wash
Ln6: Elution from Buffer B wash

Ln7: Fraction #1 post DTT cleavage
Ln8: Fraction #2 post DTT cleavage
Ln9: Fraction #3 post DTT cleavage
Ln10:Fraction #4 post DTT cleavage
Ln11:Chitin beads post DTT cleavage
Ln12:Sigma porcine DAO

Figure 2.7: Functional analysis of hDAO purified enzyme generated through the intein fusion protein. The four fractions correspond to the fractions outlined in Figure 2.6 on lane 7 through 10 where most of the DAO staining is found in the first two fractions with some in the third fraction and none in the fourth fraction were used at 5 μl per sample in the AmplexRed assay. This DAO distribution corresponds well with the DAO activity and the two observations confirm each other. All of the activity is inhibited by 10 μM DAO inhibitor, WAY-396964. Sigma porcine DAO was used as a control.

Purified DAO Fractions Are Functionally Acive and Are Inhibited With WAY-396964 (DAO Inhibitor) in AmplexRed Assay
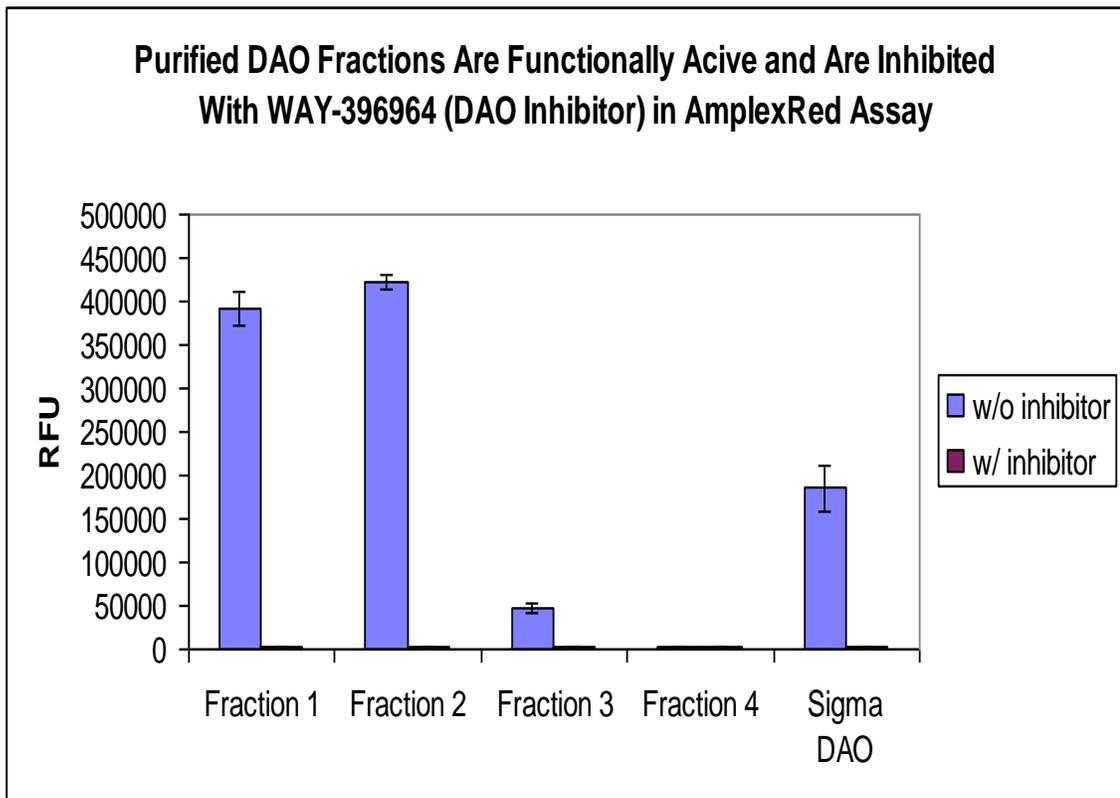
Figure 2.8: Resorufin standard curve. The resorufin standard curve was used to estimate the amount of resorufin hDAO enzyme generates in any given period of time.

Resorufin Standard Curve

[Bar chart: x-axis "Resorufin" with categories 4mM, 2mM, 1mM, 500uM, 250uM, 125uM, 62uM, 31uM, 15uM, 8uM, 4uM, 2uM, 976nM, 488nM, 244nM, 122nM, 61nM, 30nM, 15nM, 8nM, 4nM, 2nM, 0; y-axis "RFU" from 0 to 700000]
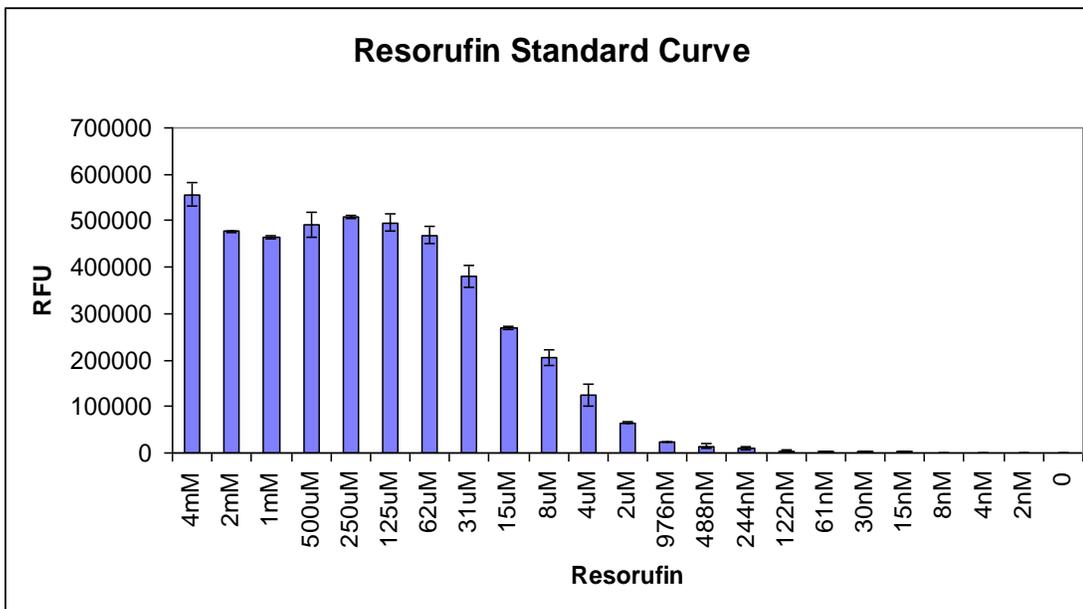
Table 2.2: Specific activity of the purified hDAO fractions. Based on the specific activity of the final DAO eluate in comparison to the bacterial lysate input we concluded that the DAO was purified about 1850 times with a yield of about 67% of the total DAO enzyme.

	Protein (mg)	Total Activity (mol Resorufin/min)	Specific Activity (mol Resorufin/min/mg)	Fold Purification
Lysate	7500	11,461,844	1,528	1
Flow through	7056	N/A	N/A	N/A
DTT eluate	2.69	7,685,714	2,857,142	~1870

3. Production and characterization of DAO polyclonal antibodies to identify DAO interactors and investigate DAO localization

3.1 Identification of DAO specific sites for immunization

One of the most important tools necessary for the investigation of DAO localization and identification of DAO interactors through co-immunoprecipitation is a specific and reliable DAO antibody. In order to obtain such a valuable reagent, commercially available antibodies were tested but none of them recognized rat species DAO on a western blot (Figure 3.1). While recognizing that lack of a signal on a western blot does not preclude an antibody from recognizing an undenatured DAO enzyme we were in need of an antibody which would recognize DAO in its denatured state on a western blot as well as natural enzymatic configuration for the immunoprecipitation experiments.

Antibodies can be made against either whole proteins or short peptides with distinct advantages and disadvantages for each method. A pure solution of recombinant proteins is necessary for a successful and specific immune response. At the time of antibody generation the purified hDAO enzyme utilized in Chapter 2 was not available and the commercially available porcine DAO was found not to be pure enough (Figure 2.6, lane 12). Furthermore, the objective was to generate a rat specific DAO antibody as rat brain tissue was readily available for the proposed experiments. Using the whole DAO protein as the antigen the tertiary structure of the enzyme and any post translational modifications would likely be part of the purified enzyme and result in antibody generation. However there would not have been any control over the region responsible for the immunogenicity, potential cross reactivity of the antibody with structurally similar proteins, and purification of the antiserum would be challenging from the perspective of preserving antigen configuration on the purification column. Since the full length of DAO and its three dimensional structure was published (Kawazoe et al., 2006; Mizutani et al., 1996) and many consensus post translational modification sequences are known (Bairoch, 1992) suitable peptides can be selected which are likely to be exposed to elicit an immune reaction, are unlikely to be found in other proteins and do not undergo post translational

modifications.   After taking all of this information into consideration short polypeptides were utilized because polypeptides are relative easy to generate and use for immunization.

Two peptides corresponding to amino terminal sequences from rat DAO were selected as antigens for use in generating immune response in rabbits. Peptide #1 (amino acid 21-38 ERYHPAQPLHMKIYADRF) was selected based on a proprietary analysis of DAO (Open Biosystems) which suggested that this region was unique to DAO and likely to be accessible to an antibody within the DAO enzyme.   Peptide   #2   (amino   acid   49-69 GLWQPYLSDPSNPQEAEWNQQ) corresponds to the sequence of a mouse DAO peptide that was previously generated against mouse DAO and shown to yield a DAO specific antibody as determined by a western blot (Almond et al., 2006). As only one amino acid is different between the rat and the mouse Peptide #2 sequence (Figure 3.2) it was anticipated that a suitable DAO antibody may be generated against the rat peptide as was the case for the mouse DAO.

The rat DAO peptide sequences were compared to corresponding mice and human DAO sequences for the purpose of future antibody validation. Both of the peptides selected against the rat DAO show about 95% amino acid similarity with the mouse sequence. In contrast, the human DAO differs considerably especially in the case of peptide #1 where five of the eighteen amino acids (~28%) were different and an extra leucine exists in the human DAO sequence. Peptide #2 was more conserved between the rat and the human DAO with three of the twenty-one amino acids differing (~17%). Furthermore, the three amino acid changes retained the same polarity and electrical charges suggesting that Peptide #2 in rat and human are functionally conserved.

Figure 3.1: Comparison of commercial DAO antibodies on SDS-PAGE gel against 20 μg of (ln1) DAO Hek293 and (ln2) Hek293 lysates. Expected molecular weight of DAO is indicated by the arrow.

A = Novus Biologicals (H00001610-M01)

B = Nordic Immunological Laboratories (NE013/7S)

C = Rockland (100-601-143)
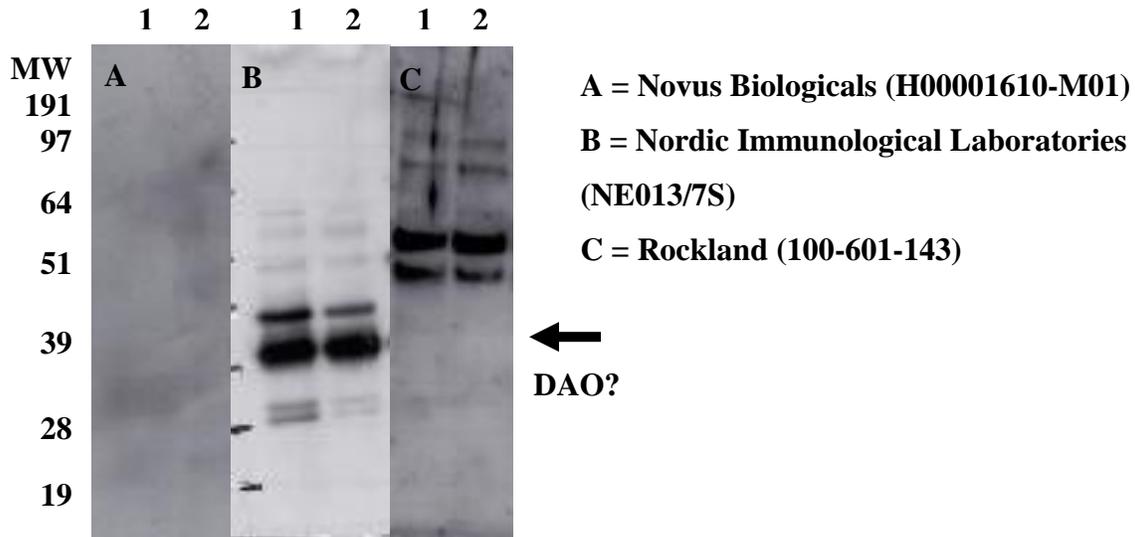
Figure 3.2: Comparison of amino acid sequences between rat, mouse and human DAO regions selected for polyclonal antibody synthesis. Both of the sequences are found on the N-terminus of the rat DAO with Peptide #1 spanning amino acids 21 through 38 and Peptide #2 ranging from 49 through 69. Amino acid differences between the sequences are highlighted in yellow and an additional leucine residue in the human Peptide #1 is highlighted in red.

	Peptide #1	Peptide #2
rDAO	^{21}ERYHPA-QPLHMKIYADRF^{38}	^{49}GLWQPYLSDPSNPQEAEWNQQ^{69}
mDAO	^{21}ERYHP**T**-QPLHMKIYADRF^{38}	^{49}GLWQPYLSDPSNPQEAEW**S**QQ^{69}
hDAO	^{21}ERYH**SVL**QPL**DI**K**V**YADRF^{39}	^{49}GLWQPYLSDP**N**NPQEA**DWS**QQ^{69}

3.2 Generation of DAO specific antibodies

Rabbits were immunized with Keyhole Limpet Hemocyanin (KLH) conjugated rDAO peptide #1 or peptide #2 according to the schedule in Table 3.1 where the initial immunization was followed by three independent boosts (Open Biosystems). Crude unpurified serum samples from day 70 collection were obtained and used to probe western blots of crude extracts containing rat DAO expressed in human embryonic kidney (Hek293) cells and rat cerebellar lysates to determine if the rabbits generated antibodies against DAO.

3.3 Characterization of crude DAO polyclonal antibody

Crude polyclonal antiserum obtained from rabbit immunized with Peptide #1 was tested for its ability to detect rat DAO expressed in Hek293 cell extract by western blotting analysis. The Peptide #1 antiserum did not result in a successful DAO antibody generation because a 39 kDa band corresponding to the expected mobility of DAO unique to the DAO Hek293 lysate was not detected (Figure 3.3A, lane 1). Although immunoreactivity against DAO Hek293 lysate is present around 39 kDa, a similar response is apparent in the Hek293 cell lysate at the same molecular weight (Figure 3.3A, lane 2) suggestive of a lack of a specific DAO antibody signal. The immunoreactivity in both of the samples was very similar suggesting that the antibody responsible for the signal was against a protein expressed in the host Hek293 cells, unlikely to be DAO.

A murine version of Peptide #2 had previously been shown to successfully generate a rabbit polyclonal against mice DAO (Almond et al., 2006). The polyclonal antiserum generated against rat Peptide #2 detected a specific 39 kDa band in rat DAO lysate and rat cerebellar lysate not present in Hek293 or rat spleen lysate (Figure 3.3, B). Both Hek293 and rat spleen lysate were used as a negative control as both are known not to express DAO. This evidence is strongly suggestive of the presence of DAO antibodies in the crude antiserum. The additional bands on the gel were presumed to be from contaminating antibodies from the rabbit serum. The serum collected from rabbit immunized with Peptide #2 was likely to result in a working DAO antibody upon further purification.

Table 3.1: Rabbit immunization schedule for DAO antibody generation. A 70 day protocol involving an initial immunization followed by three independent boosts was utilized for generation of DAO antiserum. Peptide synthesis and immunization conducted by Open Biosystem.

Procedure	Protocol Day	Description
Control serum Collection	Day 0	
Primary injection	Day 1	Primary Immunization with 0.25 mg KLH emulsified with Freund's complete adjuvant, SQ 4 sites
1st Booster	Day 14	Boost with 0.10 mg KLH emulsified with Freund's incomplete adjuvant.
Serum Collection	Day 28	~25mls per rabbit
2nd Booster	Day 42	Boost with 0.10 mg KLH emulsified with Freund's incomplete adjuvant.
Serum Collection	Day 56	~25mls per rabbit
3rd Booster	Day 56	Boost with 0.10 mg KLH emulsified with Freund's incomplete adjuvant.
Serum Collection	Day 70	Large-volume production bleeds (~50mls per rabbit)

Figure 3.3: Western blot probed with crude unpurified DAO antiserum generated against Peptide #1 (A) and Peptide #2 (B). DAO antiserum generated against Peptide #1 does not detect rat DAO at the expected molecular weight of 39 kDa (indicated by the arrow). DAO antiserum generated against Peptide #2 detects band on a Western blot in rDAO Hek293 cells and in rat cerebellum corresponding to DAO molecular weight (indicated by the arrow) not present in Hek293 cells or in rat spleen. Additional bands are present presumably corresponding to contaminating antibodies in the crude sample.
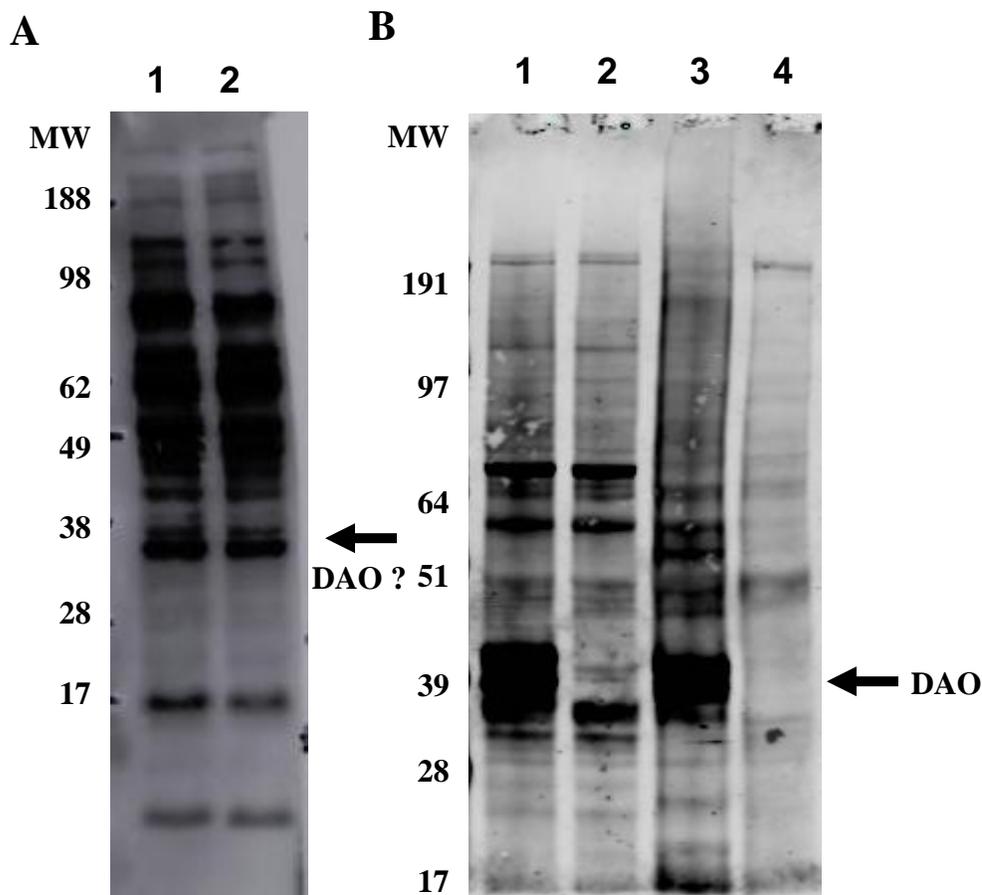
Legend:
Ln1: 20 μg rDAO Hek293
Ln2: 20 μg Hek293
Ln3: 40 μg rat cerebellar lysate
Ln4: 40 μg rat spleen lysate

3.4 Purification of DAO antibody against immunizing peptide

Due to the apparent success of the early characterization of the DAO polyclonal antibody from the rabbit immunized with Peptide #2, the serum was purified against a DAO peptide-affinity column against the immunizing peptide (performed by Open Biosystems). The resulting purified DAO antibody solution was tested by western blotting of crude lysates containing rat or human DAO expressed in Hek293 cells and rat cerebellar lysate. A pronounced DAO band of 39 kDa, predicted to be DAO, was identified in the three DAO containing samples and was absent in sham transfected Hek293 and rat spleen lysates (Figure 3.4) indicating that the DAO antibody reliably detects both rat and human DAO when over-expressed in Hek293 cells. This finding was expected given the similarity between rat and human DAO sequence within the Peptide #2 region (see Figure 3.2). In order to further test the specificity, the purified antibody was preincubated with the immunizing peptide at $1/10^{th}$ the weight of the antibody before probing the blot. The 39 kDa band was not present, strongly suggesting that the band corresponds to DAO. In addition to the expected DAO band, additional bands which migrated at about 64 kDa and 97 kDa were identified in the DAO Hek293 and Hek293 lysates. All of the bands were also pre-absorbed with the peptide suggesting that the purified DAO antibody solution has contaminating antibodies with affinity to the immunizing peptide or yet unknown DAO variants or post-translational modifications.

BLAST analysis of the region selected for the immunizing Peptide #2 provides alignment only to DAO suggesting that DAO should be the only protein detected as a result of the production of antibodies by immunization with this peptide. The presence within the purified DAO antibody solution of antibodies capable of detecting proteins other than DAO suggests that the peptide could have formed a tertiary configuration resulting in the production of unexpected antibodies after exposure to the rabbit immune system. These non-DAO peptide configurations may have been present as well in the DAO-peptide affinity column used to purify the crude serum thus retaining the contaminating antibodies within the DAO antibody solution.

Figure 3.4: Western blot probed with crude polyclonal serum purification against the immunizing peptide resulted in a cleaner DAO antibody preparation. Western blot analysis of peptide purified DAO antiserum confirmed presence of DAO antibody in the crude serum because its signal is blockable by pre-absorbtion with the immunizing peptide. Furthermore, evidence in lane 5 suggests that the antibody generated against Peptide #2 is suitable for detection of human DAO in Hek293 cells. Additional contaminating antibodies are present as depicted by unexpected bands at 64 kDa and 97 kDa. All of the unknown bands are blocked by preabsorbtion of the antibody with the peptide suggesting that the corresponding antibodies are specific to the immunizing peptide. The expected molecular weight of DAO protein is indicated by the arrow.

Legend:
Ln1: 20 μg rDAO Hek293
Ln2: 20 μg Hek293
Ln3: 40 μg rat cerebellar lysate
Ln4: 40 μg rat spleen lysate
Ln5: 20 μg hDAO Hek293
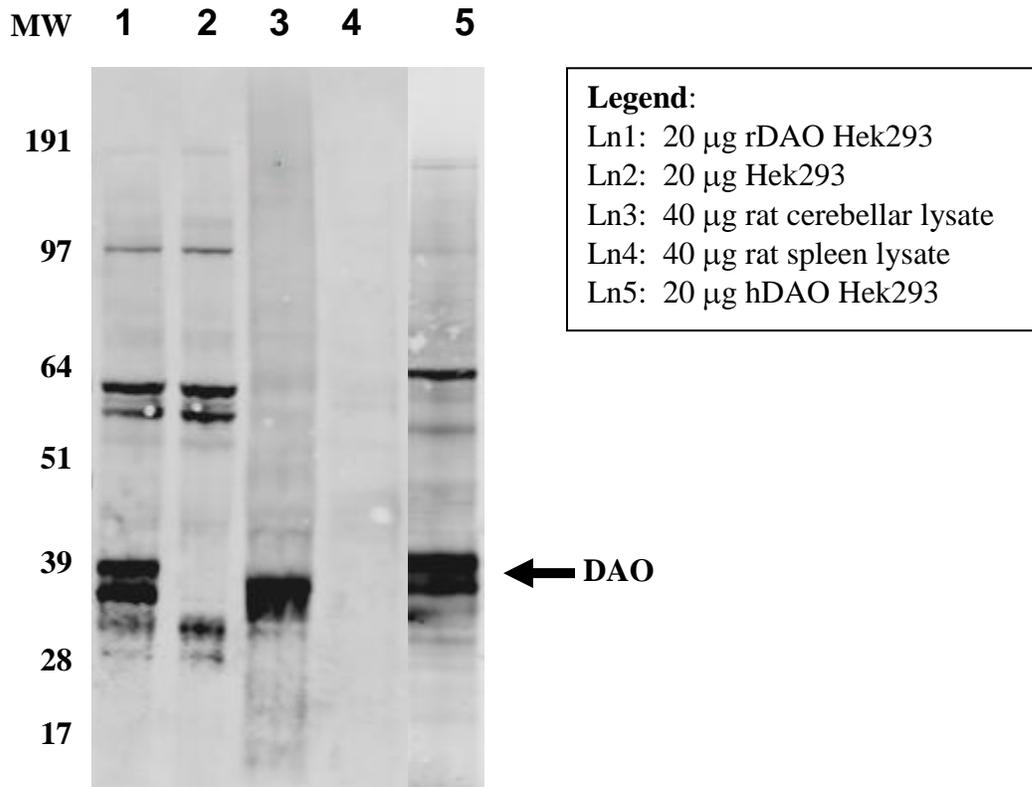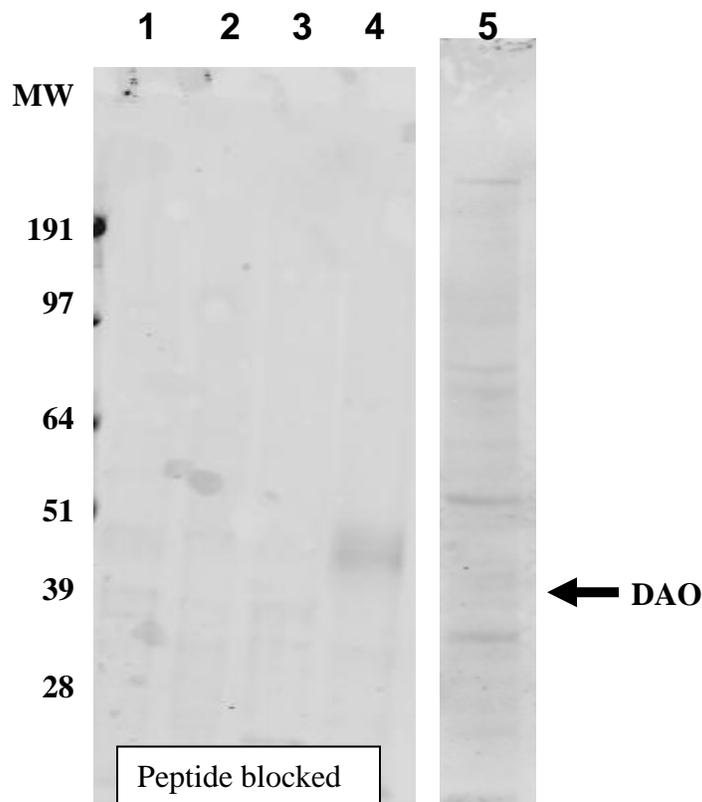
3.5 Purification of DAO antibody against purified human DAO enzyme

Since the DAO polyclonal antibody isolated through the immunizing peptide purification retained contaminating antibodies and the DAO antibody was shown to recognize both rat and human DAO enzymes the antibody preparation was subsequently purified against a pure human DAO enzyme to try to get additional purity of the preparation. Given the similarity of the two species at the immunizing peptide sequence level purification against the human or rat DAO purified protein should result in generation of purified DAO antibody. Furthermore, unlike the peptide alone purification where the peptide can apparently form unexpected configurations, the configuration of the DAO enzyme is conformationally restrained and is likely to result in a more specific antibody pool (Kaumaya et al., 1992).

After the second purification against purified hDAO, the antibody solution as tested by western blotting detected no contaminating protein bands in any of the negative controls, suggesting we had obtained a very pure DAO antibody preparation (Figure 3.5). In particular the unknown protein bands migrating at about 64 kDa and 97 kDa were not observed (see Figure 3.4). Bands were only present in DAO containing samples including human DAO Hek293 and rat cerebellar lysates. Furthermore, the DAO bands were blocked by preincubating the antibody with the immunizing peptide. Unexpectedly, two 39 kDa bands were detected in the human DAO Hek293 sample, rather than the single protein corresponding to human DAO expressed in the construct that was introduced via transient transfection in the Hek293 cells. The presence of two bands in the DAO Hek293 but none in Hek293 and the fact that both of them were blocked with the peptide preincubation suggests that both bands were DAO. One potential explanation for the presence of two forms of DAO is the incorporation of the DAO coding sequence into an expression construct in a region with an additional start codon resulting in the transcription of the original message as well as a somewhat longer message consisting of the original message plus a short fragment of Hek293 genome. Alternatively, DAO may have undergone a post-transcriptional modification such as a phosphorylation or glycosylation that takes place in Hek293 cells or underwent a c-terminal cleavage discussed in the introduction. However, it should be noted that the rat cerebellar lysate contained only one band corresponding to DAO. However, post-translational modification cannot be ruled out because human DAO may differ from the rat DAO in a key sequence exposing it to a post-translational modification, which may not be the case for rat DAO.

Figure 3.5: "Double" purified DAO antibody specifically detects DAO in human DAO Hek293 cell line and in rat cerebellar lysate on a western blot (indicated by the arrow). Membrane was probed with DAO antibody purified against the purified hDAO enzyme. Immunoreactive bands are not seen when the antibody is blocked by its peptide.

Peptide blocked
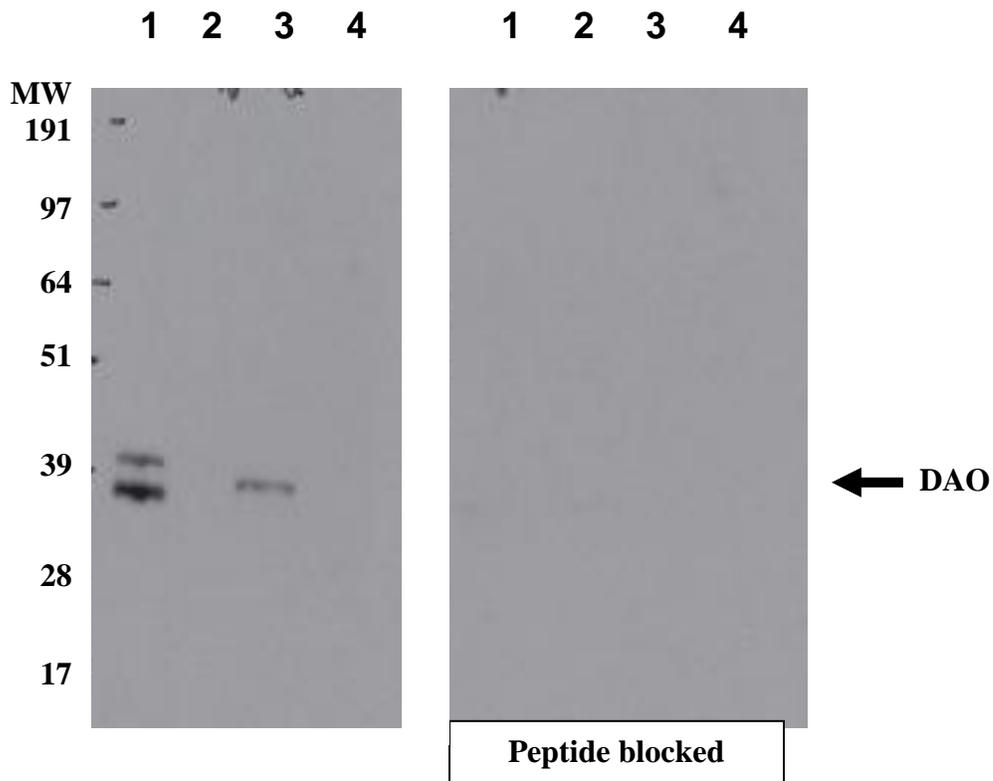
Legend:
Ln1: 20 μg hDAO Hek293 lysate
Ln2: 20 μg Hek293 lysate
Ln3: 40 μg rat cerebellar lysate
Ln4: 40 μg rat spleen lysate

3.6 DAO antibody validation against DAO KO mice lysate

The purified DAO antibody solution was tested against a DAO KO mice cerebellar lysate (a kind gift from Christine Strick, Pfizer) to further test its specificity. The KO mice were generated by knocking out exons 7-8 completely and part of exon 6 and 9 which should cause a frame shift beyond exon 9 and result in a truncated DAO protein encoding through exon 6 (manuscript in preparation). The resulting protein is expected to weight about 20 kDa, or half of the full length DAO.

Two bands around 39 kDa were observed in the WT mice cerebellar lysate (Figure 3.6 lane 1) which suggests posttranslational modifications in mice. This was not observed with the rat cerebellar lysate (Figure 3.5 lane 3) suggesting that the mice DAO construct may contain for example a phosphorylation sequence which is not found in the rat DAO sequence. Alternatively, the two bands are representation of the full length DAO and the proposed c-terminal truncated DAO (Campaner et al., 1998; Pollegioni et al., 1995). Both bands decrease in intensity in the HET mice (Figure 3.6 lane 2) but with a much more significant decrease in the lower molecular band intensity. In the KO mice both bands completely disappeared (Figure 3.6 land 3). Taken together these data suggest that both bands are corresponding to DAO. Furthermore, there is no evidence of a truncated DAO in the HET and KO mice, which, if expressed, should be detectable with the N-terminal DAO antibody. Consequently, either truncated DAO protein is degraded altogether or it is not synthesized at all. The KO mice were not available until the very end of my thesis hence these animals were not used through out my experiments as a negative control.

Figure 3.6: Examination of cerebellar lysate from DAO KO mice with the DAO antibody. WT, HET and KO mice cerebellar lysates were probed with the DAO antibody on an SDS-PAGE gel. The expected outcome would be no detectable DAO at 39 kDa but a band at ~20 kDa in the lysate from the KO mice. As expected the band corresponding to the full length DAO at 39 kDa in the KO mice lysate was not present indicating a successful KO. There was no evidence of a 20 kDa band in the cerebellar lysate from the KO mice either. In the HET cerebellar lysate where both 39 kDa and 20 kDa bands were expected at about half the intensity of the bands found in the WT mice a dimunition of the 39 kDa signal was observed without any evidence of 20 kDa band. Actin was used as a control to show that same protein concentrations were loaded for each sample. DAO is indicated by the arrow.

Legend:
Ln 1: 20 µg mice WT cerebellar lysate
Ln 2: 20 µg mice HET cerebellar lysate
Ln 3: 20 µg mice KO cerebellar lysate
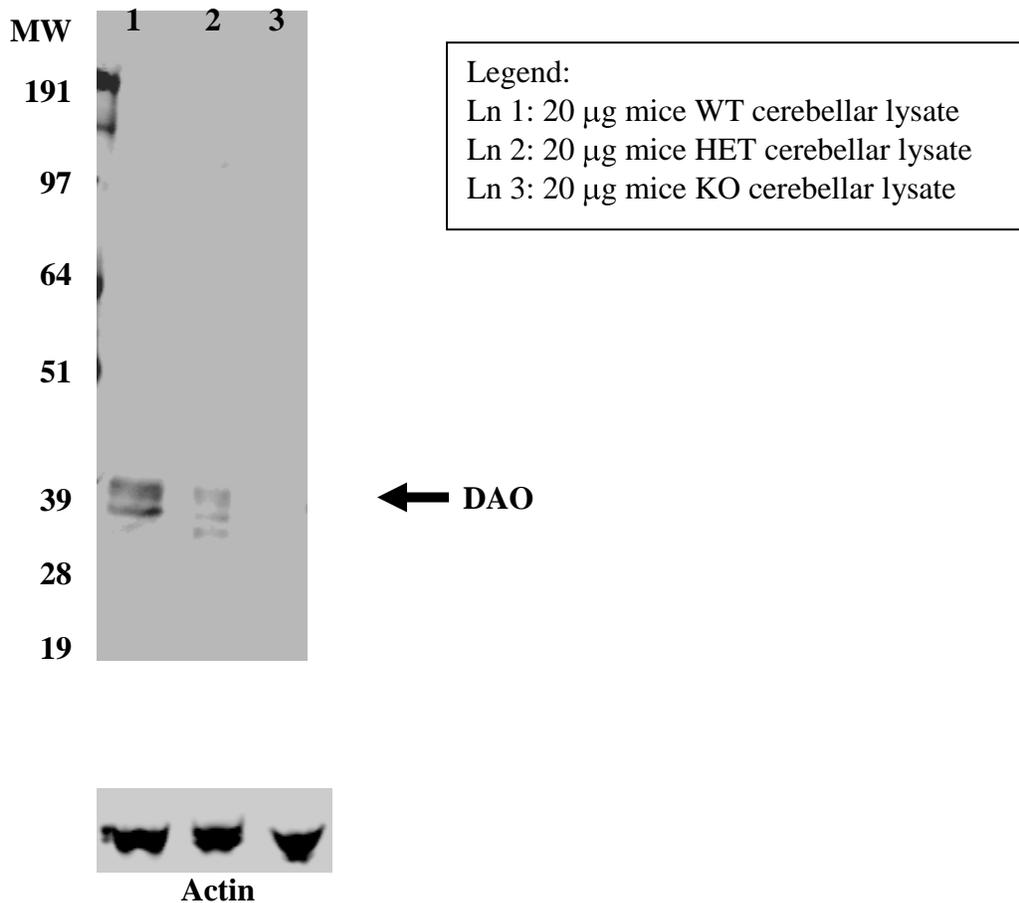
3.7 Optimization of DAO immunoprecipitation procedures

Once the DAO antibody was shown to be effectively and specifically recognizing DAO it was tested in immunoprecipitation experiments to determine if it would recognize undenatured DAO enzyme in complex co-immunoprecipitation experiments. Magnetized Dynal Protein A (Invitrogen) beads were used as a matrix for capturing and retaining the DAO antibody as outlined in Figure 3.7. The bead-antibody complex was than used to immunoprecipitate DAO from various lysate solutions.

The Dynal beads are precoated with Protein A, which has a very high affinity for most rabbit IgG antibodies (Deisenhofer, 1981). The beads were mixed with the purified antiserum to allow for capture of the antibodies by protein A. The two were then covalently crosslinked with dimethyl pimelimidate dihydrochloride (DMP) to prevent the antibodies from dissociating from the beads during washing and especially during the elution of the antigen. The beads were convenient because they can be gently separated from the rest of the solution utilizing a magnet. This allowed for retention of protein complexes, which might be otherwise disrupted during other co-immunoprecipitation procedures employing procedures such as centrifugation. In addition, the Dynal beads allowed for removal of all the wash solutions ensuring thorough washing without losing the beads.

To test the ability of the DAO antibodies coupled to Dynal beads to immunoprecipitate DAO, lysates from human DAO Hek293 cells were first used as an input for the immunoprecipitation. Increasing total protein amount from 50 μg to 750 μg of lysate were used per set of bead/antibody ratio to determine the maximal amount of DAO that can be immunoprecipitated. As seen in Figure 3.8, lanes 2 through 6, DAO antibody was able to successfully immunoprecipitate DAO enzyme. At about 100 μg of DAO Hek293 lysate (lane 3) the amount of DAO antibody was saturated as compared to 50 μg (lane 2) and 250 μg (lane 4). This bead/antibody set was used throughout further experiments and was able to pull-down as much DAO as was found in 25 μg of DAO Hek293 lysate as

Figure 3.7: Schematic diagram for preparation of DAO polyclonal antibody immunoprecipitation column. The column is composed of Dynal Protein A beads which act as a matrix for the DAO antibody.

Dynalbeads Protein A

Bind Antibody

Crosslink Antibody to Beads

Immunoprecipitate Target Antigen

Wash

Elute Target Antigen
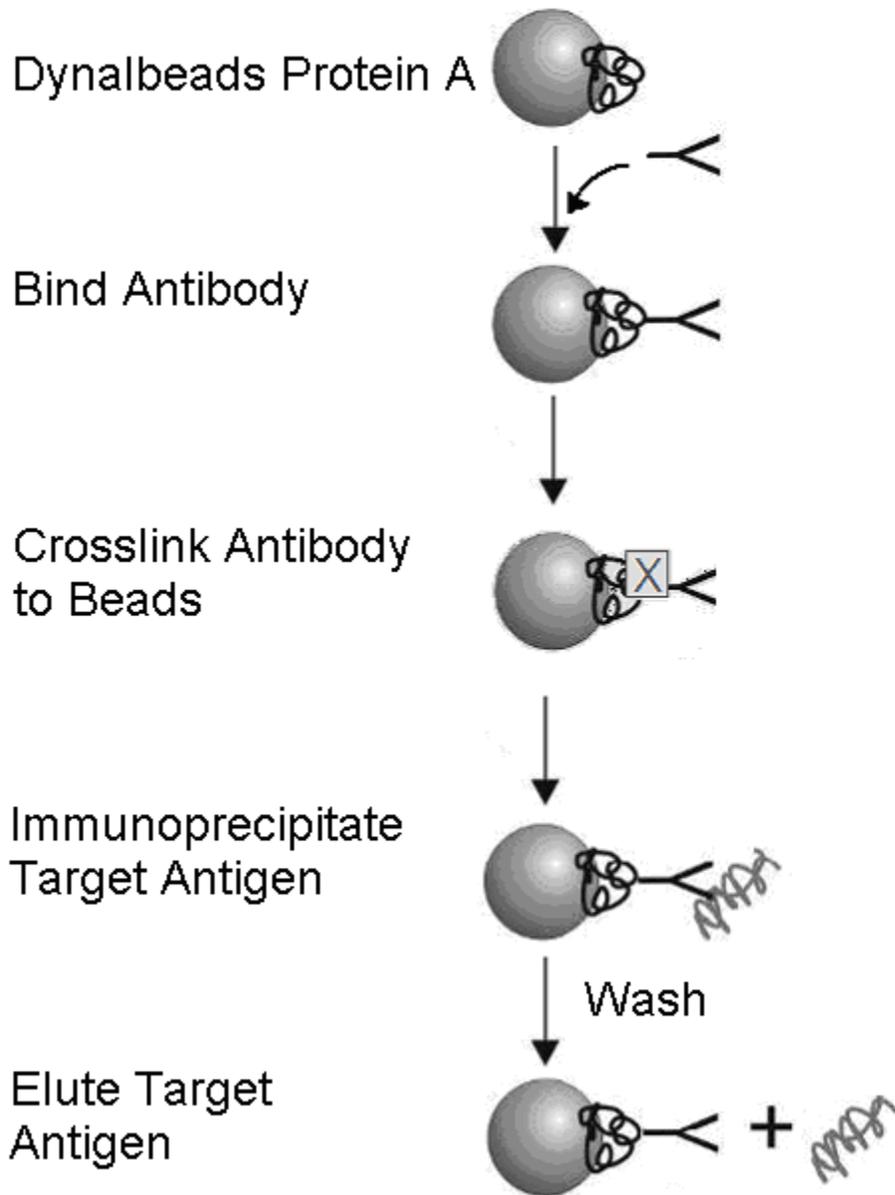
determined the by positive control with 2.5 μg of DAO-Hek293 lysate in lane 1. The additional bands found in lanes 2 through 6 around 50 kDa were probably that of the heavy IgG chain. Some of the antibody may have eluted off during the elution step despite cross-linking to the beads. Samples from lanes 7 and 8 were prepared in the same way as the other immunoprecipitation samples but prior to the addition of DAO Hek293 lysates, immunizing peptide was used to preabsorb the antibody. Lane 7 shows that 1 μg of immunizing peptide could completely block the DAO antibody from capturing DAO protein from DAO Hek293 lysate. However, at one-tenth of the peptide concentration, as depicted in lane 8, some of the DAO protein was captured and retained by the DAO antibody beads. Due to the concentration gradient of the blocking peptide the two lanes further underscore that the band being immunoprecipitated was DAO. The protein smear migrating around 62 kDa in the peptide blocked samples was perhaps the result of trace amounts of the immunizing peptide. This argument was justified by considering that in lane 8 where one-tenth of the amount used in lane 7 peptide was used was of lower intensity. Some of the high molecular weight signal may be due to antibody elution from the column and subsequent recognition by the secondary antibody. Perhaps the use of the peptide on the DAO Dynal beads resulted in the antibody elution during the stage prior to loading on the SDS-PAGE gel.

The immunoprecipitation procedure using DAO antibodies coupled to Dynal beads was further validated using rat cerebellar lysates in order to ensure that the antibody was capable of recognizing native human and rat DAO and that the DAO enzyme may be detected at physiological levels as it is in the rat cerebellum and for it to be specifically pulled-down from a lysate solution. This was critical to enable immunoprecipitation of native DAO protein complexes.

The results from western blotting analysis of immunoprecipitation from rat cerebellar lysate are presented in Figure 3.9. In lanes 3 through 7, a lysate gradient ranging from 25 μg to 500 μg was presented with an increasing retention of DAO protein. The 500 μg of rat cerebellar lysate (lane 7) corresponded to the amount of DAO captured from 100 μg of human DAO Hek293 (lane 10)

suggesting that around 500 μg of rat cerebellar lysate was necessary to saturate the beads with DAO. Since it only takes 100 μg of human DAO Hek293 lysate but 500 μg of rat cerebellar lysate this outcome suggests that there were approximatelly five times as much DAO expressed in the stable line as in the cerebellum per μg of total protein. Such an outcome was expected as in general, stable lines heterologously expressing proteins are more likely to express at a much higher than it is in native tissue. The first two lanes of Figure 3.9 show the cerebellar lysate itself at 10 μg and 50 μg both of which show presence of DAO. The relative protein band intensity between 500 μg immunoprecipitation (lane 7) and that of 50 μg lysate (lane 2) was about four-fold suggesting that the DAO antibody was capable of immunoprecipitating about forty percent of the total DAO found in the lysate. This ratio of the retained DAO on the antibody beads could be increased if the immunoprecipitation was carried out for longer then the one hour utilized in this experiment. However, such a retention rate is already high and sufficient for experimental needs. The peptide blocked DAO antibody was used in lanes 8 and 9 where either 1 μg or 0.1 μg of the immunizing peptide was used respectively. As in human DAO Hek293 sample, 1 μg of the peptide was able to completely block DAO capture by the DAO beads even when highest cerebellar lysate, 500 μg, was used. The lower peptide block partially prevented DAO capture from the cerebellar lysate.

All of the immunoprecipitation samples share the IgG heavy chain band around 50 kDa. Additional background signal was found especially in the peptide blocked samples suggesting some antibody elution from the beads and potential trace amount of the peptide as discussed previously (Figure 3.8).

Figure 3.8: Optimization of DAO immunoprecipitation protocol using DAO antibody covalently coupled to protein Dynal beads from hDAO Hek293 stable cell line lysate. The western blot was probed with DAO antibody for presence of DAO after immunoprecipitation. As the concentration of hDAO-Hek293 lysate was increased (lanes 2-6) from 50 μg to 750 μg more DAO was pulled-down until the antibody beads were saturated at about 100 μg of lysate. The pull-down was completely blocked by preabsorbtion of the antibody with 1 μg of immunizing peptide, but partially with 0.1 μg. The expected DAO protein separation on the SDS-PAGE gel is indicated by the arrow.
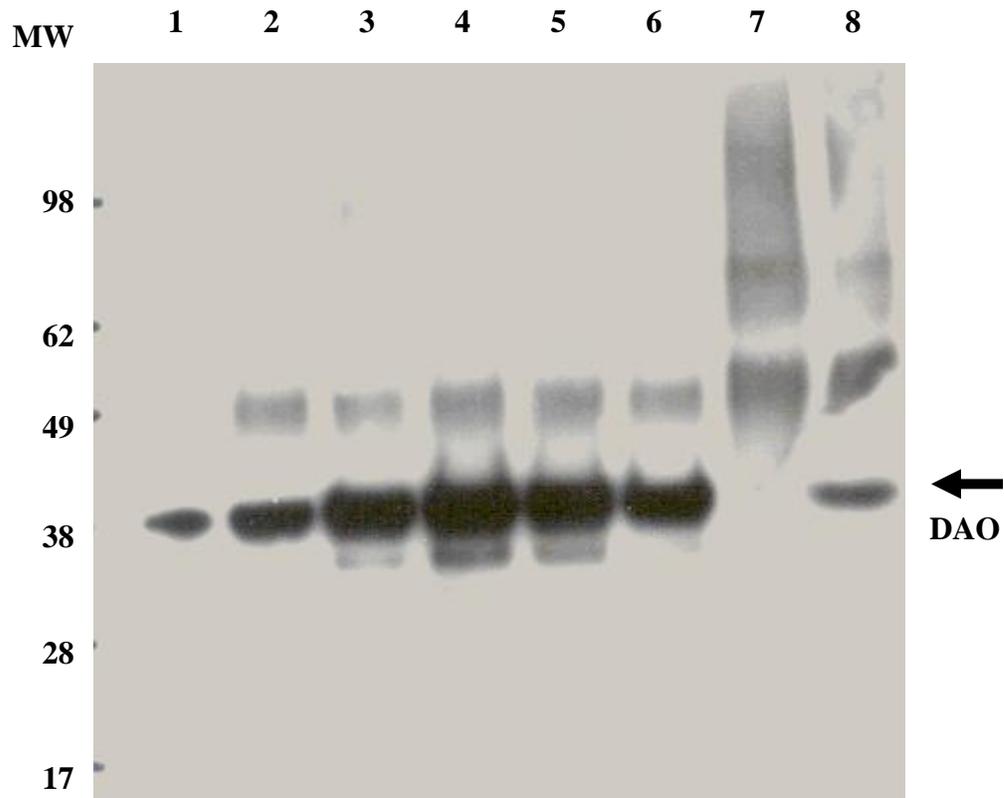

```
Legend:
Ln1:  2.5 μg hDAO Hek293 lysate
Ln2:  IP with 50 μg hDAO Hek293 lysate
Ln3:  IP with 100 μg hDAO Hek293 lysate
Ln4:  IP with 250 μg hDAO Hek293 lysate
Ln5:  IP with 500 μg hDAO Hek293 lysate
Ln6:  IP with 750 μg hDAO Hek293 lysate
Ln7:  IP with 500 μg hDAO Hek293 lysate preabsorbed with 1 μg peptide
Ln8:  IP with 500 μg hDAO Hek293 lysate preabsorbed with 0.1 μg peptide
```

Figure 3.9: Optimization of the DAO immunoprecipitation from rat cerebellar lysate using DAO antibody covalently coupled to protein A Dynal beads. As the concentration of the cerebellar lysate increases (lane 3-7) per antibody-bead sample the amount of immunoprecipitated DAO increases. The amount of DAO immunoprecipitated from 500 μg rat cerebellar lysate is equivalent to the DAO immunoprecipitated from 100 μg of hDAO-Hek293 suggesting saturation of the beads. DAO is not pulled-down when the beads are preabsorbed with 1 μg of the immunizing peptide, but see partial pull-down with 0.1 μg peptide. The expected DAO protein separation on the SDS-PAGE gel is indicated by the arrow.
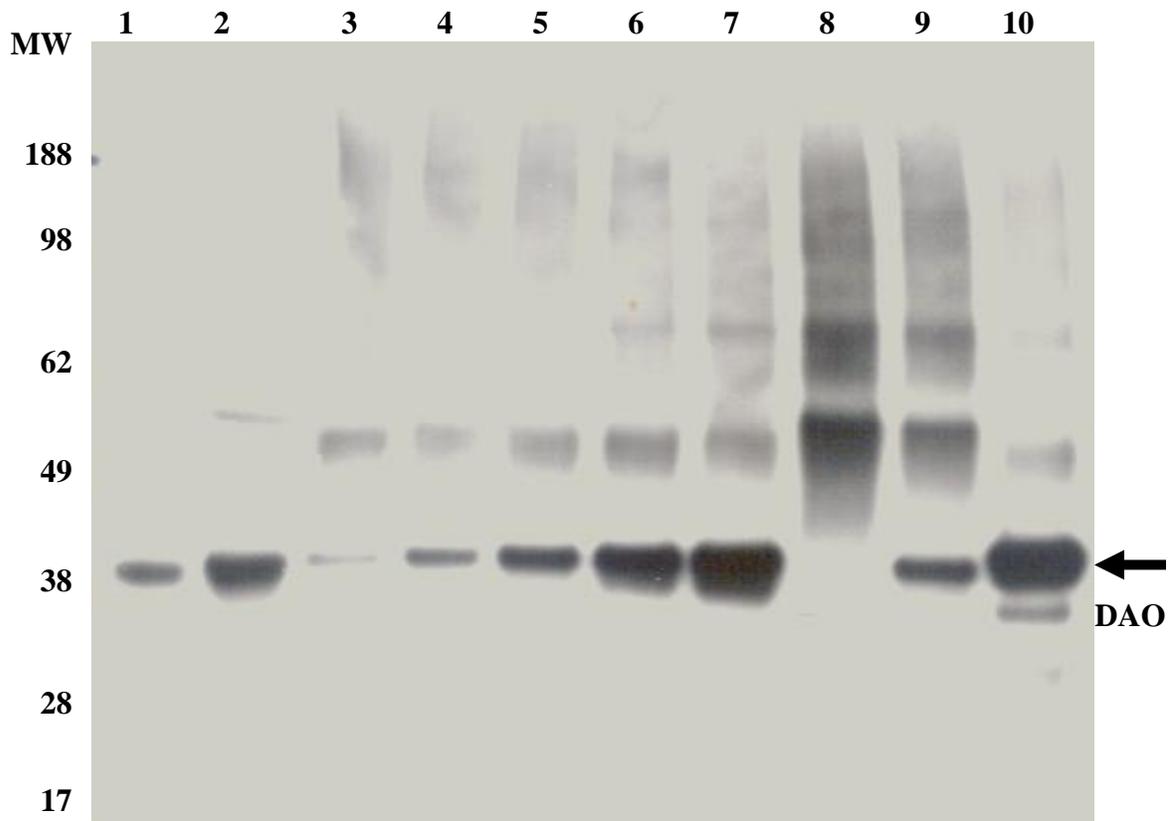
Legend:
Ln1: 10 μg rat cerebellar lysate
Ln2: 50 μg rat cerebellar lysate
Ln3: IP from 25 μg cerebellar lysate
Ln4: IP from 50 μg cerebellar lysate
Ln5: IP from 100 μg cerebellar lysate

Ln6: IP from 250 μg cerebellar lysate
Ln7: IP from 500 μg cerebellar lysate
Ln8: IP from 500 μg cerebellar lysate preabsorbed with 1 μg peptide
Ln9: IP from 500 μg cerebellar lysate preabsorbed with 0.1 μg peptide
Ln10: IP from 100 μg hDAO-Hek293 lysate

3.8 Conclusions

Two N-terminal rat DAO peptides were used to generate polyclonal antibodies in rabbits. One of the two antiserums was shown to recognize DAO lysates from both rat and human DAO stable lines while the second peptide did not yield useful DAO antiserum. The serum from the positively reactive rabbit was purified against the immunizing peptide. Due to the likely presence of contaminating antiserum a second purification against human DAO purified enzyme resulted in a very clean DAO antibody preparation. The purified antibody was successfully tested against DAO KO mice and in immunoprecipitation experiments with both rat DAO stable line and rat cerebellar lysate. Immunoprecipitation conditions for Dynal protein A beads were optimized for the maximum DAO binding capacity. These conditions were deemed suitable to be applied for a DAO interactor study.

4. Identification of putative DAO interactors through DAO antibody pull-down from rat cerebellum

4.1 Introduction

Protein-protein interactions are at the center of cellular processes including DNA replication, transcription, translation, splicing, secretion, cell cycle control, signal transduction and intermediary metabolism. Those interactions have varying degrees of affinity and specificity. The weaker interactions termed transient protein-protein interactions regulate fundamental processes such as cell growth, cell cycle, metabolic pathways and signal transduction. Thus study of protein-protein interactions plays an important role in understanding biological systems (Phizicky and Fields, 1995).

In identifying protein-protein interactions, it is important to maintain the native state of proteins to ensure identification of genuine interactors rather than aggregates of denatured proteins (Phizicky and Fields, 1995). Techniques used to asses the degree of protein interaction ultimately influence the outcome of the interactor study. Several methodologies (outlined in Table 4.1) have been widely used for the purpose of identification interacting proteins. Each of the techniques has specific benefits and disadvantages associated with them.

An understanding of the DAO interactome may give us an insight into its function and also perhaps its role in schizophrenia etiology. Knowledge of DAO interacting proteins may better allow us to understand what DAO does and the means by which its activity may be regulated through pathways which DAO has not previously been considered part of. Should DAO be found to interact with proteins known not to be expressed in the peroxisome, for example, we may be able to test its localization in relation to the new interacting partners through the likes of immunocytochemistry and electron microscopy. Such an observation would allow us to address the controversial DAO localization. Hence we propose that identification of DAO interactome, or the entire set of proteins DAO interacts with, is a valuable tool in studying the function of this enzyme.

Table 4.1: Methods used in identification of protein-protein interactions. Adapted from Howell (Howell et al., 2006)

Interaction method	Description
Yeast-2-hybrid	A high throughput screen involving use of a library fusions where the protein of interest, the bait, is fused to a DNA-binding domain and the potential interacting proteins, the prey, are fused to an activation domain. Upon a physical interaction of the bait and the prey active transcription factor is restored allowing yeast colonies to synthesize key amino acids and survive on selective media. DNA is extracted from the surviving colonies and sequenced to identify the interacting polypeptide. This approach is challenging to identify large protein interactors as those are unlikely to be part of the fusion library and may not be properly expressed.
Co-immunopre-cipitation (co-IP)	Involves specific antibody to pull-down the bait protein of interest from a protein pool or lysate and coimmunoprecipitate with it interacting proteins. After extensive washing to remove nonspecific proteins the constituents are resolved by SDS-PAGE and identified through mass spectroscopy.
Affinity chromatography	Instead of using an antibody to pull-down the bait, the bait is tagged such as with GST, TAP or His in a fusion construct. A tag-specific matrix is used to retain the bait and any interacting proteins of the bait. The tag may alter the confirmation of the bait protein thus potentially changing associated interactome. Interactors are identified via mass spectroscopy.
Phage display	A library-based method where the prey peptides are expressed as fusion proteins with the viral coat reflecting the genetic content of the virus. The phage library is exposed to the bait allowing for selection of prey virus carrying peptides capable of interacting with the bait. The genetic content of the interacting viruses is sequenced identifying the interacting peptide.
Cross-linking	This is a preferable method for identification of weaker or transient interactions. Cross-linkers quickly permeate cells and tissues allowing for stabilization of weak interactions. The preserved protein complexes containing the bait protein are separated and analyzed through mass spectroscopy. The interactome is likely dependent on the type of cross linker used.

Protein chip arrays	The bait protein is immobilized on a chip surface and exposed to potential prey proteins. Mass spectroscopy can be used to identify positive interactions.
Far-western blotting/ELISA	Involves immobilization of known prey peptides to a 2-D surface followed by addition of bait protein and detection of presence of the bait with a primary/secondary antibodies. Use of denatured proteins may alter the degree of interaction between the proteins.
Biophysical Techniques	Fluorescence resonance energy transfer is in vivo measurement of proximity between known and tagged interacting proteins. This technique is distance dependent measurement of electronic excited states of two dye molecules in which excitation from a donor is transferred onto the acceptor as long as the two are in a close proximity.

The co-immunoprecipitation (co-IP) technique for the identification of DAO interacting proteins was chosen. The use of a specific antibody allows for retention of the antigen even when the stringency of the washes are increased allowing for selection of the most robust and thus most likely true interacting proteins. This technique allows for the pull-down of DAO in its native form containing any post-translational modifications in conjunction with any preformed complexes of which DAO may be part of. DAO may not be found in the same configuration when it is synthesized with a tag in *E. coli* cells for the likes of affinity chromatography. The co-IP methodology may be less likely, however, to identify interacting proteins which are expressed at low levels (Howell et al., 2006). By using adult rat cerebellum, where DAO is highly expressed, as the source of the input for the immunoprecipitation the bait and prey concentrations are reflective of the native state preventing false positives that may result from overexpression of either the bait or the prey as could be the case in phage display.

4.2 Schematic flow of the proposed immunoprecipitation study

The immunoprecipitation with the DAO antibody and the two negative controls (described in section 4.3) led to isolation of protein complexes specific to each sample. As outlined in Figure 4.1, the samples generated through the immunoprecipitation were denatured and run on SDS-PAGE gel to separate out the proteins based on size. Each SDS-PAGE gel lane was cut into twenty even pieces and the excised bands underwent a tryptic digest resulting in shorter polypeptides representing proteins in each sample. The polypeptides generated by the tryptic digest were sequenced by mass spectroscopy and compared with the NCBI protein database to translate the identity of the proteins in each sample. The proteins identified through DAO antibody pull-down were then compared and contrasted with those of the negative controls to derive a list of DAO specific putative interacting proteins.

Figure 4.1: Schematic diagram for the proteomics strategy.

Isolation of protein complex

Biological Validation

Potential candidates

A   B   C

SDS-PAGE

Excise bands and
carry out in-gel digestion

Mass Spectroscopy

Data Analysis
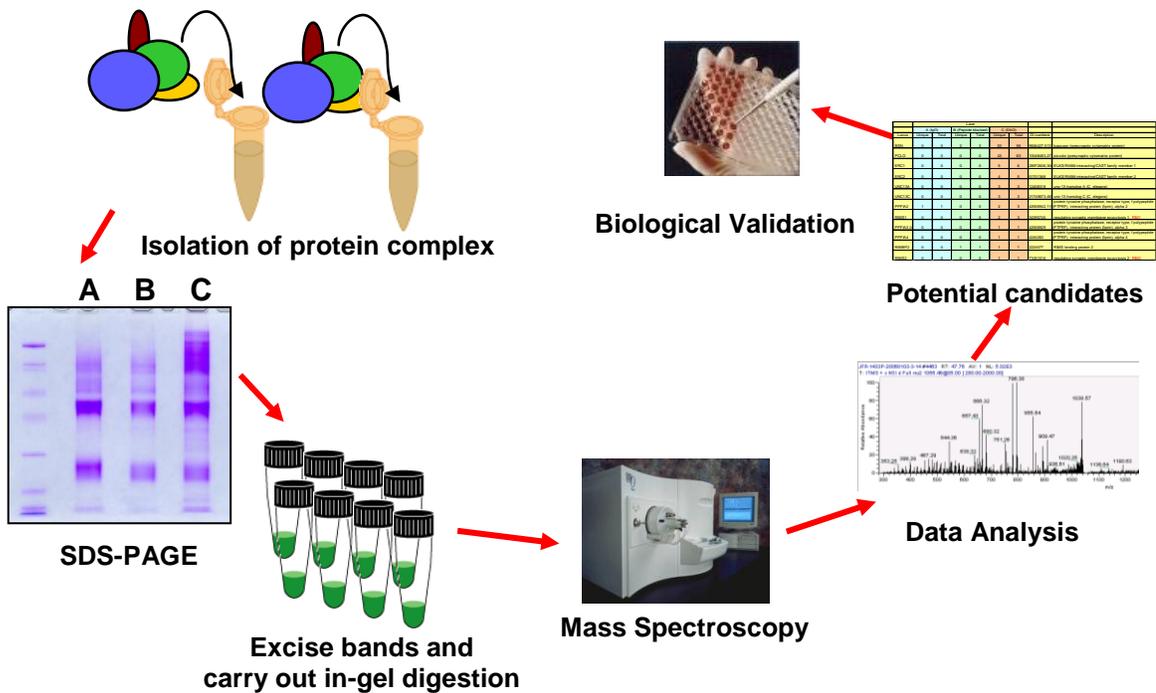
4.3 Rabbit IgG and peptide blocked DAO antibody as negative controls

Immunoprecipitation experiments are likely to yield many interacting proteins only some of which are likely attributable to a direct interaction with the bait protein. Maintaining a balance between stringency parameters to minimize nonspecific and matrix-dependent background signal while retaining the true interactors is a challenging task. Thus parameters such as prey protein concentration, ionic strength, detergent, volume and frequency of washes, and length of time/temperature for bait-prey interactions and techniques used to prepare the samples have to be optimized for best outcome (Howell et al., 2006). Furthermore, technique specific controls are critical to ascertain the likelihood of true interactors. To control for the non-specific retention of proteins by the Dynal Protein A beads or by sticking to the antibody chains two negative controls were utilized for the DAO co-immunoprecipitation: rabbit IgG and peptide blocked DAO antibody. The rabbit IgG is commonly accepted as a suitable negative control for a rabbit specific antibody so we included it in our experiment (Law et al., 2009). To more thoroughly control for non-specific sticking of proteins to the DAO antibody we prevented the capture of DAO by pre- and co-blocking the DAO antibody with the immunizing peptide during incubation with the rat cerebellar lysate. This negative control may more thoroughly control for proteins that may have affinity to our antibody then a random rabbit IgG control. As expected, both rabbit IgG pull-down and the peptide blocked DAO antibody were shown not to immunoprecipitate DAO protein from rat cerebellum as determined by SDS-PAGE gel probed with the DAO antibody (Figure 4.2). The cerebellum was used because of highly enriched DAO expression in this brain region (Verrall et al., 2007).

Figure 4.2: Optimization of negative controls for the co-IP of DAO. Two negative controls, rabbit IgG (lane 3) and peptide blocked DAO antibody (lane 2) were used to increase the confidence in the "hits" generated against the DAO antibody (lane 1). The same amount of rat cerebellar lysate was applied to the negative controls but no DAO was immunoprecipitated from the lysate. Rat cerebellar lysate, the input for the immunoprecipitation (lane 4) was used at $1/10^{th}$ the volume to verify that the lysate is expressing DAO. The resolved DAO protein on the SDS-PAGE gel is indicated by the arrow.
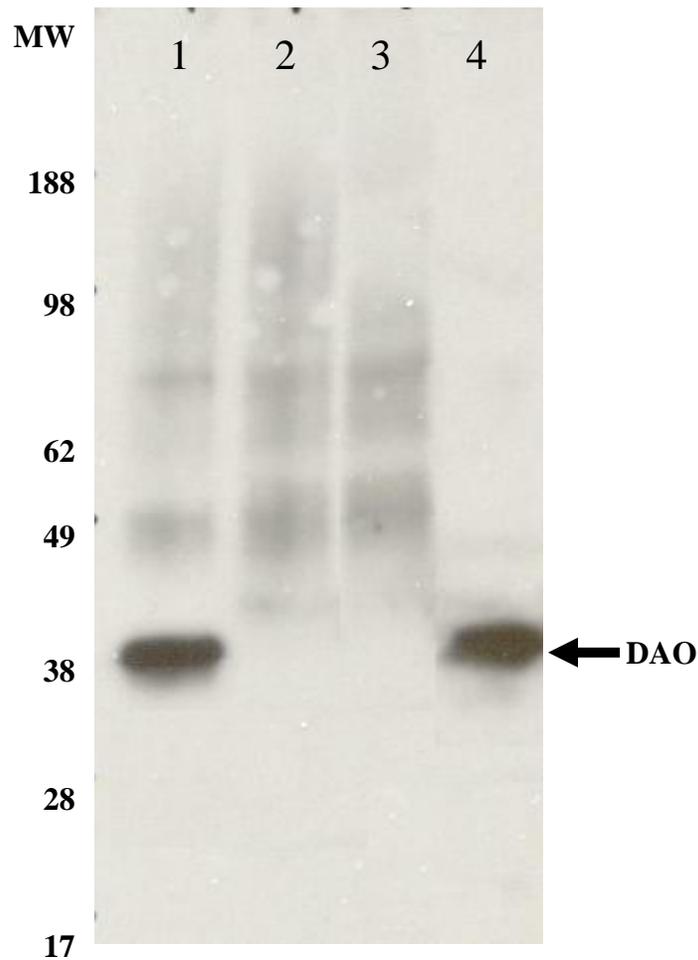
4.4 Coomassie stained gels of the eluates

The interacting proteins retained by the DAO antibody and the two negative control columns were examined for differential protein staining on the SDS-PAGE gel through visualization by the Coomassie blue stain. We expected to see enhanced protein bands in the DAO immunoprecipitation Coomassie stained SDS-PAGE lane corresponding to DAO specific interactors. This finding is especially important since we did not have a positive control. To date there are no known DAO interactors identified outside of the interaction with the product of the primate specific gene G72 (Chumakov et al., 2002).

A small portion (1/20) of the sample generated by immunoprecipitation and used for the mass spectroscopy analysis was separated on SDS-PAGE gel and stained with Coomassie stain (Figure 4.3). The possible presence of DAO in the solution from the pull-down was indicated by the green arrow. This band was not found in either of the two negative controls supporting the Western blot findings from Figure 4.2. More importantly several specific bands were present in the DAO pull-down sample represented by the greater staining at high molecular weight beyond the ~100 kDa size marker. Several small molecular weight bands of less then 20 kDa and between 30 and 40 kDa also appeared to be specific to the DAO immunoprecipitation suggesting presence of proteins that were not found in the negative controls.

Figure 4.3: Coomassie gel of the rat cerebellar immunoprecipitation input for the mass spectroscopy analysis. One-twentieth of the mass spectroscopy input was used for Coomassie stain of immunoprecipitation from rabbit IgG (lane 1), peptide blocked DAO antibody (lane 2) and DAO antibody (lane 3). Green arrow indicates band likely corresponding to DAO in the DAO pull-down column. This band is absent in the two negative controls. Black arrows highlight bands specific to the DAO immunoprecipitation sample.
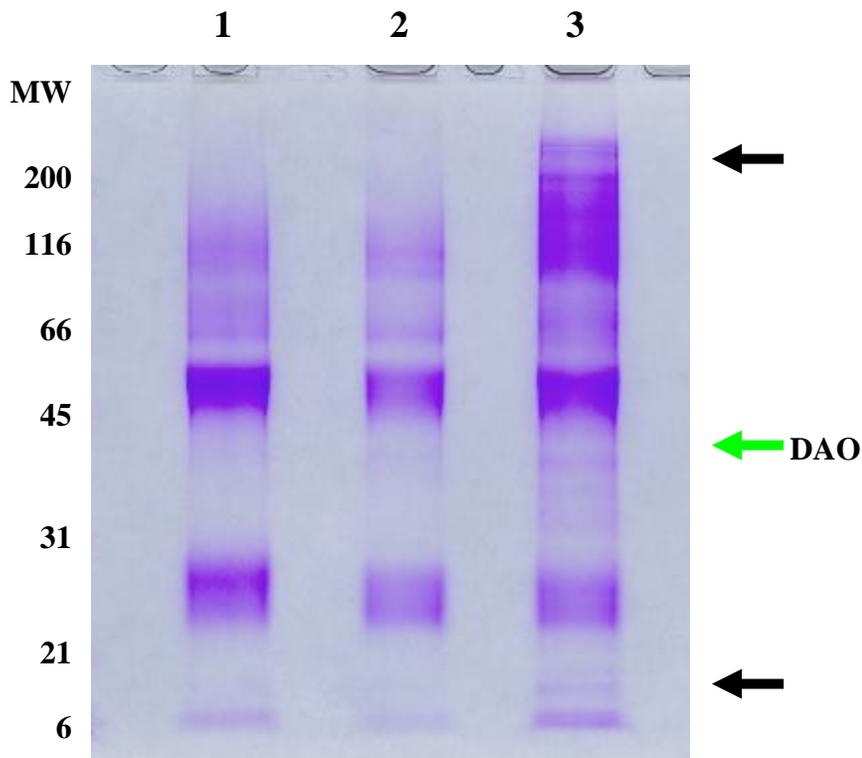
4.5 Identification of novel putative DAO interactors through mass spectroscopy using PBS as a washing buffer

While optimizing the washing conditions for the antibody containing beads we were challenged to identify an optimal procedure which would include retention of DAO interacting proteins but removal of sticky, nonspecific proteins. This was difficult to optimize because we did not have a positive control on which to rely. As a result, we decided to be conservative and use very mild washing conditions using phosphate buffered solution (PBS) in an attempt to make sure that we did not lose any of the interacting proteins. Using two negative controls we would be able to subtract out nonspecific proteins from the pool of DAO

putative interacting proteins. At the same time, having the results from the Coomassie stained SDS-PAGE gels (Figure 4.3) we had reason to believe that DAO specific interacting proteins were identified through the proposed co-immunoprecipitation from rat cerebellum.

Based on the PBS washing conditions a total of 198 putative DAO interacting proteins were identified (Table 4.2). This number represents proteins that were found in the DAO antibody immunoprecipitation column but not in either of the two negative controls. Exceptions were made for proteins that were found at very low levels (no more then two hits) in both of the two negative controls if they were identified at high concentrations in the DAO pull-down lysate. Bassoon is an example of such an exception where 52 and 94 unique and total hits respectively were identified in the DAO immunoprecipitation column but in addition 2 and 3 unique and total hits were found in the peptide blocked control respectively. The interacting proteins are highlighted in Table 4.2, where each pull-down experiment lists the abbreviated protein name, and the number of hits for each pull-down. The hits were divided into the number of unique and total hits. Unique hits were represented by the number of different polypeptides that were sequenced and identified by the mass spectroscopy and recognized as belonging to the identified protein. The greater number of unique hits may be suggestive of a stronger interacting protein or be representative of a larger protein which was digested into more fragments. Table 4.3 highlights the top 24 interacting proteins based on the number of identified hits along with their full name and molecular weight. As expected the proteins with the most hits were large proteins. Hence it was important to examine unique hits in conjunction with the total hits which represent all of the hits identified for that protein when all of the unique hits and the frequency of each unique hit were compiled together. The ideal outcome for a strong interacting protein is for a high number of unique hits to be accompanied by an even higher number of total hits. An arbitrary cut off of at least four unique hits was used to come up with the 198 interacting proteins.

Table 4.2: Putative DAO interacting proteins identified from co-immunoprecipitation experiments.

Protein Name	Sample									
	PBS Wash						RIPA Supplemented Wash			
	A (IgG)		B (Peptide blocked)		C (DAO)		D (Peptide blocked)		E (DAO)	
	Unique	Total	Unique	Total	Unique	Total	Unique	Total	Unique	Total
DYNC1H1	4	4	2	2	149	202	2	2	41	53
BSN	0	0	2	3	52	94	0	0	32	60
BAT2D1	0	0	0	0	46	100	0	0	19	46
PCLO	0	0	0	0	41	79	0	0	16	27
SACS	0	0	0	0	29	30	0	0	3	3
MYH10	0	0	0	0	20	22	2	2	4	4
ACZ	0	0	0	0	19	47	0	0	15	27
ATP6V0A1	1	1	2	2	17	51	0	0	0	0
DEPDC2	0	0	0	0	15	19	0	0	2	3
ATP6V1A	2	2	0	0	15	18	2	2	1	1
AP2A1	1	1	0	0	14	16	2	2	5	7
PRKCG	0	0	1	1	14	16	0	0	5	5
IMMT	0	0	0	0	14	16	1	1	2	3
SNIP	0	0	0	0	13	24	0	0	17	24
PC	0	0	1	1	13	14	0	0	6	7
DAO	0	0	0	0	13	28	0	0	5	7
ATP6V1B2	1	1	0	0	13	15	4	4	4	4
SDHA	2	2	0	0	13	16	0	0	0	0
NDUFA9	1	1	1	1	12	19	0	0	1	1
ANK1	1	1	0	0	12	12	0	0	1	1
AP2B1	1	1	0	0	11	11	2	2	7	8
RPS3	0	0	0	0	11	13	1	1	0	0
RAPGEF4	0	0	1	1	10	11	1	1	12	14
CEP97	0	0	0	0	10	12	0	0	4	4
SLC4A4	0	0	1	1	10	17	1	1	3	4
ARBP	0	0	1	2	10	23	1	1	1	1
MAP1A	1	1	1	1	10	13	1	1	1	1
LOC684558	0	0	0	0	10	12	0	0	1	1
SLC12A5	0	0	1	1	10	21	0	0	0	0
ERLIN2	0	0	0	0	10	13	0	0	0	0

CNTNAP1	1	1	0	0	10	13	0	0	0	0
NDUFS2	0	0	2	2	10	10	0	0	0	0
AP2A2	0	0	1	1	9	10	3	3	6	8
AP1B1	1	1	0	0	9	9	2	2	6	6
PHYHIP	0	0	0	0	9	18	0	0	5	7
MAP1B	0	0	0	0	9	12	0	0	4	4
PABPC1	1	1	2	2	9	12	0	0	4	4
PYGB	0	0	0	0	9	9	3	3	4	4
1BG3B	0	0	0	0	9	9	3	3	2	2
C1QBP	0	0	0	0	9	11	0	0	1	1
AQP4	0	0	0	0	9	85	0	0	0	0
NCAM1	1	1	0	0	9	11	1	1	0	0
ANK1	0	0	0	0	9	9	0	0	0	0
YLPM1	0	0	0	0	8	12	0	0	16	26
YLPM1	0	0	0	0	8	11	0	0	16	25
AP1B1	1	1	0	0	8	8	1	1	6	6
NAPB	1	1	0	0	8	10	2	2	4	4
DAO	0	0	0	0	8	16	0	0	2	2
TFSM	0	0	0	0	8	18	0	0	1	1
NDUFA9	1	1	1	1	8	13	0	0	1	1
MYO5A	0	0	0	0	8	9	1	1	1	1
MYH9	0	0	0	0	8	8	0	0	1	1
SLC1A2	1	1	0	0	8	21	0	0	0	0
MTCH2	0	0	0	0	8	14	0	0	0	0
ATP8A1	0	0	0	0	8	14	0	0	0	0
NDUFB5	0	0	0	0	8	10	0	0	0	0
ATP6V1C1	0	0	0	0	8	9	0	0	0	0
PRKCB	0	0	0	0	8	8	0	0	0	0
NDUFV1	0	0	1	1	8	8	1	1	0	0

ARF5	1	1	1	2	7	12	2	3	7	8
RAPGEF4	0	0	0	0	7	8	0	0	7	8
SFXN3	1	1	0	0	7	14	1	1	4	4
PPP1CB	0	0	0	0	7	7	0	0	4	6
NAPA	1	1	1	1	7	8	2	2	3	3
PYGB	0	0	0	0	7	7	2	2	3	3
RPS18	0	0	0	0	7	13	0	0	1	1
SFXN1	1	1	0	0	7	12	0	0	1	1
RAB7A	0	0	0	0	7	8	0	0	1	1
ANK2	0	0	0	0	7	7	0	0	1	1
KIF5C	0	0	0	0	7	7	0	0	1	1
NDUFB10	0	0	0	0	7	10	0	0	0	0
NEGR1	0	0	0	0	7	10	0	0	0	0
ILF2	0	0	0	0	7	9	0	0	0	0
RPS8	0	0	0	0	7	9	0	0	0	0
FLOT1	0	0	0	0	7	8	0	0	0	0
IGSF8	0	0	1	1	7	7	1	1	0	0
NDUFV2	0	0	0	0	7	7	0	0	0	0
CRMP1	1	1	0	0	6	8	1	1	16	26
CRMP1	1	1	0	0	6	8	1	1	13	24
ARF4	1	1	1	2	6	10	2	3	5	6
CHAINA	0	0	1	1	6	8	2	4	5	6
ERC1	0	0	0	0	6	8	0	0	5	5
GNB4	1	2	1	2	6	10	1	1	3	5
MAP1B	0	0	0	0	6	9	0	0	3	3
PPP1CC	0	0	0	0	6	6	1	1	3	4
MFF	0	0	0	0	6	7	0	0	2	2
ANK2	0	0	0	0	6	6	0	0	2	2
DMX2	0	0	0	0	6	6	0	0	2	2
MAP1B	0	0	1	1	6	9	0	0	1	1
ELALV1	0	0	1	1	6	8	0	0	1	1

ATP6VH1	0	0	1	1	6	8	0	0	1	1
DNM1L	0	0	0	0	6	7	1	1	1	1
RBM14	0	0	0	0	6	6	0	0	1	1
NDUFS4	0	0	0	0	6	6	0	0	1	1
NDUFB7	0	0	0	0	6	10	0	0	0	0
NDUFA12	0	0	0	0	6	9	0	0	0	0
RPS19	1	1	0	0	6	8	0	0	0	0
MAOA	0	0	0	0	6	7	0	0	0	0
DDX5	1	1	0	0	6	7	1	1	0	0
MTX2	0	0	0	0	6	7	0	0	0	0
STOML2	0	0	0	0	6	7	0	0	0	0
NDUFB8	0	0	0	0	6	6	0	0	0	0
RPL7	0	0	0	0	6	6	0	0	0	0
NDUFB11	0	0	0	0	6	6	0	0	0	0
CACNA2D1	0	0	0	0	6	6	0	0	0	0
DPP6	0	0	0	0	6	6	0	0	0	0
BIN1	0	0	0	0	6	6	0	0	0	0
CACNA2D2	0	0	0	0	6	6	0	0	0	0
SCCPDH	0	0	0	0	6	6	0	0	0	0
CLINT1	0	0	0	0	5	6	0	0	4	4
RAB2A	0	0	0	0	5	7	0	0	3	5
ENTH	0	0	0	0	5	6	0	0	3	3
EEF1A2	0	0	1	1	5	5	3	3	3	5
ANK2	0	0	0	0	5	5	0	0	3	3
DNM3	0	0	0	0	5	5	3	3	2	2
LMNB1	0	0	0	0	5	5	2	2	2	2
SYN1	1	1	0	0	5	5	2	2	2	2
RPL30	0	0	1	1	5	10	0	0	1	1
RPL14	0	0	0	0	5	6	0	0	1	1
PYGM	0	0	0	0	5	5	1	1	1	1
ELAVL1	0	0	1	1	5	5	0	0	1	1
UQCRB	1	1	0	0	5	5	0	0	1	1

NDUFA5	0	0	0	0	5	5	0	0	1	1
ATP2A3	1	1	0	0	5	10	0	0	0	0
RAP1B	0	0	0	0	5	9	2	2	0	0
NDUFS8	0	0	0	0	5	7	0	0	0	0
NFASC	0	0	0	0	5	6	1	1	0	0
HP1BP3	0	0	1	1	5	6	0	0	0	0
CAR4	0	0	0	0	5	6	0	0	0	0
KCTD12	0	0	0	0	5	5	0	0	0	0
GRIA4	0	0	0	0	5	5	0	0	0	0
RPS4X	0	0	0	0	5	5	0	0	0	0
RAA	0	0	0	0	5	5	0	0	0	0
NDUFC2	0	0	0	0	5	5	0	0	0	0
	0	0	0	0	5	5	0	0	0	0
YLPM1	0	0	0	0	4	7	0	0	9	14
DYNLL2	0	0	1	1	4	5	0	0	6	6
NCOA6	0	0	0	0	4	4	0	0	4	5
IDH3B	0	0	0	0	4	4	3	3	4	4
PURB	0	0	0	0	4	4	1	1	3	3
SLC1A6	1	1	0	0	4	7	0	0	2	2
LOC679221	1	1	0	0	4	6	0	0	2	3
MYL6	0	0	0	0	4	6	0	0	2	2
RGD1565289	0	0	1	1	4	6	0	0	2	2
GNAQ	0	0	0	0	4	6	2	2	2	2
RAB5C	0	0	0	0	4	5	1	1	2	2
RTN4	0	0	0	0	4	5	0	0	2	2
TUFM	0	0	0	0	4	4	0	0	2	2
MGST3	0	0	0	0	4	4	0	0	2	2
VAPA	0	0	0	0	4	8	1	1	1	1
TARDBP	0	0	1	1	4	7	0	0	1	1

GJA1	0	0	0	0	4	7	0	0	1	1
RPLP2	1	1	0	0	4	7	0	0	1	1
LOC685320	0	0	0	0	4	6	0	0	1	1
SEC22B	0	0	0	0	4	5	1	1	1	1
ERC2	0	0	0	0	4	5	0	0	1	1
LOC679739	0	0	0	0	4	4	0	0	1	1
DDX3X	0	0	0	0	4	4	0	0	1	1
CADM3	0	0	1	1	4	4	1	1	1	1
ANKG119	0	0	0	0	4	4	0	0	1	1
CYFIP2	0	0	0	0	4	4	0	0	1	1
NDUFA11	0	0	0	0	4	4	0	0	1	1
UQCRFS1	1	1	0	0	4	4	0	0	1	1
FAM162A	0	0	0	0	4	4	0	0	1	1
GRIA1	0	0	0	0	4	4	0	0	1	1
APOE	1	1	0	0	4	7	0	0	0	0
RPS2	1	1	0	0	4	6	0	0	0	0
SLC32A1	0	0	0	0	4	6	0	0	0	0
THY1	1	1	0	0	4	6	0	0	0	0
INPP5A	0	0	1	1	4	5	0	0	0	0
LOC683655	0	0	1	1	4	5	0	0	0	0
SDHB	0	0	0	0	4	5	0	0	0	0
RPL3	0	0	0	0	4	5	0	0	0	0
ITPR3	1	1	0	0	4	5	0	0	0	0
MAOA	0	0	0	0	4	5	0	0	0	0
MAOB	0	0	0	0	4	5	0	0	0	0
STX7	0	0	0	0	4	5	0	0	0	0
AMPH	0	0	0	0	4	5	1	1	0	0
NTM	0	0	0	0	4	5	0	0	0	0
MYH14	1	1	0	0	4	4	0	0	0	0
RGD1562953	1	1	0	0	4	4	0	0	0	0
CHCHD3	0	0	0	0	4	4	1	1	0	0

ARL8A	0	0	0	0	4	4	0	0	0	0
FINB	0	0	0	0	4	4	0	0	0	0
RPS9	0	0	0	0	4	4	0	0	0	0
RPL14	0	0	0	0	4	4	0	0	0	0
RPL22	0	0	1	1	4	4	0	0	0	0
RPS9	0	0	0	0	4	4	0	0	0	0
SLC23A12	0	0	0	0	4	4	0	0	0	0
DDOST	0	0	0	0	4	4	0	0	0	0
OGT	0	0	0	0	4	4	0	0	0	0
RPS6	0	0	0	0	4	4	0	0	0	0
DYNC1LI2	0	0	0	0	4	4	0	0	0	0
TRIM3	0	0	0	0	4	4	0	0	0	0
STX13	0	0	0	0	4	4	0	0	0	0
UNC13A	0	0	0	0	4	4	0	0	0	0
RPS6	0	0	0	0	4	4	0	0	0	0
SAMM50	0	0	0	0	4	4	0	0	0	0
DSP	0	0	0	0	0	0	0	0	11	18
DSP	0	0	0	0	0	0	0	0	6	11
CHAINB	0	0	0	0	0	0	0	0	5	5
HRNR	0	0	0	0	0	0	0	0	4	10
PFN1	0	0	0	0	0	0	0	0	4	4

Table 4.3: List of the top 24 DAO-interacting-proteins identified through the PBS washing protocol as determined by the number of unique hits. Generally there appears to be a correlation between the molecular size of the protein and the number of hits.

Abbreviation	Protein Name	Size (kDa)
DYNC1H1	Dynein heavy chain	532
BSN	Bassoon	418
BAT2D1	HBxAg transactivated protein 2	313
PCLO	Piccolo	553
PRKCG	Protein kinase C, Gamma	78
SNIP	SNAP-25-interacting protein	130
PC	Pyruvate carboxylase, mitchondrial	130
RAPGEF4	Exchange factor directly activated by cAMP 2	123
CEP97	Centrosomal protein 97	94
PHYHIP	Phyhip protein	48
MAP1B	Microtubule-associated protein 1B	270
PABPC1	Poly(A) binding protein, cytoplasmic 1	71
YLPM1	YLP motif containing 1	241
AP1B1	Adopted-related protein complex 1, beta 1	106
PPP1CB	Protein phosphate 1	37
CRMP1	Crmp 1 protein	74
ERC1	ELKS/RAB6-interacting/CAST family member	128
CLINT1	Clathrin interactor 1	68
DYNLL2	Dynein, light chain	24
NCOA6	Peroxisome proliferator activater receptor interacting protein	218
DSP	Desmoplakin 1	332
CHAINB	Chain B, perchloric acid soluble protein-a translational inhibi	14
HRNR	Homeric precursor	282
PFN1	Profilin 1	15

4.6 Optimization of harsh washing conditions

The number of putative interacting proteins identified through the mild PBS wash was much greater then could be reasonably evaluated experimentally making it difficult to select direct DAO interactors. Proteins identified in the DAO pull-down lysate may be part of larger protein complexes which were retained because a mild washing procedure was employed. A schematic of such interaction is depicted in Figure 4.4. Alternatively, some of the hits were non-

specific but retained because a mild wash was employed. Consequently, a more stringent washing was optimized to narrow down the number of interacting proteins and focus on the strongest of interactors.

Figure 4.4: A schematic diagram depicting a direct interaction of DAO (back circle) with protein x (green oval) result in immunoprecipitation of two other proteins (red and blue rectangles) which are not in a direct contact with DAO itself.

DAO antibody/bead
complex
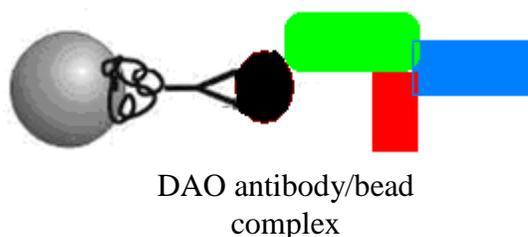
While using the PBS wash as a control other conditions including RIPA buffer alone and in combination with higher salt (NaCl) and SDS were tested. Initially the harsher washing options were tested to determine if DAO protein was washed away. This was shown not to be the case as DAO was retained during every washing condition (Figure 4.5). Subsequently, the sensitivity of the Silver stain was used to observe differences between the PBS wash and the other washes. The SDS-PAGE lane corresponding to the PBS washed samples contained the most silver staining (Figure 4.6) out of all of the samples. Consequently, the RIPA buffer supplemented with 500 mM NaCl and 0.1% SDS was selected for a repeat of the DAO immunoprecipitation from adult rat cerebellum (six weeks of age), and precipitates were separated on SDS-PAGE gel and Coomassie stained (Figure 4.7). In this gel, the DAO immunoprecipitation sample is darker with specific pronounced 200 kDa and higher molecular weight bands suggesting pull-down of specific DAO interactors. Consistent with this observation several high molecular DAO specific interacting proteins such as

bassoon, piccolo and dynein heavy chain were identified in the DAO pull-down lysate but not in the negative controls (Table 4.2). A total of 24 hits with the more stringent washing conditions were identified (Table 4.2). Thus the harsher wash conditions likely eliminated transient or weak interacting proteins and proteins that were part of a larger complex resulting in a core of proteins which are likely interacting with the DAO enzyme directly when the cerebellar cell membranes are ruptured and all of the proteins are free to interact with each other.

The proteins identified in the two immunoprecipitation experiments were grouped based on bioinformatics analysis of function and localization. This analysis resulted in identification of distinct groups consisting of presynaptic active zone, vesicle, syntaxin, RAB, NADH dehydrogenase, and ATPase/proton transporting protein subunits. Each group is described below.

Figure 4.5: Optimization of washing conditions for the DAO antibody beads using SDS-PAGE gel probed with the DAO antibody. DAO is immunoprecipitated under all of the washing conditions suggesting that once captured by the antibody it does not easily dissociate from the antibody-bead complex. DAO was immunoprecipitated from 800 μg of rat cerebellar lysate and subsequently washed with PBS (lane 1), RIPA (lane 2), Ripa supplemented with 500 mM NaCl (lane 3), RIPA with 0.1% SDS (lane 4), RIPA with 500 mM NaCl and 0.1% SDS (lane 5), RIPA with 0.5% SDS (lane 6), and the input lysate 1/10th volume (lane 7).

Figure 4.6: Optimization of washing conditions for the DAO antibody beads using SDS-PAGE gel stained with Silver stain. The immunoprecipitate using DAO specific antisera beads were washed with several stringent washing buffers to remove weak interacting proteins. The PBS wash (lane 1) leaves the most proteins on the beads as reflected by higher staining between 28 and 39 kDas then in any of the other washes: RIPA (lane 2), RIPA supplemented with 500 mM NaCl (lane 3), RIPA with 0.1% SDS (lane 4), RIPA with 500 mM NaCl and 0.1% SDS (lane 5), RIPA with 0.5% SDS (lane 6), and the input lysate (lane 7). The DAO band is visible just above the 39 kDa marker reflecting the observations made in Figure 4.5 with the DAO antibody. The expected DAO protein separation on the SDS-PAGE gel is indicated by the arrow.
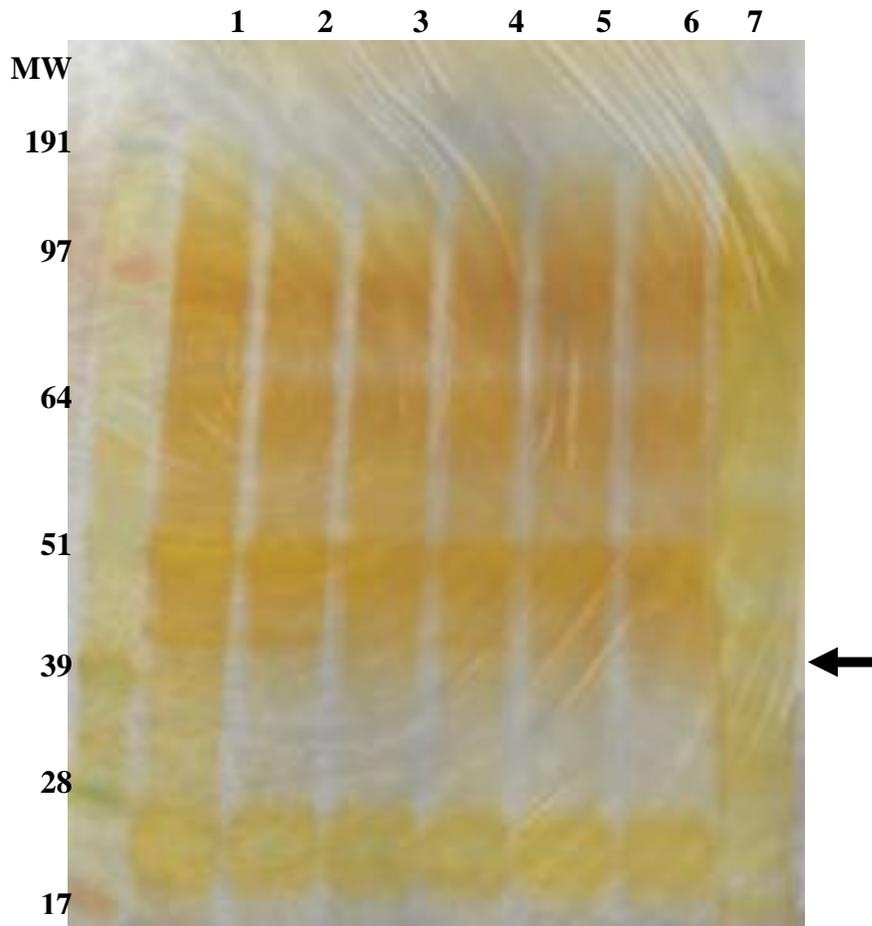
Figure 4.7: SDS-PAGE gel stained with Coomassie blue representing the samples generated using the high stringency wash for the mass spectroscopy analysis. The DAO immunoprecipitation sample, in lane 2, is darker with specific pronounced 200 kDa and higher molecular weight bands suggesting pull-down of specific DAO interactors. The expected DAO protein separation on the SDS-PAGE gel is indicated by the arrow.

Legend:
Ln 1: IP from 800 µg cerebellum preabsorbed with 1 µg peptide
Ln 2: IP from 800 µg cerebellum
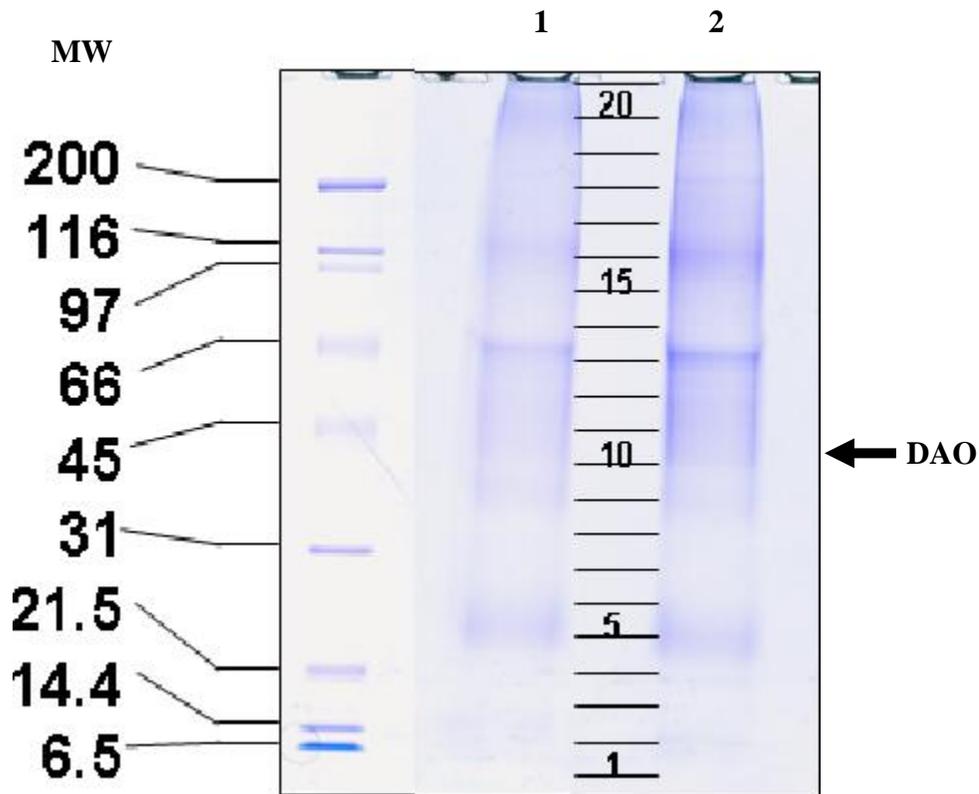
4.6.1 Presynaptic active zone interacting proteins

The presynaptic active zone, also known as 'cytomatrix assembled at active zone' (CAZ) consists of a complex network of proteins involved in the organization of docking and priming of synaptic vesicles for their release into the synaptic cleft (Figure 4.8). Thus at the CAZ electrical signals are converted into chemical messages which are propagated in the form of neurotransmitter release mediating communication with the postsynaptic membrane on adjacent neurons (Rizo and Rosenmund, 2008). Proteins including Munc13s, RIMs, ELKS, PCLO and BSN have been shown to be enriched in the active zones where they play diverse functions in vesicle fusion and neurotransmitter release (Schoch and Gundelfinger, 2006).

Many of the above mentioned proteins were identified as putative DAO interactors (Table 4.4) suggesting DAO localization within the active zone where it may contribute to D-serine metabolism or take on alternative functions. The presynaptic active zone proteins were found to be the strongest set of interacting proteins identified in both immunoprecipitation experiments as determined by the greatest number of unique and total hits as well as by the percent of the protein identified by the mass spectroscopy (Table 4.5). Out of the presynaptic proteins identified in the DAO interactome, BSN stood out as the most likely interacting protein with DAO as 29% of the entire BSN protein was identified in the DAO immunoprecipitate. This coverage is very close to that of DAO itself (30%) implying a significant interaction between the two proteins. A 30% coverage suggests a good retention of the DAO by its antibody as others have reported 18% in case of TRAF2 and NCK interacting kinase (TNIK) self immunoprecipitation (Mahmoudi et al., 2009). The percent protein coverage is not a function of a protein's size as other large proteins such as PCLO were found to be recovered and sequenced at a rate of 18%. Hence the larger the amount of any given protein that is being immunoprecipitated the greater the percent of that protein being sequenced by mass spectroscopy because the tryptic fragments are more abundant and are more likely to be picked up as hits. Finally, the CAZ interactors suggest a novel DAO localization, potentially outside of the peroxisome.

Figure 4.8: Diagram of the presynaptic active zone including the proteins that were identified through the DAO immunoprecipitation highlighted in red. Adopted from Schoch (Schoch and Gundelfinger, 2006).

Fig. 2 Schematic diagramm of interactions of CAZ proteins and the resulting network at the active zone (f
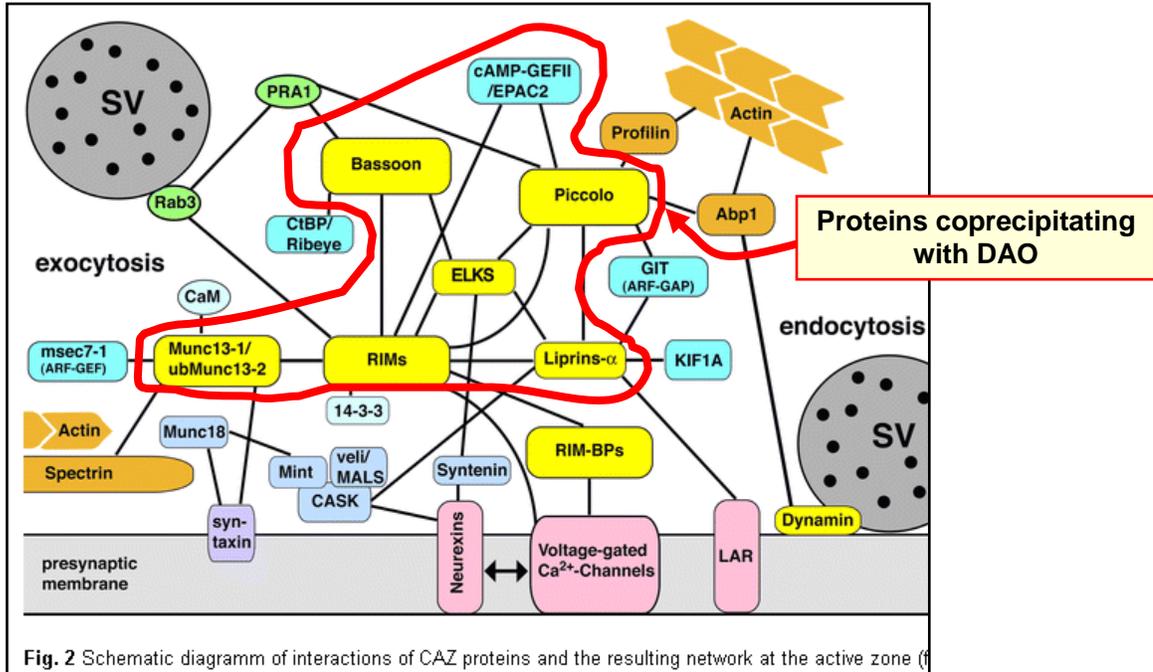
Table 4.4: Summary of the presynaptic active zone proteins identified by the mass spectroscopy from the DAO immunoprecipitation experiments from adult rat cerebellum using both mild and harsh washing conditions.

Protein Name	Sample									
	PBS Wash						RIPA Supplemented Wash			
	A (IgG)		B (Peptide blocked)		DAO		D (Peptide blocked)		DAO	
	Unique	Total	Unique	Total	Unique	Total	Unique	Total	Unique	Total
BSN	0	0	2	3	52	94	0	0	32	60
PCLO	0	0	0	0	41	79	0	0	16	27
STXBP1	7	7	4	4	28	36	7	11	13	17
DNM1	2	2	1	1	11	12	4	4	11	11
ERC1	0	0	0	0	6	8	0	0	5	5
DNM1L	0	0	0	0	6	7	1	1	1	1
DNM3	0	0	0	0	5	5	3	3	2	2
ERC2	0	0	0	0	4	5	0	0	1	1
UNC13A	0	0	0	0	4	4	0	0	0	0
RUMS1	0	0	0	0	2	3	0	0	1	1
PPFIA3	0	0	0	0	2	3	0	0	0	0
RIMS3	0	0	0	0	1	2	0	0	0	0

Table 4.5: The strength of the interaction was measured in terms of the percent protein coverage for the presynaptic active zone constituents. As a control DAO was found at 30% suggesting that Bassoon at 29% may be a strong interacting partner.

Protein	Protein MW (kDa)	% Protein Coverage
Bassoon	418	29
Piccolo	552	18
Epac2	123	25
ELKS	128	12
Munc13-1	196	5
RIM1	110	10
Liprin-α-3	149	3
DAO	39	30

4.6.2   Vesicle-associated membrane proteins (VAMPs)

The vesicle-associated membrane proteins (VAMPs) are soluble N-ethylmaleimide-sensitive factor attachment protein receptor (SNARE) proteins that are required for synaptic vesicle fusion (Chen and Scheller, 2001). Eight VAMP proteins (1-8) have been cloned and identified many of which were co-immunoprecipitated with DAO (Table 4.6). VAMP 1 and 2 (also known as synaptobrevins), found on membrane of synaptic vesicles, trigger vesicle fusion with the presynaptic membrane through an interaction with presynaptically expressed syntaxin-SNAP25 (Wang and Tang, 2006). Some of the VAMPs appear to be more critical then others. VAMP3 knockout mice were found not to be adversely affected (Yang et al., 2001) while VAMP2 knockout mice died immediately after birth and embryonic hippocampal neurons from the VAMP2 animals displayed 100-fold decrease in calcium mediated synaptic vesicle fusion as compared to hippocampal neurons from wildtype animals (Schoch et al., 2001). The difference may be due to functional redundancy in one instance but not the other.

The VAMPs represent a potential group of DAO interacting proteins which are part of the active zone. These proteins, however, are not as robustly

pulled-down as the active zone constituents outlined in Table 4.4 or the syntaxins in Table 4.7, especially with the harsh washing conditions. Furthermore, the VAMPs are much more likely to non-specifically interact with the matrix or the rabbit IgG since there are substantial hits in either the rabbit IgG or the peptide blocked negative controls as compared to the DAO pull-down (Table 4.6).

Table 4.6: Summary of the vesicle-associated membrane proteins identified by the mass spectroscopy from the DAO immunoprecipitation experiments from adult rat cerebellum using both mild and harsh washing conditions.

Protein Name	Sample									
	PBS Wash						RIPA Supplemented Wash			
	A (IgG)		B (Peptide blocked)		DAO		D (Peptide blocked)		DAO	
	Unique	Total	Unique	Total	Unique	Total	Unique	Total	Unique	Total
VAMP2	3	3	1	1	5	8	2	4	4	9
SEC22B	0	0	0	0	4	5	1	1	1	1
VAMP1	0	0	0	0	2	2	0	0	2	2
VAMP3	2	2	1	1	5	7	2	4	2	6
SV2B	0	0	1	1	1	5	0	0	0	0
VAMP5	0	0	1	1	1	1	0	0	1	1
VAPB	0	0	0	0	1	1	0	0	0	0

4.6.3   Syntaxin interacting proteins

The syntaxin family consists of 15 genes in mammals, many of which are expressed as different isoforms depending on the tissue and developmental stage (Teng et al., 2001). Syntaxin 1A interacts with SNAP-25 at the presynaptic membrane to form the target-membrane SNARE which forms a tight bond with VAMPs found on the synaptic vesicles allowing for release of neurotransmitters (Wang and Tang, 2006). The syntaxins are restricted in expression with syntaxin 18 localized to the endoplasmic reticulum, syntaxin 5 to the cis-Golgi and syntaxins 7, 8, 11, 12 and 13 to endosomes (Teng et al., 2001).

The identification of syntaxins in the DAO immunoprecipitates look relatively specific to the DAO pull-down with the exception of the strongest two

interacting proteins STX1B1 and STS1B which where also found in the negative controls (Table 4.7). Since all of the hits retained after the mild wash were removed by the harsh wash, the syntaxins may represent a transient group of DAO interacting proteins or they may have been retained by indirectly interacting with DAO.

Table 4.7: Summary of the syntaxins identified by the mass spectroscopy from the DAO immunoprecipitation experiments from adult rat cerebellum using both mild and harsh washing conditions.

Protein Name	Sample									
	PBS Wash						RIPA Supplemented Wash			
	A (IgG)		B (Peptide blocked)		DAO		D (Peptide blocked)		DAO	
	Unique	Total	Unique	Total	Unique	Total	Unique	Total	Unique	Total
STX1B1	2	2	0	0	9	19	0	0	1	1
STS1B	3	5	2	3	7	32	0	0	0	0
STX7	0	0	0	0	4	5	0	0	0	0
STX12	0	0	0	0	4	4	0	0	0	0
STX13	0	0	0	0	4	4	0	0	0	0
STXBP1	1	1	0	0	3	4	0	0	0	0
STX16	0	0	0	0	2	2	0	0	0	0
STX6	0	0	0	0	2	2	0	0	0	0
STX3	0	0	0	0	1	1	0	0	0	0
STXBP5	0	0	0	0	1	1	0	0	0	0
STXBP5L	0	0	0	0	1	1	0	0	0	0
STX1A	0	0	0	0	1	1	0	0	1	1

4.6.4 RAS oncogene family (Rab) interacting proteins

Unlike the CAZ proteins, Rabs are small (20-29 kDa) ubiquitously expressed proteins belonging to the Ras superfamily of monomeric G-proteins with more then 60 members found in mammalian cells, 28 of which were identified on neuronal synaptic vesicles (Fukuda, 2008; Schultz et al., 2000). Rabs have specific functions, for example, Rab1 and Rab 2 are involved in vesicle creation in the Golgi, while Rab3 and Rab27 assist in transport along the actin and tubulin framework and assist vesicle membrane fusion (Fukuda, 2008). Rabs cycle between cytoplasm and the membrane of the targeting organelles where

conformational changes associated with guanidine-nucleotide binding and hydrolysis regulate the activity of Rabs. GTP coupled Rabs are in the active form and are membrane bound where they are recognized by effectors while Rabs in the GDP-form are inactive (Lang and Jahn, 2008). Rabs have been shown to play a role in regulation of membrane docking, priming and stimulus dependent fusion (Grosshans et al., 2006) highlighting a potential DAO involvement in neurotransmitter release.

Among the Rabs identified through the immunoprecipitation, Rab7A and Rab2A, (Table 4.8) are more likely to represent DAO interactors because they are only found in the DAO pull-down lysate in both of the immunoprecipitation experiments and at a fairly high level given their relatively small size. Rab7A have been found to associate with Charcot-Marie-Tooth (CMT) type 2 neuropathy which is an autosomal-dominant axonal disorder (Spinosa et al., 2008). Rab2A was found to be essential for protein transport from the endoplasmic reticulum to the Golgi complex (Tisdale and Balch, 1996).

Table 4.8: Summary of the Rabs identified by the mass spectroscopy from the DAO immunoprecipitation experiments from adult rat cerebellum using both mild and harsh washing conditions.

Protein Name	Sample									
	PBS Wash						RIPA Supplemented Wash			
	A (IgG)		B (Peptide blocked)		DAO		D (Peptide blocked)		DAO	
	Unique	Total	Unique	Total	Unique	Total	Unique	Total	Unique	Total
Rab7A	0	0	0	0	7	8	0	0	1	1
ERC1	0	0	0	0	6	8	0	0	5	5
Rab35	2	3	2	2	6	11	2	3	2	3
Rab2A	0	0	0	0	5	7	0	0	3	5
Rab6B	1	2	2	4	5	9	3	7	2	8
Rab3A	1	2	4	6	5	15	3	3	5	6
Rab6A	1	2	1	1	5	9	2	2	2	3
Rab10	2	3	2	2	5	10	2	3	2	3
Rab1B	2	3	2	2	4	10	2	3	3	4
Rab1A	2	3	2	2	4	12	2	3	3	4
Rab14	1	2	1	1	4	8	1	1	2	3
Rab5C	0	0	0	0	4	5	1	1	2	2
Rab5B	0	0	0	0	3	4	1	1	1	1
Rab11B	0	0	1	1	3	5	1	1	1	1
Rab21	0	0	0	0	3	4	0	0	0	0

Rab2B	0	0	0	0	3	4	0	0	1	1
Rab8A	2	3	2	2	3	8	2	3	2	3
Rab39	1	2	1	1	2	5	1	1	1	2
Rab23	0	0	0	0	2	2	0	0	0	0
Rab3C	1	2	1	1	2	5	1	1	1	2
Rab39B	1	2	1	1	2	5	1	1	1	2
Rab5A	0	0	0	0	1	2	0	0	1	1
Rab3IP	0	0	0	0	1	1	0	0	0	0
Rab15	0	0	0	0	1	2	0	0	0	0
Rab18	0	0	0	0	1	1	0	0	1	1

4.6.5 Nicotinamide adenine dinucleotide dehydrogenase (NADH) interacting proteins

The nicotinamide adenine dinucleotide dehydrogenase interacting proteins identified through the DAO co-immunoprecipitation are part of the mammalian mitochondrial respiratory complex I. This complex consists of at least 46 subunits, seven of which are encoded by mitochondrial DNA (Carroll et al., 2003). Complex I is embedded in the inner mitochondrial membrane where it transfers electrons from NADH to ubiquinone (Benit et al., 2001). Deficiency in the complex I leads to neurological disorders such as Parkinson's disease (Schapira et al., 1990), Alzheimer's disease (Coskun et al., 2004), Huntington disease (Arenas et al., 1998) and most commonly Leigh syndrome (Iuso et al., 2006).

Most of the apparent interactions between DAO and NADH dehydrogenase proteins are weak at best as the complex I subunits were for the most part only immunoprecipitated when the weak wash was used (Table 4.9). None of the proteins were retained with the harsh wash. Furthermore, the potential expression of DAO within the mitochondria suggested by this data is in contrast to what has been published in cultured human astrocytes (Sacchi et al., 2008). Hence the likelihood of the interaction between DAO and NADH dehydrogenase proteins *in vivo* may be low. An interaction in vitro between NADH complex and DAO may explain the quantity of proteins identified through the mass spectroscopy in the immunoprecipitated lysate.

Table 4.9: Summary of the NADH dehydrogenase proteins identified by the mass spectroscopy from the DAO immunoprecipitation experiments from adult rat cerebellum using both mild and harsh washing conditions.

Protein Name	Sample									
	PBS Wash						RIPA Supplemented Wash			
	A (IgG)		B (Peptide blocked)		DAO		D (Peptide blocked)		DAO	
	Unique	Total	Unique	Total	Unique	Total	Unique	Total	Unique	Total
NDUFS1	4	4	1	1	18	31	1	1	0	0
NDUFA9	1	1	1	1	12	19	0	0	1	1
NDUFS2	0	0	2	2	10	10	0	0	0	0
NDUFS3	2	2	1	1	8	11	0	0	1	1
NDUFB5	0	0	0	0	8	10	0	0	0	0
NDUFV1	0	0	1	1	8	8	1	1	0	0
NDUFB10	0	0	0	0	7	10	0	0	0	0
NDUFV2	0	0	0	0	7	7	0	0	0	0
NDUFS4	0	0	0	0	6	6	0	0	1	1
NDUFB7	0	0	0	0	6	10	0	0	0	0
NDUFB8	0	0	0	0	6	6	0	0	0	0
NDUFB11	0	0	0	0	6	6	0	0	0	0
NDUFA13	1	1	1	1	4	4	0	0	1	1
NDUFA5	0	0	0	0	5	5	0	0	1	1
NDUFS7	1	1	1	1	5	10	0	0	0	0
NDUFS8	0	0	0	0	5	7	0	0	0	0
NDUFC2	0	0	0	0	5	5	0	0	0	0
LOC679739	0	0	0	0	4	4	0	0	1	1
NDUFA11	0	0	0	0	4	4	0	0	1	1
NDUFB4	1	1	0	0	3	3	0	0	1	1
NDUFS5	0	0	0	0	3	5	0	0	0	0
NDUFB9	0	0	0	0	3	4	0	0	0	0
NDUFA8	0	0	0	0	3	4	0	0	0	0
CYB5R3	0	0	0	0	3	4	0	0	0	0
CYB5R1	0	0	0	0	3	4	0	0	0	0
NDUFAB1	0	0	0	0	3	3	0	0	0	0
ND4	0	0	0	0	2	7	0	0	0	0
NDUFA7	0	0	0	0	2	3	0	0	0	0
ND1	0	0	0	0	2	2	0	0	0	0
NDUFA2	1	1	0	0	2	2	0	0	0	0
NDUFA6	0	0	0	0	1	3	0	0	1	1
NDUFB6	0	0	0	0	1	2	0	0	0	0
ND3	0	0	0	0	1	1	0	0	0	0
ND2	0	0	0	0	1	1	0	0	0	0

4.6.6 ATPase/H+ transporting subunits interacting proteins

Proton transporting proteins are involved in acidification of intracellular organelles including clathrin coated vesicles, endosomes, lysosomes, synaptic vesicles and others. The function of the proton pumping allows for protein processing and degradation, intracellular targeting, and receptor-mediated endocytosis (Nishi et al., 2003).

Many of the proton transporting proteins identified are not specific to the DAO immunoprecipitation suggesting non-specific interaction with the Protein A beads or to the antibody (Table 4.10). A notable exception is ATP6V0A1 which is robustly immunoprecipitated specifically with DAO pull-down. However the observed pull-down of ATP6V0A1 and of other proton transporting proteins is reduced with a harsh wash.

4.7 Conclusions

The immunoprecipitation experiment with the purified DAO antibody utilizing rat cerebellum lysate from six weeks old rats resulted in a robust pull-down of DAO (Table 4.2). This methodology in conjunction with a mild PBS wash resulted in identification of 198 putative DAO interactors which were co-immunoprecipitated with DAO but were not found at significant levels in either of the two negative controls, the rabbit IgG or the peptide blocked DAO antibody. The extent of the interacting proteins identified necessitated use of means by which only a handful of interacting proteins representing the strongest interactors would be selected. To this end, harsher washing conditions utilizing RIPA buffer supplemented with salt (NaCl) and SDS were used in subsequent immunoprecipitation experiments. The harsh wash allowed DAO retention by the DAO antibody but led to significantly fewer interacting proteins (Figure 4.5 and 4.6). The list of 198 interacting proteins identified with the mild wash was reduced to 24 proteins through application of the RIPA supplemented buffer which are likely representing stronger DAO interactors. The putative interacting proteins were grouped based on function and localization suggesting DAO presence within the active zone potentially interacting with BSN. The focus of

the next chapter will be on elaboration of the interaction between those two proteins.

Table 4.10: Summary of ATPase/H+ transporting proteins identified by the mass spectroscopy from the DAO immunoprecipitation experiments from adult rat cerebellum using both mild and harsh washing conditions.

Protein	Sample									
Name	PBS Wash						RIPA Supplemented Wash			
	A (IgG)		B (Peptide blocked)		DAO		D (Peptide blocked)		DAO	
	Unique	Total	Unique	Total	Unique	Total	Unique	Total	Unique	Total
ATP6V0A1	1	1	2	2	17	51	0	0	0	0
ATP6V1A	2	2	0	0	15	18	2	2	1	1
ATP6V1B2	1	1	0	0	13	15	4	4	4	4
ATP6V0D1	2	2	2	2	11	23	1	1	1	1
ATP5O	5	5	5	5	11	15	5	8	6	9
ATP6V1E1	2	3	1	1	8	10	2	2	5	5
ATP6V1C1	0	0	0	0	8	9	0	0	0	0
ATP5H	2	2	0	0	7	11	2	2	3	7
ATP6V1H	0	0	1	1	6	8	0	0	1	1
ATP5L	2	4	3	3	5	6	0	0	4	5
ATP12A	0	0	0	0	3	5	2	7	1	9
ATP4A	1	2	1	1	3	5	1	5	1	2
ATP5I	0	0	2	2	3	4	0	0	0	0
ATP6V1E2	0	0	0	0	3	3	0	0	0	0
ATP5J2	1	1	1	1	2	3	1	2	2	2
ATP6V0C	1	1	0	0	2	5	0	0	0	0
ATPF8	0	0	0	0	2	3	0	0	1	1
ATP5C1	1	1	1	1	2	3	1	1	1	1
ATP12A	1	1	0	0	2	2	1	1	1	1
ATP6V1D	0	0	0	0	2	2	0	0	0	0
ATP6AP1	0	0	0	0	2	2	0	0	0	0
ATP6AP2	0	0	0	0	1	1	0	0	0	0
ATP6V0D2	0	0	0	0	1	1	0	0	0	0

5. The Synapse

5.1 Introduction

The synapses of the central nervous system are contact points between neurons where messages are relayed from the presynaptic axon across the synaptic cleft to the postsynaptic dendrites. At the synapse, an electrical signal is converted into a chemical message through release of neurotransmitters from synaptic vesicles which cross the synaptic cleft and induce an electrical signal on the postsynaptic end through neurotransmitter receptors (Specht and Triller, 2008). Both the presynaptic and the postsynaptic plasma membranes at the synaptic junctions are characterized by electron-dense meshworks of proteins. The cytoskeletal protein matrix on the presynaptic side is called the 'cytometrix assembled at the active zones' (CAZ) (Garner et al., 2000). The CAZ is a specialized region where synaptic vesicles are anchored and primed prior to the membrane fusion and neurotransmitter release (Owald and Sigrist, 2009). This region is composed of dense network of filaments which extend out from the presynaptic membrane into the cytoplasm (Figure 5.1). The CAZ is thought of as a "core scaffold" for the presynaptic, cytosolic and membranous protein constituents as it is especially resistant to extraction procedures (Schoch and Gundelfinger, 2006). Despite the apparent stability of the CAZ many of its members including bassoon were found to be more fluid and "jump" between neighboring active zones (Kalla et al., 2006; Tsuriel et al., 2009). Five protein families have been found to be highly enriched in the active zone including Munc13s, which are essential for neurotransmitter release (Betz et al., 2001; Varoqueaux et al., 2002), scaffolding proteins including RIMs (Schoch et al., 2002; Wang et al., 2000), and ELKS (Takao-Rikitsu et al., 2004), liprin-α, and BSN and PCLO (Schoch and Gundelfinger, 2006). BSN and PCLO are large proteins (>400 kDa) and play a major role in the organization of the CAZ likely as scaffolding elements (Fenster et al., 2000; tom Dieck et al., 1998). Many of these and other proteins have been shown to physically associate in the active zone. For example, Munc13 has been shown to interact with RIM (Betz et al., 2001) while BSN and PCLO interact with ELKS (Takao-Rikitsu et al., 2004).

The presynaptic components are transported from the trans-Golgi to the designated axonal regions through specialized vesicular organelles that contain at least two classes of transport vesicle (Goldstein et al., 2008). The PCLO-BSN transport vesicles are dense-core 80 nm vesicles which were shown to carry the two large proteins into the nascent synapses (Zhai et al., 2001). The synaptic vesicle precursors are more heterogeneous and carry other synaptic proteins (Jin and Garner, 2008). The presynaptic proteins have been shown to be preassembled in the transport vesicles thus a functional synapse can be formed within minutes upon fusion of the vesicles in the axon.

Figure 5.1: An electron micrograph image of the synapse. The presynaptic terminus is marked by the presence of synaptic vesicles in the central part of the image (labeled with a green arrow). The synapse is between the dark stained region which represents the pre and post synaptic density (labeled with the red arrow). Taken from Siksou (Siksou et al., 2007)
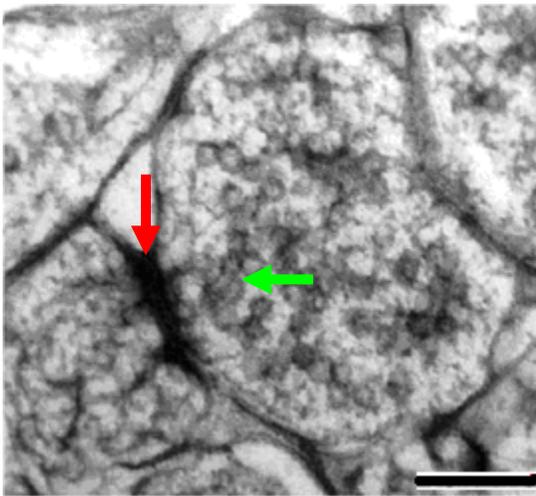
5.2 Bassoon

In an effort to determine the bassoon region responsible for synaptic targeting GFP-tagged BSN truncation mutants were generated based on functional domains (Dresbach et al., 2003). Intact full-length BSN C-terminally labeled with GFP was targeted to the axonal synapses where it was incorporated into the cytoplasmic active zone. When transiently transfected in cultured hippocampal neurons 72% of the BSN-GFP co-localized with PCLO. This construct, however, generated diffuse fluorescence in dendrites and nuclei which corresponded to a

GFP cleavage product. A BSN construct lacking the first 94 amino acids had the same presynaptic targeting properties as the full length protein but lacked the diffuse GFP cleavage product. Subsequent deletion constructs showed that neither the N-terminus (1691 amino acids) nor the C-terminus (675 amino acids) of BSN were required for presynaptic targeting. The central portion of BSN containing amino acids 1692-3263 was targeted to the presynapse and retained by the active zone (Dresbach et al., 2003). This finding is consistent with data obtained from bassoon transgenic mice lacking amino acids 505-2889 in which BSN was absent from the synapse (Altrock et al., 2003).

The N-terminal BSN construct, consisting of the first 609 amino acids, expression resembled synaptic vesicle clusters in shape and size suggesting that it may be involved in binding of synaptic organelles such as synaptic vesicles (Dresbach et al., 2003). This observation is consistent with previous studies where bassoon was found to be associated with synaptophysin-positive vesicles in a synaptic vesicle preparation (Sanmarti-Vila et al., 2000). The two double zinc finger domains found within the first 609 amino acids of bassoon are most likely to mediate the interaction with synaptic vesicles as was shown to be the case with zinc fingers of PCLO binding PRa-1 (Fenster et al., 2000) and resulting in an interaction with synaptic vesicles. The functional domains of BSN are outlined in Figure 5.2.

The BSN functional knockout (BsnΔEx4/5) mice were found to have significantly reduced concentration of N-acetyl aspartate and glutamine in the cortex and hippocampus but not cerebellum. N-acetyl aspartate is a neuron specific metabolite and its reduced concentration is indicative of a decreased neuronal population in the cortex of these mice (Angenstein et al., 2008). It is interesting that no apparent changes were found in the cerebellum since BSN was found to be widely expressed in the brain (Richter et al., 1999).

The active zone precursor vesicle hypothesis suggests that the active zone proteins are preassembled at the Golgi apparatus from where they are shipped as a complex to form presynapses (Ziv and Garner, 2004). This hypothesis is consistent with observations of an intact Golgi apparatus as necessary for delivery of BSN and PCLO to nascent synapses (Dresbach et al., 2006).

Figure 5.2: Functional domains of BSN and their published expression and localization in transiently transfected rat hippocampal neurons. Taken from Dresbach (Dresbach et al., 2003).
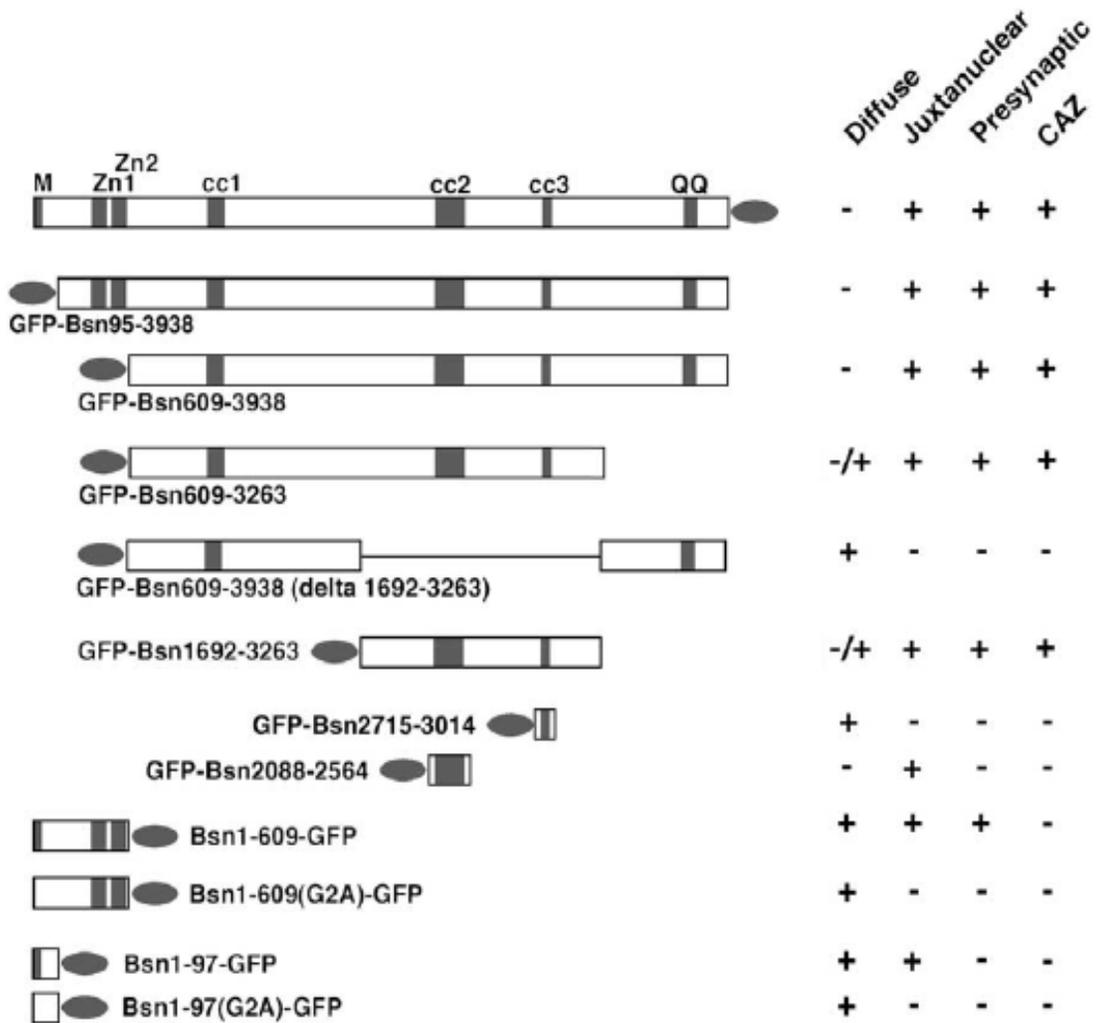
5.3 Co-immunoprecipitation of BSN with DAO from rat cerebellum

Bassoon was found to be one of the strongest, most specific, and consistent interacting proteins in the two DAO immunoprecipitation experiments. An interaction of the two proteins implies DAO presence in the presynaptic active zone where BSN has been shown to be exclusively localized (Richter et al., 1999). However, in the past DAO has been thought of as a peroxisomal enzyme (Usuda et al., 1986). Consistent with localization at the cellular periphery recent immunohistological examination of DAO in the cortex and cerebellum of human brains showed a pericellular DAO distribution (Verrall et al., 2007). This novel observation suggests DAO presence outside of the peroxisome and fits with our immunoprecipitation data suggested by interaction with non-peroxisome complexes. Consequently we chose to focus on these two proteins and study the likelihood of their interaction *in vivo* and the implications of such interactions.

Initial experiments to understand the DAO and BSN interaction were conducted from rat adult cerebellum lysate where the DAO antibody was used to immunoprecipitate DAO and the resulting isolated proteins were separated by SDS-PAGE and probed with an anti-BSN antibody (Figure 5.3). Immunoprecipitation with both DAO antibody and BSN antibody successfully pulled down BSN from adult rat cerebellum reinforcing the mass spectroscopy study and showed that the BSN antibody was capable of self immunoprecipitation. The immunoprecipitation was blocked by DAO blocking peptide. The reciprocal of this experiment where the BSN antibody was used to pull down BSN from the rat cerebellar lysate and the SDS-PAGE gel containing the respective precipitate was probed with the DAO antibody (Figure 5.3) was successful as well. Immunoprecipitation with BSN antibody but not mouse IgG resulted in the co-immunoprecipitation of DAO confirming a physical interaction between the two proteins in rat cerebellar lysate. This data was encouraging because both DAO and BSN antibodies were able to immunoprecipitate their respective target proteins and retain the interacting proteins as well. These data suggest that this apparent interaction was specific and not due to antibody reactivity with non-specific protein and that the observed co-immunoprecipitation results were instead due to a physical interaction of the two proteins.

Figure 5.3: Co-immunoprecipation of BSN with DAO antibody from rat cerebellar lysate. **A**) Immunoprecipitation with both DAO antibody and BSN antibody but not their respective negative controls successfully pulled down BSN from rat cerebellum reinforcing the mass spectroscopy study and showing that the BSN antibody was capable of self immunoprecipitation. **B**) DAO was immunoprecipitated with the DAO antibody and co-immunoprecipitated with BSN antibody but not with either of the two negative controls.

Legend:
Ln 1: BSN antibody pull down
Ln 2: Mouse IgG pull down
Ln 3: DAO antibody pull down
Ln 4: Rabbit IgG pull down
Ln 5: Input $1/10^{th}$ volume

B

MW

191
97
64
51
39
28
19

← DAO
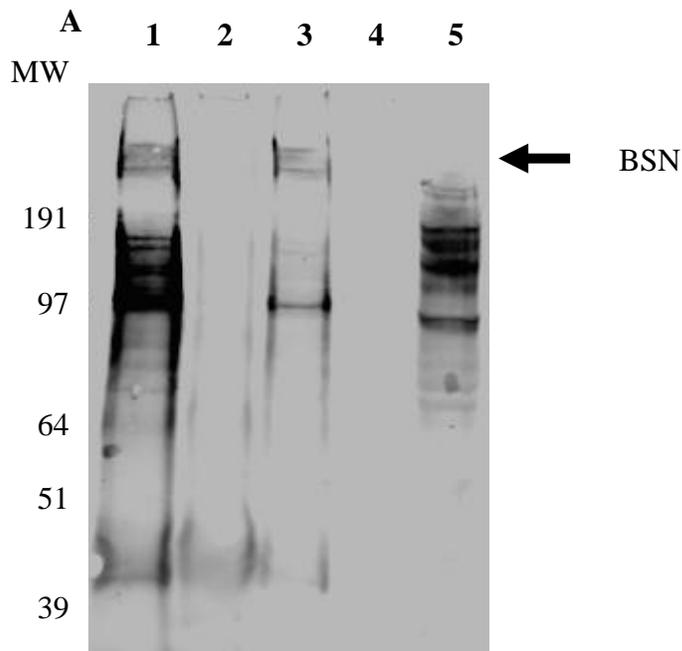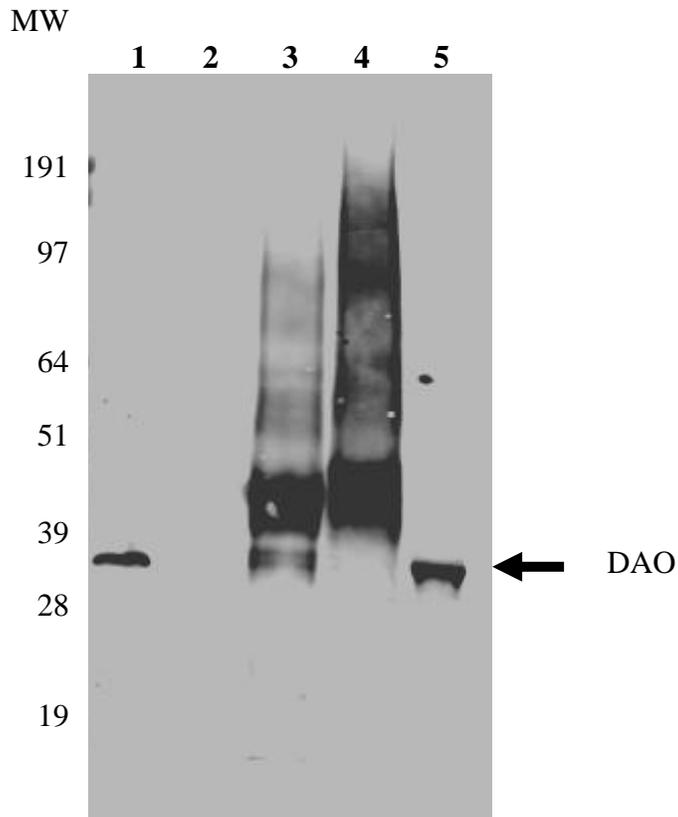
5.4 Does BSN serve as a scaffold for DAO, ASC-1 and SRR?

The identification of an interaction between DAO and BSN suggested that BSN, given its size, may act as a scaffolding protein for DAO, ASC-1 and SRR to interact and modulate D-serine concentration. This suggestion is possible since ASC-1 has been localized to cerebellar neurons and the synapse specifically (Matsuo et al., 2004). Likewise, SRR has been primarily localized in neurons (Takayasu et al., 2008; Yoshikawa et al., 2007). Hence, rat cerebellar lysates were immunoprecipitated with the BSN antibody and the immunoprecipitates were probed with ASC-1 and SRR antibodies (Figure 5.4). Neither ASC-1 nor SRR were found to interact with BSN.

Figure 5.4: ASC-1 and SRR do not co-immunoprecipitate with BSN. Immunoprecipitates generated from rat cerebellar lysate against bassoon antibody were separated on SDS-PAGE gel and probed with BSN, ASC-1 and SRR antibodies for evidence of an interaction among the proteins. Two ASC-1 antibodies were utilized, both of which detected ASC-1 in the input lysate. ASC-1 was found not to co-immunoprecipitate with bassoon. Similarly robust SRR expression in the cerebellar lysate was identified and confirmed to be that of SRR through application of SRR peptide which blocked the signal. However SRR was found not to co-immunoprecipitate with bassoon.

1   2   3

BSN

ASC-1 KosmoBio (#KAL-KE027)

ASC-1 Abcam (#ab64966)

BSN

SRR Abcam (#ab45434)

Peptide blocked SRR Abcam (#ab45543)
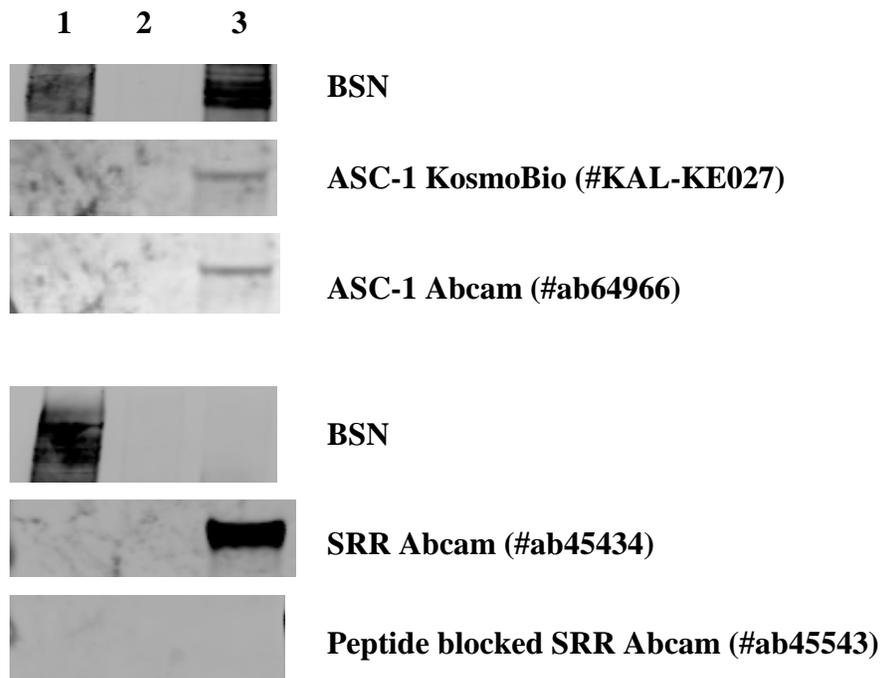
Legend:
Ln 1: BSN pull-down
Ln 2: Mouse IgG pull-down
Ln 3: $1/10^{th}$ lysate input

5.5 Immunohistochemistry localization of BSN and DAO in rat cerebellum slices

While the co-immunoprecipitation results from the rat cerebellar lysate were very encouraging, further evidence that DAO and BSN physically interact *in vivo* and are expressed in the same cerebellar regions was sought. Immunohistochemistry with the DAO and BSN antibodies was used to test if the two proteins are localized to the same cerebellar cell types. DAO immunofluorescence was found to be primarily localized to the Purkinje cellular layer, the granular layer and to a lesser extent to the molecular layer (Figure 5.5 A). The signal generated with the DAO antibody was completely blocked by preabsorbing the antibody with the peptide towards which it was generated suggesting that the staining identified with the antibody is that of DAO (Figure 5.5 B). Rat spleen does not express DAO (Figure 3.5) hence rat spleen slices were generated and examined with the DAO antibody as an additional negative control. The spleen did not display any more immunofluorescence with the DAO antibody than it did with the secondary antibody only (Figure 5.5 C and D) further suggesting DAO antibody selectively recognized DAO. Finally, the DAO immunofluorescence data was consistent with published immunostaining in the rat cerebellum (Moreno et al., 1999) but differed in respect to Purkinje cell staining from human cerebellar immunostaining utilizing DAO antibody made against the C-terminal end of human DAO (Verrall et al., 2007). While some mRNA was detected in human Purkinje cells no DAO protein was found (Verrall et al., 2007). This discrepancy may be species dependent. BSN immunofluorescence was primarily localized to the molecular layer and to a lesser extent to the granule layer with no staining detected in the Purkinje cellular layer (Figure 5.5 E). A peptide against which BSN was generated was not available so no primary antibody was used as a negative control (Figure 5.5 F). In addition, the BSN antibody was previously shown to detect BSN specifically (Tao-Cheng, 2007). When the rat cerebellar slices were co-stained with the DAO and the BSN antibodies the granule layer emerged as a likely region of co-localization with the molecular layer also possible but less likely as little yellow signal was visible (Figure 5.5 G).

Figure 5.5: Immunofluorescence localization of DAO (red) and BSN (green) in rat cerebellar and spleen slices. DAO was primarily detected in the Purkinje cellular layer, the granule layer and to a lesser extent in the molecular layer (A). This signal was completely blocked (B) by preabsorption of the antibody with the DAO peptide toward which the antibody was generated suggesting a DAO specific immunofluorescence. Rat spleen slices were used because no DAO was found in this organ when tested on SDS-PAGE gel. Lack of DAO signal on the rat spleen slices (C) as compared to secondary antibody only (D) further validated the purity of the DAO antibody. BSN was found to be localized to the molecular layer and to a lesser extent to the granule layer (E). BSN peptide was not available for antibody quenching but secondary antibody alone did not have any background signal (F). A merged image co-stained with DAO and BSN shows that the two proteins may co-localize in the granule layer and/or in the molecular layer but not likely in the purkinje cellular layer (G). ML = molecular layer; GR = granule layer; PCL = purkinje cell layer
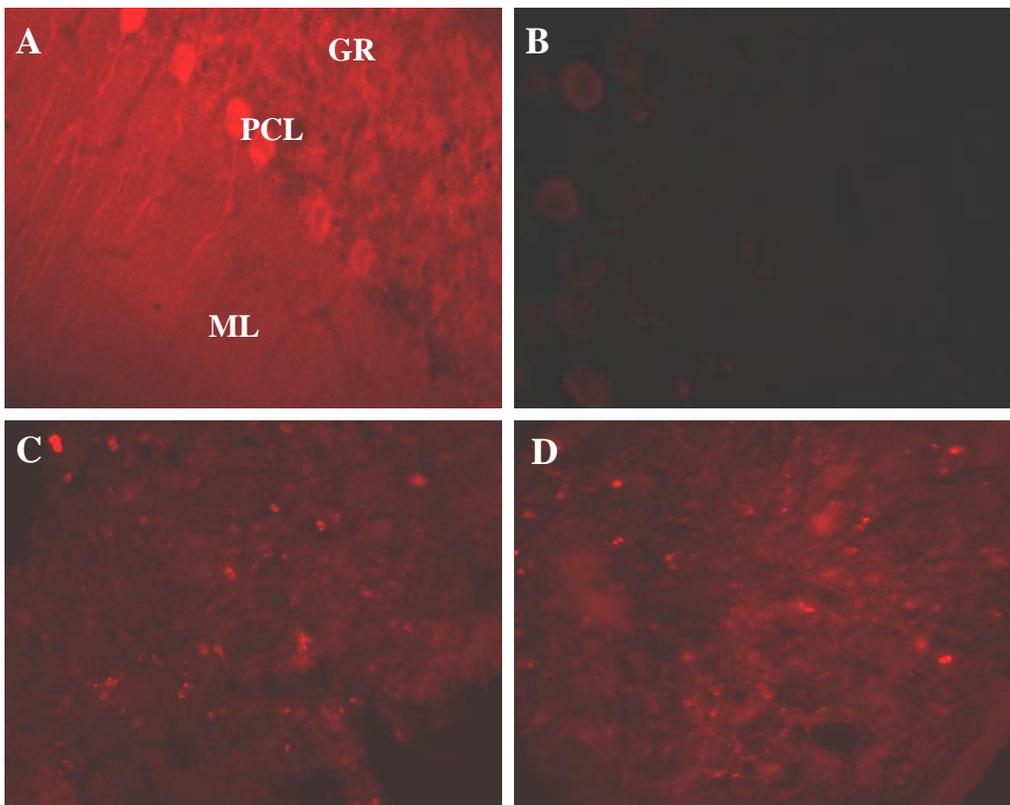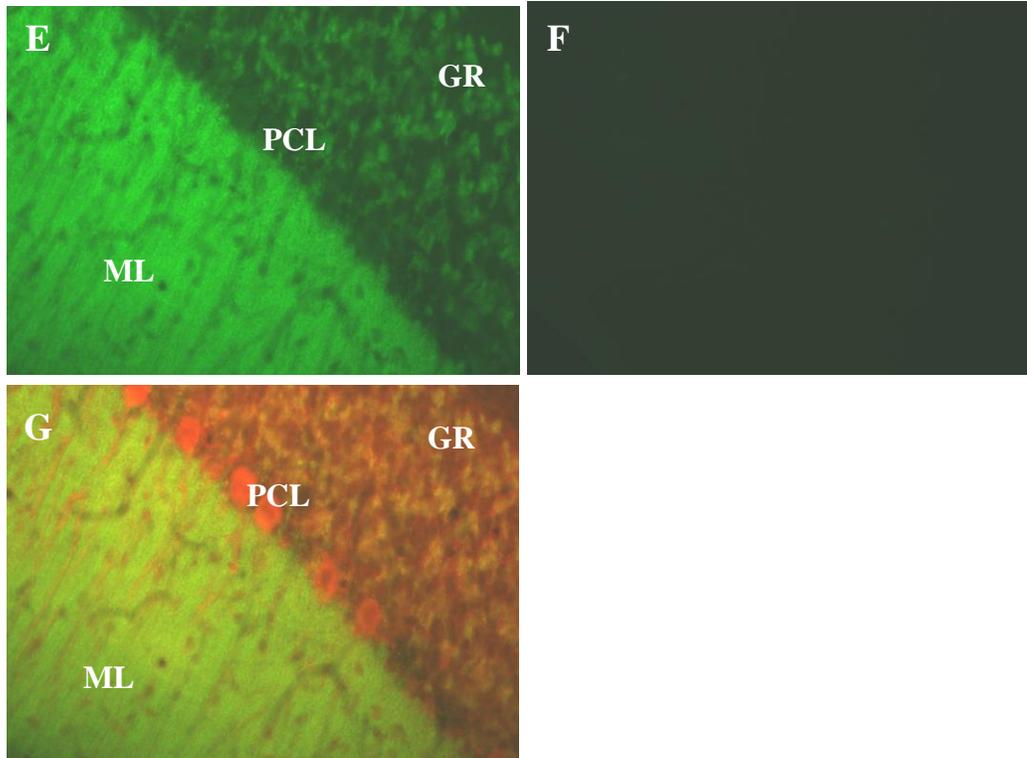
5.6 Cerebellar fractionation and localization of DAO in synaptic junction membrane fraction

While the co-immunoprecipitation and immunofluorescence results from the rat cerebellar lysate suggested colocalization of DAO and BSN, further evidence was required to prove that the two proteins physically interact *in vivo*. In order to test if the two proteins were found in synaptic junction membrane fraction free of peroxisomal markers, a subcellular fractionation experiment (schematically outlined in Figure 5.6) was employed. This approach was adopted from Altrock (Altrock et al., 2003) and results in the isolation of neuronal pre and post synaptic terminus.

Figure 5.6: Schematic diagram of the fractionation protocol employed to show presence of DAO in the synaptic junction membrane fraction without any contaminating catalase, a peroxisomal marker. The green indicates fractions that were advanced while the red shows those that were left behind.
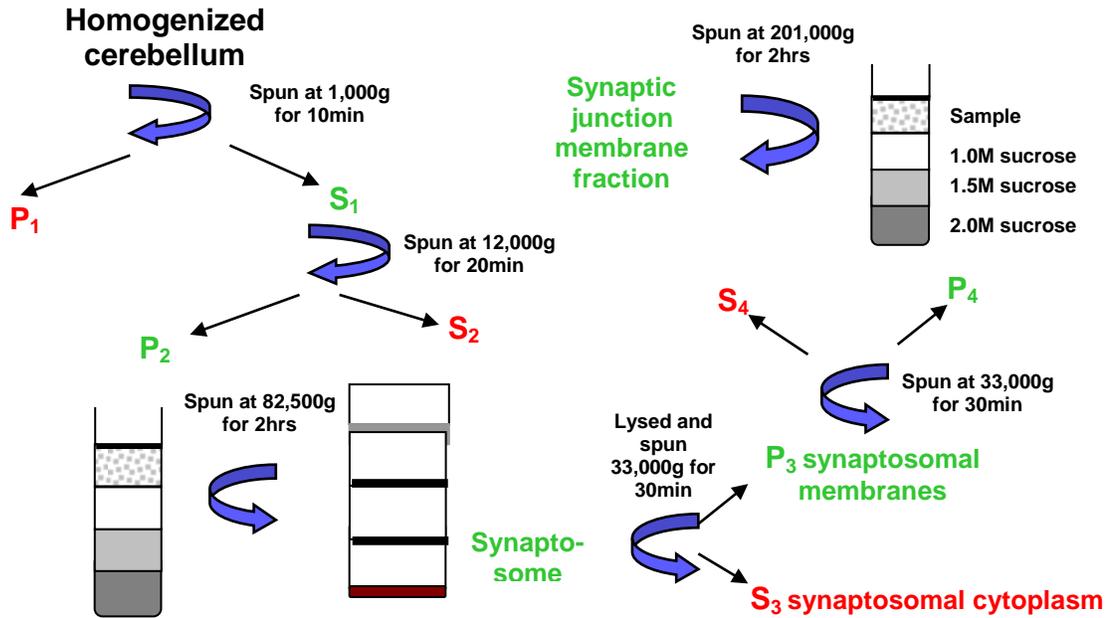
The results of the fractionation are found in Figure 5.7. Each fraction was probed for presence of markers of sub-cellular organelles including BSN, PSD-95, microtubule associated protein 2 (MAP2), DAO and catalase. BSN and PSD-95 are known pre and post synaptic markers respectively and were used to verify that the final fraction contained the proteins which this procedure is designed to purify. MAP2 is a neuron-specific cytoskeletal protein enriched in dendrites but not in the active zone. MAP2 is also comparable in size to BSN and PSD-95 making it a particularly suitable negative control. Catalase is a peroxisomal marker used to determine if any of the fractions were free of catalase but still contained DAO. Both BSN and catalase blots were overexposed to better illustrate presence or absence of the two proteins in various fractions which are

described below. All of the proteins probed for were found in the starting solution from the rat cerebellar lysate (Figure 5.7 lane 1). During the sequential fractionation MAP2 was lost when the synaptosome fraction was isolated (Figure 5.7 lane 4) but BSN, PSD-95, DAO and catalase were retained. While no BSN or PSD-95 was found in the synaptosomal cytoplasm both DAO and catalase positively identified in this fraction (Figure 5.7 lane 5). All four proteins were also found in the synaptosomal membranes (Figure 5.7 lane 6) suggesting peroxisomal association with this fraction. When the synaptosomal membranes were further fractioned to yield a pure synaptic junction membrane fraction BSN, PSD-95 and DAO were retained while catalase was lost. This finding suggests DAO localization outside of the peroxisome and within the synaptic junction membrane fraction where it may interact with BSN.

Figure 5.7: Fractionation of rat cerebellum suggests DAO localization outside of the peroxisome and among the synaptic membrane junction proteins. Three rat adult cerebellums were fractioned and analyzed for key proteins presence through Western blot. The fractions examined included S_1, S_2, P_1, synaptosomal fraction (SnpF), S_3, P_3, S_4, P_4 and synaptic junction membrane proteins (Sjmp).
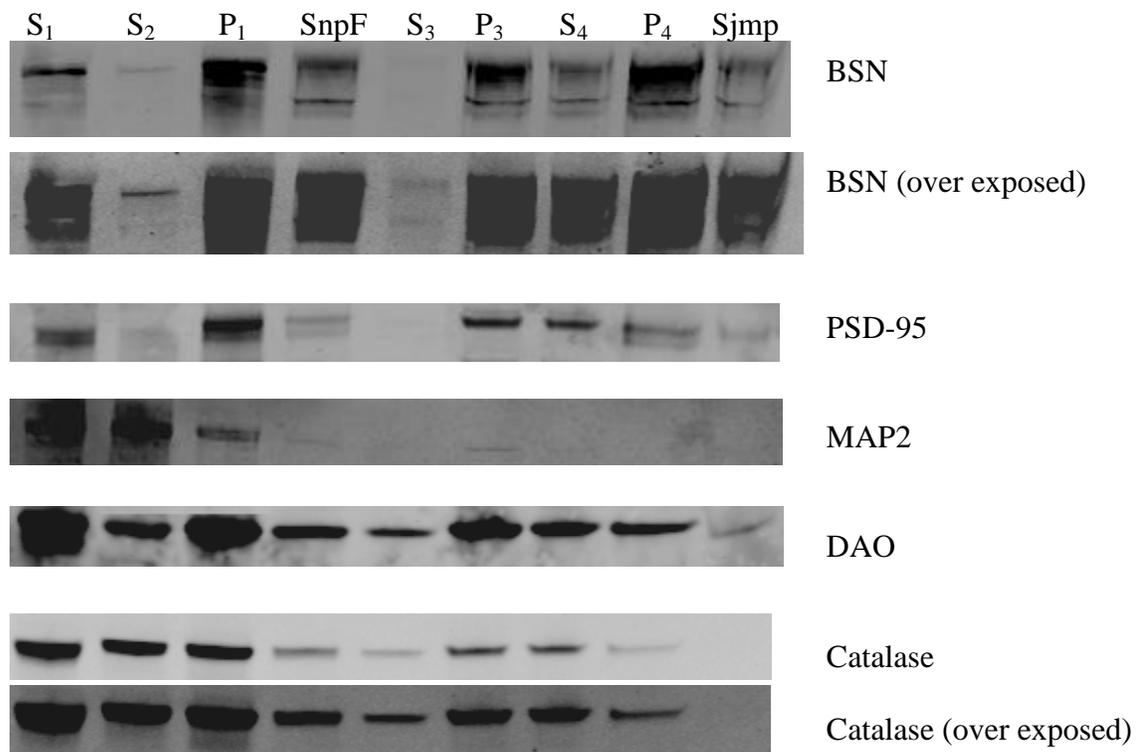
5.7 Immunohistochemistry localization studies in cerebellar granule neurons

Since mouse DAO cerebellar expression was shown to follow a neurodevelopmental pattern with no detectable DAO activity from birth until 3rd week of age (Wang and Zhu, 2003) rat cerebellar samples from two week old pups were probed for expression of DAO (Figure 5.8). Postnatal 14 day old pups were found to express cerebellar DAO albeit at about a fourth of the amount found in adult rat cerebellum. To follow up on the fractionation studies and examine DAO localization in relation to BSN, oil immersion immunocytochemistry imaging was utilized with samples from two week old cerebellar granule neurons (CGNs) from two week old rat pups. The DAO antibody showed staining within the neuronal processes (Figure 5.9 A) while the secondary antibody alone (Figure 5.9 B) and peptide blocked DAO antibody (Figure 5.9 B) did not give rise to a meaningful signal.

Figure 5.8: Verification of rat cerebellar DAO expression in two week old pups. Cerebellar DAO expression was compared between adult (ln1; 15 μg) and two week old pup (ln2; 30 μg) lysates on SDS-PAGE gel. The pups were found to express DAO at about a fourth of the amount found in the adult rat cerebellum. This data is consistent with published reports.

Figure 5.9: Immunocytochemistry of rat cerebellar granule neurons (CGNs) with DAO antibody (A), secondary antibody only (B) and peptide blocked DAO antibody (C). A fluorescent secondary antibody was used for visualization of the DAO probed CGN cells. The DAO immunofluorescence suggests punctuate DAO localization within the neuronal processes.
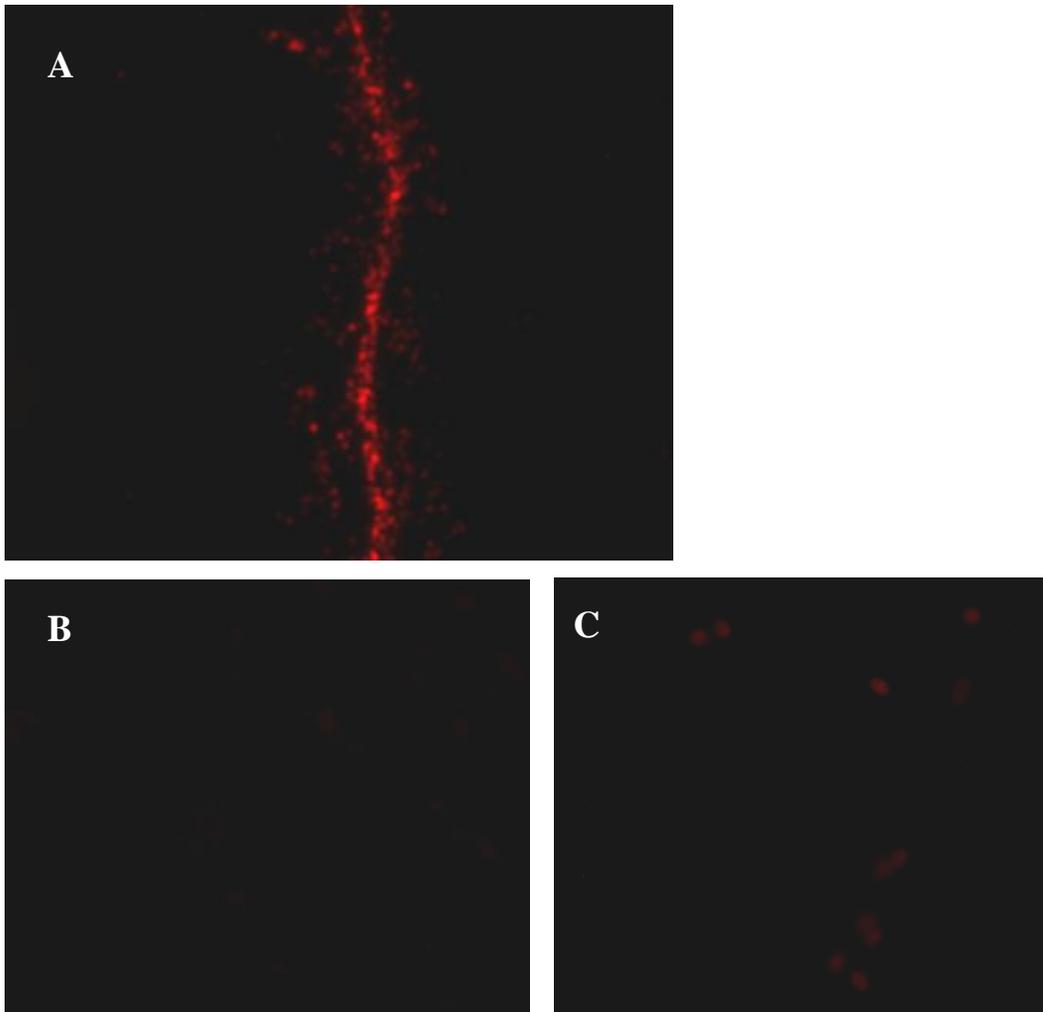
Antibodies against synaptophysin, a synaptic vesicle protein uniquely expressed at the synapse, were used in conjunction with DAO antibody to help determine DAO localization in relation to the synapses in CGNs and to compare with those of DAO and BSN. In the merged and enlarged image (Figure 5.10) DAO appears in close proximity to synaptophysin but not overlapping as would be implied by yellow spots. The lack of DAO co-localization with synaptophysin is consistent with the mass spectroscopy data as synaptophysin was not one of the putative DAO interacting proteins. However, these data suggest DAO presence within the synapse because the red fluorescence signal associated with the DAO is found within the neuronal processes.

Figure 5.10: Cerebellar granule neurons (CGNs) were cultured for two weeks before they were fixed with paraformaldehyde and used for immunocytochemistry. In the merged image, DAO and synaptophysin, a synaptic marker, were found in a proximity to each other but not co-localizing as determined by lack of yellow spots. This lack of co-localization is to be expected given that synaptophysin was not one of the DAO interactors. The fluorescence is attributable to the secondary antibody.
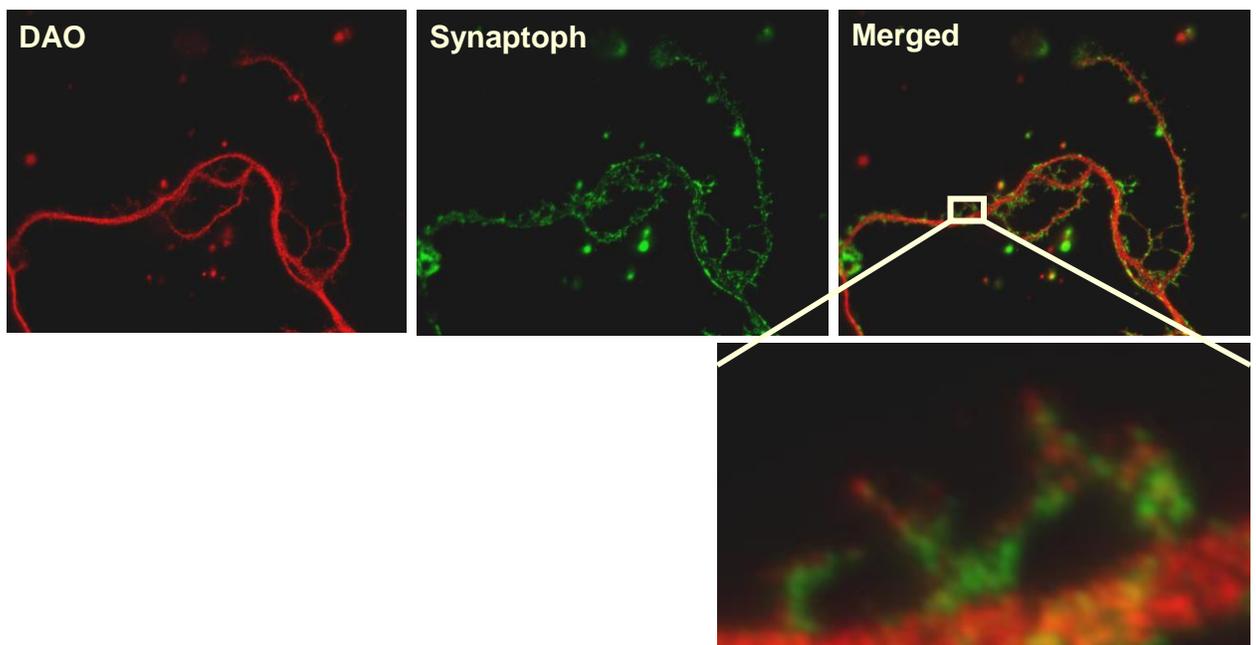
Having established initial evidence of the presence of DAO through fractionation and immunocytochemistry in neuronal presynaptic terminus we were interested if this novel DAO localization overlapped with that of BSN. CGNs were probed with DAO and BSN antibodies. While most of the DAO does not appear to overlap with BSN some co-localization between the two proteins exists as depicted by the yellow fluorescence (Figure 5.11). This moderate level of the two proteins colocalized suggests that not all BSN need be complexed with DAO.

Figure 5.11: Cerebellar granule neurons (CGNs) were cultured for two weeks before they were fixed with paraformaldehyde and used for immunocytochemistry. In the merged image, DAO and BSN may be co-localizing at the synaptic termini as depicted by the yellow spotting indicative of the two proteins in a very close proximity to each other.
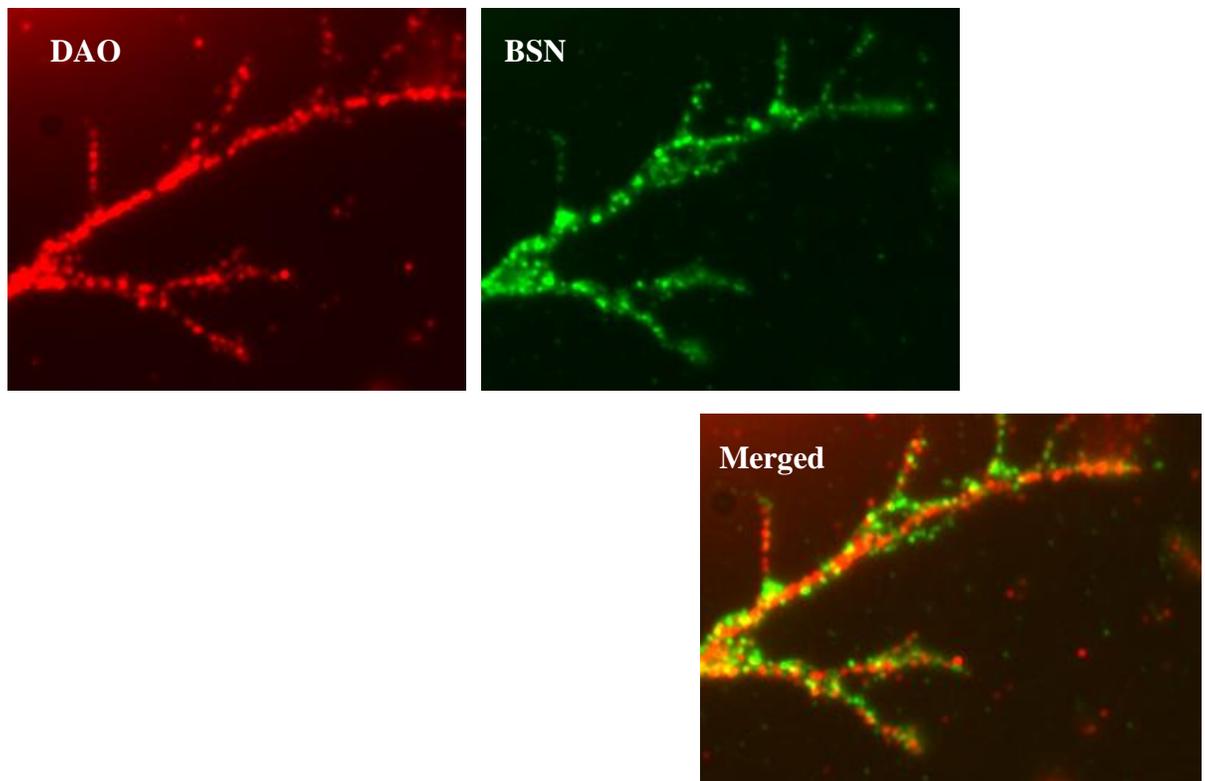
Unlike paraformaldehyde fixation which immobilizes both soluble and attached proteins in place at the time of the fixation, methanol fixation is known to wash out soluble proteins (Hoetelmans et al., 2001). The methanol fixation was shown not to wash out DAO from the presynaptic terminus (Figure 5.12) suggesting that DAO is firmly attached in the matrix. In the merged, zoom-in image DAO localization appears to partially co-localize with BSN reinforcing the data generated with paraformaldehyde fixation in Figure 5.11.

Figure 5.12: Cerebellar granule neurons (CGNs) were cultured for two weeks before they were fixed with ice cold methanol and used for immunocytochemistry. Unlike paraformaldehyde fixation, methanol fixation washes away free floating proteins. With this fixation method DAO continues to be present at the synaptic junctions. In the merged image, DAO and BSN may be co-localizing at the synaptic termini as depicted by the yellow spotting indicative of the two proteins in a very close proximity to each other.
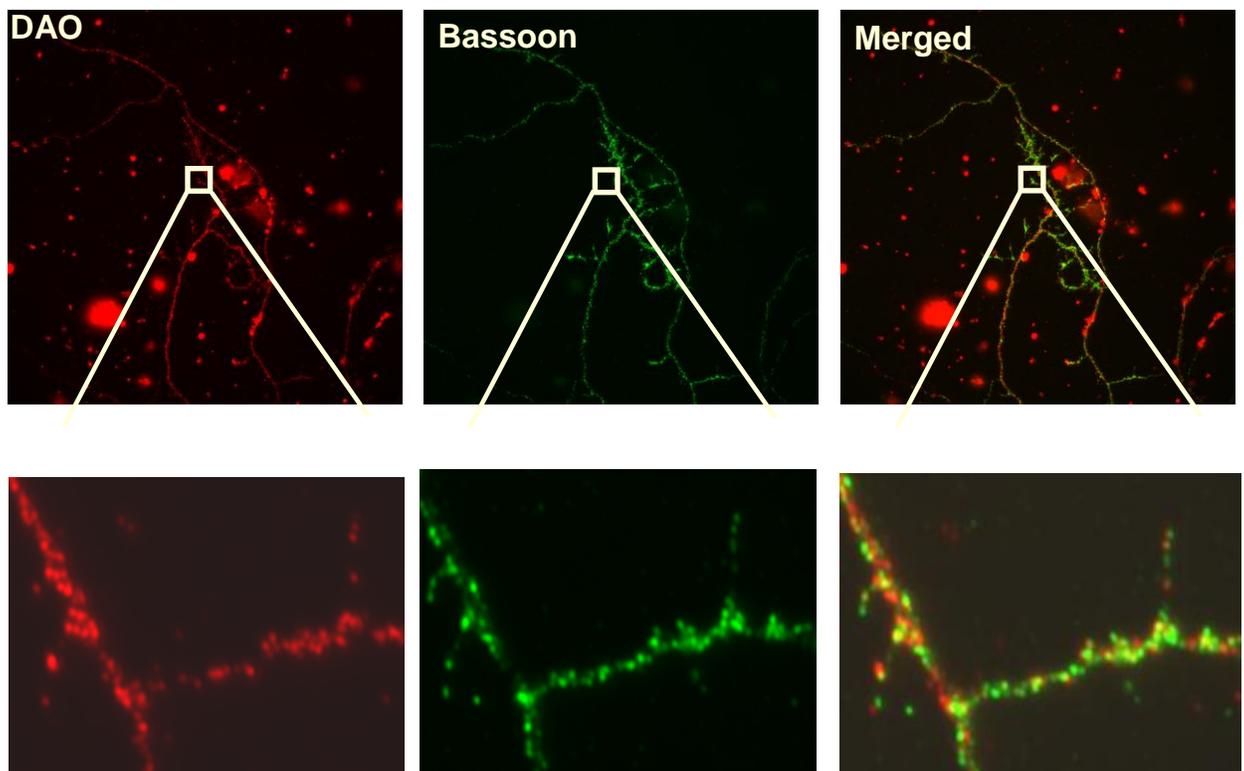
5.8 Immunoprecipitation from Hek293 cells

Hek293 cells were derived from human embryonic kidney cells hence they are unlikely to express the five members of the CAZ described in section 5.1. Consequently this immortalized cell line provides means of ascertaining a direct interaction between DAO and BSN when both proteins are co-transfected. The proposed direct interaction hypothesis is valid at least when the CAZ members are taken into account but other common proteins found in both cerebellar neurons and Hek293 cells may still be responsible for facilitating the interaction between the two proteins and cannot be ruled out as irrelevant to the described interaction.

A GFP-tagged BSN construct (kind gift from Dr. Gundelfinger, Germany) encoding BSN amino acids 95 through 3963 was transiently transfected into rDAO Hek293 stable line. The resulting lysate was shown to express the BSN fusion protein with an expected molecular weight of 397 kDa (Figure 5.13 A lane 2) and resulted in immunoprecipitation with the GFP antibody (Figure 5.13 A lane 4) but not with mouse IgG (Figure 5.13 A lane 3). The same samples were shown to co-immunoprecipitate DAO with the GFP-BSN construct (Figure 5.13 B). DAO and BSN were shown to co-localize through immunocytochemistry in the Hek293 cells overexpressing both proteins suggesting that the proteins associate in these cells (Figure 5.14).

Truncation mutants of BSN were generated to identify the region responsible for the interaction. All of the BSN truncation mutants contain N-terminal GFP tag and include amino acids 95-609, 95-3263, 1692-3263, 2715-3263 and 3263-3963 (for reference see Figure 5.2). While the zinc finger domain containing 95-609 BSN amino acids was well expressed and immunoprecipitated by GFP antibody it did not co-immunoprecipitate with DAO (Figure 5.15). The predicted coiled-coiled regions found in construct 95-3263 may play a role in the interaction with DAO as this BSN truncation mutant was able to co-immunoprecipitate DAO from rDAO Hek293 lysate (Figure 5.16). Construct 1692-3263, containing two of the three coiled-coiled regions was also able to co-immunoprecipitate DAO from the rDAO Hek293 stable line (Figure 5.17) as well as construct 2715-3263 containing a single predicted coiled-coiled region (Figure 5.18). The final 3263-3963 amino acids construct characterized by a long

glutamine chain did not express in rDAO Hek293 stable line (Figure 5.19) so we can not conclusively rule out whether this region is important for BSN-DAO interaction. We were however able to identify 2715-3263 BSN polypeptide as an important potential interaction site with DAO.

5.9 Functional effect of rBSN on rDAO enzymatic activity

The rDAO Hek293 stable line was used to ascertain if transiently transfected full length and truncation mutants of GFP-rBSN had any effect on DAO's functional activity. About 30% inhibition of DAO's enzymatic activity was observed with the full length BSN, 95-3263, 1692-3263, and 2715-3263 but not with BSN 95-609 as compared to GFP only transiently tranfected cells after 3 days post transfection (Figure 5.20). This data suggests that BSN may regulate DAO's enzymatic activity within the presynaptic active zone.

5.10 Conclusions

Following up on the mass spectroscopy results, BSN was confirmed to interact with DAO in rat cerebellar lysate through co-IP. The DAO antibody pulled-down BSN along with DAO and likewise the BSN antibody pulled-down DAO with BSN. Through a fractionation experiment of rat cerebellum DAO was found in the synaptic junction membrane fraction which contained BSN but no catalase suggesting that DAO may be found in the presynaptic terminus outside of the peroxisome where it may interact with BSN *in vivo*. Immunocytochemistry of CGNs confirmed the likely localization of DAO in neuronal processes co-localizing with BSN. In rat cerebellar slices DAO may be co-localizing with BSN in the granule and molecular layer as determined by immunohistochemistry. BSN was co-immunoprecipitated with DAO from Hek293 cells overexpressing both proteins suggesting that the two may directly interact as none of the other members of the presynaptic active zone are expressed in the Hek293 cells (Figure 5.21). Within the DAO Hek293 cells overexpression of BSN was found to inhibit DAO's enzymatic activity. Furthermore BSN region spanning amino acids 2715-3263 representing predicted single coiled coiled region was found to co-IP with DAO when both were overexpressed in Hek293 cells.

Figure 5.13: Immunoprecipitation of full-length bassoon from rDAO stable line transiently transfected with rat GFP-BSN construct and probed with GFP antibody (A) and DAO antibody (B). The bassoon fusion construct was successfully transfected into rDAO Hek293 cell line as evidenced by the presence of expected 397 kDa band in GFP-bassoon transiently transfected rDAO Hek293 cells (A, lane 2) but not in mock transfected rDAO Hek293 cells (A, lane 1). The GFP antibody was able to immunoprecipitate the fusion construct as evidenced by the presence of BSN (A, lane 4) but absence in mouse IgG immunoprecipitation (A, lane 3). DAO was found to co-immunoprecipitate along with BSN (B, lane 4) but not with mouse IgG (B, lane 3). The expected GFP-BSN truncated protein molecular weight on the SDS-PAGE gel is indicated by the arrow.
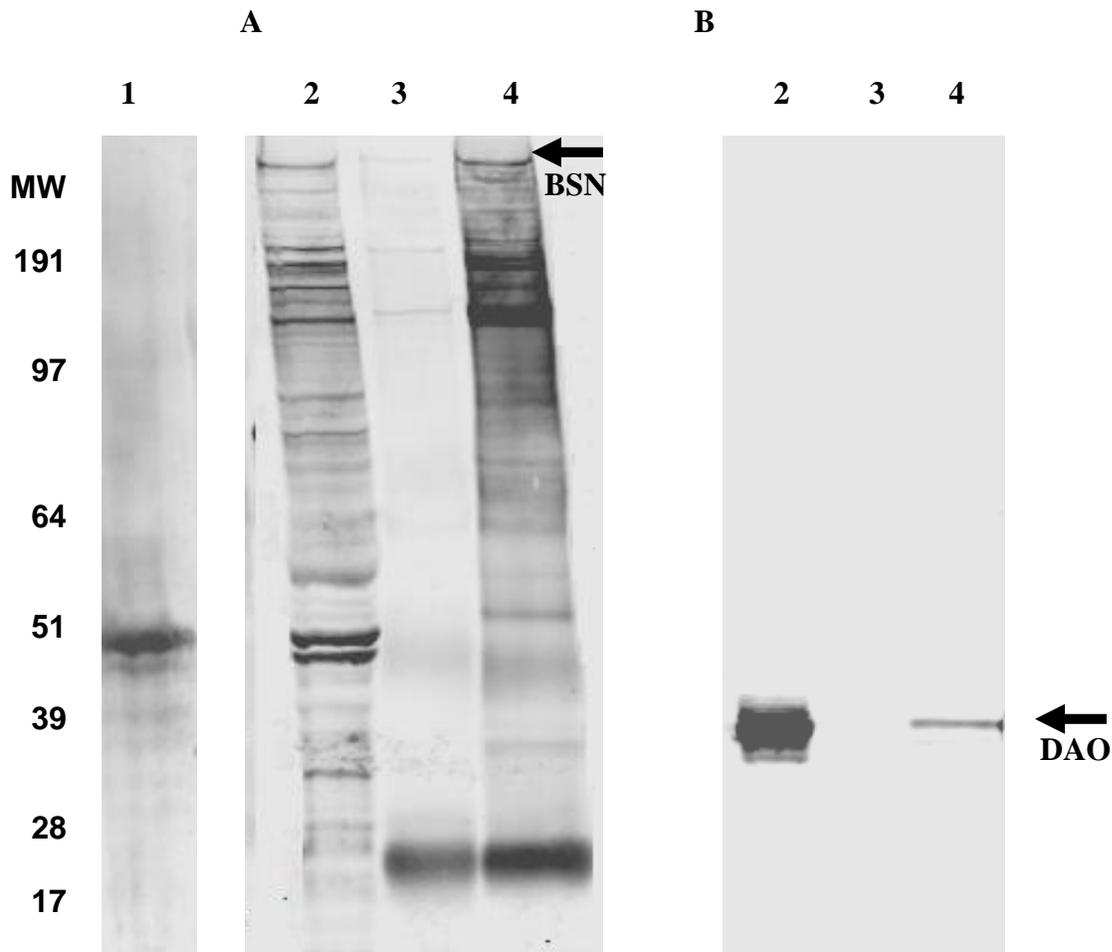
Legend:
Ln 1: Mock transfected rDAO Hek293 lysate
Ln 2: Input lysate 1/10th volume
Ln 3: Mouse IgG immunoprecipitation
Ln 4: GFP immunoprecipitation

Figure 5.14: Co-localization of DAO and BSN through immunocytochemistry in Hek293 cells. When both proteins were overexpressed in Hek293 cells they displayed a level of co-localization and proximal localization along the cell membrane (**C**). While BSN was found primarily along the cell membrane (**B**), DAO was found along the membrane and in the cytoplasm (**A**).
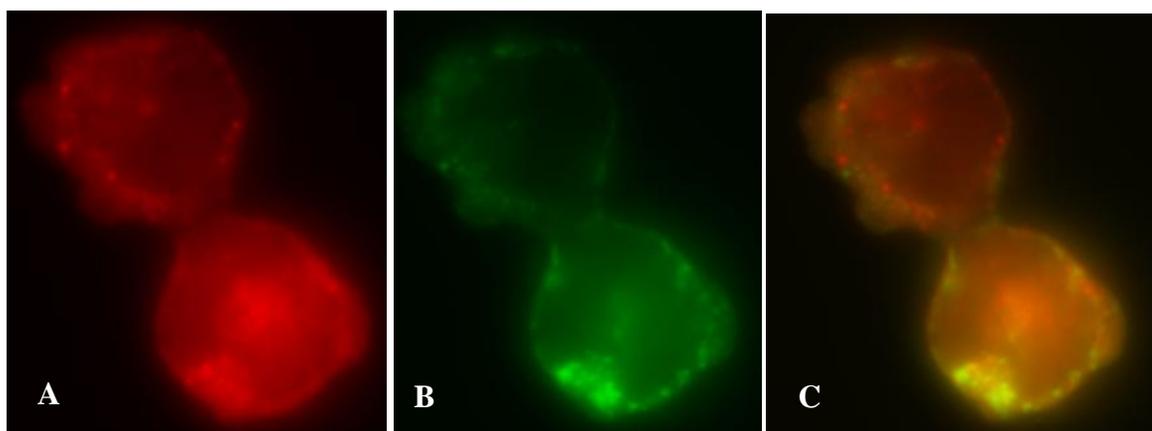
Figure 5.15: Immunoprecipitation of BSN from rDAO stable line transiently transfected with rat GFP-BSN 95-609 construct and probed with GFP antibody (A) and DAO antibody (B). The BSN fusion construct was successfully transfected into rDAO Hek293 cell line as evidenced by the presence of expected 92 kDa band in GFP-BSN transiently transfected rDAO Hek293 cells (A, lane 1). The GFP antibody was able to specifically immunoprecipitate the GFP-BSN fusion construct as shown by the presence of BSN (A, lane 3) but absence in mouse IgG immunoprecipitation (A, lane 2). DAO was found not to co-immunoprecipitate along with BSN (B, lane 3) or with mouse IgG (B, lane 3). The expected GFP-BSN truncated protein molecular weight on the SDS-PAGE gel is indicated by the arrow.
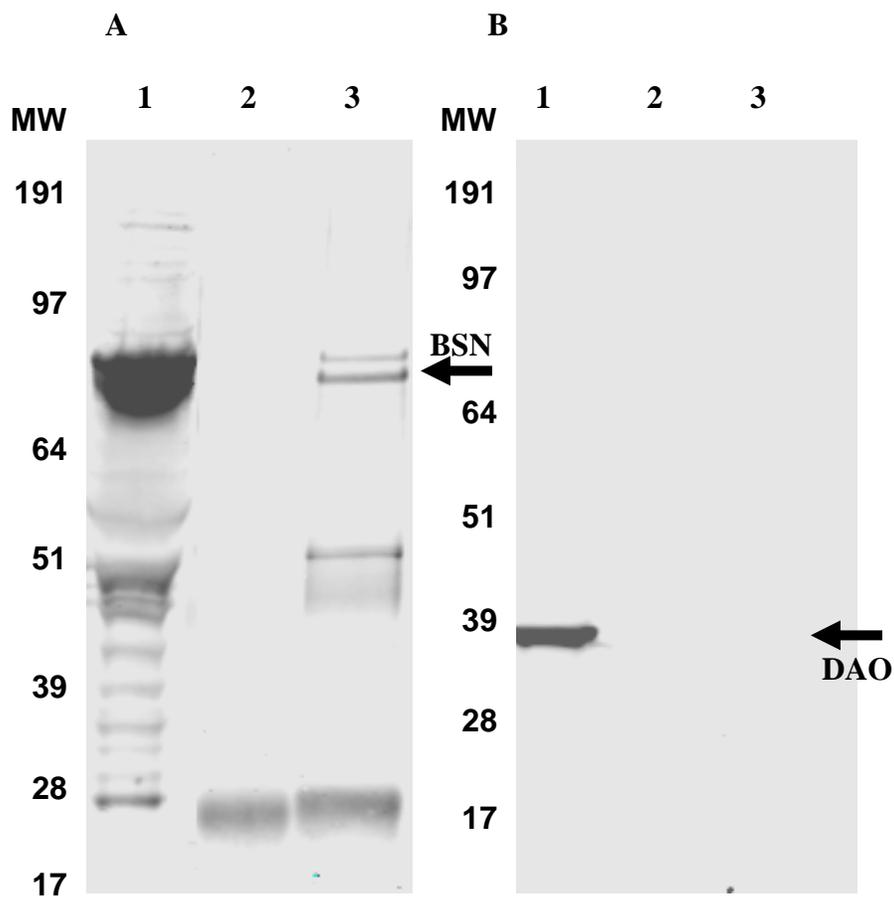
Legend:
Ln 1: Input lysate 1/10th volume
Ln 2: Mouse IgG immunoprecipitation
Ln 3: GFP immunoprecipitation

Figure 5.16: Immunoprecipitation of BSN from rDAO stable line transiently transfected with rat GFP-BSN 95-3263 construct and probed with GFP antibody (A) and DAO antibody (B). The BSN fusion construct was successfully transfected into rDAO Hek293 cell line as evidenced by the presence of expected 377 kDa band in GFP-BSN transiently transfected rDAO Hek293 cells (A, lane 1). The GFP antibody was able to immunoprecipitate the fusion construct as evidenced by the presence of BSN (A, lane 3) but absence in mouse IgG immunoprecipitation (A, lane 2). DAO was found to co-immunoprecipitate along with BSN (B, lane 3) but not with mouse IgG (B, lane 2). The expected GFP-BSN truncated protein molecular weight on the SDS-PAGE gel is indicated by the arrow.

Legend:
Ln 1: Input lysate $1/10^{th}$ volume
Ln 2: Mouse IgG immunoprecipitation
Ln 3: GFP immunoprecipitation

Figure 5.17: Immunoprecipitation of BSN from rDAO stable line transiently transfected with rat GFP-BSN 1692-3263 construct and probed with GFP antibody (A) and DAO antibody (B). The BSN fusion construct was successfully transfected into rDAO Hek293 cell line as evidenced by the presence of expected 204 kDa band in GFP-BSN transiently transfected rDAO Hek293 cells (A, lane 1). The GFP antibody was able to immunoprecipitate the fusion construct as evidenced by the presence of BSN (A, lane 3) but absence in mouse IgG immunoprecipitation (A, lane 2). DAO was found to co-immunoprecipitate along with BSN (B, lane 3) but not with mouse IgG (B, lane 2). The expected GFP-BSN truncated protein molecular weight on the SDS-PAGE gel is indicated by the arrow.

Legend:
Ln 1: Input lysate 1/10th volume
Ln 2: Mouse IgG immunoprecipitation
Ln 3: GFP immunoprecipitation

Figure 5.18: Immunoprecipitation of BSN from rDAO stable line transiently transfected with rat GFP-BSN 2715-3263 construct and probed with GFP antibody (A) and DAO antibody (B). The BSN fusion construct was successfully transfected into rDAO Hek293 cell line as evidenced by the presence of expected 64 kDa band in GFP-BSN transiently transfected rDAO Hek293 cells (A, lane 1). The GFP antibody was able to immunoprecipitate the fusion construct as evidenced by the presence of BSN (A, lane 3) but absence in mouse IgG immunoprecipitation (A, lane 2). DAO was found to co-immunoprecipitate along with BSN (B, lane 3) but not with mouse IgG (B, lane 2). The expected GFP-BSN truncated protein molecular weight on the SDS-PAGE gel is indicated by the arrow.

Legend:
Ln 1: Input lysate 1/10th volume
Ln 2: Mouse IgG immunoprecipitation
Ln 3: GFP immunoprecipitation

Figure 5.19: Immunoprecipitation of BSN from rDAO stable line transiently transfected with rat GFP-BSN 3263-3963 construct and probed with GFP antibody (A) and DAO antibody (B). The BSN fusion construct was found not to express as evidenced by lack of presence of expected 111 kDa band in GFP-BSN transiently transfected rDAO Hek293 cells (A, lane 1). Blot B was probed with DAO antibody.
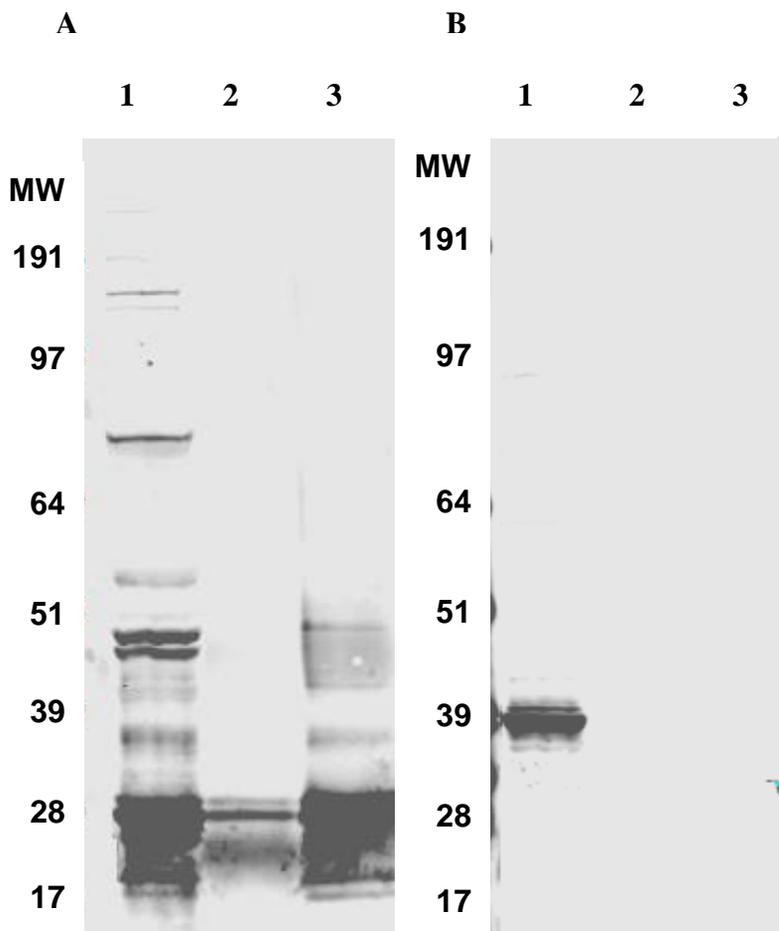
Legend:
Ln 1: Input lysate $1/10^{th}$ volume
Ln 2: Mouse IgG immunoprecipitation
Ln 3: GFP immunoprecipitation

Figure 5.20: Transiently transfected GFP-BSN inhibits DAO's enzymatic activity as measured by the AmplexRed assay. Transiently transfected full length GFP-BSN (95-3963), 1692-3263 BSN, and 2715-3263 BSN partially inhibited DAO's acitivity in relation to GPF only and 95-609 BSN.

Activity of Transiently Transfected DAO Stable Line With BSN or GFP
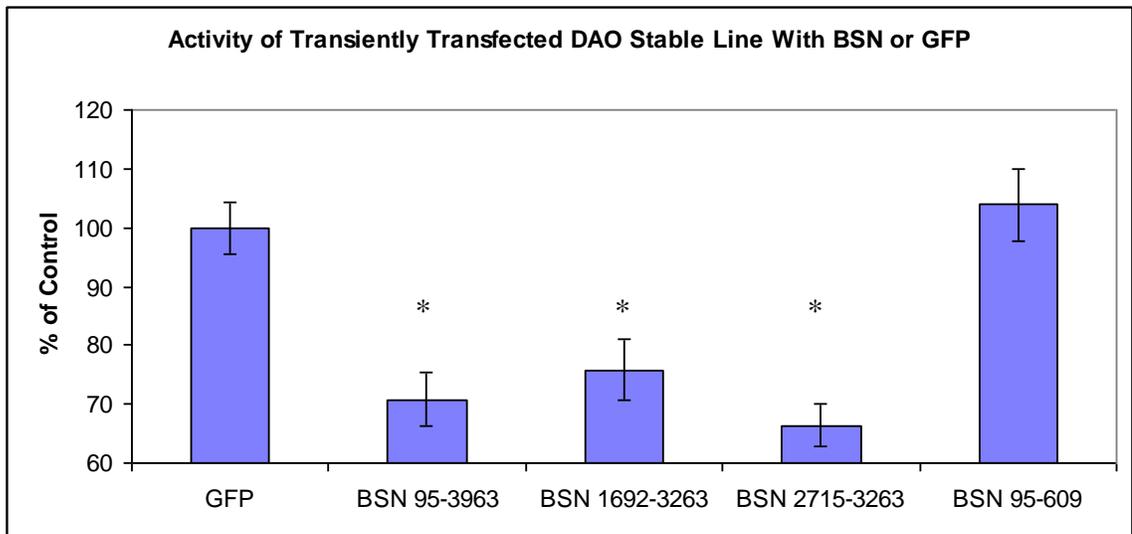
* P < 0.01 as compared to the GFP control based on One-way ANOVA according to Dunnett's method.

Figure 5.21: No evidence of BSN, PCLO or Liprin-α-3 expression in Hek293 cell lysate. SDS-PAGE gel containing Hek293 and rat cerebellar lysates was probed for presence of the above mentioned presynaptic active zone proteins with respective antibodies. Anti-actin antibody was used to show equal protein concentration in the two samples.

Legend:
Ln 1: 20 μg rat cerebellar lysate
Ln 2: 20 μg Hek293 lysate
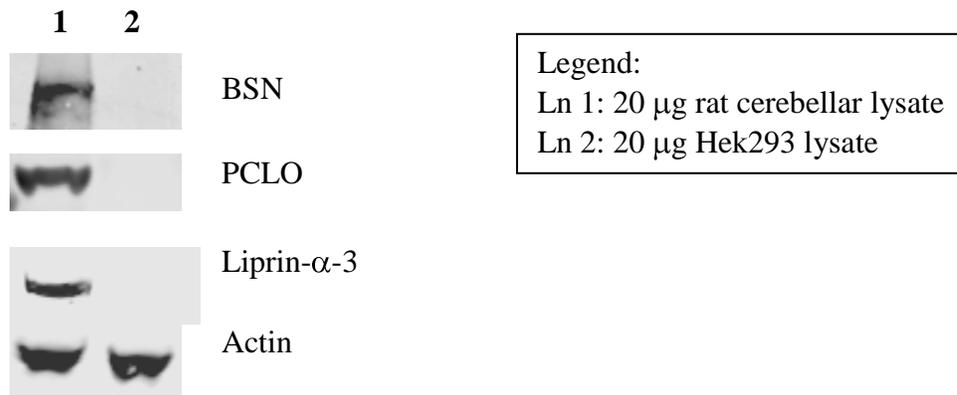
6. Yeast-two-hybrid screen for identification of DAO interacting proteins from human fetal brain

6.1 Introduction

Yeast-two-hybrid (Y2H) is a high-throughput technique used to identify protein-protein interactions (Young, 1998). As summarized in Table 4.1 and illustrated in Figure 6.1, this molecular biology tool relies on the observation that the GAL4 transcriptional factor may be divided into functional regions, the binding domain (BD) and the activating domain (AD), which act coordinately to activate reporter gene(s) under control of the GAL upstream activating sequence (UAS). The BD interacts with GAL4 UAS while the activating domain initiates transcription (Joung et al., 2000). Neither the AD nor the BD on its own can activate the reporter genes but when both are in a close physical proximity they form a functional transcriptional factor (Verschure et al., 2006). Since the AD and BD are two separate entities which otherwise do not interact with each other, they can be brought together by fusion with proteins that have an affinity for each other. Hence in a yeast-two-hybrid screen, plasmids containing the BD are constructed as fusion with known proteins, e.g. DAO, which serves as a "bait" protein. The AD plasmid is engineered with DNA encoding protein fragments representing a pool of proteins transcribed from a given organism or tissue which represents the "prey" in this instance from human brain. The AD containing fusion protein with an affinity for the BD-DAO fusion protein will allow for the AD and BD to come to a close proximity and initiate transcription of reporter genes. The yeast strains utilized in the Y2H screen are genetically modified to lack key biosynthetic enzymes essential for amino acids or nucleic acids synthesis. When grown on dropout media, or media lacking the necessary nutrients, the strains will not grow unless the transcription factor is functional through an interaction of the bait with the prey which promotes expression of enzymes need for the biosynthesis of essential nutrients and survival on the drop out media. Y2H is a commonly used technique has been repeatedly and successfully used in identifying physiological relevant protein-protein interactors (Millar et al., 2005).

While this approach has been successful it has been plagued with occasional shortcomings including a high degree of false positives and negatives. Amongst the explanations is that the proteins are over expressed which may force an interaction which otherwise would not be possible. Since the proteins are expressed as fusion constructs their three dimensional configuration may be altered. Large proteins are unlikely to be expressed at a full length and may be represented as fragments resulting in lack of interaction in cases where the protein must be intact to form the interacting domain. Both bait and prey proteins may undergo posttranslational modifications *in vivo* which may not happen in the yeast cells altering affinity between proteins. The proteins may never be expressed in the same cell type *in vivo* or in the same cellular compartment or alternatively they may be co-expressed in a certain organelle while they have to be expressed in the yeast nucleus to come up as a hit. All of these factors contribute to false positive rates of as much as 50% and necessitate further confirmatory studies and independent methodologies such as co-immunoprecipitation to confirm the preliminary findings (Deane et al., 2002).

Figure 6.1: Schematic diagram of the yeast-two-hybrid principle. Two proteins, the bait and the prey, are separately expressed in yeast as fusion constructs with the BD and the AD respectively. In an event of an interaction between the bait and the prey the GAL4 transcriptional factor is reconfigured by virtue of physical proximity of the BD and the AD resulting in transcription of reporter gene(s).
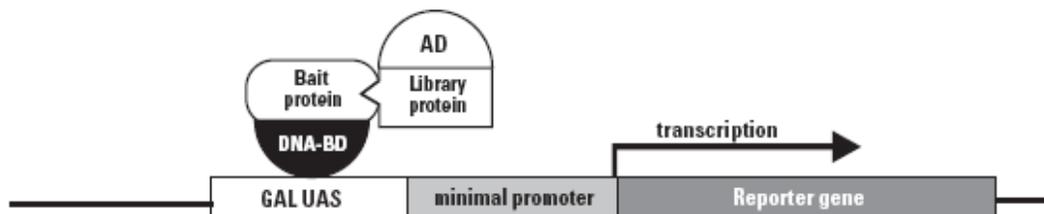
Taken from Clontech Matchmaker user manual.

6.2 The Matchmaker Pretransformed Library

A fetal brain library generated through poly-T primer by Clontech Laboratories (#638831) was used for the yeast-two-hybrid screen. The poly-T primer is complementary to the poly-A tails found on mRNAs allowing for reverse transcription of the mRNA found in the human fetal brain. The poly-T primer generates a library encoding mostly C-terminal fragments of proteins especially in case of large proteins. Through application of this approach we would be highly unlikely to identify large DAO interactors or those that may be interacting at the N-terminus. The poly-T library was cloned into pACT2 vector and transformed into Y187 MATα yeast strain. Human DAO lacking the peroxisomal targeting sequence was cloned into pGBKT7 vector and transformed into AH109 MATa strain (Figure 6.2). The yeast strains used in this screen were genetically engineered to lack capabilities of synthesizing adenine (Ade), histidine (His), leucine (Leu), and tryptophan (Trp). Thus they cannot survive on media lacking any one of those nutrients unless they have been transformed with both the bait and prey vectors conferring expression of tryptophan and leucine biosynthetic enzymes respectively as selectable markers for maintaining the presence of the plasmids within the cells and fusion proteins that interact with each other conferring transcription of adenine and histidine biosynthetic enzymes. When the strains express interacting proteins they also can break down X-α-Gal through expression of MEL1 and LacZ enzymes transforming otherwise white colonies into blue colonies (Figure 6.2).

Figure 6.2: Schematic for the yeast-two-hybrid mating and selection. The two yeast haploid strains, AH109 and Y187, were transformed with pGBKT7-DAO and pACT2-library vectors respectively and mated. The resulting diploids expressing proteins conferring interaction with DAO survived on quadruple dropout media and turned blue color.
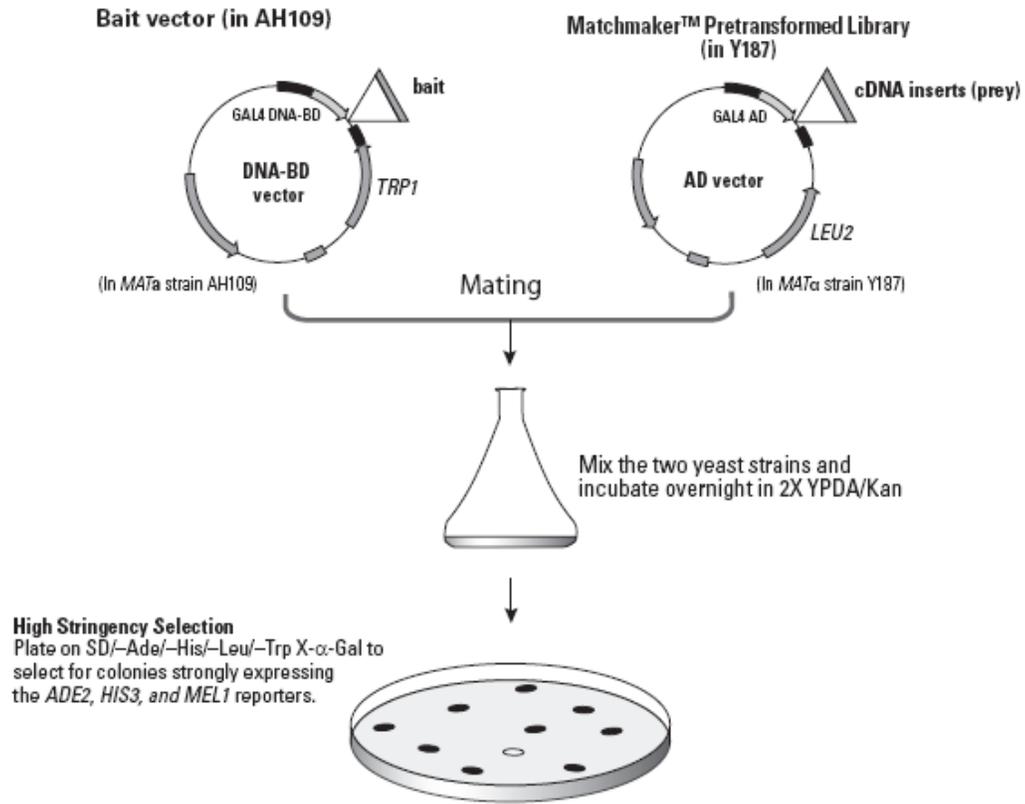
Taken from Clontech Matchmaker user manual.
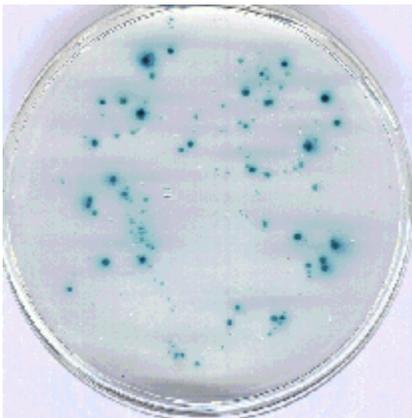
This plate is an example of successful mating and a robust interaction between the bait and the prey resulting in growth of blue colonies.

6.3 Yeast-two-hybrid Control Experiments

Prior to the Y2H screen the pGBKT7-DAO construct was tested for auto activation. This is a critical experiment in which the bait construct was transformed into the AH109 yeast strain and plated out on tryptophan dropout and quadruple dropout media. In our case, the yeast strain transformed with the pGBKT7-DAO construct grew on tryptophan dropout media while mock transformed yeast did not, confirming successful transformation of cells. More importantly, no colonies were identified on the quadruple dropout medium even after seven days post transformation suggesting that the BD-DAO on its own cannot activate the transcription of reporter genes.

The DAO construct was also tested for toxicity. Growth rates of transformed yeast cells with the pGBKT7-DAO were compared to those transformed with the bait vector without DAO. The number of colonies and the colony sizes between the two transformations did not differ when grown on tryptophan dropout media suggesting that the DAO bait construct is not toxic to the yeast cells. Through this set of control experiments we determined that DAO was a suitable candidate for a Y2H screen.

6.4 DAO Truncation Mutants

DAO truncation mutants were generated to assist in identification of the DAO interacting site with the yeast-two-hybrid interacting proteins. An interacting site is a polypeptide or a single amino acid within the protein responsible for the interaction with the interacting protein. Identification of an interactor with a truncated DAO protein may be used as a confirmation step for the Y2H screen and allows for an eventual recognition of the amino acids responsible for the physical interaction. DAO truncation mutants were generated through polymerase chain reaction (PCR) of the 5' primer and a 3' primer progressively closer to the 5' end. This resulted in generation of progressively shorter DAO fragments in increments of about 50 amino acids for a total of five truncation mutants and the full length DAO without the peroxisomal targeting sequence (Figure 6.3). The PCR bands generated during the synthesis of the DAO truncation are illustrated in Figure 6.4 while the corresponding Western blot

with the fusion protein between DAO and the transcriptional factor binding domain are in Figure 6.5.

Figure 6.3: Schematic diagram of the DAO truncation mutants. The DAO fragments were synthesized in increments of about 50 amino acids extending out from the 5' end until the entire protein length was covered.
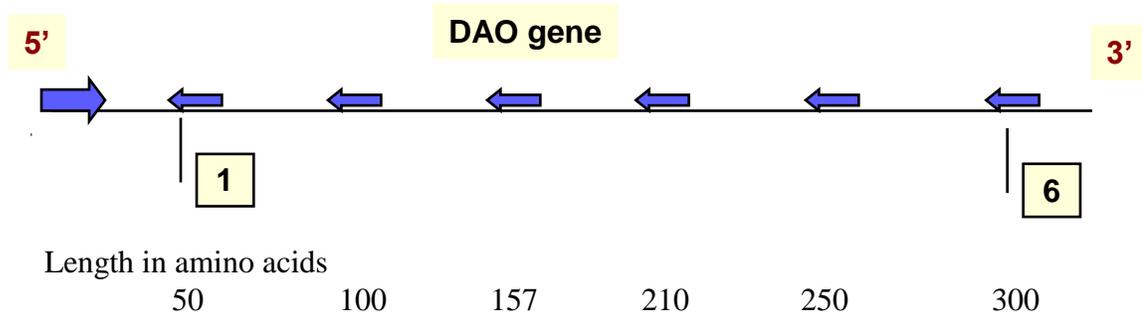
Figure 6.4: DNA fragments generated through PCR during synthesis of DAO truncation mutants. Primers complementary to the 5' end and a truncated 3' end of the DAO sequence were used to synthesize truncated DAO encoding constructs. Sample of the constructs are shown below on ethydium bromide agar gel visualized under UV light.

Legend:
Ln 1: DAO truncation 1 ~150bp
Ln 2: DAO truncation 2 ~ 300bp
Ln 3: DAO truncation 3 ~ 450bp
Ln 4: DAO truncation 4 ~ 600bp
Ln 5: DAO truncation 5 ~ 750bp
Ln 6: Full length DAO ~ 1000bp

153
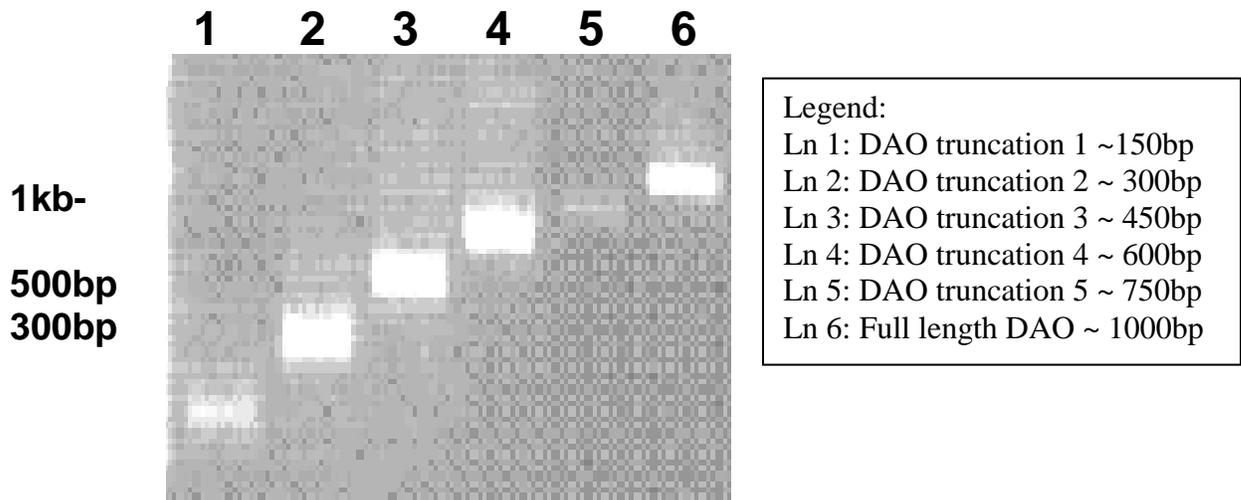
Figure 6.5: Western blot showing expression of the truncated DAO fusion proteins. The DAO fragments generated through PCR were cloned into the pGBKT7 vector resulting in expression of the DAO fusion proteins of the expected molecular weight. This blot was probed with Gal4 antibody.

Legend:
Ln 1: DAO truncation 1 ~ 23kDa
Ln 2: DAO truncation 2 ~ 28kDa
Ln 3: DAO truncation 3 ~ 33kDa
Ln 4: DAO truncation 4 ~ 38kDa
Ln 5: DAO truncation 5 ~ 43kDa
Ln 6: Full length DAO ~ 49kDa
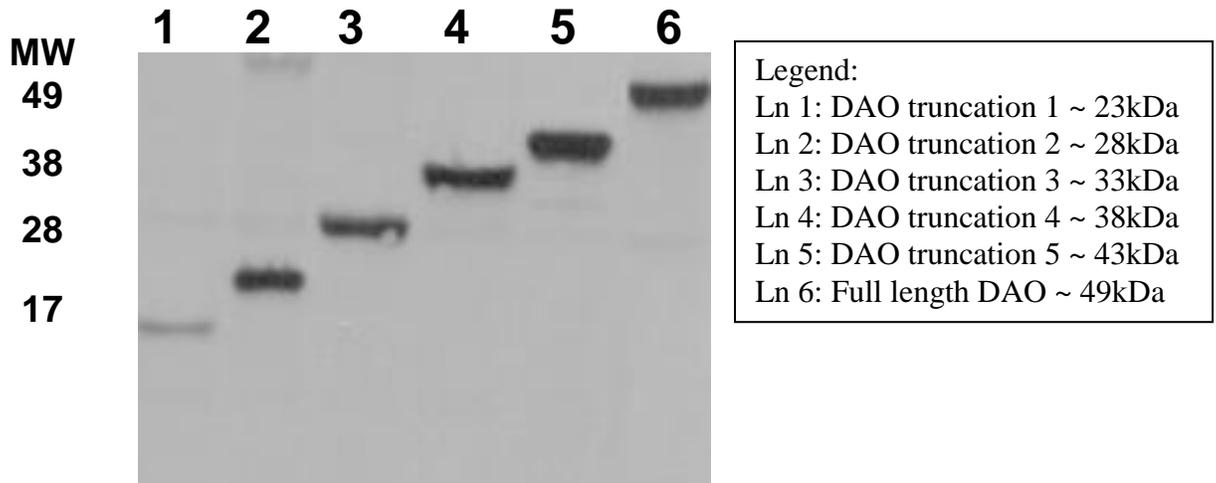
6.5 Results from the Mating Screen

A pretransformed human fetal brain library from Clontech (#638831) was used to mate with the DAO AH109 yeast cells. A mating efficiency of 9% was obtained between the DAO AH109 and human fetal brain library in Y187 yeast. A total of 1.85 million colonies were screened. One million colonies is the minimum recommended by Clontech to screen the entire library. Sixteen colonies were identified, fifteen of which were blue on the quadruple dropout media after three to four days post mating. The prey vectors were extracted, amplified and sequenced to identify the interactors. Yeasts were retransformed with the isolated prey vector to test for auto activation and in conjunction with the DAO bait vector to verify the initial observations. None of the sixteen colonies displayed auto activation and all of them grew on the quadruple dropout media.

Out of the sixteen colonies that grew on the quadruple dropout media, two colonies were represented by WW domain binding protein 2 (WBP-2). The remaining fourteen colonies ranged in size from 5 to 153 polypeptides when configured in frame with the AD but did not have corresponding protein

154

sequences in the NCBI library. The two WBP-2 clones identified encoded in-frame 124 amino acid peptide suggesting that both originated from the same colony. Similarly three 94 amino acid peptides corresponding to an unknown protein from a chromosome 1 genomic contig probably originated from the same starting colony as each had the exact same sequence. Eight of the peptides without a corresponding NCBI sequence were identifiable proteins in a different reading frame from that of the expected based on the prey vector cloning. However, since it is unlikely for any of the constructs to be expressed in other frame then the expected we did not pursue analysis of the impact of the unknown polypeptides on DAO. None of the clones displayed auto activation on their own or when expressed with pGBKT7 vector suggesting that in yeast they formed a physical interaction with the DAO protein.

6.6 Characterization of DAO and WBP-2 interaction

WBP-2 is a 139 amino acid protein. Through the yeast-two-hybrid screen we identified a 124 amino-acid peptide which represents nearly 90% of the entire length of the protein. There was a perfect homology between the yeast-two-hybrid protein and that of the expected NCBI WBP-2 sequence (Figure 6.6). WBP-2 has been shown to play an important role in activation of progesterone receptor and estrogen receptor (Dhananjayan et al., 2006). It has been shown to interact with and activate Pax8, a protein required for morphogenesis of the thyroid gland (Nitsch et al., 2004). WBP-2 has also been shown to interact with Yes kinase-associated protein (Sudol et al., 1995).

Both WBP-2 fragments identified were tested with the DAO truncation mutants to ascertain if any portion of the DAO protein was responsible for the physical interaction with WBP-2. Neither the vector nor the N-terminal 50 amino acids of DAO interacted with the WBP-2 fragment as no colonies grew on the quadruple dropout media post mating. However, longer DAO fragments of 100, 150, 200 and 250 amino acids successfully interacted with the WBP-2 (Figure 6.7). This suggests that the portion of DAO responsible for the interaction with WBP-2 in yeast cells is between n-terminal 50 and 100 amino acids.

Figure 6.6: Alignment of the NCBI WBP-2 amino acid sequence and that of our yeast-two-hybrid polypeptide. WBP-2 is a 139 amino acid long protein which was identified as a putative DAO interacting protein based on identification of 124 interacting polypeptide. The identified polypeptide has a complete homology to the WBP-2 sequence.

```
>☐ gb|EAW89327.1| G WW domain binding protein 2, isoform CRA_c [Homo sapiens]
Length=139

 Score =  154 bits (390),  Expect = 1e-36, Method: Composition-based stats.
 Identities = 124/124 (100%), Positives = 124/124 (100%), Gaps = 0/124 (0%)

Query  1     PEPTVLPSVPPSPSGALLGARSIPCSCFTLSFSPRRDSLATSSTAVQLPQSGTHCYTQPH  60
             PEPTVLPSVPPSPSGALLGARSIPCSCFTLSFSPRRDSLATSSTAVQLPQSGTHCYTQPH
Sbjct  16    PEPTVLPSVPPSPSGALLGARSIPCSCFTLSFSPRRDSLATSSTAVQLPQSGTHCYTQPH  75

Query  61    EPLQTSQVSSRALPDPAHIPSAGLCWSQKATAPAFHSARVQLQPPPPFLPFPVLGHVVAT  120
             EPLQTSQVSSRALPDPAHIPSAGLCWSQKATAPAFHSARVQLQPPPPFLPFPVLGHVVAT
Sbjct  76    EPLQTSQVSSRALPDPAHIPSAGLCWSQKATAPAFHSARVQLQPPPPFLPFPVLGHVVAT  135

Query  121   LCDF  124
             LCDF
Sbjct  136   LCDF  139
```

Figure 6.7: Mapping of the DAO interacting site with WBP-2. C-terminal DAO truncation mutants every 50 amino acids were used to ascertain the DAO region responsible for the physical interaction with WBP-2. Neither the vector nor the n-terminal 50 amino acid long DAO fragment formed an interaction with WBP-2. However, longer DAO fragments of 100, 150, 200 and 250 amino acids successfully interacted with the WBP-2. These data suggest that the DAO region responsible for the interaction with WBP-2 is found between n-terminal 50 and 100 amino acids.

	Vector	DAO 1	DAO 2	DAO 3	DAO 4	DAO 5	DAO C
WBP2	X	X	Y	Y	Y	Y	Y
WBP2	X	X	Y	Y	Y	Y	Y

Through the Allen Brain Atlas which shows mRNA expression profiles we were able to conclude that WBP-2 is likely to be expressed in the cerebellum where DAO expression is especially high (Figure 6.8). This data suggests that the two proteins may exist in the same tissue and be relevant interactors *in vivo*.

Figure 6.8: The mouse mRNA expression profile of WBP-2

Taken from Allen Brain Atlas.

A FLAG-tagged C-terminal full length human WBP-2 was expressed in hDAO stable line to ascertain its effect on the DAO activity. Increasing amounts of the WBP-2 construct ranging from 1 to 100 ng per 50,000 DAO cells in 96-well plate were transiently transfected but the DAO enzymatic activity remained unchanged (Figure 6.9).

Expression of the flag-tagged WBP-2 was confirmed in the hDAO Hek293 lysate by probing SDS-PAGE gel with a flag antibody. However, WBP-2 was not immunoprecipitated with DAO by DAO antibody from the DAO stable line lysate over expressing WBP-2 (Figure 6.10).

The mass spectroscopy data described in chapter 4 was examined for presence of WBP-2. Interestingly, WBP-2 was found to be co-immunoprecipitated with DAO by DAO antibody from rat cerebellar lysate when the mild wash conditions were utilized (Figure 6.11). WBP-2 was not identified in any of the negative controls or in the DAO immunoprecipitate with the harsh washing. The Y2H and the co-immunoprecipitation screens suggest that WBP-2

157

may be a relevant DAO interacting protein. However it is likely that WBP-2 a very weak DAO interactor or WBP-2 has a very low cerebellar expression profile.

Figure 6.9: Analysis of functional impact of WBP-2 expression on DAO activity. Overexpression of WBP-2 in hDAO stable line did not effect the DAO enzymatic activity.
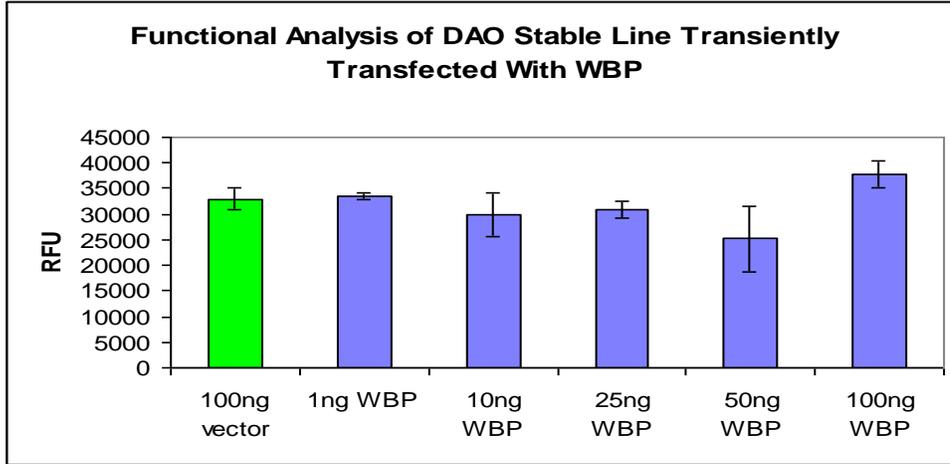
Figure 6.10: WBP-2 does not immunoprecipitate with DAO when over expressed in the hDAO stable line. DAO was immunoprecipitated with the DAO antibody and probed for the flag-WBP-2 presence. While WBP-2 was detected with FLAG antibody in the input lysate, none was found in the immunprecipitation lanes. The expected molecular weight of WBP-2 is designated with the arrow.

Legend:
Ln 1: Lysate input ($1/10^{th}$ volume)
Ln 2: Peptide blocked IP with DAO
         antibody
Ln 3: IP with DAO antibody
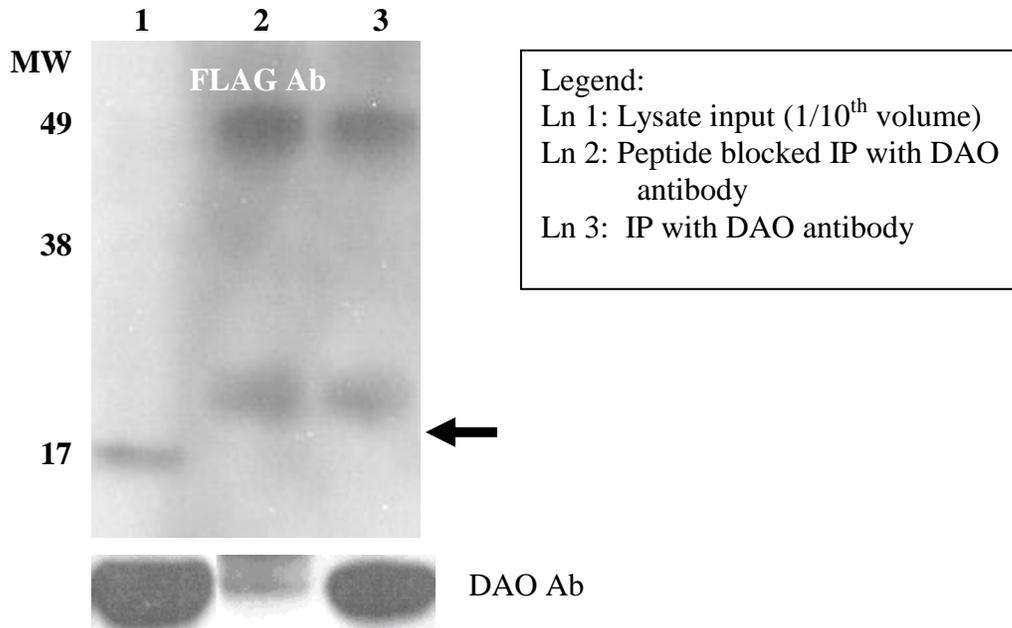
Figure 6.11: The mass spectroscopy data suggest that WBP-2 is specifically immunoprecipitated with DAO via DAO antibody from rat cerebellar lysate. Despite the specificity of WBP-2 to DAO column the single polypeptide identified may be a random event, representing a very weak interaction or indicative of a low WBP-2 expression.

Protein Name	Sample									
	PBS Wash						RIPA Supplemented Wash			
	A (IgG)		B (Peptide blocked)		C (DAO)		D (Peptide blocked)		E (DAO)	
	Unique	Total	Unique	Total	Unique	Total	Unique	Total	Unique	Total
WBP-2	0	0	0	0	1	1	0	0	0	0

6.7 Y2H screening of human adult brain library

To complement our Y2H screen of human fetal brain library we collaborated with Hybrigenics to perform a Y2H screen on a human adult brain library. A different library was tested to account for DAO developmental expression changes described in chapter 1. While Hybrigenics used the same GAL4 screening strategy as we have they used a library synthesized through random primers instead of the poly-T primer. The difference between the two libraries is that with a random primer approach potentially a better coverage of the library is possible especially with large proteins. Through the Hybrigenics screen four hits were identified. An important advantage to the Hybrigenics screen is the proprietary algorithm used to determine the strength of and likelihood of the interaction allowing for a ranking of the hits. Of the four putative interacting proteins, mitochondrial tumor suppressor-1 (MTUS1) was identified as having a very high likelihood of interaction, one unidentified protein with a moderate likelihood of an interaction and TAF1 and COPS5 with a very low likelihood. None of these proteins were identified in either the Y2H fetal brain library screen or the rat brain immunoprecipitation.

6.8 Conclusions

The Matchmaker pretransformed human fetal brain library and collaboration with Hybrigenics were successfully used in identification of DAO interacting proteins through yeast-two-hybrid screens. Through these approaches twenty colonies on the quadruple dropout media were identified representing seventeen putative DAO interacting proteins. Of the group four corresponded to identifiable proteins based on the NCBI alignment matching with a perfect homology. Our confirmatory experiments focused on WBP-2. The interaction between DAO and WBP-2 was characterized through DAO truncation mutants suggesting that WBP-2 interacts between amino acid 50 and 100 of DAO protein. mRNA expression pattern suggests that WBP-2 may be highly transcribed in the cerebellum suggesting that it may be found in the same tissue as DAO. However, WBP-2 was shown not to affect activity of DAO when both proteins were over expressed in Hek293 cells. More importantly, the interaction identified in the yeast-two-hybrid did not confirm in co-immunoprecipitation from the over expressed Hek293 cell lysates. Interestingly, WBP-2 was found to be a very weak DAO interacting protein through the DAO immunoprecipitation from rat cerebellar lysate suggesting that the two proteins may have a weak affinity for each other.

6.9 Conclusions and Future Studies

I started my doctorate work by focusing on necessary tools for identification and characterization of DAO interacting proteins. As such, one specific DAO antibody was generated, purified and validated. This antibody was shown to detect human, rat and mouse DAO on SDS-PAGE gel and to immunoprecipitate DAO protein from lysate. The DAO antibody in conjunction with Dynal beads was used to co-immunoprecipitate DAO and its interacting proteins from rat cerebellar lysate. The interacting proteins were then identified through mass spectroscopy. As part of this experiment, two negative controls were used, a rabbit IgG and a peptide blocked DAO antibody, to eliminate sticky, non-specific proteins from being considered as putative DAO interacators. Furthermore, the co-immunoprecipitation was performed with a mild and a harsh

washing conditions to identify the strongest DAO interacting proteins. DAO yeast expression constructs were also generated to explore DAO interacting proteins through a Y2H methodology. Additional tools generated for validation and characterization of the interacting proteins include purified human DAO enzyme, and rat and human DAO stable lines. Amplex Red assay was found to reliably measure DAO's activity and was used to ascertain effect of DAO's interacting proteins on DAO's activity.

Through co-IP and Y2H approaches many putative DAO interacting proteins have been identified. Those interacting proteins represent several different groups of proteins suggesting DAO expression outside of the traditionally assumed peroxisome region and speculate to explore consequences of such an altered expression and potentially alternative DAO functions. The number of interacting proteins identified made it difficult to pursue them all hence we focused on WBP-2 and BSN. WBP-2 was identified in both Y2H and the co-IP experiments. The interation between the two proteins was confirmed in Y2H and it is likely that WBP-2 interacts between DAO's 50th and 100th amino acid. However, no functional effects were observed on DAO's activity when both proteins were over expressed in Hek293 cells. The DAO antibody did not immunoprecipitate WBP-2 from Hek293 lysate over expressing both proteins either suggesting that in the context of Hek293 cells there is no relevant interaction between the two proteins. On the other hand, the outcome of co-IPs, fractionations, and immunocytochemistry studies suggest that DAO interacts with BSN within the presynaptic active zone where its enzymatic activity is modulated by BSN. It is yet unknown what function DAO plays at the presynaptic active zone. If DAO is FAD bound then it is likely to be enzymatically active but this has to be explored in future studies as well as any other functions DAO may have at the synapse. Such DAO localization may directly play into modulating synaptic D-serine concentration as this neurotransmitter is reabsorbed from the synapse by Asc-1 into neurons. Before D-serine is recycled back into the synapses some of it may be degraded by DAO. However, metabolism of D-serine at the CAZ poses a threat of oxidative stress on the synapse due to the hydrogen peroxide synthesis. Hence DAO's activity, if unchecked can lead to excessive

synaptic pruning. Does this occur, to what extent, and does it contribute to schizophrenia? Do the interacting proteins represent dirct interactors and if so are those interactions true for other species than rat DAO? The DAO KO mice represent a tool to start addressing these questions in the future.

Chapter 7: Discussion

7.1: Dynein: a potential DAO interacting protein

      We used Spotfire software designed in-house by Andrew Hill to cluster the putative DAO interacting proteins resulting in the main six groups described in sections 4.6.1 through 4.6.6. In addition to these six clusters, individual proteins such as the heavy and light chains of dynein have been identified in the co-immunoprecipitation experiments with the DAO antibody utilizing both PBS and modified RIPA buffer washes (Table 4.2). The robust retention of dynein polypeptide chains by the DAO antibody, which was abrogated by immunogenic peptide and absent in non-immune IgG control experiments (Table 4.2), suggests a potential interaction between DAO and dynein. Nevertheless, we did not pursue this finding because we were interested in the novelty posed by presynaptic active zone proteins in the context of DAO localization. However, DAO transport to the CAZ may be explained by an interaction with dynein. Since dynein is a motor protein that uses ATP-derived energy for transport of intracellular cargo from the cell center to the periphery (Mallik et al., 2004; Reck-Peterson et al., 2006; Vallee et al., 2004), a DAO interaction with dynein may be relevant for DAO movement from the cytoplasm into the CAZ.

7.2: Discrepancies with published literature

      As depicted in Figure 5.5, DAO immunofluorescence in the rat cerebellar sections appears to be concentrated to the Purkinje cells of the Purkinje cell layer. This observation is further supported by DAO specific immunofluorescence in the molecular layer originating from Purkinje cell dendrites. It is unlikely that the immunofluorescence attributable to the Purkinje cells stems from other cells that may be either synapsing upon or in a close proximity to the Purkinje cells. Our findings are supported by a published report showing DAO immunoreactivity in Purkinje cells (Moreno et al., 1999) but the DAO antibody used in this study was later shown to cross-react with D-aspartate oxidase (Shleper et al., 2005) suggesting that the Purkinje cell immunoreactivity may not be specific to DAO itself. In contrast to our findings, other reports, examining mRNA and protein

DAO expression in human and rat, reported a distinct lack of DAO presence in the Purkinje cells (Ono et al., 2009; Verrall et al., 2007). Furthermore, we failed to show DAO immunoreactivity in Bergmann glia, which was reported earlier (Ono et al., 2009; Verrall et al., 2007). To understand this apparent discrepancy we could examine DAO expression through the avidin-biotin-peroxidase technique using the Vectastain Elite ABC kit (Vector Labs, Burlingame, CA), as in aforementioned published reports, instead of the immunofluorescence. Alternatively, we could test for DAO mRNA expression in the Purkinje cells through in situ hybridization. We chose to do the former. When the same tissue used for immunofluorescence was instead visualized with the avidin-biotin-peroxidase, DAO immunoreactivity was much more consistent with that of the above mentioned reports (Figure 7.1). Specifically, we no longer observed Purkinje cell staining but did see predominant Purkinje cell layer immunoreactivity likely to be that of Bergmann glia as depicted by the small round cells. In addition we observed moderate staining of small round cells in the molecular layer.

It is hard to reconcile this noticeable difference between the immunofluorescence and avidin-biotin-peroxidase immunoreactivity as the only difference between the two experiments was the secondary antibody and the visualization method. In each instance the secondary antibody was shown not to have any signal of its own suggesting that the observed difference is not due to the secondary antibody.

The DAO expression utilizing the avidin-biotin-peroxidase visualization do not preclude it from co-localization with BSN as rat cerebellar slices also displayed immunoreactivity to small round cells in the Purkinje cell layer and the molecular layer (Figure 7.1). However, this method does not allow for co-staining with both antibodies so we cannot be completely sure of their co-localization.

Figure 7.1: DAO and BSN immunoreactivity in rat cerebellar slices. When the rat cerebellar slices were prepared in the exact same way as for the immunofluorescence but visualized using avidin-biotin-peroxidase technique the DAO was mainly shown to localize to small cells likely to be Bergmann glia within the Purkinje cell layer but not to the Purkinje cells themselves and modestly to small round cells in the molecular layer (A). This immunoreactivity was abolished when rabbit IgG was used instead of the DAO antibody (B). A zoom in of DAO stained image (C) clearly shows immunoreactivity of small round cells surrounding the Purkinje cell (*). BSN immunoreactivity also was found in small round cells of the Purkinje cell layer, small round cells of the molecular layer and modestly to the Purkinje cells and small round cells in the granule layer (D). No immunoreactivity was observed when a mouse IgG was used instead of BSN antibody (E).

A

B

C
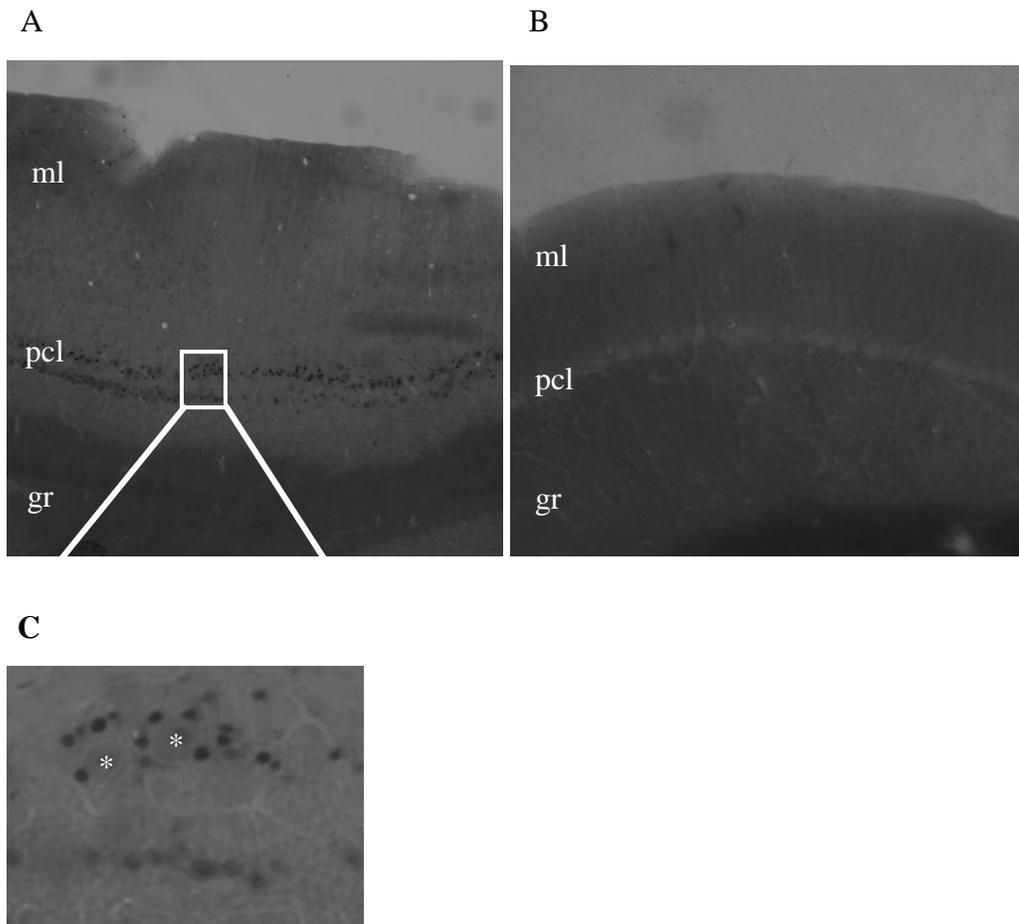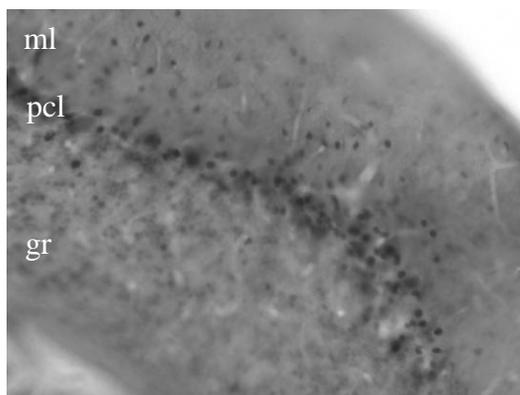
D   **E**
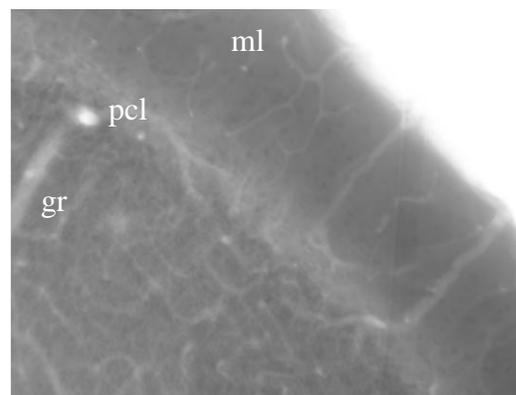
ml = molecular layer, pcl = Purkinje cell layer; gr = granule layer; * = Purkinje cell

7.3: Additional imaging studies

In the past, substantial discrepancies have emerged with respect to DAO localization on regional, cellular and subcellular levels (described earlier and review in (Verrall et al., 2010).   As depicted in this thesis the detection method utilizing the same antibody may result in a different outcome.   To build confidence in DAO localization it would be ideal to probe for DAO with multiple DAO antibodies generated against different regions of the DAO polypeptide. Also, an Electron microscopy imaging of the rat cerebellum may more definitely pinpoint DAO localization and address its likely presynaptic localization. In particular, Electron microscopy immunogold would allow us to pinpoint the subcellular localization, cell types, and address co-localization with BSN.

7.4: Thesis summary

Through a co-immunoprecipitation and mass spectrometry approach we have identified twenty-four putative DAO interacting proteins from rat cerebellum (Table 4.3).   Many of the proteins, including BSN, PCLO, SNIP, ERC1, and RAPGEF4 are enriched in the presynaptic active zone (Chin et al., 2000; Dresbach et al., 2003; Li et al., 2006; Wang et al., 1999; Wang et al., 2002) suggesting an alternative subcellular localization for DAO to that of the widely accepted astrocytic, peroxisome bound DAO (Cristiano et al., 2001; Usuda et al.,

1986; Wanders and Waterham, 2006). Our findings are supported by recent observations of DAO expression 1) in neurons, as exemplified by reports of DAO expression in Golgi and Purkinje cells of the rat cerebellum (Moreno et al., 1999) and pyramidal neurons of human hippocampus and cerebral cortex (Verrall et al., 2007); 2) in the extra-peroxisomal space, as exemplified by a pericellular distribution of DAO in human brain combined with the lack of an overlap between DAO and peroxisomal markers in human astrocyte cultures (Sacchi et al., 2008; Verrall et al., 2007). Thus, since published reports hint at DAO localization outside of the peroxisome, we explored an alternative localization for DAO at the presynaptic active zone by virtue of its interaction with BSN.

BSN was confirmed to interact with DAO in rat cerebellar detergent extracts through co-immunoprecipitation combined with western blotting using DAO- and BSN-specific antibodies (Figure 5.3). Subcellular fractionation studies of rat cerebellum showed that DAO is present in the synaptic junction membrane fraction which contained BSN but not catalase (Figure 5.7). This data suggests a DAO localization outside of the peroxisome, where DAO was historically believed to be localized (De Duve and Baudhuin, 1966). In light of our immunoprecipitation findings, these fractionation data suggest that DAO may be found in the presynaptic terminus where it may interact with BSN *in vivo*. Immunocytochemistry of cultured CGNs confirmed the localization of DAO in neuronal processes partially colocalizing with BSN (Figures 5.11 and 5.12).

BSN was co-immunoprecipitated with DAO from HEK293 cells over expressing both proteins (Figure 5.13) suggesting that the two may directly interact as none of the major members of the presynaptic active zone are expressed in the HEK293 cells (Figure 5.21). The presence of other presynaptic active zone proteins in the DAO immunoprecipitate suggests that they may have been pulled-down with DAO or indirectly through an interaction with BSN itself (Wang et al., 2009). While the carboxyl terminus of BSN was shown to be responsible for an interaction with many of the other presynaptic active zone proteins (Wang et al., 2009), the BSN region spanning amino acids 2715-3263, representing a predicted single coiled coil domain, was found to co-immunoprecipitate with DAO when both were over-expressed in HEK293 cells

(Figure 5.18). This data suggests that an interaction of BSN with other members of the presynaptic active zone would not be disrupted by a DAO-BSN interaction as it involves a different region of BSN.

The presynaptic cytoskeletal protein matrix, called the 'cytometrix assembled at the active zones' (CAZ) (Garner et al., 2000), is a specialized subcellular domain where synaptic vesicles are anchored and primed prior to membrane fusion and neurotransmitter release (Owald and Sigrist, 2009). BSN and PCLO play a major role in the organization of the CAZ likely as scaffolding elements (Fenster et al., 2000; tom Dieck et al., 1998). Another member of the presynaptic terminus, Asc-1, a D-serine uptake transporter, has a major role in D-serine clearance from the synapse in forebrain and cerebellum (Fukasawa et al., 2000; Helboe et al., 2003; Matsuo et al., 2004; Nakauchi et al., 2000; Rutter et al., 2007; Shao et al., 2009). The presence of DAO at the CAZ suggests that some of the reabsorbed D-serine may be metabolized; further fine-tuning the D-serine concentration within the synapse and influencing NMDAR activation. Our findings are important in light of a recent report of D-serine release from neurons via a nonvesicular mechanism (Rosenberg et al., 2010), suggesting that this nonvesicular pool of D-serine might be readily metabolized by presynaptically-localized DAO.

The interaction of DAO with BSN may be especially relevant in the forebrain where DAO has been reported to be predominantly expressed in neurons (Kapoor et al., 2006; Sacchi et al., 2008; Verrall et al., 2007). Such expression, in conjunction with our observation of an inhibitory effect of BSN on the activity of DAO, may in part explain why the enzymatic activity of DAO has been consistently undetectable in the forebrain (Neims et al., 1966; Weimar and Neims, 1977). In the hindbrain, however, where DAO is more likely to be expressed in glia rather than in neurons, BSN would not be expected to influence DAO's activity since BSN is not expressed in glia. In fact, within the brain, DAO activity is most robust in hindbrain when compared to all other brain regions (Arnold et al., 1979; Horiike et al., 1994; Madeira et al., 2008; Weimar and Neims, 1977).

A loss of the inhibitory effect of BSN on neuronal DAO activity may also explain observations made in BSN functional knockout mice(Altrock et al., 2003). These mice express a fragment of BSN that lacks amino acids 505-2889, a region that partially overlaps with the DAO binding site identified in the present study (Figure 5.18). Moreover, this BSN fragment only partially partitions (between 10 and 30%) with the synaptic protein fraction. Hippocampal cultures derived from these mice have been shown to express twice as many functionally silent synapses than wild-type mice (Altrock et al., 2003). The functional silence may be a direct consequence of lack of sufficient NMDAR activation as exemplified by reduced LTP in striatal medium spiny neurons of the BSN mutant mice (Ghiglieri et al., 2009). Therefore, in the neuronal hippocampal cultures from the BSN functional knockout mice, DAO may still act within the presynaptic active zone without the inhibitory effect elicited by BSN. It is tempting to speculate that presynaptic DAO, in the absence of the inhibitory influence of BSN, as would be the case in these BSN mutant mice, is functionally overactive, metabolizing synaptic D-serine and resulting in NMDAR hypoactivity.

The mechanism underlying the inhibition of DAO enzymatic activity by BSN is yet unknown. Since human DAO catalytic activity has been shown to be absent in flavin adenine dinucleotide-unbound DAO (Caldinelli et al., 2009), BSN may compete with flavin adenine dinucleotide (FAD) binding rendering DAO inactive. BSN inhibition of presynaptic active zone DAO may be critical to maintaining healthy synapses. Uncontrolled and excessive DAO catalytic activity may be cytotoxic through hydrogen peroxide production (Park et al., 2006), resulting in excessive synaptic pruning and a reduction of synapses. However, the connection between BSN and these molecular and cellular consequences have yet to be experimentally established.

It is as yet unknown what function DAO plays at the presynaptic active zone. If DAO is FAD-bound, then it is likely to be enzymatically active but must be explored directly in future studies. The metabolism of D-serine by DAO at the CAZ poses a threat of oxidative damage to synaptic components due to excessive hydrogen peroxide synthesis. Hence the catalytic activity of DAO, if unchecked,

can lead to excessive synaptic pruning as well as other pathological cellular consequences. BSN may be playing an important homeostatic role, inhibiting excessive DAO activity at the presynaptic active zone. Whether this occurs, to what extent, and whether it may serve as a contributing factor to NMDAR hypofunction are critical questions that need to be addressed.

7.5: Relevance of our findings

Synaptic D-serine is critical to NMDAR activity. Our findings of DAO localization at the CAZ, outside of the peroxisome, suggest a direct involvement of DAO in modulating how much D-serine is available for synaptic release. In the absence of an inhibitory effect mediated by BSN on DAO, the presynaptic DAO activity may excessively metabolize D-serine resulting in a decreased concentration of readily releasable D-serine into the synaptic cleft. This decreased level of D-serine, in turn, may contribute to the NMDAR hypofunction observed in schizophrenic patients. Our data suggests that a potent DAO inhibitor may at least in part reverse NMDAR hypofunction by increasing synaptic D-serine concentration.

8. Materials and Methods

8.1 Molecular Biology

8.1.1 Bacterial and yeast strains

Subcloning and PCR cloning were performed unless otherwise stated using the One Shot^R MAX Efficiency^R DH5α^{TM} – T1^R Chemical Competent *E. coli* (Invitrogen; 12297-016).

BL21 (DE3) competent cells were purchased from Stratagene for the purpose of generating purified hDAO enzyme.

Saccharomyces cerevisiae host strain Y187 pretransformed with the human fetal brain library were purchased from Clontech Laboratories. For mating and subcloning untransfected AH109 (Clontech; 630444) and Y187 yeast strains (Clontech; 630457) were used.

8.1.2 Growth media and agar plates

Luria-Bertani (LB) broth containing 1% tryptone, 0.5% yeast extract and 0.5% NaCl (Gibco; 10855) was used to grow all of the bacterial cultures. For plasmids encoding Ampicillin resistance, Ampicillin (amp) (EMD Biosciences; 171254), was added to a concentration of 100 μg/ml and for Kanamycin resistance, Kanamycin (kan) (EMD Biosciences; 420311) was added to a concentration of 50 μg/ml.

Luria-Bertani (LB) agar plates containing antibiotic were purchased from Teknova (50 μg/ml Ampicillin – L1150-02; 50 μg/ml Kanamycin – L1025).

S.O.C medium (2% Tryptone, 0.5% Yeast Extract, 10 mM NaCl, 25 mM KCl, 10 mM MgCl$_2$, 10 mM MgSO$_4$, 20 mM glucose) was purchased from Invitrogen (15544-034).

Yeast media purchased from Clontech include YPD (a blend of yeast extract, peptone, and dextrose) medium (630409), YPD agar medium (630410), minimal synthetically defined (SD) base medium (630411), minimal SD agar base (630412), Trp dropout (DO) supplement (630413), Leu DO supplement (630414), His DO supplement (630415), Ura DO supplement (630416), Leu/Trp DO supplement (630417), His/Leu DO supplement (630418), His/Leu/Trp DO supplement (630419) and Ade/His/Leu/Trp DO supplement (630428).

8.1.3 Chemical transformation protocol

Competent bacterial cells were thawed out on ice and 0.1-1 μg (in a total volume of 1 μl) of plasmid was mixed into 50 μl of cell solution in 14 ml Falcon tubes (Beckton Dickinson; 352059), incubated on ice for 30 min, heat shocked for 45 seconds at 42°C and cooled on ice for 2 min. The cells were removed from ice bath and mixed with 200 μl of S.O.C medium and incubated for 45 min at 37°C in a shaker at 150 rmp. The entire solution and 1/10 and 1/100 dilutions there of were spread out on selective LB plates for incubation overnight at 37°C. Individual colonies were selected the following day.

8.1.4 DNA electrophoresis

See Sambrooke et al (1989) chapter 6

Briefly, agarose was added 1x TAE (Invitrogen; 15558-042) and melted in a microwave oven. The concentration of agarose used depended on the size of fragments to be resolved, on a scale of 0.6% for large fragments (>5kb) up to 2.5% for small fragmens (<0.5 kb). Ethydium bromide (BioRad; 161-0433) was added to a concentration of 100 ng/ml. A 6x loading buffer (Promega; 25223001) was added to samples prior to loading on the gel. Samples were run in 1x TAE buffer at a constant voltage of 60-130V depending on the gel box size. DNA was visualized by placing the gel on the UV transilluminator.

8.1.5 Ethanol precipitation of DNA

To concentrate DNA from aqueous solution, 0.1 volume of 3M Sodium Acetate pH 5.2 (Rockland; RLMB-041) followed by 2 volumes of 100% ethanol were

added, and incubated in -20°C for at least 10 min. For small amounts of DNA, such as ligations and preparation of fragments prior to ligation, 1 µl of glycogen (1mg/ml) was added before the salt and ethanol. After centrifugation at 13,000 rpms for 15 min, the pellet was washed with 70% ethanol and dried at room temperature for 5 min before it was resuspended in sterile water.

8.1.6 Gel extraction

The QIAquick Gel Extraction Kit (Qiagen; 28704) was used to extract DNA from agar. Briefly, the DNA sample was run on agarose and the band of interest was excised and weighted. The sample was dissolved in three times its weight in buffer QG at 42°C before isopropyl alcohol was added at one times the sample weight. The solution was spun down at 13,000 rpm at room temperature for 1 min in the QIAquick spin column before 500 µl of buffer QG was reapplied to the filter QIA tubes. The tubes were again spun down at 13,000 rpm for 1 min and the DNA containing filter was washed with 750 µl of buffer PE spun down for 1 min. The residual solution was discarded followed by one more spin. The sample was eluted off with 20 µl of sterile water into an eppendorf tube.

8.1.7 PCR purification

The QIAquick PCR purification kit (Qiagen; 28104) was used to purify PCR product from contaminating enzymes and oligos. Briefly, five volumes of buffer PBI were added to one volume of PCR sample. The mixture was centrifuged for 1 min at 13,000 rpms in the QIAquick column. The column was washed with 750 µl of buffer PE and centrifuged at 13,000 rpm for 1 min. Flow through was discarded and the sample was spun down for another minute. DNA was collected by applying 20 µl and spinning the sample for 1 min.

8.1.8 Subcloining with TOPO TA and Zero Blunt TOPO

When cloning, PCR constructs were first cloned into the TOPO TA pCR^{R}II-TOPO^{R} (Invitrogen; K4620-01) or Zero Blunt^{R} TOPO^{R} PCR cloning vector (Invitrogen; K2800-20). The TOPO TA allows for a one-step cloning strategy of

Taq polymerase-amplified PCR products into the TOPO vector without ligase because the TOPO vector contains topoisomerase facilitating the ligation reaction. The Zero Blunt TOPO allows for direct insertion of a blunt-end PCR products into the plasmid vector. Both vectors allowed for a quick and convenient selection of plasmid containing cells and growth for a mini-DNA preparation for sequencing. Upon sequencing results, mutation-free clones where digested out of the TOPO vector with restriction endonucleases and ligated into expression vectors.

The PCR reaction was run on agarose gel and the band of interest was excised using gel extraction kit (Qiagen) and resuspended into 20 µl of sterile water (EMD; 7732-18-5). For the TOPO reaction, 4 µl of the PCR product was mixed with 1 µl with salt solution (included in the kit) and 1 µl of TOPO vector. The mixture was incubated at room temperature for 5 min. Chemically competent bacteria cells were transformed with 1 µl of the TOPO solution.

8.1.9 DNA Maxi- and mini-preparations

For preparation of purified DNA on both small and large scale Qiagen mini (27106) and maxi (12662) kits were utilized. 5 ml or 150 ml of bacterial culture containing plasmid of choice were grown on selective media overnight for the mini or the maxi DNA preparations respectively. The cells were centrifuged at 5,000 rpm for 20 min at 4^oC and the resulting pellets were resuspened in 250 µl or 10 ml of buffer P1. Cells were lysed with 250 µl or 10 ml with buffer P2 for no more then 5 min. The lysis buffer was neutralized with equal volume of buffer P3. For the mini kit the solution was centrifuged at 13,000 rpm for 10 min at room temperature to remove genomic DNA and cellular debris. The solution was captured in a filter through a 1 min spin in the provided collection tubes, washed with buffer PE and finally eluted off of the filter with 20 µl of sterile water. For the maxi kit the resulting solution was passed through a filter to remove genomic DNA and cell debris, washed with 60 ml of buffer QC. The DNA was eluted off with 15 ml of buffer QF and precipitated with 10.5 ml of isopropyl alcohol. This

solution was passed through the QIA filter which retained the DNA plasmid. It was washed with 70% ethanol before a final elution into 1 ml of sterile water.

8.1.10 DNA digestion with restriction endonucleases

All of the restriction endonucleases unless otherwise stated were purchased from New England Biosciences.

Approximately, 5-10 µg of DNA was digested in a total volume of 25 µl with the appropriate restriction enzymes and buffer. Approximately, 2 µl or 40 units were used per digest carried out at 37°C for 2 hrs. In a double digestion, if the enzymes had compatible buffer requirements then both digestions were concurrently run otherwise single digestion was prepared. The resulting fragment was run on agarose gel and excised through gel extraction kit before the second digestion with another restriction enzyme.

8.1.11 DNA ligation

All of the ligation reactions were 5 min reactions at room temperature utilizing Rapid DNA Ligation kit (Roche; 11635379001). For the ligation, 7 µl of insert DNA was mixed with 1 µl of the vector DNA and 2 µl of DNA dilution buffer. An additional 10 µl of T4 DNA ligation buffer was added and 1 µl of T4 DNA ligase.

8.1.12 Polymerase chain reaction (PCR)

To generate fusion proteins containing either bassoon truncations or the full length DAO construct, regions were amplified by the polymerase chain reaction (PCR) using primers to introduce restriction sites into the products which would allow for in-frame cloning into the appropriate pcDNA 3.1 (Invitrogen; V790-20) and pTYB2 (New England Biolabs; N6702S)(for DAO), pCSM-EGFP (Clonetech; 6101-1)(for bassoon).

8.1.12.1 Preparation of vector fragments

Both human and rat DAO were cloned into pcDNA3.1 vector (Invitrogen). EcoRI (5') and NotI (3') were used for the rDAO and HindIII (5') and XbaI (3') were used for the hDAO.

Primers for rDAO include

5'   AAAAGAATTCACCATGCGCGTGGCCGTGATTGGAGCG

3'   TTTTGCGGCCGCTCAGAGGTGGGATGGAGGCATC

Primers for hDAO include

5'   AAAGCTTACCATGCGTGTGGTGGTGATT

3'   TTTTCTAGATCAGAGGTGGGATGGTGGCATTCTG

The pCSM-EGFP vector containing rat Bsn95-3963 was obtained kindly from the lab of Dr. Gundelfinger (Leibniz Insitute for Neurobiology, Germany). The bassoon construct was cloned into the vector using HindIII (5') and SacII (3') with the GFP fused at the N-terminus. This construct was subsequently used by me to synthesize truncation mutants representative of various functional domains of this protein.

8.1.12.2 Preparation of inserts synthesized by PCR

PCR reactions were carried out with the following KOD Xtreme[TM] Hot Start DNA Polymerase reaction mixture from Novagen (71975):

12.5 μl   2x Xtreme buffer

5 μl   dNTPs (2 mM each)

7 μl   PCR grade water

0.4 μl   Sense (5') primer (100 μM)

0.4 μl   Anti-sense (3') primer (100 μM)

0.1 μl   Template DNA

0.5 μl   KOD Xtreme hot start DNA polymerase

Reaction was run in a total volume of 26 μl.

The reaction mixture was subject to 25 cycles of the following program on a BioRad Gene Cycler: 10 sec at 98°C, 30 sec at 55°C, 1 min per kb length at 68°C.

The PCR reaction was run on agarose gel (section 6.1.6), appropriate DNA band was extracted from gel (section 6.1.6) and subcloned into TOPO vector (section 6.1.8).

List of primers used for synthesizing bassoon PCR cloning inserts each containing 5' HindIII and 3' SacII restriction sites.

All are written in a 5' to 3' direction.

Bsn95-609

5'   CAGATCTCGAGCTCAAGCTTCTGCTACTGCTCCT

3'   TTTTTCCGCGGGATCCCTGTCTTCTTTTCCGGG

Bsn2715-3014

5'   AAAAAAGCTTATGGGCAGGCTCAGGGTGTGGCTGGGCC

3'   TTTTCCGCGGCCGCAGCTGGTTGAGCTCGCTGTCAGACA

Bsn1692-3263

5'   AAAAAAGCTTTTCCAGGCCGCCAGTCAACCGCCGTGCA

3'   TTTTCCGCGGGGGATCCTTCCCGGGACGCCCACTGA

Bsn95-3263

5'   CAGATCTCGAGCTCAAGCTTCTGCTACTGCTCCT

3'   TTTTCCGCGGGGGATCCTTCCCGGGACGCCCACTGA

Bsn3263-3963

5'   AAAAAAAAGCTTAGAGAACCAGCTGTCCTAGAGGGACCC

3'   TTTTTCCGCGGCCAGAATGAGGAAAATTTTTTGCC

8.1.13 Sequencing

All of the samples were sent out to internal Wyeth sequencing department. Sequences of the inserts were sent back electronically indicating the exact content of the insert which was compared to the template to make sure that it reflected the expected sequence.

8.1.14 Preparation of competent yeast cells

Streaked yeast on YPDA agar and incubated upside down for 3 days at 30°C. Inoculated 3 mls YPDA medium in sterile 15 Falcon tube with single colony with a diameter of 2-3 mm. Incubated at 30°C for 8-12 hrs and shaked at 200 rpm. Tranfered 5 μl of the culture to 250 ml flast containing 50 mls of YPDA. Incubated the cells at 30°C while shaking for ~16 hrs until OD_{600} reached 0.15-0.3. Centrifuged down the cells for 5 min at 700 g at room temperature and resuspend the pellet in 100 mls of fresh YPDA. Incubated the cells at 30°C while shaking until they reach OD_{600} of $0.4 - 0.5$ (about 3-5 hrs). Spun 50 mls of culture as before and resuspend the pellet in 30 mls of sterile, deionized water. Spun the cells again and resuspend the pellet in 1.5 ml of 1.1xTE/LiAc. Pelleted the cells in a table top centrifuge at top speed for 15 sec. Resuspend the pellet in 600 μl of 1.1xTE/LiAc.

8.1.15 Yeast transformation

In a prechilled 1.5 ml microfuge mixed 100 ng of plasmid DNA with 5 μl Herring Testes Carrier DNA (10 ml/ml) and 50 μl of competent cells. Added 0.5 ml PEG/LiAc and gently mixed. Incubated for 30°C for 30 min with occasionally mix of the cells. Added 20 μl DMSO and mixed. Incubated at 42°C for 15 min with an occasional mix. Pelleted the cells in a table top centrifuge at top speed for 15 sec. Resuspend the pellet in 1 ml of YPD liquid medium and incubated with shaking at 30°C for 90 min. Pelleted the cells in a table top centrifuge at top speed for 15 sec. Resuspended cells in 1 ml of 0.9% (w/v) NaCl and plated out the cells on appropriate dropout plates. Incubate upside down at 30°C.

8.1.16 Yeast mating

Streaked out yeast cells containing the prey vector and the bait vector on appropriate single dropout media and grew at 30°C for 3 days. Picked single colony about 2-3 mm from each plate (one for bait and one for prey containing strain) into 1.5 ml centrifuge tube containing 500 μl of 2xYPDA and vortexed to mix. Incubated overnight while shaking at 200 rpm at 30°C. Spreaded the mated culture on double and quadruple dropout media and incubated at 30°C for 3 to 5 days. The double dropout was used to determine mating efficiency while the quadruple dropout for interactor study.

8.1.17 Yeast DNA extraction

Done with the Yeastmaker yeast plasmid isolation kit (Clontech; 630441). Inoculated single colony into 0.5 ml of appropriate SD liquid mdium and incubated at 30°C overnight with vigorous shaking (250 rpm). Pelleted the cells through centrifugation at 14,000 rpm for 5 min. Resuspended in 50 μl of potassium phosphate (67 mM KH$_2$PO$_4$; pH 7.5) and mixed with 10 μl of Lyticase solution. Incubated at 37°C fro 30 min. Added 10 μl of 20% SDS and vortexd for 1 min. Prepared a Chroma Spin-1000 DEPC-water column by vortexing the spin column until resuspended the gel matrix, removed the cap and broke off the tip, placed the column into 2 ml polypropylene tube, centrifuged column for 5 min at 700 x g and saved the column in a fresh microcentrifuge tube. Applied the cell sample to the center of the gel bed's flat surface. Spun the column for 5 min at 700 x g. The purified DNA was in the eluate.

8.2 Biochemistry

8.2.1 Sodium Dodecyl Sulphate Polyacrylamide Gel Electrophoresis (SDS-PAGE)

SDS-PAGE sample buffer (3x) (80 mM Tris-HCl pH 6.8, 100 mM DTT, 10% glycerol, 2% SDS and 0.1% bromophenol blue) was added to samples before they were boiled for 3 min and loaded onto gels.

Samples were run in 4-12% gradient w/v polyacrylamide (Invitrogen;NP0321BOX). gels were run in MOPS (NuPage; NP0001) at 130V for about 2 hrs.

8.2.1.1 Coomassie Blue staining

If proteins were to be visualized directly, gel was fixed and stained with 1% Coomassie Blue (BioRad; 161-0436) in 10% acetic acid and 20% methanol for 30 min at room temperature. The gels were destained in 10% acetic acid and 20% methanol.

8.2.1.2 Silver stain

For more sensitive protein detection Silver stain was utilized. A brief protocol for Silver stain kit (Invitrogen; LC6100) includes fixing the SDS-PAGE gels with 200 ml of fixing solution for 10 min, 2 x 10 min x 100 ml washes in sensitizing solution, 2 x 5 min x 200 ml washes in pure water, 15 min incubation in 100 ml of staining solution, 2 x 5min x 200 ml of rinse with pure water, 5 min incubation in developing solution, and stopping the reaction with 5 ml of the stopping solution.

8.2.2 Western blotting

The SDS-PAGE gel was placed against pre-wetted 0.45 μm nitrocellulose (BioRad; 162-0215) with two pieces of Whatman 3mm filter paper on each side into a BioRad western blot cassette. Transfer was carried out in a BioRad western blotting apparatus with 1x Transfer buffer at 30V. Transfer normally lasted between 60 and 90 min. After transfer the positions of proteins lanes and molecular weight markers were indented. The blot was blocked with blocking buffer (Rockland; MB-070) for 30 min. The antibodies were diluted at 1:1000 dilution unless otherwise stated into the blocking buffer and applied to the filter for at least 1 hr with vigorous shaking. Excess antibody was washed off with 0.1% Tween-20 in 100 mM PBS (Gibco; 14190) 5min x 3. Secondary antibody was conjugated to red fluorescence or green fluorescence (Invitrogen; A21109; Rockland; 610-131-121). The blots were visualized on the Odyssey (Li-Cor).

8.2.2.1 Primary antibodies used in this study for western blotting

DAO (rabbit polyclonal custom made through OpenBiosystems as described in chapter 2)

Catalase	Sigma; C0979
Bassoon	StressGen; VAM-PS003
PSD-95	UC Davis/NINDS/NIMH NeuroMab ; 75-028
MAP2	Sigma; M2320
Actin	Sigma; A-2066
Synaptophysin	Sigma; S5768
GFP	Clontech; 632375
GAL4 DNA-BD	Clontech; 630403
Mouse IgG	SantaCruz; sc-2025
Rabbit IgG	Abcam; ab37415-5

8.2.3 Synaptic junction membrane fractionation experiments

The fractionation experiment was derived from tom Dieck (tom Dieck et al., 1998), Wyneken (Wyneken et al., 2001) and Carlin (Carlin et al., 1980). Rat cerebellum from four animals was collected for a total weight of about 2 g of wet tissue was homogenized by hand 10 times in 8 ml of solution A (320 mM sucrose/ 5 mM HEPES / protease inhibitors). The resulting lysate was centrifuged for 10 min at 1,000g at 4^oC. The resulting supernatant (S_1) was centrifuged at 12,000g for 20 min at 4^oC. For every 1 g of pellet (P_2), 2.4 ml of solution A was used to resuspend it into solution. This solution was layered onto a sucrose gradient consisting of 10 ml each of 0.85 M, 1.0 M, and 1.2 M. The gradient was centrifuged for 2 hrs at 82,500g. The synaptosomal fraction was collected between the 1.0M and 1.2M and it was layered on top of the 1.0M fraction. This fraction was lysed for 30 min on ice in 5x volume of solution B (5 mM Tris-HCl pH 8.1/ 1 mM DTT). The solution was centrifuged at 33,000g for 30 min and the resulting pellet (P_3) was resuspended in solution C (320 mM sucrose / 2 mM DTT / 12 mM Tris-HCl pH 8.1) at a volume of 60 ml/ 10 g of starting material. The resuspended P_3 was mixed with equal volume of 320 mM sucrose / 1% Triton X-100 and incubated on ice for 15 min. The sample was centrifuged at 4^oC for 30

min at 33,000g and the resulting pellet (P_4) was resuspended in solution A. The resuspended P_4 was layered on top of sucrose gradient composed of 1.0 M, 1.5 M and 2.0 M and centrifuged at 4°C for 2 hr at 201,000g. The pellet resulting from this centrifugation represents the synaptic junction membrane fraction.

8.2.4 Amplex Red DAO assay

The hDAO enzymatic assay was run in 20 mM Tris-HCl pH 7.5, 1.0 % glycerol, 0.01% Brij-35 and 0.01% BSA buffer. Each 384 well in 384 well plate (Matrix; 4328) was loaded with 20 μl of purified DAO enzyme at 7 ng per well, 10 μl of 4x compound in 8% DMSO (WAY-396964 or just buffer) and following 5-10 minute incubation 10 μl of D-alanine (5 mM) (VWR; IC10028025), Amplex Red (100 μM)(Invitrogen; A36006), HRP (1 U/ml)(Sigma; P8375-100KU) was added. The reaction took place in the dark at room temperature for 30 min before the RFU were read on Victor2 (PerkinElmer) using 544nm excitation, and 590 nm emission.

For the hDAO and rDAO stable line 20 k cells per well in 384 well plates were plated overnight. The media was replaced with 35 μl of 50 mM NaHPO$_4$ pH 7.4 and 5 μl of 10x compound in 3% DMSO or just assay buffer was added for 5-10 min incubation prior to adding 10 μl of 50 mM D-alanine, 100 μM Amplex Red, 1 U/ml HRP. The cells were incubated at room temperature for 45-60 min in the dark prior to reading the fluorescence on Victor2 with 544 nm excitation wavelength and 596 nm emission.

8.2.5 Bacterial culture preparation and chitin column hDAO purification

BL21 (DE3) *E. coli* cells were transiently transfected with the hDAO/pTYB2 construct and plated on LB amp plates overnight at 37°C. A single colony was selected and incubated at 37°C in 100 ml of LB amp at 175 rpm until the solution reached optical density of 0.6 at 600 nm. The solution was then ten fold diluted into LB amp supplemented with 0.5 mM IPTG. The cells grew overnight at 30°C

in a shaker at 200 rpms. The following day the cells were centrifuged at 5,000 rpms for 20 min and the pellet was frozen and kept at -80°C.

The cell pellet was processed according to Raibek (2000). For every 10g of wet pellet 80 ml of cold 50 mM Tris-HCl pH 8.0, 1 mM sodium benzoate, 1 mM EDTA, 1 mM ATP, and protease inhibitor solution was used to resuspend the cells. The solution was thoroughly sonicated and centrifuged at 13,000 rpms for 15 min at 4°C to remove cellular debris. The remaining supernatant was normalized with NaCl (to a concentration of 1 M) before the solution was applied to an equilibrated 5-ml affinity column (Chitin beads from Stratagene) with solution A (50 mM Tris-HCl pH 8.0, 1 mM sodium benzoate, 1 mM EDTA, 1 M NaCl). The beads were subsequently washed with 100 ml of buffer A and 20 ml of buffer B (buffer A without the NaCl or sodium benzoate). Finally, the column was washed with 10 ml of buffer C (buffer B with 50 mM hydroxylamine) and left at 4°C overnight in buffer C solution. The cleaved hDAO was collected the following day and examined for purity on SDS-PAGE gel stained with Coomassie Blue and for activity with the Amplex Red assay.

8.2.6 Protein assay

Protein concentration was determined based on a standard protein curve as measured with BioRad DC protein assay. A total of 20 µl of reagent S per 1.0 ml of reagent A were added to make the working reagent. Several dilutions of a protein standard containing 0.2 mg/ml to 1.5 mg/ml protein were prepared (Pierce; prediluted protein standards). A total volume of 100 µl of standards and samples were added to cuvetts and mixed with 500 µl of working reagent followed by addition of 4 ml of reagent B. The samples were incubated for 15 min at room temperature before absorbance was read at 750 nm on Spectromax.

8.3 Cell Culture
8.3.1 Maintenance of HEK293 cells

Human embryonic kidney cell fibroblasts were grown at 37°C with 5% CO^{2} in Dulbecco's Modified Eagles Medium (DMEM; Gibco) containing 10% (v/v) fetal

183

calf serum (FCS; Gibco) and 1% (v/v) penicillin and streptomycin (Gibco). At approximately 90% confluence, cells were passaged by treatment in 5 ml prewarmed trypsin (0.25% w/v) (Gibco). Once in suspension the cells were diluted 1:10 with prewarmed DMEM (as above), and seeded out onto T175 (BD Falcon).

8.3.2 Transient transfection of Hek293

One 10 cm poly-D-lysine coated dish (Becton Dickinson) containing 30-50% confluence was used per transfection with Lipofectamine 2000 (Invitrogen). 15 µg of DNA was suspended in 500 µl of OptiMem (Gibco) in 5 ml polystyrene tube (Falcon). In another polystyrene tube 30 µl of lifopectamine 2000 was suspended in 500 µl of OptiMem and both solutions were incubated individually at room temperature for 5 min. The tube containing the DNA was then mixed with the tube containing the lipofectamine and incubated at room temperature for 20 min before the solution was added to the dish containing the cells. The cells were harvested 24-72 hr post transfection depending on the expression level of the recombinant protein.

8.3.3 Stable line generation

T175 flast was grown to 90% confluency before the cells were harvested and resuspended in 0.5 ml Optimem. The cells were transferred to a 0.4 cm electroporation cuvette (BioRad) and 10 µg total plasmid DNA was added. Electroporation was carried out with the settings 400 V, 250 µFm $\infty\Omega$. The cells were then added to 20 ml DMEM and plated out at 100 µl and at dilutions of 1:10 and 1:100 on 96-well plates. After 24 hr incubation additional 100 µl of DMEM media containing 1.6 mg/ml of hygromycin or G418 were added. The cells were left in the incubator for 2 weeks before they where examined for growth. Wells containing single colonies per well were selected and screened for presence of the recombinant gene through western blotting and functional activity screening.

8.3.4 Culturing of cerebellar granule neurons

Animal handling in accordance with animal welfare regulations. Cerebellum was dissected from postnatal day 14-21 rat pups, the meninges were removed under a dissecting microscope and the tissue was stored in ice cold PBS. The tissue was dissociated using papain solution (Worthington). The tissue was incubated for 30 min at 37°C in 250 μl of DNase (tube 3) and 5 ml papain (tube 2). The solution was then removed and the tissue was triturated in 2 ml of DNase (vial 3)/ inhibitor (vial 4)/ EBSS (vial 1) 10x with a 1 ml tips. Once the tissue settled down the supernatant was removed into a separate tube and the trituration was repeated 3 more times with 6 more ml on the pelleted tissue sample. All of the supernatants were pulled together and centrifuged at 300g for 5 min. The pellet was resuspended in 2 ml of DNase (vial 3)/ inhibitor (vial 4)/ EBSS (vial 1) and layered on top of 6 ml of inhibitor (vial 4). This solution was centrifuged at 300g for 5 min and the pelleted cells were resuspended in Neurobasal complete media (500 ml of neurobasal media w/o L-glutamine, 10 ml of B27 supplement 50x, 0.75 g of KCl, 200 mM glutamine, 6.6 mg/ml Aphidicolin, and 1% penicillin and streptomycin. The cells were counted and plated out at 50,000 cells per 24-well poly-D-lysine coated coverslips and incubated at 37°C with 5% CO_2 for two weeks without changing the media. After the two weeks the cells were processed for imaging.

8.4 Immunofluorescence

8.4.1 Cerebellar granule neurons preparation for immunofluorescence

The CGN containing coverslips were washed 5 x 5 min in cold PBS. To remove autofluorescence the cells were washed with 1% sodium borohydride 3 x 5 min and then washed with cold PBS to wash out the sodium borohydride. They were then soaked in 0.5% Triton X-100 in PBS for 1 hr at 4°C and washed twice for 5 min in cold PBS. 1 hr block in 5% normal goat serum (Vector) with 0.2% Triton X-100 in cold PBS followed. Primary antibody was added to the blocking solution at 1:100 dilution for 1-3 hr before wash in cold PBS 5 x 5 min. Secondary antibody at 1:200 dilution suspended in the blocking reagent was then

185

applied to the coverslips for 1 hr. It was then washed away with 5 x 5 min PBS.
The coverslips were mounted onto slides with prolong gold (Invitrogen) and
visualized under fluorescent microscopy.

8.4.2 Rat cerebellar immunofluorescence preparation

Fresh 4% paraformaldehyde for rat perfusion was made according to the
following protocol for 1L: 40 g of paraformaldehyde was mixed into 500 ml of
water heated to $60^{o}C$. NaOH was titrated into this solution until all of the
paraformaldehyde solubilized from a milky appearance to clear solution. Then
500 ml of 0.2 M phosphate buffer was added and the pH was adjcuted to 7.4.

Animal handling in accordance with animal welfare regulations. Animals were
anestized prior to any work. Through a cardiac tap 100 ml of PBS was infused to
wash out blood out of the blood vessels. After the PBS wash the solution was
switched to perfusion with 500 ml/animal of 4% paraformaldehyde running at
about 50 ml per minute. The intact cerebellum was dissociated and soaked in 4%
paraformaldehyde for additional 10 min. The cerebellum was then soaked in 30%
sucrose solution for about 2 days until the tissue sunk to the bottom of the vessel.

The cerebellar tissue was frozen by application of dry ice on the stage of
microtome and cut into 20 μm slices. The slices were washed 5 x 5 min in cold
PBS and treated with 1% sodium borohydrate 3 x 5 min to remove
autofluorescence. The slices were washed with cold PBS 2 x 5 min and soaked in
0.5% Trion X-100 for 1 hr. They were washed 2 x 5 min in PBS and blocked for
1 hr in 5% normal goat serum with 0.2% Triton X-100. Primary antibody was
added to the blocking buffer at 1:100 dilution and incubated overnight while
gently racking at $4^{o}C$. The following day the slices were washed in cold PBS 5 x
5 min. Secondary antibody diluted in the blocking buffer at 1:200 dilution was
added to the slices for 1 hr and then washed away with 5 x 5 min PBS. The slices
were mounted on slides and preserved with prolong gold. The sections were
imaged on fluorescent microscope.

8.5 Immunoprecipitation

8.5.1 Application of Dynal Protein A beads

Dynal protein A beads (Invitrogen) have a strong binding capacity for rabbit IgG hence they were used to capture DAO antibody and consequently immunoprecipite DAO from cellular lysate such as the rat cerebellum or the DAO stable line. More background information on the Dynal beads can be found in chapter 2 where the principle is more thoroughly outlined.

The beads were thoroughly mixed through vortexing to make sure that they are in solution before 100 μl was removed into ependorf tube. The tube was placed on a Dynal MPC magnet which separated the beads out of the solution. Media was removed and replaced with 0.5 ml of 0.1 M NaPO$_4$ pH 8.0. The beads were resuspended and again precipitated with the magnet, sodium phosphate was removed and replaced with fresh sodium phosphate solution two more times. The beads were resuspended in 90 μl of sodium phosphate buffer and 10 μl rabbit antibody solution was added to the bead solution. This solution was gently mixed for 10 min at room temperature to all the beads to capture the antibody. The beads were then applied to the magnet and the solution was removed and replaced with 0.5 ml of sodium phosphate buffer 3 x 5 min. The antibody was crosslinked to the beads by removing the sodium phosphate buffer and replacing it with 1 ml of 0.2 M triethanolamide pH 8.2, 3 x 2 min. The beads were resuspended in freshly made 1 ml of 0.2 M triethanolamide pH 8.2 supplemented with 20 mM DMP (dimethyl pimelimidate dihydrochloride) (Pierce) and incubated for 30 min at room temperature with a gentle rotation. The reaction was stopped by removing the solution and replacing it with 50 mM Tris pH 7.5 for 15 min at room temperature with a gentle rotation. The beads were washed 3 x 5 min in PBS and resuspended in 100 μl of PBS. The protein A beads are now coated with the rabbit antibody which is covalently coupled to the beads. Fresh cellular or tissue lysates in RIPA buffer were added to the bead-antibody complex and incubated for 1 hr at 4°C with gentle rocking. The lysate was washed away with PBS or stronger washing detergents 3 x 5 min at room temperature and the beads

were resuspended in 20 µl of PBS. SDS-PAGE loading dye was added to this solution and it was boiled for 3 min to extract attached proteins.

8.5.2 Application of Dynal Protein G beads

Dynal protein G beads (Invitrogen) have a strong binding capacity for monoclonal IgG (Akerstrom 1985) hence they were used to capture bassoon and GFP antibodies which were then used to immunoprecipite bassoon and GFP-tagged bassoon from cellular lysate such as the rat cerebellum or transiently transfected cells.

The Dynal protein G beads were vortexed to resuspend them in solution and 100 µl sample was removed. The beads were separated from the solution via a magnet and resuspended in 0.5 ml of 0.1 M citrate-phosphate buffer pH 5.0. The washing was repeated two more times and the beads were resuspended in 50 µl of the citrate-phosphate buffer. 10 µl of monoclonal antibody solution was added to the bead solution and incubated for 40 min at room temperature while gently rocking. The supernatant was then removed and the beads were washed 3 x 5 min with 0.5 ml of the citrate-phosphate buffer. The antibody was crosslinked to the beads in the same manner as the rabbit IgG was to protein A beads (see 6.5.1). After the crosslinking, the beads were resuspended in 100 µl of PBS and cellular or tissue lysate was added to this solution for 1 hr incubation at 4°C with gentle rocking. The beads were then washed with PBS or stronger washing detergent 3 x 5 min at room temperature and the beads were resuspended in 20 µl of PBS. SDS buffer was added to this solution and it was boiled for 3 min to extract attached proteins.

8.6 Mass spectroscopy

Immunoprecipitate collected from the DAO immunoprecipitation column was loaded and separated on 10-20% Tricine SDS-PAGE gel (Invitrogen). The proteins on the SDS-PAGE gel were stained with Imperial Protein Stain Solution (Pierce). Each gel lane was cut into twenty pieces of about 1 x 1 mm^{2}. The

pieces were excised and the stain was removed by dehydration in acetonitrile (ACN), rehydrated, and washed in 25 mM sodium phosphate (pH 6.0), and dehydrated again in ACN. Proteins within the gel pieces were digested in a solution containing 0.5 μg of trypsin in 25 mM sodium phosphate (pH 6.0) at 37°C for 4 hrs. The trypsonized peptides were extracted from gel with 60% ACN / 1 % fomic acid (FA) followed by extraction with 90 % ACN / 5 % FA. The eluates were concentrated to near dryness by vacuum and reconstituted in 20 μl of 2% ACN / 0.1 % FA in preparation for the mass spectroscopic analysis.

Agilent 1100 nanoflow system connected to a linear ion trap mass spectrometer (LTQ, ThermoFinnigan) was used for the mass spectrometric analysis. The peptide samples were pressure-loaded onto a C18 PicoFrit microcapillary column (New Objective) packed with Magic C18 beads (5 μm, 75 μm x 11 cm, Michron BioResources) and desalted on-line with solvent A (2% ACN and 0.1% FA). The peptides were eluted with a gradient from 4 to 60% solvent B (90% ACN and 0.1% FA) over 70 min with a flow rate of 250 nl/min. The fragment ion spectra (MS/MS scan) were acquired in a data-dependent manner in which each fragment ion scan was followed by consecutive MS/MS scan on the first three most intense ions from the MS scan.

References

(2008). Rare chromosomal deletions and duplications increase risk of schizophrenia. Nature *455*, 237-241.

Adler, C. M., Malhotra, A. K., Elman, I., Goldberg, T., Egan, M., Pickar, D., and Breier, A. (1999). Comparison of ketamine-induced thought disorder in healthy volunteers and thought disorder in schizophrenia. Am J Psychiatry *156*, 1646-1649.

Akazawa, C., Shigemoto, R., Bessho, Y., Nakanishi, S., and Mizuno, N. (1994). Differential expression of five N-methyl-D-aspartate receptor subunit mRNAs in the cerebellum of developing and adult rats. J Comp Neurol *347*, 150-160.

Akbarian, S., Sucher, N. J., Bradley, D., Tafazzoli, A., Trinh, D., Hetrick, W. P., Potkin, S. G., Sandman, C. A., Bunney, W. E., Jr., and Jones, E. G. (1996). Selective alterations in gene expression for NMDA receptor subunits in prefrontal cortex of schizophrenics. J Neurosci *16*, 19-30.

Almond, S. L., Fradley, R. L., Armstrong, E. J., Heavens, R. B., Rutter, A. R., Newman, R. J., Chiu, C. S., Konno, R., Hutson, P. H., and Brandon, N. J. (2006). Behavioral and biochemical characterization of a mutant mouse strain lacking D-amino acid oxidase activity and its implications for schizophrenia. Mol Cell Neurosci *32*, 324-334.

Altrock, W. D., tom Dieck, S., Sokolov, M., Meyer, A. C., Sigler, A., Brakebusch, C., Fassler, R., Richter, K., Boeckers, T. M., Potschka, H.*, et al.* (2003). Functional inactivation of a fraction of excitatory synapses in mice deficient for the active zone protein bassoon. Neuron *37*, 787-800.

Alvir, J. M., Lieberman, J. A., Safferman, A. Z., Schwimmer, J. L., and Schaaf, J. A. (1993). Clozapine-induced agranulocytosis. Incidence and risk factors in the United States. N Engl J Med *329*, 162-167.

Andersen, J. D., and Pouzet, B. (2004). Spatial memory deficits induced by perinatal treatment of rats with PCP and reversal effect of D-serine. Neuropsychopharmacology *29*, 1080-1090.

Andreasen, N. C. (1995). Symptoms, signs, and diagnosis of schizophrenia. Lancet *346*, 477-481.

Andreasen, N. C., Flaum, M., Swayze, V., 2nd, O'Leary, D. S., Alliger, R., Cohen, G., Ehrhardt, J., and Yuh, W. T. (1993). Intelligence and brain structure in normal individuals. Am J Psychiatry *150*, 130-134.

Andreasen, N. C., O'Leary, D. S., Cizadlo, T., Arndt, S., Rezai, K., Ponto, L. L., Watkins, G. L., and Hichwa, R. D. (1996). Schizophrenia and cognitive

dysmetria: a positron-emission tomography study of dysfunctional prefrontal-thalamic-cerebellar circuitry. Proc Natl Acad Sci U S A *93*, 9985-9990.

Andreasen, N. C., and Pierson, R. (2008). The role of the cerebellum in schizophrenia. Biol Psychiatry *64*, 81-88.

Angenstein, F., Hilfert, L., Zuschratter, W., Altrock, W. D., Niessen, H. G., and Gundelfinger, E. D. (2008). Morphological and metabolic changes in the cortex of mice lacking the functional presynaptic active zone protein bassoon: a combined 1H-NMR spectroscopy and histochemical study. Cereb Cortex *18*, 890-897.

Angermuller, S., and Fahimi, H. D. (1988). Heterogenous staining of D-amino acid oxidase in peroxisomes of rat liver and kidney. A light and electron microscopic study. Histochemistry *88*, 277-285.

Aragon, C., and Lopez-Corcuera, B. (2003). Structure, function and regulation of glycine neurotransporters. Eur J Pharmacol *479*, 249-262.

Arenas, J., Campos, Y., Ribacoba, R., Martin, M. A., Rubio, J. C., Ablanedo, P., and Cabello, A. (1998). Complex I defect in muscle from patients with Huntington's disease. Ann Neurol *43*, 397-400.

Arnold, G., Liscum, L., and Holtzman, E. (1979). Ultrastructural localization of D-amino acid oxidase in microperoxisomes of the rat nervous system. J Histochem Cytochem *27*, 735-745.

Arnold, S. E., Franz, B. R., Gur, R. C., Gur, R. E., Shapiro, R. M., Moberg, P. J., and Trojanowski, J. Q. (1995). Smaller neuron size in schizophrenia in hippocampal subfields that mediate cortical-hippocampal interactions. Am J Psychiatry *152*, 738-748.

Arnold, S. E., Ruscheinsky, D. D., and Han, L. Y. (1997). Further evidence of abnormal cytoarchitecture of the entorhinal cortex in schizophrenia using spatial point pattern analyses. Biol Psychiatry *42*, 639-647.

Badner, J. A., and Gershon, E. S. (2002). Meta-analysis of whole-genome linkage scans of bipolar disorder and schizophrenia. Mol Psychiatry *7*, 405-411.

Bairoch, A. (1992). PROSITE: a dictionary of sites and patterns in proteins. Nucleic Acids Res *20 Suppl*, 2013-2018.

Basu, A. C., Tsai, G. E., Ma, C. L., Ehmsen, J. T., Mustafa, A. K., Han, L., Jiang, Z. I., Benneyworth, M. A., Froimowitz, M. P., Lange, N.*, et al.* (2009). Targeted disruption of serine racemase affects glutamatergic neurotransmission and behavior. Mol Psychiatry *14*, 719-727.

Baumgart, F., and Rodriguez-Crespo, I. (2008). D-amino acids in the brain: the biochemistry of brain serine racemase. FEBS J *275*, 3538-3545.

Bendikov, I., Nadri, C., Amar, S., Panizzutti, R., De Miranda, J., Wolosker, H., and Agam, G. (2007). A CSF and postmortem brain study of D-serine metabolic parameters in schizophrenia. Schizophr Res *90*, 41-51.

Beneyto, M., and Meador-Woodruff, J. H. (2004). Expression of transcripts encoding AMPA receptor subunits and associated postsynaptic proteins in the macaque brain. J Comp Neurol *468*, 530-554.

Benit, P., Chretien, D., Kadhom, N., de Lonlay-Debeney, P., Cormier-Daire, V., Cabral, A., Peudenier, S., Rustin, P., Munnich, A., and Rotig, A. (2001). Large-scale deletion and point mutations of the nuclear NDUFV1 and NDUFS1 genes in mitochondrial complex I deficiency. Am J Hum Genet *68*, 1344-1352.

Benzel, I., Kew, J. N., Viknaraja, R., Kelly, F., de Belleroche, J., Hirsch, S., Sanderson, T. H., and Maycox, P. R. (2008). Investigation of G72 (DAOA) expression in the human brain. BMC Psychiatry *8*, 94.

Berger, U. V., Luthi-Carter, R., Passani, L. A., Elkabes, S., Black, I., Konradi, C., and Coyle, J. T. (1999). Glutamate carboxypeptidase II is expressed by astrocytes in the adult rat nervous system. J Comp Neurol *415*, 52-64.

Bertolino, A., Esposito, G., Callicott, J. H., Mattay, V. S., Van Horn, J. D., Frank, J. A., Berman, K. F., and Weinberger, D. R. (2000). Specific relationship between prefrontal neuronal N-acetylaspartate and activation of the working memory cortical network in schizophrenia. Am J Psychiatry *157*, 26-33.

Betz, A., Thakur, P., Junge, H. J., Ashery, U., Rhee, J. S., Scheuss, V., Rosenmund, C., Rettig, J., and Brose, N. (2001). Functional interaction of the active zone proteins Munc13-1 and RIM1 in synaptic vesicle priming. Neuron *30*, 183-196.

Black, J. E., Kodish, I. M., Grossman, A. W., Klintsova, A. Y., Orlovskaya, D., Vostrikov, V., Uranova, N., and Greenough, W. T. (2004). Pathology of layer V pyramidal neurons in the prefrontal cortex of patients with schizophrenia. Am J Psychiatry *161*, 742-744.

Boyer, P., Phillips, J. L., Rousseau, F. L., and Ilivitsky, S. (2007). Hippocampal abnormalities and memory deficits: new evidence of a strong pathophysiological link in schizophrenia. Brain Res Rev *54*, 92-112.

Braff, D. L., Geyer, M. A., Light, G. A., Sprock, J., Perry, W., Cadenhead, K. S., and Swerdlow, N. R. (2001). Impact of prepulse characteristics on the detection of sensorimotor gating deficits in schizophrenia. Schizophr Res *49*, 171-178.

Breier, A., Adler, C. M., Weisenfeld, N., Su, T. P., Elman, I., Picken, L., Malhotra, A. K., and Pickar, D. (1998). Effects of NMDA antagonism on striatal dopamine release in healthy subjects: application of a novel PET approach. Synapse *29*, 142-147.

Brown, A. S., Schaefer, C. A., Wyatt, R. J., Goetz, R., Begg, M. D., Gorman, J. M., and Susser, E. S. (2000). Maternal exposure to respiratory infections and adult schizophrenia spectrum disorders: a prospective birth cohort study. Schizophr Bull *26*, 287-295.

Browne, S., Roe, M., Lane, A., Gervin, M., Morris, M., Kinsella, A., Larkin, C., and Callaghan, E. O. (1996). Quality of life in schizophrenia: relationship to sociodemographic factors, symptomatology and tardive dyskinesia. Acta Psychiatr Scand *94*, 118-124.

Browning, M. D., Dudek, E. M., Rapier, J. L., Leonard, S., and Freedman, R. (1993). Significant reductions in synapsin but not synaptophysin specific activity in the brains of some schizophrenics. Biol Psychiatry *34*, 529-535.

Buchanan, R. W., Javitt, D. C., Marder, S. R., Schooler, N. R., Gold, J. M., McMahon, R. P., Heresco-Levy, U., and Carpenter, W. T. (2007). The Cognitive and Negative Symptoms in Schizophrenia Trial (CONSIST): the efficacy of glutamatergic agents for negative symptoms and cognitive impairments. Am J Psychiatry *164*, 1593-1602.

Buka, S. L., Tsuang, M. T., Torrey, E. F., Klebanoff, M. A., Bernstein, D., and Yolken, R. H. (2001a). Maternal infections and subsequent psychosis among offspring. Arch Gen Psychiatry *58*, 1032-1037.

Buka, S. L., Tsuang, M. T., Torrey, E. F., Klebanoff, M. A., Wagner, R. L., and Yolken, R. H. (2001b). Maternal cytokine levels during pregnancy and adult psychosis. Brain Behav Immun *15*, 411-420.

Buller, A. L., Larson, H. C., Schneider, B. E., Beaton, J. A., Morrisett, R. A., and Monaghan, D. T. (1994). The molecular basis of NMDA receptor subtypes: native receptor diversity is predicted by subunit composition. J Neurosci *14*, 5471-5484.

Bunney, B. S., Walters, J. R., Roth, R. H., and Aghajanian, G. K. (1973). Dopaminergic neurons: effect of antipsychotic drugs and amphetamine on single cell activity. J Pharmacol Exp Ther *185*, 560-571.

Burnet, P. W., Eastwood, S. L., Bristow, G. C., Godlewska, B. R., Sikka, P., Walker, M., and Harrison, P. J. (2008a). D-amino acid oxidase activity and expression are increased in schizophrenia. Mol Psychiatry *13*, 658-660.

Burnet, P. W., Hutchinson, L., von Hesling, M., Gilbert, E. J., Brandon, N. J., Rutter, A. R., Hutson, P. H., and Harrison, P. J. (2008b). Expression of D-serine and glycine transporters in the prefrontal cortex and cerebellum in schizophrenia. Schizophr Res *102*, 283-294.

Caldinelli, L., Molla, G., Sacchi, S., Pilone, M. S., and Pollegioni, L. (2009). Relevance of weak flavin binding in human D-amino acid oxidase. Protein Sci *18*, 801-810.

Campaner, S., Pollegioni, L., Ross, B. D., and Pilone, M. S. (1998). Limited proteolysis and site-directed mutagenesis reveal the origin of microheterogeneity in Rhodotorula gracilis D-amino acid oxidase. Biochem J *330 (Pt 2)*, 615-621.

Cannon, T. D., Thompson, P. M., van Erp, T. G., Toga, A. W., Poutanen, V. P., Huttunen, M., Lonnqvist, J., Standerskjold-Nordenstam, C. G., Narr, K. L., Khaledy, M.*, et al.* (2002). Cortex mapping reveals regionally specific patterns of genetic and disease-specific gray-matter deficits in twins discordant for schizophrenia. Proc Natl Acad Sci U S A *99*, 3228-3233.

Carlin, R. K., Grab, D. J., Cohen, R. S., and Siekevitz, P. (1980). Isolation and characterization of postsynaptic densities from various brain regions: enrichment of different types of postsynaptic densities. J Cell Biol *86*, 831-845.

Carlsson, A. (1988). The current status of the dopamine hypothesis of schizophrenia. Neuropsychopharmacology *1*, 179-186.

Carlsson, A., Waters, N., Holm-Waters, S., Tedroff, J., Nilsson, M., and Carlsson, M. L. (2001). Interactions between monoamines, glutamate, and GABA in schizophrenia: new evidence. Annu Rev Pharmacol Toxicol *41*, 237-260.

Carroll, J., Fearnley, I. M., Shannon, R. J., Hirst, J., and Walker, J. E. (2003). Analysis of the subunit composition of complex I from bovine heart mitochondria. Mol Cell Proteomics *2*, 117-126.

Cascella, N. G., Macciardi, F., Cavallini, C., and Smeraldi, E. (1994). d-cycloserine adjuvant therapy to conventional neuroleptic treatment in schizophrenia: an open-label study. J Neural Transm Gen Sect *95*, 105-111.

Chen, Y. A., and Scheller, R. H. (2001). SNARE-mediated membrane fusion. Nat Rev Mol Cell Biol *2*, 98-106.

Chin, L. S., Nugent, R. D., Raynor, M. C., Vavalle, J. P., and Li, L. (2000). SNIP, a novel SNAP-25-interacting protein implicated in regulated exocytosis. J Biol Chem *275*, 1191-1200.

Chouinard, M. L., Gaitan, D., and Wood, P. L. (1993). Presence of the N-methyl-D-aspartate-associated glycine receptor agonist, D-serine, in human temporal cortex: comparison of normal, Parkinson, and Alzheimer tissues. J Neurochem *61*, 1561-1564.

Christopoulos, A., and Kenakin, T. (2002). G protein-coupled receptor allosterism and complexing. Pharmacol Rev *54*, 323-374.

Chumakov, I., Blumenfeld, M., Guerassimenko, O., Cavarec, L., Palicio, M., Abderrahim, H., Bougueleret, L., Barry, C., Tanaka, H., La Rosa, P.*, et al.* (2002). Genetic and physiological data implicating the new human gene G72 and the gene for D-amino acid oxidase in schizophrenia. Proc Natl Acad Sci U S A *99*, 13675-13680.

Cline, M. J., and Lehrer, R. I. (1969). D-amino acid oxidase in leukocytes: a possible D-amino-acid-linked antimicrobial system. Proc Natl Acad Sci U S A *62*, 756-763.

Conley, R. R., and Buchanan, R. W. (1997). Evaluation of treatment-resistant schizophrenia. Schizophr Bull *23*, 663-674.

Conrad, A. J., Abebe, T., Austin, R., Forsythe, S., and Scheibel, A. B. (1991). Hippocampal pyramidal cell disarray in schizophrenia as a bilateral phenomenon. Arch Gen Psychiatry *48*, 413-417.

Conti, F., Barbaresi, P., Melone, M., and Ducati, A. (1999). Neuronal and glial localization of NR1 and NR2A/B subunits of the NMDA receptor in the human cerebral cortex. Cereb Cortex *9*, 110-120.

Cook, S. P., Galve-Roperh, I., Martinez del Pozo, A., and Rodriguez-Crespo, I. (2002). Direct calcium binding results in activation of brain serine racemase. J Biol Chem *277*, 27782-27792.

Corrigan, J. J. (1969). D-amino acids in animals. Science *164*, 142-149.

Corvin, A., Donohoe, G., McGhee, K., Murphy, K., Kenny, N., Schwaiger, S., Nangle, J. M., Morris, D., and Gill, M. (2007). D-amino acid oxidase (DAO) genotype and mood symptomatology in schizophrenia. Neurosci Lett *426*, 97-100.

Coskun, P. E., Beal, M. F., and Wallace, D. C. (2004). Alzheimer's brains harbor somatic mtDNA control-region mutations that suppress mitochondrial transcription and replication. Proc Natl Acad Sci U S A *101*, 10726-10731.

Costa, J., Khaled, E., Sramek, J., Bunney, W., Jr., and Potkin, S. G. (1990). An open trial of glycine as an adjunct to neuroleptics in chronic treatment-refractory schizophrenics. J Clin Psychopharmacol *10*, 71-72.

Cotter, D., Mackay, D., Chana, G., Beasley, C., Landau, S., and Everall, I. P. (2002). Reduced neuronal size and glial cell density in area 9 of the dorsolateral prefrontal cortex in subjects with major depressive disorder. Cereb Cortex *12*, 386-394.

Coyle, J. T. (2006). Glutamate and schizophrenia: beyond the dopamine hypothesis. Cell Mol Neurobiol *26*, 365-384.

Coyle, J. T., and Tsai, G. (2004a). NMDA receptor function, neuroplasticity, and the pathophysiology of schizophrenia. Int Rev Neurobiol *59*, 491-515.

Coyle, J. T., and Tsai, G. (2004b). The NMDA receptor glycine modulatory site: a therapeutic target for improving cognition and reducing negative symptoms in schizophrenia. Psychopharmacology (Berl) *174*, 32-38.

Creese, I., Burt, D. R., and Snyder, S. H. (1976). Dopamine receptor binding predicts clinical and pharmacological potencies of antischizophrenic drugs. Science *192*, 481-483.

Cristiano, L., Bernardo, A., and Ceru, M. P. (2001). Peroxisome proliferator-activated receptors (PPARs) and peroxisomes in rat cortical and cerebellar astrocytes. J Neurocytol *30*, 671-683.

Crow, T. J. (1985). The two-syndrome concept: origins and current status. Schizophr Bull *11*, 471-486.

Cull-Candy, S. G., and Leszkiewicz, D. N. (2004). Role of distinct NMDA receptor subtypes at central synapses. Sci STKE *2004*, re16.

Curras, M. C., and Pallotta, B. S. (1996). Single-channel evidence for glycine and NMDA requirement in NMDA receptor activation. Brain Res *740*, 27-40.

D'Aniello, A., Vetere, A., and Petrucelli, L. (1993). Further study on the specificity of D-amino acid oxidase and D-aspartate oxidase and time course for complete oxidation of D-amino acids. Comp Biochem Physiol B *105*, 731-734.

Davidsson, P., Gottfries, J., Bogdanovic, N., Ekman, R., Karlsson, I., Gottfries, C. G., and Blennow, K. (1999). The synaptic-vesicle-specific proteins rab3a and synaptophysin are reduced in thalamus and related cortical brain regions in schizophrenic brains. Schizophr Res *40*, 23-29.

Davis, J. M., Chen, N., and Glick, I. D. (2003). A meta-analysis of the efficacy of second-generation antipsychotics. Arch Gen Psychiatry *60*, 553-564.

Davis, K. L., Buchsbaum, M. S., Shihabuddin, L., Spiegel-Cohen, J., Metzger, M., Frecska, E., Keefe, R. S., and Powchik, P. (1998). Ventricular enlargement in poor-outcome schizophrenia. Biol Psychiatry *43*, 783-793.

Davis, K. L., Kahn, R. S., Ko, G., and Davidson, M. (1991). Dopamine in schizophrenia: a review and reconceptualization. Am J Psychiatry *148*, 1474-1486.

De Duve, C., and Baudhuin, P. (1966). Peroxisomes (microbodies and related particles). Physiol Rev *46*, 323-357.

De Miranda, J., Panizzutti, R., Foltyn, V. N., and Wolosker, H. (2002). Cofactors of serine racemase that physiologically stimulate the synthesis of the N-methyl-D-aspartate (NMDA) receptor coagonist D-serine. Proc Natl Acad Sci U S A *99*, 14542-14547.

Deane, C. M., Salwinski, L., Xenarios, I., and Eisenberg, D. (2002). Protein interactions: two methods for assessment of the reliability of high throughput observations. Mol Cell Proteomics *1*, 349-356.

Deisenhofer, J. (1981). Crystallographic refinement and atomic models of a human Fc fragment and its complex with fragment B of protein A from Staphylococcus aureus at 2.9- and 2.8-A resolution. Biochemistry *20*, 2361-2370.

Detera-Wadleigh, S. D., and McMahon, F. J. (2006). G72/G30 in schizophrenia and bipolar disorder: review and meta-analysis. Biol Psychiatry *60*, 106-114.

Dhananjayan, S. C., Ramamoorthy, S., Khan, O. Y., Ismail, A., Sun, J., Slingerland, J., O'Malley, B. W., and Nawaz, Z. (2006). WW domain binding protein-2, an E6-associated protein interacting protein, acts as a coactivator of estrogen and progesterone receptors. Mol Endocrinol *20*, 2343-2354.

Dingledine, R., Borges, K., Bowie, D., and Traynelis, S. F. (1999). The glutamate receptor ion channels. Pharmacol Rev *51*, 7-61.

Dingledine, R., Kleckner, N. W., and McBain, C. J. (1990). The glycine coagonist site of the NMDA receptor. Adv Exp Med Biol *268*, 17-26.

Dresbach, T., Hempelmann, A., Spilker, C., tom Dieck, S., Altrock, W. D., Zuschratter, W., Garner, C. C., and Gundelfinger, E. D. (2003). Functional regions of the presynaptic cytomatrix protein bassoon: significance for synaptic targeting and cytomatrix anchoring. Mol Cell Neurosci *23*, 279-291.

Dresbach, T., Torres, V., Wittenmayer, N., Altrock, W. D., Zamorano, P., Zuschratter, W., Nawrotzki, R., Ziv, N. E., Garner, C. C., and Gundelfinger, E. D. (2006). Assembly of active zone precursor vesicles: obligatory trafficking of presynaptic cytomatrix proteins Bassoon and Piccolo via a trans-Golgi compartment. J Biol Chem *281*, 6038-6047.

Duncan, E. J., Szilagyi, S., Schwartz, M. P., Bugarski-Kirola, D., Kunzova, A., Negi, S., Stephanides, M., Efferen, T. R., Angrist, B., Peselow, E*., et al.* (2004). Effects of D-cycloserine on negative symptoms in schizophrenia. Schizophr Res *71*, 239-248.

Dunlop, D. S., and Neidle, A. (2005). Regulation of serine racemase activity by amino acids. Brain Res Mol Brain Res *133*, 208-214.

Einhorn, L. C., Johansen, P. A., and White, F. J. (1988). Electrophysiological effects of cocaine in the mesoaccumbens dopamine system: studies in the ventral tegmental area. J Neurosci *8*, 100-112.

Elvevag, B., and Goldberg, T. E. (2000). Cognitive impairment in schizophrenia is the core of the disorder. Crit Rev Neurobiol *14*, 1-21.

Falkai, P., and Bogerts, B. (1986). Cell loss in the hippocampus of schizophrenics. Eur Arch Psychiatry Neurol Sci *236*, 154-161.

Falls, D. L. (2003). Neuregulins: functions, forms, and signaling strategies. Exp Cell Res *284*, 14-30.

Fang, Q. K., Hopkins, S., and Jones, S. (2005). Benzol[d]isoxazol-3-ol DAAO inhibitors. In, (US).

Farah, A. (2005). Atypicality of atypical antipsychotics. Prim Care Companion J Clin Psychiatry *7*, 268-274.

Farde, L., Wiesel, F. A., Stone-Elander, S., Halldin, C., Nordstrom, A. L., Hall, H., and Sedvall, G. (1990). D2 dopamine receptors in neuroleptic-naive schizophrenic patients. A positron emission tomography study with [11C]raclopride. Arch Gen Psychiatry *47*, 213-219.

Feinberg, I. (1990). Cortical pruning and the development of schizophrenia. Schizophr Bull *16*, 567-570.

Fenster, S. D., Chung, W. J., Zhai, R., Cases-Langhoff, C., Voss, B., Garner, A. M., Kaempf, U., Kindler, S., Gundelfinger, E. D., and Garner, C. C. (2000). Piccolo, a presynaptic zinc finger protein structurally related to bassoon. Neuron *25*, 203-214.

Fenton, W. S., Blyler, C. R., and Heinssen, R. K. (1997). Determinants of medication compliance in schizophrenia: empirical and clinical findings. Schizophr Bull *23*, 637-651.

Foltyn, V. N., Bendikov, I., De Miranda, J., Panizzutti, R., Dumin, E., Shleper, M., Li, P., Toney, M. D., Kartvelishvily, E., and Wolosker, H. (2005). Serine racemase modulates intracellular D-serine levels through an alpha,beta-elimination activity. J Biol Chem *280*, 1754-1763.

Freedman, R. (2003). Schizophrenia. N Engl J Med *349*, 1738-1749.

Fuchs, S. A., De Barse, M. M., Scheepers, F. E., Cahn, W., Dorland, L., de Sain-van der Velden, M. G., Klomp, L. W., Berger, R., Kahn, R. S., and de Koning, T. J. (2008). Cerebrospinal fluid D-serine and glycine concentrations are unaltered and unaffected by olanzapine therapy in male schizophrenic patients. Eur Neuropsychopharmacol *18*, 333-338.

Fukasawa, Y., Segawa, H., Kim, J. Y., Chairoungdua, A., Kim, D. K., Matsuo, H., Cha, S. H., Endou, H., and Kanai, Y. (2000). Identification and characterization of a Na(+)-independent neutral amino acid transporter that associates with the 4F2 heavy chain and exhibits substrate selectivity for small neutral D- and L-amino acids. J Biol Chem *275*, 9690-9698.

Fukuda, M. (2008). Regulation of secretory vesicle traffic by Rab small GTPases. Cell Mol Life Sci *65*, 2801-2813.

Fukui, K., and Miyake, Y. (1992). Molecular cloning and chromosomal localization of a human gene encoding D-amino-acid oxidase. J Biol Chem *267*, 18631-18638.

Furukawa, H., and Gouaux, E. (2003). Mechanisms of activation, inhibition and specificity: crystal structures of the NMDA receptor NR1 ligand-binding core. EMBO J *22*, 2873-2885.

Gao, X. M., Sakai, K., Roberts, R. C., Conley, R. R., Dean, B., and Tamminga, C. A. (2000). Ionotropic glutamate receptors and expression of N-methyl-D-aspartate receptor subunits in subregions of human hippocampus: effects of schizophrenia. Am J Psychiatry *157*, 1141-1149.

Garner, C. C., Kindler, S., and Gundelfinger, E. D. (2000). Molecular determinants of presynaptic active zones. Curr Opin Neurobiol *10*, 321-327.

Geddes, J. (1999). Prenatal and perinatal and perinatal risk factors for early onset schizophrenia, affective psychosis, and reactive psychosis. BMJ *318*, 426.

Geddes, J., Freemantle, N., Harrison, P., and Bebbington, P. (2000). Atypical antipsychotics in the treatment of schizophrenia: systematic overview and meta-regression analysis. BMJ *321*, 1371-1376.

Ghiglieri, V., Picconi, B., Sgobio, C., Bagetta, V., Barone, I., Paille, V., Di Filippo, M., Polli, F., Gardoni, F., Altrock, W.*, et al.* (2009). Epilepsy-induced abnormal striatal plasticity in Bassoon mutant mice. Eur J Neurosci *29*, 1979-1993.

Glantz, L. A., and Lewis, D. A. (2000). Decreased dendritic spine density on prefrontal cortical pyramidal neurons in schizophrenia. Arch Gen Psychiatry *57*, 65-73.

Goff, D. C., and Coyle, J. T. (2001). The emerging role of glutamate in the pathophysiology and treatment of schizophrenia. Am J Psychiatry *158*, 1367-1377.

Goff, D. C., Henderson, D. C., Evins, A. E., and Amico, E. (1999). A placebo-controlled crossover trial of D-cycloserine added to clozapine in patients with schizophrenia. Biol Psychiatry *45*, 512-514.

Goff, D. C., Herz, L., Posever, T., Shih, V., Tsai, G., Henderson, D. C., Freudenreich, O., Evins, A. E., Yovel, I., Zhang, H., and Schoenfeld, D. (2005). A six-month, placebo-controlled trial of D-cycloserine co-administered with conventional antipsychotics in schizophrenia patients. Psychopharmacology (Berl) *179*, 144-150.

Goff, D. C., Tsai, G., Manoach, D. S., and Coyle, J. T. (1995). Dose-finding trial of D-cycloserine added to neuroleptics for negative symptoms in schizophrenia. Am J Psychiatry *152*, 1213-1215.

Goldenberg, H., Huttinger, M., Ludwig, R., Kramar, R., and Bock, P. (1975). Catalase-positive particles ("microperoxisomes") from rat preputial gland and bovine adrenal cortex. Exp Cell Res *93*, 438-442.

Goldstein, A. Y., Wang, X., and Schwarz, T. L. (2008). Axonal transport and the delivery of pre-synaptic components. Curr Opin Neurobiol *18*, 495-503.

Gossrau, R. (1991). Catalytic histochemistry of acid and neutral hydrolases in plant seedlings. Histochem J *23*, 483-489.

Gotesman, I. (1991). Schizophrenia Genesis: The origins of Madness. , (New York Freeman Press).

Grosshans, B. L., Ortiz, D., and Novick, P. (2006). Rabs and their effectors: achieving specificity in membrane traffic. Proc Natl Acad Sci U S A *103*, 11821-11827.

Gu, Z., Jiang, Q., Fu, A. K., Ip, N. Y., and Yan, Z. (2005). Regulation of NMDA receptors by neuregulin signaling in prefrontal cortex. J Neurosci *25*, 4974-4984.

Guidotti, A., Auta, J., Davis, J. M., Di-Giorgi-Gerevini, V., Dwivedi, Y., Grayson, D. R., Impagnatiello, F., Pandey, G., Pesold, C., Sharma, R.*, et al.* (2000). Decrease in reelin and glutamic acid decarboxylase67 (GAD67) expression in schizophrenia and bipolar disorder: a postmortem brain study. Arch Gen Psychiatry *57*, 1061-1069.

Gur, R. E., Cowell, P., Turetsky, B. I., Gallacher, F., Cannon, T., Bilker, W., and Gur, R. C. (1998). A follow-up magnetic resonance imaging study of schizophrenia. Relationship of neuroanatomical changes to clinical and neurobehavioral measures. Arch Gen Psychiatry *55*, 145-152.

Gustafson, E. C., Stevens, E. R., Wolosker, H., and Miller, R. F. (2007). Endogenous D-serine contributes to NMDA-receptor-mediated light-evoked responses in the vertebrate retina. J Neurophysiol *98*, 122-130.

Habl, G., Zink, M., Petroianu, G., Bauer, M., Schneider-Axmann, T., von Wilmsdorff, M., Falkai, P., Henn, F. A., and Schmitt, A. (2009). Increased D: -amino acid oxidase expression in the bilateral hippocampal CA4 of schizophrenic patients: a post-mortem study. J Neural Transm.

Halassa, M. M., Fellin, T., and Haydon, P. G. (2007). The tripartite synapse: roles for gliotransmission in health and disease. Trends Mol Med *13*, 54-63.

Halim, N. D., Weickert, C. S., McClintock, B. W., Hyde, T. M., Weinberger, D. R., Kleinman, J. E., and Lipska, B. K. (2003). Presynaptic proteins in the prefrontal cortex of patients with schizophrenia and rats with abnormal prefrontal development. Mol Psychiatry *8*, 797-810.

Hall, W., and Degenhardt, L. (2000). Cannabis use and psychosis: a review of clinical and epidemiological evidence. Aust N Z J Psychiatry *34*, 26-34.

Hamase, K., Konno, R., Morikawa, A., and Zaitsu, K. (2005). Sensitive determination of D-amino acids in mammals and the effect of D-amino-acid oxidase activity on their amounts. Biol Pharm Bull *28*, 1578-1584.

Harrison, P. J. (1999). The neuropathology of schizophrenia. A critical review of the data and their interpretation. Brain *122 (Pt 4)*, 593-624.

Harrison, P. J., and Eastwood, S. L. (2001). Neuropathological studies of synaptic connectivity in the hippocampal formation in schizophrenia. Hippocampus *11*, 508-519.

Harrison, P. J., Law, A. J., and Eastwood, S. L. (2003). Glutamate receptors and transporters in the hippocampus in schizophrenia. Ann N Y Acad Sci *1003*, 94-101.

Harrison, P. J., and Owen, M. J. (2003). Genes for schizophrenia? Recent findings and their pathophysiological implications. Lancet *361*, 417-419.

Harrison, P. J., and Weinberger, D. R. (2005). Schizophrenia genes, gene expression, and neuropathology: on the matter of their convergence. Mol Psychiatry *10*, 40-68; image 45.

Hashimoto, A., Kumashiro, S., Nishikawa, T., Oka, T., Takahashi, K., Mito, T., Takashima, S., Doi, N., Mizutani, Y., Yamazaki, T., and et al. (1993a). Embryonic development and postnatal changes in free D-aspartate and D-serine in the human prefrontal cortex. J Neurochem *61*, 348-351.

Hashimoto, A., Nishikawa, T., Hayashi, T., Fujii, N., Harada, K., Oka, T., and Takahashi, K. (1992). The presence of free D-serine in rat brain. FEBS Lett *296*, 33-36.

Hashimoto, A., Nishikawa, T., Konno, R., Niwa, A., Yasumura, Y., Oka, T., and Takahashi, K. (1993b). Free D-serine, D-aspartate and D-alanine in central nervous system and serum in mutant mice lacking D-amino acid oxidase. Neurosci Lett *152*, 33-36.

Hashimoto, A., Nishikawa, T., Oka, T., and Takahashi, K. (1993c). Endogenous D-serine in rat brain: N-methyl-D-aspartate receptor-related distribution and aging. J Neurochem *60*, 783-786.

Hashimoto, A., Oka, T., and Nishikawa, T. (1995a). Anatomical distribution and postnatal changes in endogenous free D-aspartate and D-serine in rat brain and periphery. Eur J Neurosci *7*, 1657-1663.

Hashimoto, A., Oka, T., and Nishikawa, T. (1995b). Extracellular concentration of endogenous free D-serine in the rat brain as revealed by in vivo microdialysis. Neuroscience *66*, 635-643.

Hashimoto, A., Yoshikawa, M., Niwa, A., and Konno, R. (2005a). Mice lacking D-amino acid oxidase activity display marked attenuation of stereotypy and ataxia induced by MK-801. Brain Res *1033*, 210-215.

Hashimoto, K., Engberg, G., Shimizu, E., Nordin, C., Lindstrom, L. H., and Iyo, M. (2005b). Reduced D-serine to total serine ratio in the cerebrospinal fluid of drug naive schizophrenic patients. Prog Neuropsychopharmacol Biol Psychiatry *29*, 767-769.

Hashimoto, K., Fujita, Y., Horio, M., Kunitachi, S., Iyo, M., Ferraris, D., and Tsukamoto, T. (2009). Co-administration of a D-amino acid oxidase inhibitor potentiates the efficacy of D-serine in attenuating prepulse inhibition deficits after administration of dizocilpine. Biol Psychiatry *65*, 1103-1106.

Hashimoto, K., Fukushima, T., Shimizu, E., Komatsu, N., Watanabe, H., Shinoda, N., Nakazato, M., Kumakiri, C., Okada, S., Hasegawa, H.*, et al.* (2003). Decreased serum levels of D-serine in patients with schizophrenia: evidence in support of the N-methyl-D-aspartate receptor hypofunction hypothesis of schizophrenia. Arch Gen Psychiatry *60*, 572-576.

Haydon, P. G. (2001). GLIA: listening and talking to the synapse. Nat Rev Neurosci *2*, 185-193.

Heckers, S., and Konradi, C. (2002). Hippocampal neurons in schizophrenia. J Neural Transm *109*, 891-905.

Helboe, L., Egebjerg, J., Moller, M., and Thomsen, C. (2003). Distribution and pharmacology of alanine-serine-cysteine transporter 1 (asc-1) in rodent brain. Eur J Neurosci *18*, 2227-2238.

Heresco-Levy, U., Ermilov, M., Shimoni, J., Shapira, B., Silipo, G., and Javitt, D. C. (2002). Placebo-controlled trial of D-cycloserine added to conventional neuroleptics, olanzapine, or risperidone in schizophrenia. Am J Psychiatry *159*, 480-482.

Heresco-Levy, U., Javitt, D. C., Ermilov, M., Mordel, C., Horowitz, A., and Kelly, D. (1996a). Double-blind, placebo-controlled, crossover trial of glycine adjuvant therapy for treatment-resistant schizophrenia. Br J Psychiatry *169*, 610-617.

Heresco-Levy, U., Javitt, D. C., Ermilov, M., Mordel, C., Silipo, G., and Lichtenstein, M. (1999). Efficacy of high-dose glycine in the treatment of enduring negative symptoms of schizophrenia. Arch Gen Psychiatry *56*, 29-36.

Heresco-Levy, U., Silipo, G., and Javitt, D. C. (1996b). Glycinergic augmentation of NMDA receptor-mediated neurotransmission in the treatment of schizophrenia. Psychopharmacol Bull *32*, 731-740.

Hess, S. D., Daggett, L. P., Crona, J., Deal, C., Lu, C. C., Urrutia, A., Chavez-Noriega, L., Ellis, S. B., Johnson, E. C., and Velicelebi, G. (1996). Cloning and functional characterization of human heteromeric N-methyl-D-aspartate receptors. J Pharmacol Exp Ther *278*, 808-816.

Hoetelmans, R. W., Prins, F. A., Cornelese-ten Velde, I., van der Meer, J., van de Velde, C. J., and van Dierendonck, J. H. (2001). Effects of acetone, methanol, or paraformaldehyde on cellular structure, visualized by reflection contrast microscopy and transmission and scanning electron microscopy. Appl Immunohistochem Mol Morphol *9*, 346-351.

Hollister, J. M., Laing, P., and Mednick, S. A. (1996). Rhesus incompatibility as a risk factor for schizophrenia in male adults. Arch Gen Psychiatry *53*, 19-24.

Honey, G. D., Pomarol-Clotet, E., Corlett, P. R., Honey, R. A., McKenna, P. J., Bullmore, E. T., and Fletcher, P. C. (2005). Functional dysconnectivity in schizophrenia associated with attentional modulation of motor function. Brain *128*, 2597-2611.

Hons, J., Zirko, R., Ulrychova, M., Cermakova, E., and Libiger, J. (2008). D-serine serum levels in patients with schizophrenia: relation to psychopathology and comparison to healthy subjects. Neuro Endocrinol Lett *29*, 485-492.

Horiike, K., Tojo, H., Arai, R., Nozaki, M., and Maeda, T. (1994). D-amino-acid oxidase is confined to the lower brain stem and cerebellum in rat brain: regional differentiation of astrocytes. Brain Res *652*, 297-303.

Horiike, K., Tojo, H., Arai, R., Yamano, T., Nozaki, M., and Maeda, T. (1987). Localization of D-amino acid oxidase in Bergmann glial cells and astrocytes of rat cerebellum. Brain Res Bull *19*, 587-596.

Howell, J. M., Winstone, T. L., Coorssen, J. R., and Turner, R. J. (2006). An evaluation of in vitro protein-protein interaction techniques: assessing contaminating background proteins. Proteomics *6*, 2050-2069.

Howes, O. D., Egerton, A., Allan, V., McGuire, P., Stokes, P., and Kapur, S. (2009). Mechanisms underlying psychosis and antipsychotic treatment response in schizophrenia: insights from PET and SPECT imaging. Curr Pharm Des *15*, 2550-2559.

Howes, O. D., and Kapur, S. (2009). The dopamine hypothesis of schizophrenia: version III--the final common pathway. Schizophr Bull *35*, 549-562.

Huettner, J. E. (2003). Kainate receptors and synaptic transmission. Prog Neurobiol *70*, 387-407.

Huntley, G. W., Vickers, J. C., and Morrison, J. H. (1997). Quantitative localization of NMDAR1 receptor subunit immunoreactivity in inferotemporal

and prefrontal association cortices of monkey and human. Brain Res *749*, 245-262.

Ichimiya, T., Okubo, Y., Suhara, T., and Sudo, Y. (2001). Reduced volume of the cerebellar vermis in neuroleptic-naive schizophrenia. Biol Psychiatry *49*, 20-27.

Itil, T., Keskiner, A., Kiremitci, N., and Holden, J. M. (1967). Effect of phencyclidine in chronic schizophrenics. Can Psychiatr Assoc J *12*, 209-212.

Iuso, A., Scacco, S., Piccoli, C., Bellomo, F., Petruzzella, V., Trentadue, R., Minuto, M., Ripoli, M., Capitanio, N., Zeviani, M., and Papa, S. (2006). Dysfunctions of cellular oxidative metabolism in patients with mutations in the NDUFS1 and NDUFS4 genes of complex I. J Biol Chem *281*, 10374-10380.

Jaaro-Peled, H., Hayashi-Takagi, A., Seshadri, S., Kamiya, A., Brandon, N. J., and Sawa, A. (2009). Neurodevelopmental mechanisms of schizophrenia: understanding disturbed postnatal brain maturation through neuregulin-1-ErbB4 and DISC1. Trends Neurosci *32*, 485-495.

Javitt, D. C., and Zukin, S. R. (1991). Recent advances in the phencyclidine model of schizophrenia. Am J Psychiatry *148*, 1301-1308.

Javitt, D. C., Zylberman, I., Zukin, S. R., Heresco-Levy, U., and Lindenmayer, J. P. (1994). Amelioration of negative symptoms in schizophrenia by glycine. Am J Psychiatry *151*, 1234-1236.

Jentsch, J. D., and Roth, R. H. (1999). The neuropsychopharmacology of phencyclidine: from NMDA receptor hypofunction to the dopamine hypothesis of schizophrenia. Neuropsychopharmacology *20*, 201-225.

Jin, Y., and Garner, C. C. (2008). Molecular mechanisms of presynaptic differentiation. Annu Rev Cell Dev Biol *24*, 237-262.

Johkura, K., Usuda, N., Liang, Y., and Nakazawa, A. (1998). Immunohistochemical localization of peroxisomal enzymes in developing rat kidney tissues. J Histochem Cytochem *46*, 1161-1173.

Jones, P. B., Barnes, T. R., Davies, L., Dunn, G., Lloyd, H., Hayhurst, K. P., Murray, R. M., Markwick, A., and Lewis, S. W. (2006). Randomized controlled trial of the effect on Quality of Life of second- vs first-generation antipsychotic drugs in schizophrenia: Cost Utility of the Latest Antipsychotic Drugs in Schizophrenia Study (CUtLASS 1). Arch Gen Psychiatry *63*, 1079-1087.

Joung, J. K., Ramm, E. I., and Pabo, C. O. (2000). A bacterial two-hybrid selection system for studying protein-DNA and protein-protein interactions. Proc Natl Acad Sci U S A *97*, 7382-7387.

Kahn, R. S., Fleischhacker, W. W., Boter, H., Davidson, M., Vergouwe, Y., Keet, I. P., Gheorghe, M. D., Rybakowski, J. K., Galderisi, S., Libiger, J*., et al.* (2008).

Effectiveness of antipsychotic drugs in first-episode schizophrenia and schizophreniform disorder: an open randomised clinical trial. Lancet *371*, 1085-1097.

Kalla, S., Stern, M., Basu, J., Varoqueaux, F., Reim, K., Rosenmund, C., Ziv, N. E., and Brose, N. (2006). Molecular dynamics of a presynaptic active zone protein studied in Munc13-1-enhanced yellow fluorescent protein knock-in mutant mice. J Neurosci *26*, 13054-13066.

Kalus, P., Muller, T. J., Zuschratter, W., and Senitz, D. (2000). The dendritic architecture of prefrontal pyramidal neurons in schizophrenic patients. Neuroreport *11*, 3621-3625.

Kane, J., Honigfeld, G., Singer, J., and Meltzer, H. (1988). Clozapine for the treatment-resistant schizophrenic. A double-blind comparison with chlorpromazine. Arch Gen Psychiatry *45*, 789-796.

Kapoor, R., Lim, K. S., Cheng, A., Garrick, T., and Kapoor, V. (2006). Preliminary evidence for a link between schizophrenia and NMDA-glycine site receptor ligand metabolic enzymes, d-amino acid oxidase (DAAO) and kynurenine aminotransferase-1 (KAT-1). Brain Res *1106*, 205-210.

Kapur, S., Zipursky, R., Jones, C., Shammi, C. S., Remington, G., and Seeman, P. (2000). A positron emission tomography study of quetiapine in schizophrenia: a preliminary finding of an antipsychotic effect with only transiently high dopamine D2 receptor occupancy. Arch Gen Psychiatry *57*, 553-559.

Karson, C. N., Mrak, R. E., Schluterman, K. O., Sturner, W. Q., Sheng, J. G., and Griffin, W. S. (1999). Alterations in synaptic proteins and their encoding mRNAs in prefrontal cortex in schizophrenia: a possible neurochemical basis for 'hypofrontality'. Mol Psychiatry *4*, 39-45.

Katsetos, C. D., Hyde, T. M., and Herman, M. M. (1997). Neuropathology of the cerebellum in schizophrenia--an update: 1996 and future directions. Biol Psychiatry *42*, 213-224.

Kaumaya, P. T., VanBuskirk, A. M., Goldberg, E., and Pierce, S. K. (1992). Design and immunological properties of topographic immunogenic determinants of a protein antigen (LDH-C4) as vaccines. J Biol Chem *267*, 6338-6346.

Kawazoe, T., Tsuge, H., Imagawa, T., Aki, K., Kuramitsu, S., and Fukui, K. (2007). Structural basis of D-DOPA oxidation by D-amino acid oxidase: alternative pathway for dopamine biosynthesis. Biochem Biophys Res Commun *355*, 385-391.

Kawazoe, T., Tsuge, H., Pilone, M. S., and Fukui, K. (2006). Crystal structure of human D-amino acid oxidase: context-dependent variability of the backbone conformation of the VAAGL hydrophobic stretch located at the si-face of the flavin ring. Protein Sci *15*, 2708-2717.

Kegeles, L. S., Abi-Dargham, A., Zea-Ponce, Y., Rodenhiser-Hill, J., Mann, J. J., Van Heertum, R. L., Cooper, T. B., Carlsson, A., and Laruelle, M. (2000). Modulation of amphetamine-induced striatal dopamine release by ketamine in humans: implications for schizophrenia. Biol Psychiatry *48*, 627-640.

Kim, D. H., Maneen, M. J., and Stahl, S. M. (2009). Building a better antipsychotic: receptor targets for the treatment of multiple symptom dimensions of schizophrenia. Neurotherapeutics *6*, 78-85.

Kim, J. S., Kornhuber, H. H., Schmid-Burgk, W., and Holzmuller, B. (1980). Low cerebrospinal fluid glutamate in schizophrenic patients and a new hypothesis on schizophrenia. Neurosci Lett *20*, 379-382.

Kim, P. M., Aizawa, H., Kim, P. S., Huang, A. S., Wickramasinghe, S. R., Kashani, A. H., Barrow, R. K., Huganir, R. L., Ghosh, A., and Snyder, S. H. (2005). Serine racemase: activation by glutamate neurotransmission via glutamate receptor interacting protein and mediation of neuronal migration. Proc Natl Acad Sci U S A *102*, 2105-2110.

Kinney, G. G., O'Brien, J. A., Lemaire, W., Burno, M., Bickel, D. J., Clements, M. K., Chen, T. B., Wisnoski, D. D., Lindsley, C. W., Tiller, P. R.*, et al.* (2005). A novel selective positive allosteric modulator of metabotropic glutamate receptor subtype 5 has in vivo activity and antipsychotic-like effects in rat behavioral models. J Pharmacol Exp Ther *313*, 199-206.

Kirkpatrick, B., Buchanan, R. W., Ross, D. E., and Carpenter, W. T., Jr. (2001). A separate disease within the syndrome of schizophrenia. Arch Gen Psychiatry *58*, 165-171.

Kirov, G., O'Donovan, M. C., and Owen, M. J. (2005). Finding schizophrenia genes. J Clin Invest *115*, 1440-1448.

Koibuchi, N., Konno, R., Matsuzaki, S., Ohtake, H., Niwa, A., and Yamaoka, S. (1995). Localization of D-amino acid oxidase mRNA in the mouse kidney and the effect of testosterone treatment. Histochem Cell Biol *104*, 349-355.

Konno, R. (2001). Assignment of D-amino-acid oxidase gene to a human and a mouse chromosome. Amino Acids *20*, 401-408.

Konno, R. (2003). Rat cerebral serine racemase: amino acid deletion and truncation at carboxy terminus. Neurosci Lett *349*, 111-114.

Konno, R., Yamamoto, K., Niwa, A., and Yasumura, Y. (1991). Presence of D-amino-acid oxidase protein in mutant mice lacking D-amino-acid oxidase activity. Int J Biochem *23*, 1301-1305.

Konno, R., and Yasumura, Y. (1983). Mouse mutant deficient in D-amino acid oxidase activity. Genetics *103*, 277-285.

Korostishevsky, M., Kaganovich, M., Cholostoy, A., Ashkenazi, M., Ratner, Y., Dahary, D., Bernstein, J., Bening-Abu-Shach, U., Ben-Asher, E., Lancet, D.*, et al.* (2004). Is the G72/G30 locus associated with schizophrenia? single nucleotide polymorphisms, haplotypes, and gene expression analysis. Biol Psychiatry *56*, 169-176.

Korostishevsky, M., Kremer, I., Kaganovich, M., Cholostoy, A., Murad, I., Muhaheed, M., Bannoura, I., Rietschel, M., Dobrusin, M., Bening-Abu-Shach, U.*, et al.* (2006). Transmission disequilibrium and haplotype analyses of the G72/G30 locus: suggestive linkage to schizophrenia in Palestinian Arabs living in the North of Israel. Am J Med Genet B Neuropsychiatr Genet *141B*, 91-95.

Krystal, J. H., Karper, L. P., Seibyl, J. P., Freeman, G. K., Delaney, R., Bremner, J. D., Heninger, G. R., Bowers, M. B., Jr., and Charney, D. S. (1994). Subanesthetic effects of the noncompetitive NMDA antagonist, ketamine, in humans. Psychotomimetic, perceptual, cognitive, and neuroendocrine responses. Arch Gen Psychiatry *51*, 199-214.

Kumashiro, S., Hashimoto, A., and Nishikawa, T. (1995). Free D-serine in post-mortem brains and spinal cords of individuals with and without neuropsychiatric diseases. Brain Res *681*, 117-125.

Kurz, M., Hummer, M., Oberbauer, H., and Fleischhacker, W. W. (1995). Extrapyramidal side effects of clozapine and haloperidol. Psychopharmacology (Berl) *118*, 52-56.

Kvajo, M., Dhilla, A., Swor, D. E., Karayiorgou, M., and Gogos, J. A. (2008). Evidence implicating the candidate schizophrenia/bipolar disorder susceptibility gene G72 in mitochondrial function. Mol Psychiatry *13*, 685-696.

Labrie, V., Fukumura, R., Rastogi, A., Fick, L. J., Wang, W., Boutros, P. C., Kennedy, J. L., Semeralul, M. O., Lee, F. H., Baker, G. B.*, et al.* (2009a). Serine racemase is associated with schizophrenia susceptibility in humans and in a mouse model. Hum Mol Genet *18*, 3227-3243.

Labrie, V., Wang, W., Barger, S. W., Baker, G. B., and Roder, J. C. (2009b). Genetic loss of D-amino acid oxidase activity reverses schizophrenia-like phenotypes in mice. Genes Brain Behav.

Lahti, A. C., Koffel, B., LaPorte, D., and Tamminga, C. A. (1995). Subanesthetic doses of ketamine stimulate psychosis in schizophrenia. Neuropsychopharmacology *13*, 9-19.

Lahti, A. C., Weiler, M. A., Holcomb, H. H., Tamminga, C. A., Carpenter, W. T., and McMahon, R. (2006). Correlations between rCBF and symptoms in two independent cohorts of drug-free patients with schizophrenia. Neuropsychopharmacology *31*, 221-230.

Lane, H. Y., Huang, C. L., Wu, P. L., Liu, Y. C., Chang, Y. C., Lin, P. Y., Chen, P. W., and Tsai, G. (2006). Glycine transporter I inhibitor, N-methylglycine (sarcosine), added to clozapine for the treatment of schizophrenia. Biol Psychiatry *60*, 645-649.

Lang, T., and Jahn, R. (2008). Core proteins of the secretory machinery. Handb Exp Pharmacol, 107-127.

Laruelle, M., Abi-Dargham, A., Gil, R., Kegeles, L., and Innis, R. (1999). Increased dopamine transmission in schizophrenia: relationship to illness phases. Biol Psychiatry *46*, 56-72.

Laurie, D. J., and Seeburg, P. H. (1994). Ligand affinities at recombinant N-methyl-D-aspartate receptors depend on subunit composition. Eur J Pharmacol *268*, 335-345.

Law, I. K., Liu, L., Xu, A., Lam, K. S., Vanhoutte, P. M., Che, C. M., Leung, P. T., and Wang, Y. (2009). Identification and characterization of proteins interacting with SIRT1 and SIRT3: implications in the anti-aging and metabolic effects of sirtuins. Proteomics *9*, 2444-2456.

Leiderman, E., Zylberman, I., Zukin, S. R., Cooper, T. B., and Javitt, D. C. (1996). Preliminary investigation of high-dose oral glycine on serum levels and negative symptoms in schizophrenia: an open-label trial. Biol Psychiatry *39*, 213-215.

Leighton, F., Poole, B., Beaufay, H., Baudhuin, P., Coffey, J. W., Fowler, S., and De Duve, C. (1968). The large-scale separation of peroxisomes, mitochondria, and lysosomes from the livers of rats injected with triton WR-1339. Improved isolation procedures, automated analysis, biochemical and morphological properties of fractions. J Cell Biol *37*, 482-513.

Leucht, S., Corves, C., Arbter, D., Engel, R. R., Li, C., and Davis, J. M. (2009). Second-generation versus first-generation antipsychotic drugs for schizophrenia: a meta-analysis. Lancet *373*, 31-41.

Lewis, C. M., Levinson, D. F., Wise, L. H., DeLisi, L. E., Straub, R. E., Hovatta, I., Williams, N. M., Schwab, S. G., Pulver, A. E., Faraone, S. V.*, et al.* (2003). Genome scan meta-analysis of schizophrenia and bipolar disorder, part II: Schizophrenia. Am J Hum Genet *73*, 34-48.

Lewis, D. A., and Gonzalez-Burgos, G. (2006). Pathophysiologically based treatment interventions in schizophrenia. Nat Med *12*, 1016-1022.

Lewis, D. A., and Lieberman, J. A. (2000). Catching up on schizophrenia: natural history and neurobiology. Neuron *28*, 325-334.

Li, D., and He, L. (2007). G72/G30 genes and schizophrenia: a systematic meta-analysis of association studies. Genetics *175*, 917-922.

Li, F., and Tsien, J. Z. (2009). Memory and the NMDA receptors. N Engl J Med *361*, 302-303.

Li, Y., Asuri, S., Rebhun, J. F., Castro, A. F., Paranavitana, N. C., and Quilliam, L. A. (2006). The RAP1 guanine nucleotide exchange factor Epac2 couples cyclic AMP and Ras signals at the plasma membrane. J Biol Chem *281*, 2506-2514.

Li, Y. H., and Han, T. Z. (2007). Glycine binding sites of presynaptic NMDA receptors may tonically regulate glutamate release in the rat visual cortex. J Neurophysiol *97*, 817-823.

Lieberman, J. A., Kane, J. M., and Alvir, J. (1987). Provocative tests with psychostimulant drugs in schizophrenia. Psychopharmacology (Berl) *91*, 415-433.

Lieberman, J. A., Stroup, T. S., McEvoy, J. P., Swartz, M. S., Rosenheck, R. A., Perkins, D. O., Keefe, R. S., Davis, S. M., Davis, C. E., Lebowitz, B. D*., et al.* (2005). Effectiveness of antipsychotic drugs in patients with chronic schizophrenia. N Engl J Med *353*, 1209-1223.

Linderholm, K. R., Andersson, A., Olsson, S., Olsson, E., Snodgrass, R., Engberg, G., and Erhardt, S. (2007). Activation of rat ventral tegmental area dopamine neurons by endogenous kynurenic acid: a pharmacological analysis. Neuropharmacology *53*, 918-924.

Liu, X., He, G., Wang, X., Chen, Q., Qian, X., Lin, W., Li, D., Gu, N., Feng, G., and He, L. (2004). Association of DAAO with schizophrenia in the Chinese population. Neurosci Lett *369*, 228-233.

Liu, Y., Li, Q., Zhu, H., and Yang, J. (2009). High soluble expression of D-amino acid oxidase in Escherichia coli regulated by a native promoter. Appl Biochem Biotechnol *158*, 313-322.

Liu, Y. L., Fann, C. S., Liu, C. M., Chang, C. C., Wu, J. Y., Hung, S. I., Liu, S. K., Hsieh, M. H., Hwang, T. J., Chan, H. Y*., et al.* (2006). No association of G72 and D-amino acid oxidase genes with schizophrenia. Schizophr Res *87*, 15-20.

Luby, E. D., Cohen, B. D., Rosenbaum, G., Gottlieb, J. S., and Kelley, R. (1959). Study of a new schizophrenomimetic drug; sernyl. AMA Arch Neurol Psychiatry *81*, 363-369.

Lynch, D. R., and Guttmann, R. P. (2001). NMDA receptor pharmacology: perspectives from molecular biology. Curr Drug Targets *2*, 215-231.

Ma, J., Qin, W., Wang, X. Y., Guo, T. W., Bian, L., Duan, S. W., Li, X. W., Zou, F. G., Fang, Y. R., Fang, J. X*., et al.* (2006). Further evidence for the association between G72/G30 genes and schizophrenia in two ethnically distinct populations. Mol Psychiatry *11*, 479-487.

Madeira, C., Freitas, M. E., Vargas-Lopes, C., Wolosker, H., and Panizzutti, R. (2008). Increased brain D-amino acid oxidase (DAAO) activity in schizophrenia. Schizophr Res *101*, 76-83.

Maekawa, M., Watanabe, M., Yamaguchi, S., Konno, R., and Hori, Y. (2005). Spatial learning and long-term potentiation of mutant mice lacking D-amino-acid oxidase. Neurosci Res *53*, 34-38.

Mahmoudi, T., Li, V. S., Ng, S. S., Taouatas, N., Vries, R. G., Mohammed, S., Heck, A. J., and Clevers, H. (2009). The kinase TNIK is an essential activator of Wnt target genes. EMBO J.

Mallik, R., Carter, B. C., Lex, S. A., King, S. J., and Gross, S. P. (2004). Cytoplasmic dynein functions as a gear in response to load. Nature *427*, 649-652.

Manto, M. (2009). Mechanisms of human cerebellar dysmetria: experimental evidence and current conceptual bases. J Neuroeng Rehabil *6*, 10.

Marino, M. J., Knutsen, L. J., and Williams, M. (2008). Emerging opportunities for antipsychotic drug discovery in the postgenomic era. J Med Chem *51*, 1077-1107.

Martina, M., Krasteniakov, N. V., and Bergeron, R. (2003). D-Serine differently modulates NMDA receptor function in rat CA1 hippocampal pyramidal cells and interneurons. J Physiol *548*, 411-423.

Matsui, T., Sekiguchi, M., Hashimoto, A., Tomita, U., Nishikawa, T., and Wada, K. (1995). Functional comparison of D-serine and glycine in rodents: the effect on cloned NMDA receptors and the extracellular concentration. J Neurochem *65*, 454-458.

Matsuo, H., Kanai, Y., Tokunaga, M., Nakata, T., Chairoungdua, A., Ishimine, H., Tsukada, S., Ooigawa, H., Nawashiro, H., Kobayashi, Y.*, et al.* (2004). High affinity D- and L-serine transporter Asc-1: cloning and dendritic localization in the rat cerebral and cerebellar cortices. Neurosci Lett *358*, 123-126.

Matthysse, S. (1973). Antipsychotic drug actions: a clue to the neuropathology of schizophrenia? Fed Proc *32*, 200-205.

McBain, C. J., Kleckner, N. W., Wyrick, S., and Dingledine, R. (1989). Structural requirements for activation of the glycine coagonist site of N-methyl-D-aspartate receptors expressed in Xenopus oocytes. Mol Pharmacol *36*, 556-565.

McDonald, J. W., Penney, J. B., Johnston, M. V., and Young, A. B. (1990). Characterization and regional distribution of strychnine-insensitive [3H]glycine binding sites in rat brain by quantitative receptor autoradiography. Neuroscience *35*, 653-668.

McEvoy, J. P., Lieberman, J. A., Stroup, T. S., Davis, S. M., Meltzer, H. Y., Rosenheck, R. A., Swartz, M. S., Perkins, D. O., Keefe, R. S., Davis, C. E*., et al.* (2006). Effectiveness of clozapine versus olanzapine, quetiapine, and risperidone in patients with chronic schizophrenia who did not respond to prior atypical antipsychotic treatment. Am J Psychiatry *163*, 600-610.

McGlashan, T. H., and Fenton, W. S. (1993). Subtype progression and pathophysiologic deterioration in early schizophrenia. Schizophr Bull *19*, 71-84.

Mednick, S. A., Machon, R. A., Huttunen, M. O., and Bonett, D. (1988). Adult schizophrenia following prenatal exposure to an influenza epidemic. Arch Gen Psychiatry *45*, 189-192.

Medoff, D. R., Holcomb, H. H., Lahti, A. C., and Tamminga, C. A. (2001). Probing the human hippocampus using rCBF: contrasts in schizophrenia. Hippocampus *11*, 543-550.

Meltzer, H. Y. (1997). Treatment-resistant schizophrenia--the role of clozapine. Curr Med Res Opin *14*, 1-20.

Messias, E. L., Chen, C. Y., and Eaton, W. W. (2007). Epidemiology of schizophrenia: review of findings and myths. Psychiatr Clin North Am *30*, 323-338.

Meyer-Lindenberg, A., Miletich, R. S., Kohn, P. D., Esposito, G., Carson, R. E., Quarantelli, M., Weinberger, D. R., and Berman, K. F. (2002). Reduced prefrontal activity predicts exaggerated striatal dopaminergic function in schizophrenia. Nat Neurosci *5*, 267-271.

Middleton, F. A., and Strick, P. L. (1994). Anatomical evidence for cerebellar and basal ganglia involvement in higher cognitive function. Science *266*, 458-461.

Millar, J. K., Pickard, B. S., Mackie, S., James, R., Christie, S., Buchanan, S. R., Malloy, M. P., Chubb, J. E., Huston, E., Baillie, G. S*., et al.* (2005). DISC1 and PDE4B are interacting genetic factors in schizophrenia that regulate cAMP signaling. Science *310*, 1187-1191.

Mirnics, K., Middleton, F. A., Stanwood, G. D., Lewis, D. A., and Levitt, P. (2001). Disease-specific changes in regulator of G-protein signaling 4 (RGS4) expression in schizophrenia. Mol Psychiatry *6*, 293-301.

Misztal, M., Skangiel-Kramska, J., Niewiadomska, G., and Danysz, W. (1996). Subchronic intraventricular infusion of quinolinic acid produces working memory impairment--a model of progressive excitotoxicity. Neuropharmacology *35*, 449-458.

Miyamoto, S., Duncan, G. E., Marx, C. E., and Lieberman, J. A. (2005). Treatments for schizophrenia: a critical review of pharmacology and mechanisms of action of antipsychotic drugs. Mol Psychiatry *10*, 79-104.

Mizutani, H., Miyahara, I., Hirotsu, K., Nishina, Y., Shiga, K., Setoyama, C., and Miura, R. (1996). Three-dimensional structure of porcine kidney D-amino acid oxidase at 3.0 A resolution. J Biochem *120*, 14-17.

Molla, G., Sacchi, S., Bernasconi, M., Pilone, M. S., Fukui, K., and Polegioni, L. (2006). Characterization of human D-amino acid oxidase. FEBS Lett *580*, 2358-2364.

Momoi, K., Fukui, K., Watanabe, F., and Miyake, Y. (1988). Molecular cloning and sequence analysis of cDNA encoding human kidney D-amino acid oxidase. FEBS Lett *238*, 180-184.

Monyer, H., Burnashev, N., Laurie, D. J., Sakmann, B., and Seeburg, P. H. (1994). Developmental and regional expression in the rat brain and functional properties of four NMDA receptors. Neuron *12*, 529-540.

Moreno, S., Nardacci, R., Cimini, A., and Ceru, M. P. (1999). Immunocytochemical localization of D-amino acid oxidase in rat brain. J Neurocytol *28*, 169-185.

Mothet, J. P., Parent, A. T., Wolosker, H., Brady, R. O., Jr., Linden, D. J., Ferris, C. D., Rogawski, M. A., and Snyder, S. H. (2000). D-serine is an endogenous ligand for the glycine site of the N-methyl-D-aspartate receptor. Proc Natl Acad Sci U S A *97*, 4926-4931.

Mulle, J. G., Chowdari, K. V., Nimgaonkar, V., and Chakravarti, A. (2005). No evidence for association to the G72/G30 locus in an independent sample of schizophrenia families. Mol Psychiatry *10*, 431-433.

Mustafa, A. K., van Rossum, D. B., Patterson, R. L., Maag, D., Ehmsen, J. T., Gazi, S. K., Chakraborty, A., Barrow, R. K., Amzel, L. M., and Snyder, S. H. (2009). Glutamatergic regulation of serine racemase via reversal of PIP2 inhibition. Proc Natl Acad Sci U S A *106*, 2921-2926.

Nagata, Y., Borghi, M., Fisher, G. H., and D'Aniello, A. (1995). Free D-serine concentration in normal and Alzheimer human brain. Brain Res Bull *38*, 181-183.

Nakauchi, J., Matsuo, H., Kim, D. K., Goto, A., Chairoungdua, A., Cha, S. H., Inatomi, J., Shiokawa, Y., Yamaguchi, K., Saito, I.*, et al.* (2000). Cloning and characterization of a human brain Na(+)-independent transporter for small neutral amino acids that transports D-serine with high affinity. Neurosci Lett *287*, 231-235.

Need, A. C., Ge, D., Weale, M. E., Maia, J., Feng, S., Heinzen, E. L., Shianna, K. V., Yoon, W., Kasperaviciute, D., Gennarelli, M.*, et al.* (2009). A genome-wide investigation of SNPs and CNVs in schizophrenia. PLoS Genet *5*, e1000373.

Neidle, A., and Dunlop, D. S. (2002). Allosteric regulation of mouse brain serine racemase. Neurochem Res *27*, 1719-1724.

Neims, A. H., Zieverink, W. D., and Smilack, J. D. (1966). Distribution of D-amino acid oxidase in bovine and human nervous tissues. J Neurochem *13*, 163-168.

Nelson, M. D., Saykin, A. J., Flashman, L. A., and Riordan, H. J. (1998). Hippocampal volume reduction in schizophrenia as assessed by magnetic resonance imaging: a meta-analytic study. Arch Gen Psychiatry *55*, 433-440.

Newcomer, J. W., Farber, N. B., Jevtovic-Todorovic, V., Selke, G., Melson, A. K., Hershey, T., Craft, S., and Olney, J. W. (1999). Ketamine-induced NMDA receptor hypofunction as a model of memory impairment and psychosis. Neuropsychopharmacology *20*, 106-118.

Niemi, L. T., Suvisaari, J. M., Tuulio-Henriksson, A., and Lonnqvist, J. K. (2003). Childhood developmental abnormalities in schizophrenia: evidence from high-risk studies. Schizophr Res *60*, 239-258.

Nishi, T., Kawasaki-Nishi, S., and Forgac, M. (2003). Expression and function of the mouse V-ATPase d subunit isoforms. J Biol Chem *278*, 46396-46402.

Nitsch, R., Di Palma, T., Mascia, A., and Zannini, M. (2004). WBP-2, a WW domain binding protein, interacts with the thyroid-specific transcription factor Pax8. Biochem J *377*, 553-560.

Nordahl, T. E., Kusubov, N., Carter, C., Salamat, S., Cummings, A. M., O'Shora-Celaya, L., Eberling, J., Robertson, L., Huesman, R. H., Jagust, W., and Budinger, T. F. (1996). Temporal lobe metabolic differences in medication-free outpatients with schizophrenia via the PET-600. Neuropsychopharmacology *15*, 541-554.

Numakawa, T., Yagasaki, Y., Ishimoto, T., Okada, T., Suzuki, T., Iwata, N., Ozaki, N., Taguchi, T., Tatsumi, M., Kamijima, K*., et al.* (2004). Evidence of novel neuronal functions of dysbindin, a susceptibility gene for schizophrenia. Hum Mol Genet *13*, 2699-2708.

O'Brien, E. M., Tipton, K. F., Strolin Benedetti, M., Bonsignori, A., Marrari, P., and Dostert, P. (1991). Is the oxidation of milacemide by monoamine oxidase a major factor in its anticonvulsant actions? Biochem Pharmacol *41*, 1731-1737.

O'Brien, K. B., and Bowser, M. T. (2006). Measuring D-serine efflux from mouse cortical brain slices using online microdialysis-capillary electrophoresis. Electrophoresis *27*, 1949-1956.

O'Donovan, M. C., Craddock, N., Norton, N., Williams, H., Peirce, T., Moskvina, V., Nikolov, I., Hamshere, M., Carroll, L., Georgieva, L*., et al.* (2008). Identification of loci associated with schizophrenia by genome-wide association and follow-up. Nat Genet *40*, 1053-1055.

Oliet, S. H., and Mothet, J. P. (2006). Molecular determinants of D-serine-mediated gliotransmission: from release to function. Glia *54*, 726-737.

Ono, K., Shishido, Y., Park, H. K., Kawazoe, T., Iwana, S., Chung, S. P., Abou El-Magd, R. M., Yorita, K., Okano, M., Watanabe, T.*, et al.* (2009). Potential pathophysiological role of D-amino acid oxidase in schizophrenia: immunohistochemical and in situ hybridization study of the expression in human and rat brain. J Neural Transm *116*, 1335-1347.

Otte, D. M., Bilkei-Gorzo, A., Filiou, M. D., Turck, C. W., Yilmaz, O., Holst, M. I., Schilling, K., Abou-Jamra, R., Schumacher, J., Benzel, I.*, et al.* (2009). Behavioral changes in G72/G30 transgenic mice. Eur Neuropsychopharmacol *19*, 339-348.

Owald, D., and Sigrist, S. J. (2009). Assembling the presynaptic active zone. Curr Opin Neurobiol *19*, 311-318.

Panatier, A., Theodosis, D. T., Mothet, J. P., Touquet, B., Pollegioni, L., Poulain, D. A., and Oliet, S. H. (2006). Glia-derived D-serine controls NMDA receptor activity and synaptic memory. Cell *125*, 775-784.

Panizzutti, R., Rausch, M., Zurbrugg, S., Baumann, D., Beckmann, N., and Rudin, M. (2005). The pharmacological stimulation of NMDA receptors via co-agonist site: an fMRI study in the rat brain. Neurosci Lett *380*, 111-115.

Paoletti, P., and Neyton, J. (2007). NMDA receptor subunits: function and pharmacology. Curr Opin Pharmacol *7*, 39-47.

Paradiso, S., Andreasen, N. C., O'Leary, D. S., Arndt, S., and Robinson, R. G. (1997). Cerebellar size and cognition: correlations with IQ, verbal memory and motor dexterity. Neuropsychiatry Neuropsychol Behav Neurol *10*, 1-8.

Park, H. K., Shishido, Y., Ichise-Shishido, S., Kawazoe, T., Ono, K., Iwana, S., Tomita, Y., Yorita, K., Sakai, T., and Fukui, K. (2006). Potential role for astroglial D-amino acid oxidase in extracellular D-serine metabolism and cytotoxicity. J Biochem *139*, 295-304.

Paulson, L., Martin, P., Persson, A., Nilsson, C. L., Ljung, E., Westman-Brinkmalm, A., Eriksson, P. S., Blennow, K., and Davidsson, P. (2003). Comparative genome- and proteome analysis of cerebral cortex from MK-801-treated rats. J Neurosci Res *71*, 526-533.

Peacock, L., Solgaard, T., Lublin, H., and Gerlach, J. (1996). Clozapine versus typical antipsychotics. A retro- and prospective study of extrapyramidal side effects. Psychopharmacology (Berl) *124*, 188-196.

Peroutka, S. J., and Synder, S. H. (1980). Relationship of neuroleptic drug effects at brain dopamine, serotonin, alpha-adrenergic, and histamine receptors to clinical potency. Am J Psychiatry *137*, 1518-1522.

Phizicky, E. M., and Fields, S. (1995). Protein-protein interactions: methods for detection and analysis. Microbiol Rev *59*, 94-123.

Pierri, J. N., Volk, C. L., Auh, S., Sampson, A., and Lewis, D. A. (2001). Decreased somal size of deep layer 3 pyramidal neurons in the prefrontal cortex of subjects with schizophrenia. Arch Gen Psychiatry *58*, 466-473.

Pollegioni, L., Ceciliani, F., Curti, B., Ronchi, S., and Pilone, M. S. (1995). Studies on the structural and functional aspects of Rhodotorula gracilis D-amino acid oxidase by limited trypsinolysis. Biochem J *310 (Pt 2)*, 577-583.

Pollegioni, L., Piubelli, L., Sacchi, S., Pilone, M. S., and Molla, G. (2007). Physiological functions of D-amino acid oxidases: from yeast to humans. Cell Mol Life Sci *64*, 1373-1394.

Porton, B., and Wetsel, W. C. (2007). Reduction of synapsin III in the prefrontal cortex of individuals with schizophrenia. Schizophr Res *94*, 366-370.

Potkin, S. G., Costa, J., Roy, S., Jin, Y., and Gulasekaram, B. (1992). Glycine in the treatment of Schizophrenia. In: Meltzer HY (ed) Glycine in the treatment of Schizophrenia (New York: Raven Press).

Priestley, T., Laughton, P., Myers, J., Le Bourdelles, B., Kerby, J., and Whiting, P. J. (1995). Pharmacological properties of recombinant human N-methyl-D-aspartate receptors comprising NR1a/NR2A and NR1a/NR2B subunit assemblies expressed in permanently transfected mouse fibroblast cells. Mol Pharmacol *48*, 841-848.

Purcell, S. M., Wray, N. R., Stone, J. L., Visscher, P. M., O'Donovan, M. C., Sullivan, P. F., and Sklar, P. (2009). Common polygenic variation contributes to risk of schizophrenia and bipolar disorder. Nature *460*, 748-752.

Pycock, C. J., Kerwin, R. W., and Carter, C. J. (1980). Effect of lesion of cortical dopamine terminals on subcortical dopamine receptors in rats. Nature *286*, 74-76.

Rajkowska, G., Selemon, L. D., and Goldman-Rakic, P. S. (1998). Neuronal and glial somal size in the prefrontal cortex: a postmortem morphometric study of schizophrenia and Huntington disease. Arch Gen Psychiatry *55*, 215-224.

Reck-Peterson, S. L., Yildiz, A., Carter, A. P., Gennerich, A., Zhang, N., and Vale, R. D. (2006). Single-molecule analysis of dynein processivity and stepping behavior. Cell *126*, 335-348.

Richter, K., Langnaese, K., Kreutz, M. R., Olias, G., Zhai, R., Scheich, H., Garner, C. C., and Gundelfinger, E. D. (1999). Presynaptic cytomatrix protein bassoon is localized at both excitatory and inhibitory synapses of rat brain. J Comp Neurol *408*, 437-448.

Rizo, J., and Rosenmund, C. (2008). Synaptic vesicle fusion. Nat Struct Mol Biol *15*, 665-674.

Robinson, J. M., Briggs, R. T., and Karnovsky, M. J. (1978). Localization of D-amino acid oxidase on the cell surface of human polymorphonuclear leukocytes. J Cell Biol *77*, 59-71.

Rosenberg, D., Kartvelishvily, E., Shleper, M., Klinker, C. M., Bowser, M. T., and Wolosker, H. (2010). Neuronal release of D-serine: a physiological pathway controlling extracellular D-serine concentration. FASEB J *24*, 2951-2961.

Rosse, R. B., Fay-McCarthy, M., Kendrick, K., Davis, R. E., and Deutsch, S. I. (1996). D-cycloserine adjuvant therapy to molindone in the treatment of schizophrenia. Clin Neuropharmacol *19*, 444-450.

Rosse, R. B., Schwartz, B. L., Davis, R. E., and Deutsch, S. I. (1991). An NMDA intervention strategy in schizophrenia with "low-dose" milacemide. Clin Neuropharmacol *14*, 268-272.

Rosse, R. B., Schwartz, B. L., Leighton, M. P., Davis, R. E., and Deutsch, S. I. (1990). An open-label trial of milacemide in schizophrenia: an NMDA intervention strategy. Clin Neuropharmacol *13*, 348-354.

Rosso, I. M., Cannon, T. D., Huttunen, T., Huttunen, M. O., Lonnqvist, J., and Gasperoni, T. L. (2000). Obstetric risk factors for early-onset schizophrenia in a Finnish birth cohort. Am J Psychiatry *157*, 801-807.

Rutter, A. R., Fradley, R. L., Garrett, E. M., Chapman, K. L., Lawrence, J. M., Rosahl, T. W., and Patel, S. (2007). Evidence from gene knockout studies implicates Asc-1 as the primary transporter mediating d-serine reuptake in the mouse CNS. Eur J Neurosci *25*, 1757-1766.

Sacchi, S., Bernasconi, M., Martineau, M., Mothet, J. P., Ruzzene, M., Pilone, M. S., Pollegioni, L., and Molla, G. (2008). pLG72 modulates intracellular D-serine levels through its interaction with D-amino acid oxidase: effect on schizophrenia susceptibility. J Biol Chem *283*, 22244-22256.

Sakata, K., Fukushima, T., Minje, L., Ogurusu, T., Taira, H., Mishina, M., and Shingai, R. (1999). Modulation by L- and D-isoforms of amino acids of the L-glutamate response of N-methyl-D-aspartate receptors. Biochemistry *38*, 10099-10106.

Sanmarti-Vila, L., tom Dieck, S., Richter, K., Altrock, W., Zhang, L., Volknandt, W., Zimmermann, H., Garner, C. C., Gundelfinger, E. D., and Dresbach, T. (2000). Membrane association of presynaptic cytomatrix protein bassoon. Biochem Biophys Res Commun *275*, 43-46.

Sasaki, M., Konno, R., Nishio, M., Niwa, A., Yasumura, Y., and Enami, J. (1992). A single-base-pair substitution abolishes D-amino-acid oxidase activity in the mouse. Biochim Biophys Acta *1139*, 315-318.

Satel, S. L., and Edell, W. S. (1991). Cocaine-induced paranoia and psychosis proneness. Am J Psychiatry *148*, 1708-1711.

Sawada, K., Barr, A. M., Nakamura, M., Arima, K., Young, C. E., Dwork, A. J., Falkai, P., Phillips, A. G., and Honer, W. G. (2005). Hippocampal complexin proteins and cognitive dysfunction in schizophrenia. Arch Gen Psychiatry *62*, 263-272.

Sawada, K., Young, C. E., Barr, A. M., Longworth, K., Takahashi, S., Arango, V., Mann, J. J., Dwork, A. J., Falkai, P., Phillips, A. G., and Honer, W. G. (2002). Altered immunoreactivity of complexin protein in prefrontal cortex in severe mental illness. Mol Psychiatry *7*, 484-492.

Saykin, A. J., Gur, R. C., Gur, R. E., Mozley, P. D., Mozley, L. H., Resnick, S. M., Kester, D. B., and Stafiniak, P. (1991). Neuropsychological function in schizophrenia. Selective impairment in memory and learning. Arch Gen Psychiatry *48*, 618-624.

Saykin, A. J., Shtasel, D. L., Gur, R. E., Kester, D. B., Mozley, L. H., Stafiniak, P., and Gur, R. C. (1994). Neuropsychological deficits in neuroleptic naive patients with first-episode schizophrenia. Arch Gen Psychiatry *51*, 124-131.

Schapira, A. H., Cooper, J. M., Dexter, D., Clark, J. B., Jenner, P., and Marsden, C. D. (1990). Mitochondrial complex I deficiency in Parkinson's disease. J Neurochem *54*, 823-827.

Schell, M. J. (2004). The N-methyl D-aspartate receptor glycine site and D-serine metabolism: an evolutionary perspective. Philos Trans R Soc Lond B Biol Sci *359*, 943-964.

Schell, M. J., Brady, R. O., Jr., Molliver, M. E., and Snyder, S. H. (1997). D-serine as a neuromodulator: regional and developmental localizations in rat brain glia resemble NMDA receptors. J Neurosci *17*, 1604-1615.

Schell, M. J., Molliver, M. E., and Snyder, S. H. (1995). D-serine, an endogenous synaptic modulator: localization to astrocytes and glutamate-stimulated release. Proc Natl Acad Sci U S A *92*, 3948-3952.

Schluter, K., Figiel, M., Rozyczka, J., and Engele, J. (2002). CNS region-specific regulation of glial glutamate transporter expression. Eur J Neurosci *16*, 836-842.

Schmahmann, J. D. (2004). Disorders of the cerebellum: ataxia, dysmetria of thought, and the cerebellar cognitive affective syndrome. J Neuropsychiatry Clin Neurosci *16*, 367-378.

Schmitz, D., Mellor, J., and Nicoll, R. A. (2001). Presynaptic kainate receptor mediation of frequency facilitation at hippocampal mossy fiber synapses. Science *291*, 1972-1976.

Schoch, S., Castillo, P. E., Jo, T., Mukherjee, K., Geppert, M., Wang, Y., Schmitz, F., Malenka, R. C., and Sudhof, T. C. (2002). RIM1alpha forms a protein scaffold for regulating neurotransmitter release at the active zone. Nature *415*, 321-326.

Schoch, S., Deak, F., Konigstorfer, A., Mozhayeva, M., Sara, Y., Sudhof, T. C., and Kavalali, E. T. (2001). SNARE function analyzed in synaptobrevin/VAMP knockout mice. Science *294*, 1117-1122.

Schoch, S., and Gundelfinger, E. D. (2006). Molecular organization of the presynaptic active zone. Cell Tissue Res *326*, 379-391.

Schousboe, A. (2003). Role of astrocytes in the maintenance and modulation of glutamatergic and GABAergic neurotransmission. Neurochem Res *28*, 347-352.

Schultz, J., Doerks, T., Ponting, C. P., Copley, R. R., and Bork, P. (2000). More than 1,000 putative new human signalling proteins revealed by EST data mining. Nat Genet *25*, 201-204.

Schumacher, J., Jamra, R. A., Freudenberg, J., Becker, T., Ohlraun, S., Otte, A. C., Tullius, M., Kovalenko, S., Bogaert, A. V., Maier, W.*, et al.* (2004). Examination of G72 and D-amino-acid oxidase as genetic risk factors for schizophrenia and bipolar affective disorder. Mol Psychiatry *9*, 203-207.

Schwarcz, R., Rassoulpour, A., Wu, H. Q., Medoff, D., Tamminga, C. A., and Roberts, R. C. (2001). Increased cortical kynurenate content in schizophrenia. Biol Psychiatry *50*, 521-530.

Schwieler, L., Erhardt, S., Nilsson, L., Linderholm, K., and Engberg, G. (2006). Effects of COX-1 and COX-2 inhibitors on the firing of rat midbrain dopaminergic neurons--possible involvement of endogenous kynurenic acid. Synapse *59*, 290-298.

Seeman, P., Lee, T., Chau-Wong, M., and Wong, K. (1976). Antipsychotic drug doses and neuroleptic/dopamine receptors. Nature *261*, 717-719.

Selemon, L. D., Rajkowska, G., and Goldman-Rakic, P. S. (1998). Elevated neuronal density in prefrontal area 46 in brains from schizophrenic patients: application of a three-dimensional, stereologic counting method. J Comp Neurol *392*, 402-412.

Shao, Z., Kamboj, A., and Anderson, C. M. (2009). Functional and immunocytochemical characterization of D-serine transporters in cortical neuron and astrocyte cultures. J Neurosci Res *87*, 2520-2530.

Sheinin, A., Shavit, S., and Benveniste, M. (2001). Subunit specificity and mechanism of action of NMDA partial agonist D-cycloserine. Neuropharmacology *41*, 151-158.

Shenton, M. E., Dickey, C. C., Frumin, M., and McCarley, R. W. (2001). A review of MRI findings in schizophrenia. Schizophr Res *49*, 1-52.

Shi, J., Badner, J. A., Gershon, E. S., and Liu, C. (2008). Allelic association of G72/G30 with schizophrenia and bipolar disorder: a comprehensive meta-analysis. Schizophr Res *98*, 89-97.

Shi, W. X., Pun, C. L., Smith, P. L., and Bunney, B. S. (2000). Endogenous DA-mediated feedback inhibition of DA neurons: involvement of both D(1)- and D(2)-like receptors. Synapse *35*, 111-119.

Shim, S. S., Hammonds, M. D., and Kee, B. S. (2008). Potentiation of the NMDA receptor in the treatment of schizophrenia: focused on the glycine site. Eur Arch Psychiatry Clin Neurosci *258*, 16-27.

Shleper, M., Kartvelishvily, E., and Wolosker, H. (2005). D-serine is the dominant endogenous coagonist for NMDA receptor neurotoxicity in organotypic hippocampal slices. J Neurosci *25*, 9413-9417.

Shoji, K., Mariotto, S., Ciampa, A. R., and Suzuki, H. (2006a). Mutual regulation between serine and nitric oxide metabolism in human glioblastoma cells. Neurosci Lett *394*, 163-167.

Shoji, K., Mariotto, S., Ciampa, A. R., and Suzuki, H. (2006b). Regulation of serine racemase activity by D-serine and nitric oxide in human glioblastoma cells. Neurosci Lett *392*, 75-78.

Siksou, L., Rostaing, P., Lechaire, J. P., Boudier, T., Ohtsuka, T., Fejtova, A., Kao, H. T., Greengard, P., Gundelfinger, E. D., Triller, A., and Marty, S. (2007). Three-dimensional architecture of presynaptic terminal cytomatrix. J Neurosci *27*, 6868-6877.

Simeon, J., Fink, M., Itil, T. M., and Ponce, D. (1970). d-Cycloserine therapy of psychosis by symptom provocation. Compr Psychiatry *11*, 80-88.

Smith, S. M., Uslaner, J. M., Yao, L., Mullins, C. M., Surles, N. O., Huszar, S. L., McNaughton, C. H., Pascarella, D. M., Kandebo, M., Hinchliffe, R. M.*, et al.* (2009). The behavioral and neurochemical effects of a novel D-amino acid oxidase inhibitor compound 8 [4H-thieno [3,2-b]pyrrole-5-carboxylic acid] and D-serine. J Pharmacol Exp Ther *328*, 921-930.

Snyder, S. H. (1976). The dopamine hypothesis of schizophrenia: focus on the dopamine receptor. Am J Psychiatry *133*, 197-202.

Snyder, S. H. (2006). Dopamine receptor excess and mouse madness. Neuron *49*, 484-485.

Specht, C. G., and Triller, A. (2008). The dynamics of synaptic scaffolds. Bioessays *30*, 1062-1074.

Spinosa, M. R., Progida, C., De Luca, A., Colucci, A. M., Alifano, P., and Bucci, C. (2008). Functional characterization of Rab7 mutant proteins associated with Charcot-Marie-Tooth type 2B disease. J Neurosci *28*, 1640-1648.

Stefanini, S., Farrace, M. G., and Argento, M. P. (1985). Differentiation of liver peroxisomes in the foetal and newborn rat. Cytochemistry of catalase and D-aminoacid oxidase. J Embryol Exp Morphol *88*, 151-163.

Stefanini, S., Serafini, B., Cimini, A., and Sartori, C. (1994). Differentiation of kidney cortex peroxisomes in fetal and newborn rats. Biol Cell *82*, 185-193.

Stevens, E. R., Esguerra, M., Kim, P. M., Newman, E. A., Snyder, S. H., Zahs, K. R., and Miller, R. F. (2003). D-serine and serine racemase are present in the vertebrate retina and contribute to the physiological activation of NMDA receptors. Proc Natl Acad Sci U S A *100*, 6789-6794.

Straub, R. E., and Weinberger, D. R. (2006). Schizophrenia genes - famine to feast. Biol Psychiatry *60*, 81-83.

Strisovsky, K., Jiraskova, J., Barinka, C., Majer, P., Rojas, C., Slusher, B. S., and Konvalinka, J. (2003). Mouse brain serine racemase catalyzes specific elimination of L-serine to pyruvate. FEBS Lett *535*, 44-48.

Strisovsky, K., Jiraskova, J., Mikulova, A., Rulisek, L., and Konvalinka, J. (2005). Dual substrate and reaction specificity in mouse serine racemase: identification of high-affinity dicarboxylate substrate and inhibitors and analysis of the beta-eliminase activity. Biochemistry *44*, 13091-13100.

Sudol, M., Chen, H. I., Bougeret, C., Einbond, A., and Bork, P. (1995). Characterization of a novel protein-binding module--the WW domain. FEBS Lett *369*, 67-71.

Sullivan, P. F., Kendler, K. S., and Neale, M. C. (2003). Schizophrenia as a complex trait: evidence from a meta-analysis of twin studies. Arch Gen Psychiatry *60*, 1187-1192.

Susser, E., Neugebauer, R., Hoek, H. W., Brown, A. S., Lin, S., Labovitz, D., and Gorman, J. M. (1996). Schizophrenia after prenatal famine. Further evidence. Arch Gen Psychiatry *53*, 25-31.

Takahata, R., and Moghaddam, B. (2000). Target-specific glutamatergic regulation of dopamine neurons in the ventral tegmental area. J Neurochem *75*, 1775-1778.

Takao-Rikitsu, E., Mochida, S., Inoue, E., Deguchi-Tawarada, M., Inoue, M., Ohtsuka, T., and Takai, Y. (2004). Physical and functional interaction of the active zone proteins, CAST, RIM1, and Bassoon, in neurotransmitter release. J Cell Biol *164*, 301-311.

Takayasu, N., Yoshikawa, M., Watanabe, M., Tsukamoto, H., Suzuki, T., Kobayashi, H., and Noda, S. (2008). The serine racemase mRNA is expressed in both neurons and glial cells of the rat retina. Arch Histol Cytol *71*, 123-129.

Talbot, K., Eidem, W. L., Tinsley, C. L., Benson, M. A., Thompson, E. W., Smith, R. J., Hahn, C. G., Siegel, S. J., Trojanowski, J. Q., Gur, R. E.*, et al.* (2004). Dysbindin-1 is reduced in intrinsic, glutamatergic terminals of the hippocampal formation in schizophrenia. J Clin Invest *113*, 1353-1363.

Tamminga, C., Cascella, N., Fakouhi, T., and Herting, R. (1992). Enhancement of NMDA-mediated transmission in schizophrenia, (New York: Raven Press).

Tanii, Y., Nishikawa, T., Hashimoto, A., and Takahashi, K. (1994). Stereoselective antagonism by enantiomers of alanine and serine of phencyclidine-induced hyperactivity, stereotypy and ataxia in the rat. J Pharmacol Exp Ther *269*, 1040-1048.

Tao-Cheng, J. H. (2007). Ultrastructural localization of active zone and synaptic vesicle proteins in a preassembled multi-vesicle transport aggregate. Neuroscience *150*, 575-584.

Tarelli, G. T., Vanoni, M. A., Negri, A., and Curti, B. (1990). Characterization of a fully active N-terminal 37-kDa polypeptide obtained by limited tryptic cleavage of pig kidney D-amino acid oxidase. J Biol Chem *265*, 21242-21246.

Teng, F. Y., Wang, Y., and Tang, B. L. (2001). The syntaxins. Genome Biol *2*, REVIEWS3012.

Thompson, P. M., Sower, A. C., and Perrone-Bizzozero, N. I. (1998). Altered levels of the synaptosomal associated protein SNAP-25 in schizophrenia. Biol Psychiatry *43*, 239-243.

Tisdale, E. J., and Balch, W. E. (1996). Rab2 is essential for the maturation of pre-Golgi intermediates. J Biol Chem *271*, 29372-29379.

tom Dieck, S., Sanmarti-Vila, L., Langnaese, K., Richter, K., Kindler, S., Soyke, A., Wex, H., Smalla, K. H., Kampf, U., Franzer, J. T.*, et al.* (1998). Bassoon, a novel zinc-finger CAG/glutamine-repeat protein selectively localized at the active zone of presynaptic nerve terminals. J Cell Biol *142*, 499-509.

Torrey, E. F., Rawlings, R. R., Ennis, J. M., Merrill, D. D., and Flores, D. S. (1996). Birth seasonality in bipolar disorder, schizophrenia, schizoaffective disorder and stillbirths. Schizophr Res *21*, 141-149.

Tran, K. D., Smutzer, G. S., Doty, R. L., and Arnold, S. E. (1998). Reduced Purkinje cell size in the cerebellar vermis of elderly patients with schizophrenia. Am J Psychiatry *155*, 1288-1290.

Tsai, G., and Coyle, J. T. (2002). Glutamatergic mechanisms in schizophrenia. Annu Rev Pharmacol Toxicol *42*, 165-179.

Tsai, G., Lane, H. Y., Yang, P., Chong, M. Y., and Lange, N. (2004). Glycine transporter I inhibitor, N-methylglycine (sarcosine), added to antipsychotics for the treatment of schizophrenia. Biol Psychiatry *55*, 452-456.

Tsai, G., Passani, L. A., Slusher, B. S., Carter, R., Baer, L., Kleinman, J. E., and Coyle, J. T. (1995). Abnormal excitatory neurotransmitter metabolism in schizophrenic brains. Arch Gen Psychiatry *52*, 829-836.

Tsai, G., Yang, P., Chung, L. C., Lange, N., and Coyle, J. T. (1998). D-serine added to antipsychotics for the treatment of schizophrenia. Biol Psychiatry *44*, 1081-1089.

Tsai, G. E., Yang, P., Chang, Y. C., and Chong, M. Y. (2006). D-alanine added to antipsychotics for the treatment of schizophrenia. Biol Psychiatry *59*, 230-234.

Tsuang, M. (2000). Schizophrenia: genes and environment. Biol Psychiatry *47*, 210-220.

Tsuriel, S., Fisher, A., Wittenmayer, N., Dresbach, T., Garner, C. C., and Ziv, N. E. (2009). Exchange and redistribution dynamics of the cytoskeleton of the active zone molecule bassoon. J Neurosci *29*, 351-358.

Tuominen, H. J., Tiihonen, J., and Wahlbeck, K. (2005). Glutamatergic drugs for schizophrenia: a systematic review and meta-analysis. Schizophr Res *72*, 225-234.

Turner, T. (2007). Chlorpromazine: unlocking psychosis. BMJ *334 Suppl 1*, s7.

Usuda, N., Yokota, S., Hashimoto, T., and Nagata, T. (1986). Immunocytochemical localization of D-amino acid oxidase in the central clear matrix of rat kidney peroxisomes. J Histochem Cytochem *34*, 1709-1718.

Vallee, R. B., Williams, J. C., Varma, D., and Barnhart, L. E. (2004). Dynein: An ancient motor protein involved in multiple modes of transport. J Neurobiol *58*, 189-200.

van Berckel, B. N., Evenblij, C. N., van Loon, B. J., Maas, M. F., van der Geld, M. A., Wynne, H. J., van Ree, J. M., and Kahn, R. S. (1999). D-cycloserine increases positive symptoms in chronic schizophrenic patients when administered in addition to antipsychotics: a double-blind, parallel, placebo-controlled study. Neuropsychopharmacology *21*, 203-210.

van Berckel, B. N., Hijman, R., van der Linden, J. A., Westenberg, H. G., van Ree, J. M., and Kahn, R. S. (1996). Efficacy and tolerance of D-cycloserine in drug-free schizophrenic patients. Biol Psychiatry *40*, 1298-1300.

Varoqueaux, F., Sigler, A., Rhee, J. S., Brose, N., Enk, C., Reim, K., and Rosenmund, C. (2002). Total arrest of spontaneous and evoked synaptic transmission but normal synaptogenesis in the absence of Munc13-mediated vesicle priming. Proc Natl Acad Sci U S A *99*, 9037-9042.

Vawter, M. P., Howard, A. L., Hyde, T. M., Kleinman, J. E., and Freed, W. J. (1999). Alterations of hippocampal secreted N-CAM in bipolar disorder and synaptophysin in schizophrenia. Mol Psychiatry *4*, 467-475.

Veen, N. D., Selten, J. P., van der Tweel, I., Feller, W. G., Hoek, H. W., and Kahn, R. S. (2004). Cannabis use and age at onset of schizophrenia. Am J Psychiatry *161*, 501-506.

Verdoux, H., Geddes, J. R., Takei, N., Lawrie, S. M., Bovet, P., Eagles, J. M., Heun, R., McCreadie, R. G., McNeil, T. F., O'Callaghan, E.*, et al.* (1997). Obstetric complications and age at onset in schizophrenia: an international collaborative meta-analysis of individual patient data. Am J Psychiatry *154*, 1220-1227.

Verma, A., and Moghaddam, B. (1996). NMDA receptor antagonists impair prefrontal cortex function as assessed via spatial delayed alternation performance in rats: modulation by dopamine. J Neurosci *16*, 373-379.

Verrall, L., Burnet, P. W., Betts, J. F., and Harrison, P. J. (2010). The neurobiology of D-amino acid oxidase and its involvement in schizophrenia. Mol Psychiatry *15*, 122-137.

Verrall, L., Walker, M., Rawlings, N., Benzel, I., Kew, J. N., Harrison, P. J., and Burnet, P. W. (2007). d-Amino acid oxidase and serine racemase in human brain: normal distribution and altered expression in schizophrenia. Eur J Neurosci *26*, 1657-1669.

Verschure, P. J., Visser, A. E., and Rots, M. G. (2006). Step out of the groove: epigenetic gene control systems and engineered transcription factors. Adv Genet *56*, 163-204.

Volk, D. W., Austin, M. C., Pierri, J. N., Sampson, A. R., and Lewis, D. A. (2000). Decreased glutamic acid decarboxylase67 messenger RNA expression in a subset of prefrontal cortical gamma-aminobutyric acid neurons in subjects with schizophrenia. Arch Gen Psychiatry *57*, 237-245.

Vollenweider, F. X., Vontobel, P., Oye, I., Hell, D., and Leenders, K. L. (2000). Effects of (S)-ketamine on striatal dopamine: a [11C]raclopride PET study of a model psychosis in humans. J Psychiatr Res *34*, 35-43.

Volterra, A., and Meldolesi, J. (2005). Astrocytes, from brain glue to communication elements: the revolution continues. Nat Rev Neurosci *6*, 626-640.

Wanders, R. J., and Waterham, H. R. (2006). Biochemistry of mammalian peroxisomes revisited. Annu Rev Biochem *75*, 295-332.

Wang, L. Z., and Zhu, X. Z. (2003). Spatiotemporal relationships among D-serine, serine racemase, and D-amino acid oxidase during mouse postnatal development. Acta Pharmacol Sin *24*, 965-974.

Wang, X., He, G., Gu, N., Yang, J., Tang, J., Chen, Q., Liu, X., Shen, Y., Qian, X., Lin, W.*, et al.* (2004). Association of G72/G30 with schizophrenia in the Chinese population. Biochem Biophys Res Commun *319*, 1281-1286.

Wang, X., Hu, B., Zieba, A., Neumann, N. G., Kasper-Sonnenberg, M., Honsbein, A., Hultqvist, G., Conze, T., Witt, W., Limbach, C.*, et al.* (2009). A protein interaction node at the neurotransmitter release site: domains of Aczonin/Piccolo, Bassoon, CAST, and rim converge on the N-terminal domain of Munc13-1. J Neurosci *29*, 12584-12596.

Wang, X., Kibschull, M., Laue, M. M., Lichte, B., Petrasch-Parwez, E., and Kilimann, M. W. (1999). Aczonin, a 550-kD putative scaffolding protein of presynaptic active zones, shares homology regions with Rim and Bassoon and binds profilin. J Cell Biol *147*, 151-162.

Wang, Y., Liu, X., Biederer, T., and Sudhof, T. C. (2002). A family of RIM-binding proteins regulated by alternative splicing: Implications for the genesis of synaptic active zones. Proc Natl Acad Sci U S A *99*, 14464-14469.

Wang, Y., Sugita, S., and Sudhof, T. C. (2000). The RIM/NIM family of neuronal C2 domain proteins. Interactions with Rab3 and a new class of Src homology 3 domain proteins. J Biol Chem *275*, 20033-20044.

Wang, Y., and Tang, B. L. (2006). SNAREs in neurons--beyond synaptic vesicle exocytosis (Review). Mol Membr Biol *23*, 377-384.

Watanabe, M., Inoue, Y., Sakimura, K., and Mishina, M. (1992). Developmental changes in distribution of NMDA receptor channel subunit mRNAs. Neuroreport *3*, 1138-1140.

Waziri, R. (1988). Glycine therapy of schizophrenia. Biol Psychiatry *23*, 210-211.

Weickert, C. S., Straub, R. E., McClintock, B. W., Matsumoto, M., Hashimoto, R., Hyde, T. M., Herman, M. M., Weinberger, D. R., and Kleinman, J. E. (2004). Human dysbindin (DTNBP1) gene expression in normal brain and in schizophrenic prefrontal cortex and midbrain. Arch Gen Psychiatry *61*, 544-555.

Weimar, W. R., and Neims, A. H. (1977). The development of D-amino acid oxidase in rat cerebellum. J Neurochem *29*, 649-656.

Weinberger, D. R. (1987). Implications of normal brain development for the pathogenesis of schizophrenia. Arch Gen Psychiatry *44*, 660-669.

Weinberger, D. R., and Kleinman, J. E. (1986). Observations on the brain in schizophrenia. In Psychiatry update: the American Psychiatric Association annual review, A.J. Frances, and R.E. Hales, eds. (Alexandria, VA: American Psychiatry Press, Inc).

Weinberger, D. R., Kleinman, J. E., Luchins, D. J., Bigelow, L. B., and Wyatt, R. J. (1980). Cerebellar pathology in schizophrenia: a controlled postmortem study. Am J Psychiatry *137*, 359-361.

Weiss, A. P., Dewitt, I., Goff, D., Ditman, T., and Heckers, S. (2005). Anterior and posterior hippocampal volumes in schizophrenia. Schizophr Res *73*, 103-112.

Weiss, A. P., Goff, D., Schacter, D. L., Ditman, T., Freudenreich, O., Henderson, D., and Heckers, S. (2006). Fronto-hippocampal function during temporal context monitoring in schizophrenia. Biol Psychiatry *60*, 1268-1277.

Weiss, A. P., and Heckers, S. (2001). Neuroimaging of declarative memory in schizophrenia. Scand J Psychol *42*, 239-250.

Williams, M. (2009). Commentary: genome-based CNS drug discovery: D-amino acid oxidase (DAAO) as a novel target for antipsychotic medications: progress and challenges. Biochem Pharmacol *78*, 1360-1365.

Witcher, M. R., Kirov, S. A., and Harris, K. M. (2007). Plasticity of perisynaptic astroglia during synaptogenesis in the mature rat hippocampus. Glia *55*, 13-23.

Wolf, G., Keilhoff, G., Fischer, S., and Hass, P. (1990). Subcutaneously applied magnesium protects reliably against quinolinate-induced N-methyl-D-aspartate (NMDA)-mediated neurodegeneration and convulsions in rats: are there therapeutical implications. Neurosci Lett *117*, 207-211.

Wolosker, H., Blackshaw, S., and Snyder, S. H. (1999a). Serine racemase: a glial enzyme synthesizing D-serine to regulate glutamate-N-methyl-D-aspartate neurotransmission. Proc Natl Acad Sci U S A *96*, 13409-13414.

Wolosker, H., Dumin, E., Balan, L., and Foltyn, V. N. (2008). D-amino acids in the brain: D-serine in neurotransmission and neurodegeneration. FEBS J *275*, 3514-3526.

Wolosker, H., Sheth, K. N., Takahashi, M., Mothet, J. P., Brady, R. O., Jr., Ferris, C. D., and Snyder, S. H. (1999b). Purification of serine racemase: biosynthesis of the neuromodulator D-serine. Proc Natl Acad Sci U S A *96*, 721-725.

Wood, L. S., Pickering, E. H., and Dechairo, B. M. (2007). Significant support for DAO as a schizophrenia susceptibility locus: examination of five genes putatively associated with schizophrenia. Biol Psychiatry *61*, 1195-1199.

Wood, P. L., Emmett, M. R., Rao, T. S., Mick, S., Cler, J., and Iyengar, S. (1989). In vivo modulation of the N-methyl-D-aspartate receptor complex by D-serine:

potentiation of ongoing neuronal activity as evidenced by increased cerebellar cyclic GMP. J Neurochem *53*, 979-981.

Wood, P. L., Rao, T. S., Iyengar, S., Lanthorn, T., Monahan, J., Cordi, A., Sun, E., Vazquez, M., Gray, N., and Contreras, P. (1990). A review of the in vitro and in vivo neurochemical characterization of the NMDA/PCP/glycine/ion channel receptor macrocomplex. Neurochem Res *15*, 217-230.

Wright, I. C., Rabe-Hesketh, S., Woodruff, P. W., David, A. S., Murray, R. M., and Bullmore, E. T. (2000). Meta-analysis of regional brain volumes in schizophrenia. Am J Psychiatry *157*, 16-25.

Wroblewska, B., Wroblewski, J. T., Pshenichkin, S., Surin, A., Sullivan, S. E., and Neale, J. H. (1997). N-acetylaspartylglutamate selectively activates mGluR3 receptors in transfected cells. J Neurochem *69*, 174-181.

Wu, E. Q., Birnbaum, H. G., Shi, L., Ball, D. E., Kessler, R. C., Moulis, M., and Aggarwal, J. (2005). The economic burden of schizophrenia in the United States in 2002. J Clin Psychiatry *66*, 1122-1129.

Wyatt, R. J. (1991). Early intervention with neuroleptics may decrease the long-term morbidity of schizophrenia. Schizophr Res *5*, 201-202.

Wyneken, U., Smalla, K. H., Marengo, J. J., Soto, D., de la Cerda, A., Tischmeyer, W., Grimm, R., Boeckers, T. M., Wolf, G., Orrego, F., and Gundelfinger, E. D. (2001). Kainate-induced seizures alter protein composition and N-methyl-D-aspartate receptor function of rat forebrain postsynaptic densities. Neuroscience *102*, 65-74.

Xia, M., Liu, Y., Figueroa, D. J., Chiu, C. S., Wei, N., Lawlor, A. M., Lu, P., Sur, C., Koblan, K. S., and Connolly, T. M. (2004). Characterization and localization of a human serine racemase. Brain Res Mol Brain Res *125*, 96-104.

Xie, X., Dumas, T., Tang, L., Brennan, T., Reeder, T., Thomas, W., Klein, R. D., Flores, J., O'Hara, B. F., Heller, H. C., and Franken, P. (2005). Lack of the alanine-serine-cysteine transporter 1 causes tremors, seizures, and early postnatal death in mice. Brain Res *1052*, 212-221.

Yamada, K., Ohnishi, T., Hashimoto, K., Ohba, H., Iwayama-Shigeno, Y., Toyoshima, M., Okuno, A., Takao, H., Toyota, T., Minabe, Y., *et al.* (2005). Identification of multiple serine racemase (SRR) mRNA isoforms and genetic analyses of SRR and DAO in schizophrenia and D-serine levels. Biol Psychiatry *57*, 1493-1503.

Yang, C., Mora, S., Ryder, J. W., Coker, K. J., Hansen, P., Allen, L. A., and Pessin, J. E. (2001). VAMP3 null mice display normal constitutive, insulin- and exercise-regulated vesicle trafficking. Mol Cell Biol *21*, 1573-1580.

Yang, C. R., and Svensson, K. A. (2008). Allosteric modulation of NMDA receptor via elevation of brain glycine and D-serine: the therapeutic potentials for schizophrenia. Pharmacol Ther *120*, 317-332.

Yang, S., Qiao, H., Wen, L., Zhou, W., and Zhang, Y. (2005). D-serine enhances impaired long-term potentiation in CA1 subfield of hippocampal slices from aged senescence-accelerated mouse prone/8. Neurosci Lett *379*, 7-12.

Yoshikawa, M., Takayasu, N., Hashimoto, A., Sato, Y., Tamaki, R., Tsukamoto, H., Kobayashi, H., and Noda, S. (2007). The serine racemase mRNA is predominantly expressed in rat brain neurons. Arch Histol Cytol *70*, 127-134.

Young, C. E., Arima, K., Xie, J., Hu, L., Beach, T. G., Falkai, P., and Honer, W. G. (1998). SNAP-25 deficit and hippocampal connectivity in schizophrenia. Cereb Cortex *8*, 261-268.

Young, K. H. (1998). Yeast two-hybrid: so many interactions, (in) so little time. Biol Reprod *58*, 302-311.

Yurimoto, H., Hasegawa, T., Sakai, Y., and Kato, N. (2000). Physiological role of the D-amino acid oxidase gene, DAO1, in carbon and nitrogen metabolism in the methylotrophic yeast Candida boidinii. Yeast *16*, 1217-1227.

Zafra, F., Gomeza, J., Olivares, L., Aragon, C., and Gimenez, C. (1995). Regional distribution and developmental variation of the glycine transporters GLYT1 and GLYT2 in the rat CNS. Eur J Neurosci *7*, 1342-1352.

Zahniser, N. R., and Doolen, S. (2001). Chronic and acute regulation of Na+/Cl- -dependent neurotransmitter transporters: drugs, substrates, presynaptic receptors, and signaling systems. Pharmacol Ther *92*, 21-55.

Zhai, R. G., Vardinon-Friedman, H., Cases-Langhoff, C., Becker, B., Gundelfinger, E. D., Ziv, N. E., and Garner, C. C. (2001). Assembling the presynaptic active zone: a characterization of an active one precursor vesicle. Neuron *29*, 131-143.

Zhou, M., Diwu, Z., Panchuk-Voloshina, N., and Haugland, R. P. (1997). A stable nonfluorescent derivative of resorufin for the fluorometric determination of trace hydrogen peroxide: applications in detecting the activity of phagocyte NADPH oxidase and other oxidases. Anal Biochem *253*, 162-168.

Ziv, N. E., and Garner, C. C. (2004). Cellular and molecular mechanisms of presynaptic assembly. Nat Rev Neurosci *5*, 385-399.

Zornberg, G. L., Buka, S. L., and Tsuang, M. T. (2000). Hypoxic-ischemia-related fetal/neonatal complications and risk of schizophrenia and other nonaffective psychoses: a 19-year longitudinal study. Am J Psychiatry *157*, 196-202.

Zou, F., Li, C., Duan, S., Zheng, Y., Gu, N., Feng, G., Xing, Y., Shi, J., and He, L. (2005). A family-based study of the association between the G72/G30 genes and schizophrenia in the Chinese population. Schizophr Res *73*, 257-261.